Fundamental group actions on derived categories

Kite, Alexandre

Awarding institution:
King's College London

Fundamental Group Actions on Derived Categories

Alexandre Fabrice Kite

Department of Mathematics
King's College London

A thesis presented for the degree of
Doctor of Philosophy in Pure Mathematics

December 2018

Contents

Abstract. The study of the gauged linear sigma model in physics has led to a prediction that the fundamental groupoid of a space of physically meaningful parameters (the FI parameters) acts on the derived categories of certain Calabi–Yau varieties. These varieties occur as GIT quotients of a linear space by a torus action. The auto-equivalences of the derived category corresponding to some "large radius" loops in the parameter space are well understood and are so-called "window shifts". These arise naturally from the representation theory and we can try to use them to construct the conjectural representation. This has been carried out successfully for certain toric examples by Donovan and Segal in [18] and for all so-called "quasi-symmetric" examples by Halpern-Leistner and Sam in [24]. In both cases, the authors rely on the existence of special configurations of line bundles called "magic windows" (introduced in [18]) to prove relations between the various window shifts.

In this thesis, we move beyond these examples and construct a representation of the fundamental groupoid on two basepoints of an open subset of the FI parameter space whenever this space is 2-dimensional. This relies on a generalisation of windows called "fractional windows" which were introduced by Halpern-Leistner and Shipman in [25]. Moreover, we describe several examples where we can extend this representation over the whole parameter space.

When the dimension of this space becomes larger, constructing the representation becomes more complicated. Nonetheless, we construct such a representation in a new example whose parameter space is 3-dimensional using the Lefschetz hyperplane theorem. We also discuss an approach to the same problem using finite covers of the parameter space (based on [18]). Finally, we recall a conjecture of Aspinwall, Plesser and Wang [4] about how to construct a representation more generally. This leads us to conjecture a relationship between some intersection multiplicities and semi-orthogonal decompositions of derived categories and we prove that this relationship is at least well-defined.

1. Introduction

Start with a representation $T_L \curvearrowright \mathbb{C}^n$ of a connected torus T_L over $\mathbb{C}$. The weights of this representation $\beta_1, \dots, \beta_n$ lie in $L^\vee$, where L is the lattice of cocharacters of T_L. A torus representation can be viewed geometrically through the associated *toric variation of GIT* (VGIT). From this perspective, a choice of $\beta \in L^\vee$ determines an equivariant polarisation $\mathcal{O}(\beta)$ on $\mathbb{C}^n$ and we can form the associated GIT quotient X_β. For us, X_β is always a smooth toric stack (see Definition 3.20) and not a singular toric variety.

The real span of the space of parameters for the VGIT is therefore $L^\vee_{\mathbb{R}}$ and there is a natural fan in $L^\vee_{\mathbb{R}}$, called the *secondary fan* (see Definition 3.13). The cones in this fan naturally index the possible GIT quotients for our T_L-action in the sense that any two $\beta \in L^\vee$ lying in the interior of a given cone correspond to the same GIT quotient X_β. In particular, if β lies in a *chamber* C – that is, the interior of a maximal cone of this fan – we denote this GIT quotient by X_C and this is a smooth

DM stack. We call X_C a *phase* of the VGIT and crossing a wall in the secondary fan corresponds to a birational modification of X_C.

We are particularly interested in the case when our representation is *Calabi–Yau* – that is, when the sum of the weights is 0 – and if this holds, then X_β is *Calabi–Yau* for any β in the sense that $K_{X_\beta} \cong \mathcal{O}_{X_\beta}$. In this case, the secondary fan can be enhanced to a *stacky fan* (see Definition 3.22) called the *stacky secondary fan* (see Definition 3.37). Any stacky fan has an associated toric stack and the one associated to the stacky secondary fan is called the *secondary stack* [16]. We denote this by $\mathfrak{F}$. Then $\mathfrak{F}$ is a proper (see Remark 3.40) toric stack compactifying $T_{L^\vee}$. Moreover, the chambers C of the secondary fan naturally correspond to torus fixed points in $\mathfrak{F}$, which we therefore denote p_C. So the points p_C in $\mathfrak{F}$ – which physicists refer to as "large radius limits" – naturally index the phases of our VGIT.

The reason for our interest in the Calabi–Yau case, is that, in general, birational modifications of Calabi–Yaus are expected to induce equivalences between their derived categories and, in particular, all the phases of a toric Calabi–Yau VGIT should be derived equivalent. In fact, this has been proved, using the theory of windows, in [6, 22]. However such derived equivalences are not unique and so we would like to understand the global story of how they all fit together.

A priori it seems difficult to guess what relations one expects between these equivalences. Yet physicists came up with a remarkable prediction, which we shall now explain. They first tell us to complexify the space of VGIT parameters. We do this by associating to our VGIT a particular type of 2-dimensional quantum field theory, called a *gauged linear sigma model* (GLSM). Here the "gauging" refers to the T_L action and the "linear" to the fact that T_L acts on the linear space $\mathbb{C}^n$. Physicists impose the Calabi–Yau condition to ensure that this GLSM is not *anomalous*. Our VGIT parameters $\beta \in L^\vee_{\mathbb{R}}$ give parameters in this theory. These should be thought of as Kähler parameters – indeed the polarisation $\mathcal{O}(\beta)$ descends to one on X_β. There are other "Kähler-type" parameters in this theory, analogous to B-fields on a Calabi–Yau variety. Together these parameters form a complex orbifold called the *Fayet–Iliopoulos parameter space* (FIPS), which, to first approximation, is roughly $T_{L^\vee}$, or $\mathfrak{F}$ if we include limits points. This parameter space is a version of the "stringy Kähler moduli space" of a Calabi–Yau variety.

For a general reductive gauge group, it is hard to make precise mathematical sense of the FIPS, though it should be closely related to the space of Bridgeland stability conditions [9] on the derived category $D^b(X_C)$ of some phase. However, when the gauge group is a connected torus, we can use toric mirror symmetry to identify the FIPS with the "complex parameter space" of the mirror GLSM. The "complex parameters" in a GLSM parametrise "superpotentials" – that is, a certain class of Laurent polynomials (see Definition 3.1) – which don't have critical points, up to reparamatrisation. The exact notion of this "discriminant locus", where the superpotentials develop critical points, is given by zeros of the *principal A-determinant* E_A (see Definition 3.6) introduced by Gelfand, Kapranov and

Zelevinsky [20]. This is exactly the degeneracy locus of the "GKZ system" of differential equations ([20], Ch. 10, Remark 1.8). As such, the FIPS can be identified with the complement of the discriminant locus inside this space of superpotentials (see Definition 3.9). As $\mathfrak{F}$ is a compactification of this space of superpotentials, it follows that the FIPS is an open substack inside $\mathfrak{F}$ and the walls of the secondary fan are capturing the asymptotic behaviour of the discriminant locus near the toric boundary in $\mathfrak{F}$.

So we have a family of GLSMs whose Kähler structure is parametrised by the FIPS. In these physical theories there are dynamical objects known as "D-branes" which form a category. In certain regions of the FIPS, these D-brane categories can be understood geometrically as follows. Near each large radius limit p_C in $\mathfrak{F}$, there is an open subset $V_C \subset \text{FIPS}$ called the "large radius region" near p_C (see §5.1). When the FI parameters lie inside V_C, the D-brane category can be identified with the derived category $D^b(X_C)$. Unfortunately, for other FI parameters it is harder to understand this category geometrically. Yet, starting with a D-brane in a particular phase, physicists claim they can canonically transport it to different phases as we vary the FI parameters. However mathematicians have yet to make "D-brane transport", or indeed the GLSM itself, rigorous. Nonetheless, the existence of this "local system of categories" over the FIPS is a testable mathematical statement.

We want to make a precise mathematical statement out of this heuristic picture coming from physics with the fundamental groupoid acting on the derived categories of all of the phases. To this end, we need to pick a basepoint q_C near each large limit p_C, since p_C itself usually lies in the discriminant. In §5.1, we explain how to makes these choices, up to canonical homotopy. Then the following becomes a precise conjecture:

Conjecture A. *There is a representation ρ of the (orbifold) fundamental groupoid $\pi_1(\mathit{FIPS}, \{q_C\})$ into $\boldsymbol{Cat}_1$ such that $\rho(q_C) \cong D^b(X_C)$ for all chambers C of the secondary fan.*

Here $\mathbf{Cat}_1$ denotes the category of small categories with morphisms given by functors up to natural isomorphism – that is, the natural 1-category associated to the 2-category of categories. If the FIPS has a non-trivial orbifold structure, we need to use the orbifold fundamental groupoid (see [34], Ch. 13).

Several people have constructed representations along these lines. Of particular relevance to us are Donovan–Segal's [18] examples arising from A_n surface singularities. In [18], the authors explicitly identify the FIPS with a hyperplane complement and show that its fundamental group(oid) acts on the derived category of the phases. Recently, generalising [18], Halpern-Leistner–Sam [24] have considered VGITs arising from so-called *quasi-symmetric* representations, using work of Špenko–Van den Bergh [33] on non-commutative crepant resolutions. In this setting, they construct a representation of the fundamental group of a certain hyperplane complement on the phases of this VGIT. Similar representations

of fundamental groups of hyperplane complements also arise in work of Donovan and Wemyss [19] but in a non-commutative setting.

In this thesis, we shall push these ideas further and discuss a strategy for proving Conjecture A in many cases when our VGIT is not quasi-symmetric, where the geometry of the discriminant is much richer than a hyperplane complement. The general theme of this thesis is that nonetheless Conjecture A still seems to hold.

The outline of this thesis is as follows: §2-5 contain largely introductory material and §6-10 contain the new results. In §2, we give more background and context for the problem and explain our results. In particular, we explicitly describe the case when the FIPS is 1-dimensional in §2.1. In §3, we recall the theory of GKZ discriminants in the toric setting from [20] and introduce the FIPS formally. §4 recaps the theory of derived equivalences between phases coming from grade restriction windows. In §5, we describe how to use these equivalences to construct the representation in Conjecture A on certain *large radius* paths. In §6 we use the theory of "fractional grade restriction windows" to extend this to a representation on *all* paths near a curve in the toric boundary of a 2d FIPS. In §7, we then prove that, in two examples, we can extend this representation to the whole of the FIPS. In higher dimensions, the problem becomes more complicated. Nonetheless we prove in §8 that for a quasi-symmetric representation the FIPS is a hyperplane complement and, in fact, the underlying hyperplane arrangement agrees with the one in [24]. Using the theory of "magic windows", this is enough to prove Conjecture A in the quasi-symmetric case. We then move on to the higher-dimensional non-quasi-symmetric case in §9 and describe an example in detail where, following the strategy outlined in §2.4.1, we can prove Conjecture A completely. In §9.3, we discuss how this relates to Donovan and Segal's work [18] and construct an analogous finite cover of the FIPS for this example. Finally, in §10 we discuss a conjecture about how to construct a representation more generally. As part of this, we prove a Jordan-Hölder-type theorem for certain semi-orthogonal decompositions of derived categories.

Acknowledgements: I am indebted to my main supervisor Ed Segal for introducing me to this topic and for all that he has taught me. Needless to say, this thesis owes a huge debt to him. I would particularly like to thank him for the clarity and patience he brings to every discussion and for all the suggestions he has given towards improving this thesis.

I would also like to thank Tom Coates for all that he has explained to me, particularly during the early years of my PhD, and for reading through some sections of this thesis. Likewise, I would like to express my gratitude to Konni Rietsch for all the support she has provided over the years.

This work was supported by the Engineering and Physical Sciences Research Council [EP/L015234/1] through the EPSRC Centre for Doctoral Training in Geometry and Number Theory (The London School of Geometry and Number Theory), University College London. My thanks go out to all the first cohort of this

programme for all they have taught me (both mathematical and not), for the continuing inspiration they provide and for the good times we had together.

Finally, I would like to thank my family for everything they have done for me over the years – in so many ways, this thesis would not have been possible without them. In particular, special thanks to my dad for kindling my interest in mathematics, to my mum for inspiring me and to Harrison for putting up with me whilst I wrote this thesis.

Notation: Let e_i denote the ith standard basis vector for $\mathbb{Z}^n$ and $e_i^\vee$ denote the ith standard basis vector for $(\mathbb{Z}^n)^\vee$. Let L be the lattice of *cocharacters* or *one-parameter subgroups* (1-PS) of T_L – that is, $L := \mathrm{Hom}(\mathbb{C}^*, T_L)$ – and hence $L^\vee$ is the lattice of *characters* of T_L. We let $T_{L^\vee}^{S^1} := L^\vee \otimes S^1$ denote the compact torus inside $T_{L^\vee}$ and $T_{L^\vee}^{\mathbb{R}} = L^\vee \otimes \mathbb{R}_{>0}^\times$ the connected real subtorus in $T_{L^\vee}$. The inclusions into $T_{L^\vee}$ are induced by the isomorphism $\mathbb{R}_{>0}^\times \times S^1 \cong \mathbb{C}^*$ coming from polar coordinates.

A linear toric VGIT $T_L \circlearrowright \mathbb{C}^n$ is specified by its set of *weights* $Q(e_i^\vee) := \beta_i \in L^\vee$, which can be packaged as a map $Q : (\mathbb{Z}^n)^\vee \to L^\vee$. We shall assume that Q is surjective and set $k := \mathrm{rank}(L)$. If we let $M := \ker(Q), N := M^\vee$ (both lattices of rank $n-k$), then there are exact sequences:

$$\begin{aligned} &0 \to L \xrightarrow{Q^\vee} \mathbb{Z}^n \xrightarrow{A} N \to 0 \\ &0 \to M \xrightarrow{A^\vee} (\mathbb{Z}^n)^\vee \xrightarrow{Q} L^\vee \to 0 \end{aligned} \tag{1}$$

The map A here is called the *ray map* and $\omega_i := A(e_i)$ is the ith *ray*. We assume that the rays are distinct and non-zero. As $\ker A = \mathrm{Im} Q^\vee$, the linear toric VGIT $T_L \circlearrowright \mathbb{C}^n$ can equivalently be specified by A; cf. [17].

For an element l in a lattice L, its lattice length $|l|$ is the positive integer such that $l = |l| u_l$ where $u_l \in L$ is the primitive generator of the ray through l. We abbreviate the rank of L to $\mathrm{Rk}(L)$. For any field $\mathbb{F}$ and abelian group L, $L_{\mathbb{F}} := L \otimes_{\mathbb{Z}} \mathbb{F}$. We also set $H_l := \{y \in L_{\mathbb{R}}^\vee \mid \langle l, y \rangle = 0\}$. $\mathfrak{R}(z)$ and $\mathfrak{I}(z)$ denote the real and imaginary parts of a complex number $z \in \mathbb{C}$ respectively.

For a (stacky – see Definition 3.22) fan Σ in $N_{\mathbb{R}}$, we let X_Σ be the corresponding toric variety (stack). For a k-dimensional cone σ in Σ, we let $Z(\sigma) \subset X_\Sigma$ be the codimension k torus-invariant subvariety (substack) which is the closure of the torus orbit corresponding to σ (see [14], §3.2). We also denote the torus-invariant divisor in X_Σ corresponding to ω_i by D_i and so $D_i = Z(\omega_i)$. Similarly, if we pick a polarisation on X_Σ with corresponding polytope $P \subset M_{\mathbb{R}}$, then if F is a k-dimensional face of P, we let $Z(F) := Z(\sigma) \subset X_\Sigma$ where σ is the codimension k cone of Σ dual to F.

We abbreviate *semi-orthogonal decomposition* to SOD.

For a set of basepoints $\{p_i\}$ in X, $\pi_1(X, \{p_i\})$ denotes the orbifold fundamental groupoid of X on these basepoints. $\pi_1(X, p_1, p_2)$ denotes the elements of the orbifold fundamental groupoid going from p_1 to p_2.

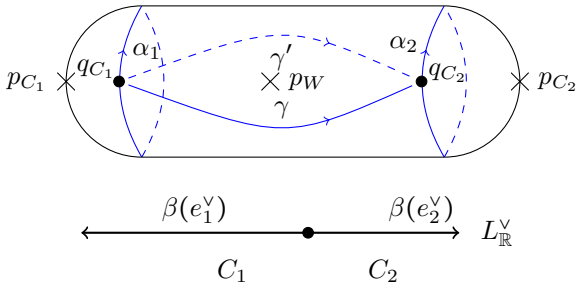

FIGURE 1. The secondary stack $\mathfrak{F}$ with the two large radius limits p_{C_i} and principal discriminant p_W marked (T) (for top) and its stacky secondary fan (B) (for bottom).

2. Extended introduction

2.1. **The case of a 1d FIPS.** We first describe the simplest case of Conjecture A when the FIPS is 1-dimensional. This is well-understood (see for example [18], §2.1.1) and corresponds to the case of $T_L = \mathbb{C}^* \circlearrowright \mathbb{C}^n$. The secondary fan (see Definition 3.13), which is a fan in $L_{\mathbb{R}}^\vee \cong \mathbb{R}$, is schematically shown at the bottom of Figure 1. Because of the Calabi–Yau condition, the secondary fan always has two chambers C_1 and C_2. As the secondary fan parametrises the possible GIT quotients, we therefore have two phases (see Definition 3.21) denoted by X_{C_1} and X_{C_2} and we let $i_j : X_{C_j} \subset [\mathbb{C}^n / \mathbb{C}^*]$ be the open immersion induced by the inclusion of the semistable locus corresponding to C_j into $\mathbb{C}^n$.

To get the correct stack structure for the FIPS, we have to enhance the secondary fan to a so-called "stacky fan" (see Definition 3.22). In the 1d case, this "stacky secondary fan" (see Definition 3.37) just consists of an element $\beta(e_i^\vee) \in L^\vee \cap C_i$ for $i = 1, 2$, which is given by $\beta(e_i^\vee) := \operatorname{lcm}(\beta_j | \beta_j \in C_i)$ (see [16], Proposition 2.12). The corresponding toric stack is called the *secondary stack* $\mathfrak{F}$ (see Definition 3.38) and is $\mathbb{P}(\ell_1, \ell_2)/\mu_r$ where $r := \gcd(|\beta(e_1^\vee)|, |\beta(e_2^\vee)|)$, $\ell_i := |\beta(e_i^\vee)|/r \in \mathbb{Z}_{>0}$ and, if we pick $a_1, a_2 \in \mathbb{Z}$ such that $a_1\ell_1 + a_2\ell_2 = -1$, then $\zeta \in \mu_r$ acts by $(\zeta^{a_2}, \zeta^{a_1})$. Thus $\mathfrak{F}$ (shown at the top of Figure 1) has no stacky points in the open torus orbit but may have some orbifold points at the two large radius limits – that is, torus fixed points – labelled p_{C_i}.

In any dimension, the discriminant is defined by GKZ's *principal A-determinant* (see Definition 3.6) and, in the 1d case, this consists of between 1 and 3 points. There is always a unique point, which we denote p_W here, in the open torus orbit of $\mathfrak{F}$ and we call it the *principal component* (see Definition 3.11). Then the torus fixed point p_{C_i} is in the discriminant precisely when there are multiple weights lying in the chamber C_i. In the case when only a single weight, β_j say, lies in C_i, p_{C_i} is not in the discriminant and is a $\mathbb{Z}_{|\beta_j|}$-orbifold point. As such, the FIPS, which is the complement of the discriminant in $\mathfrak{F}$, is an (orbifolded) $\mathbb{P}^1$ with at most 3 points missing (see Figure 1).

In light of Conjecture A, we now want to construct an action of the fundamental groupoid $\pi_1(\text{FIPS}, \{q_{C_1}, q_{C_2}\})$ where q_{C_i} is a real (see Definition 5.3) basepoint in the FIPS near p_{C_i}. In dimension 1, this fundamental groupoid is easy to describe – namely, it is generated by the paths α_1, α_2 and γ shown in blue in Figure 1. If there are no orbifold points in the FIPS – that is, both p_{C_i} are in the discriminant – then it is the free groupoid on these generators. Otherwise, if we have an orbifold point of order d at p_{C_i} then the only relations are $\alpha_i^d = e$. We will refer to the paths α_i as *toric loops* as they are loops which are invariant under the action of the compact torus $T^{S^1}_{L^\vee} \coloneqq L^\vee \otimes S^1$ and the path γ as a *large radius* path.

With this presentation of $\pi_1(\text{FIPS}, \{q_{C_1}, q_{C_2}\})$ to hand, we see that the path α_i must act by an auto-equivalence of X_{C_i} and we'll choose this to be tensoring by a certain line bundle on X_{C_i}. In fact, if we pick a small, possibly punctured, disk V_{C_i} in the FIPS about p_{C_i}, there is a canonical way to identify $\pi_1(V_{C_i}, q_{C_i})$ with $\text{Pic}(X_{C_i})$ and hence there is a canonical line bundle associated to α_i. We use this line bundle to define our action of α_i on $D^b(X_{C_i})$.

We make this identification $\pi_1(V_{C_i}, q_{C_i}) \cong \text{Pic}(X_{C_i})$ in the 1d case as follows. We've already seen that $\pi_1(V_{C_i}, q_{C_i}) \cong \langle \alpha_i \rangle$ and this is either $\mathbb{Z}$ or $\mathbb{Z}_{|\beta_j|}$, where the latter case happens precisely when β_j is the only weight in C_i. To understand $\text{Pic}(X_{C_i})$, it helps to think about our VGIT in terms of fans in $N_\mathbb{R}$ whose rays are a subset of the n rays ω_j defined by the short exact sequence (1) and with support equal to the full-dimensional cone generated by all the rays ω_j (see the discussion before Remark 3.23). Since all phases of our VGIT are DM stacks, by standard toric geometry (see [14], Proposition 6.4.1), we can identify $\text{Pic}(X_{C_i}) \cong L^\vee$ whenever the corresponding fan for X_{C_i} uses all the n rays ω_j. Note that $\text{Rk}(L) = 1$ implies that we only have 1 more ray than the number of dimensions and so, if we don't use all the rays, we must use all but one. If ω_j denotes the ray we don't use, the same standard toric geometry tells us that $\text{Pic}(X_{C_i}) \cong L^\vee / \langle \beta_j \rangle \cong \mathbb{Z}_{|\beta_j|}$. To complete the argument, we can use the short exact sequences (1) to check that ω_j is not in the fan for X_{C_i} precisely when β_j is the only weight in C_i.

As such, to get the full action ρ of $\pi_1(\text{FIPS}, \{q_{C_1}, q_{C_2}\})$, all that remains is to freely assign an equivalence between $D^b(X_{C_1})$ and $D^b(X_{C_2})$ to γ. In the context of linear toric Calabi–Yau VGITs, one can construct such an equivalence using *windows* (see Definition 4.8), which were introduced in [32].

Remark 2.1. As we shall see below, there are infinitely many windows and these are naturally indexed by $\mathbb{Z}$. As such, there are correspondingly infinitely many equivalences we could assign to γ. Hence this approach allows us to construct infinitely many actions ρ and there seems not to be a canonical one, though this ambiguity is naturally fixed by choosing an integer associated to γ.

To describe our windows, we first note that there is a positive number η naturally associated to the wall given by the origin in $L^\vee_\mathbb{R}$, namely the absolute value of the sum of the weights in C_i for either i. We note that η is independent of i because of

the Calabi–Yau condition. Then, in this case, a window is just a full subcategory $\mathcal{W}$ of $D^b([\mathbb{C}^n/\mathbb{C}^*])$ generated by $\mathbb{C}^*$-equivariant line bundles on $\mathbb{C}^n$ whose weights lie in an interval of width $\eta-1$. Such a window therefore depends on a choice of $w\in\mathbb{Z}$ and given such a w, the corresponding window $\mathcal{W}(w)=\langle\mathcal{O}(d)\mid d\in[w,w+\eta-1]\rangle$. The key property of windows in the Calabi–Yau setting (c.f. Corollary 4.16) is that, for either j and any w, the restriction $i_j^*:\mathcal{W}(w)\to D^b(X_{C_j})$ is an equivalence. Then the *window equivalence* ϕ_w from $D^b(X_{C_1})$ to $D^b(X_{C_2})$ is $i_2^*\circ(i_1^*)^{-1}$ – that is, we lift from $D^b(X_{C_1})$ into $\mathcal{W}(w)$ and then restrict to $D^b(X_{C_2})$.

Remark 2.2. We note that if, instead of γ, we had chosen any path from q_{C_1} to q_{C_2} which together with the α_i freely generates $\pi_1(\mathrm{FIPS},\{q_{C_1},q_{C_2}\})$, then the same argument as above would produce a different action. The particular choice above was motivated by physics (see [27]).

In particular, if we had chosen the path γ' shown in Figure 1 instead of γ and if we fix $\rho(\gamma)=\phi_w$, it is natural to ask what the equivalence $\rho(\gamma')$ is. Noting that $\gamma'=\alpha_2^{-1}\circ\gamma\circ\alpha_1$ in $\pi_1(\mathrm{FIPS},\{q_{C_1},q_{C_2}\})$, one checks that $\rho(\gamma')=\phi_{w+1}$ can also be described as a window equivalence but using the window $\mathcal{W}(w+1)$ instead of $\mathcal{W}(w)$.

With both of these functors to hand, we can try to think more geometrically about our action ρ by studying the auto-equivalence of $D^b(X_{C_1})$ given by $\rho((\gamma')^{-1}\circ\gamma)$. This auto-equivalence is called a *window shift* (see Definition 4.18). It turns out (see [25], Proposition 3.4) that window shifts can be described as a twist about a spherical functor whose source category is the derived category of the $\mathbb{C}^*$-fixed locus in $\mathbb{C}^n$ (see Remark 4.19 for details). In particular, if our representation has no 0 weights, the $\mathbb{C}^*$-fixed locus is the origin and the window shift is a spherical twist about a sheaf supported on the flopping locus.

2.2. **At and near large radius in a higher-dimensional FIPS.** So when the FIPS is 1-dimensional we can solve Conjecture A. In higher dimensions life is not so easy, one reason being that we don't have such an easy explicit presentation for $\pi_1(\mathrm{FIPS},\{q_C\})$. Nonetheless, as in the 1d case, we can try to focus on regions of the FIPS where the topology is simpler and try to construct actions of the fundamental groupoids of these regions.

Recall that the large-radius limits p_C are the torus fixed points in $\mathfrak{F}$ and there is one for each chamber C of the secondary fan. As we shall see in §5.1 the, possibly punctured, disk V_{C_i} near the large radius limit p_{C_i} in the 1d case generalises to a certain analytic open region of the FIPS – called a "large radius region" (see Definition 5.2) – whose closure in $\mathfrak{F}$ contains the large radius limit p_{C_i}. Loops α in $\pi_1(V_{C_i},q_{C_i})$ are again called "toric loops" as they are the higher-dimensional analogue of our toric loops α_i from the 1d case. Moreover, we still have the same correspondence (see Lemma 5.4) between toric loops α and line bundles on X_{C_i} and hence a canonical action of such loops.

Now that we understand how to define our action in the region $V_{C_i} \subset \text{FIPS}$ near each large radius limit, we turn to constructing an action in another region of the FIPS, called a "near large radius region". To make this precise, fix a wall W in the secondary fan for the rest of this section. Given such a wall W between two chambers C_1 and C_2, recall that there is a unique torus-invariant rational curve in $\mathfrak{F}$ joining p_{C_1} and p_{C_2}. We will denote this curve by $Z(W)$, shown in Figure 2 (L) (for left). Then there is a near large radius region $V_W \subset \text{FIPS}$ associated to W (see §5.2), which connects V_{C_1} with V_{C_2}. This region lies "near" $Z(W)$ in the sense that its closure in $\mathfrak{F}$ meets $Z(W)$ in a subset with non-empty interior.

As a warm-up to Conjecture A, for the rest of this section we focus on constructing a representation of the fundamental groupoid $\pi_1(V_W, \{q_{C_1}, q_{C_2}\})$ with two basepoints, one near p_{C_1} and one near p_{C_2}, on $D^b(X_{C_1})$ and $D^b(X_{C_2})$. We call this fundamental groupoid the *near large radius groupoid* associated to W (see Definition 5.9) and it is designed to capture the topology of the FIPS near the rational curve $Z(W)$. Apart from toric loops at each of the basepoints, there are additional paths in V_W which connect q_{C_1} with q_{C_2}. To understand the near large radius groupoid, it is helpful to single out such a path which is an analogue of the path γ from the 1d case. We'll denote a choice of such a path by $\gamma^0_{C_1,C_2}$, where our notation is designed to keep track of the two chambers.

A first guess for $\gamma^0_{C_1,C_2}$ is a path in $Z(W)$, going from q_{C_1} to q_{C_2}, such as γ_{C_1,C_2} in Figure 2 (L). However, $Z(W)$ is often in the discriminant locus and so, as $\gamma^0_{C_1,C_2}$ has to lie in the FIPS, we can't choose such a path in general.

Instead, we use the fact that V_W is fibred in cylinders over some base. As $V_W \subset \text{FIPS}$, these cylinders are punctured at points of the discriminant and we can assume, without loss of generality, that our basepoints both lie on the boundary of the same fibre. A schematic fibre is shown in Figure 2 (R), where the crosses indicate the discriminant and where we have drawn a potential choice of $\gamma^0_{C_1,C_2}$. The reason that this is a good analogue of γ is that, if we take the limit of our fibre and the two basepoints in it under the 1-PS of $T_{L^\vee}$ associated to a generic element of $L^\vee \cap W$, then $\gamma^0_{C_1,C_2}$ limits to the path γ_{C_1,C_2} in $Z(W)$ we initially wanted to choose as an analogue of γ. We say that the path $\gamma^0_{C_1,C_2}$ in V_W is a "push-off" of the path γ_{C_1,C_2} in $Z(W)$.

We can see this limiting behaviour of $\gamma^0_{C_1,C_2}$ as the fibre approaches $Z(W)$ – that is, as the cylinder from Figure 2 (R) get closer and closer to Figure 2 (L) – as follows. By construction of V_W, all the points of the discriminant in the cylinder fibre converge to the point p_W. If we let m_W be the intersection multiplicity of the open torus orbit in $Z(W)$ with the discriminant, it follows that, for a fibre sufficiently close to $Z(W)$, we can find a disk D, such as the one shown in Figure 2 (R), which contains all these m_W punctures. Moreover, since our choice of $\gamma^0_{C_1,C_2}$ is outside D, it doesn't interact with these punctures as the fibre tends to $Z(W)$ and so $\gamma^0_{C_1,C_2}$ extends across $Z(W)$. We call the subgroupoid of the near large radius groupoid generated by the generalisations of the α and γ paths from the 1d case

the *large radius groupoid* associated to W (see Definition 5.12) and denote it by $\mathcal{G}_{LR}^W$. It represents the closest thing we have near $Z(W)$ in a higher-dimensional FIPS to the fundamental groupoid from the 1d FIPS.

Remark 2.3. In general, the large radius groupoid is a *strict* subgroupoid of the near large radius groupoid. Explicitly, any path in the punctured cylinder fibre in Figure 2 (R) which is not homotopic in the fibre to a path completely outside the disk D is not in the large radius groupoid. We call such paths in V_W *near large radius paths* and observe that they arise whenever $m_W > 1$ – that is, whenever the discriminant intersects the open orbit in $Z(W)$ non-transversely. Since in general the discriminant is reducible (see Definition 3.6), this non-transversal intersection can arise when one component intersects the open orbit in $Z(W)$ non-transversely or whenever multiple components intersect it.

We now turn to constructing the representation on $\pi_1(V_W, \{q_{C_1}, q_{C_2}\})$. We start by considering what happens on the subgroupoid $\mathcal{G}_{LR}^W$. Given we know how toric loops act, this boils down to constructing the derived equivalence $\rho(\gamma^0_{C_1,C_2})$ between X_{C_1} and X_{C_2}. In complete analogy with the 1d case, this is given by a window equivalence, using the general theory of windows introduced in §4.

Remark 2.4. We can think about this more general window equivalence in a way which makes the analogy with the 1d case clearer as follows. Namely, X_{C_1} and X_{C_2} are "connected" by a VGIT with $\mathrm{Rk}(L) = 1$ in the sense that one can find (see [20], Ch. 7, Theorem 2.10) open toric substacks $Y_{C_i} \subset X_{C_i}$ such that $X_{C_1} \backslash Y_{C_1} = X_{C_2} \backslash Y_{C_2}$ and Y_{C_i} are the two phases of a toric Calabi–Yau VGIT with $\mathrm{Rk}(L) = 1$. Then our more general window equivalence can be thought of as taking a window equivalence between Y_{C_1} and Y_{C_2}, as described in the 1d case, and then extending this by the identity to X_{C_i}.

If we continue this line of thought, the secondary stack for the VGIT for Y is exactly $Z(W)$ and, by the properties of the discriminant E_A (see Theorem 3.33), the FIPS for the VGIT for Y is the complement in $Z(W)$ of the components of the discriminant in $\mathfrak{F}$ which don't contain $Z(W)$. In particular, if $Z(W)$ is not completely in the discriminant in $\mathfrak{F}$, then the FIPS for the VGIT for Y is where the FIPS of the VGIT for X meets $Z(W)$.

Putting the representation on the analogues of α_i and γ together, we arrive (in Proposition 5.20) at a representation $\rho^W : \mathcal{G}_{LR}^W \to \mathbf{Cat}_1$ which assigns to the analogue of the paths α/γ from the 1d case tensoring by a line bundle/a window equivalence. Here the superscript on ρ reminds us that we are only considering paths in V_W.

Remark 2.5. Exactly as in the 1d case (see Remark 2.1), there are infinitely many possible window equivalences between X_{C_1} and X_{C_2} we could choose from and these are naturally indexed by $\mathbb{Z}$. As such, there are infinitely many representations ρ^W of $\mathcal{G}_{LR}^W$ and no canonical choice amongst these.

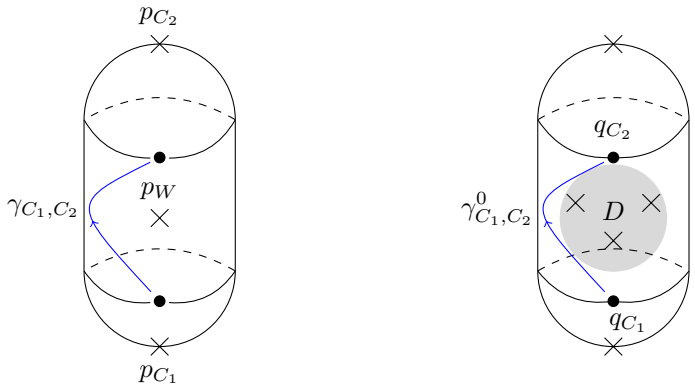

FIGURE 2. The torus-invariant curve $Z(W)$ with large radius limits p_{C_i} and point p_W in the discriminant (L) and a curve "near large radius" with 3 points in the discriminant (R)

As $\mathcal{G}^W_{LR}$ is typically a strict subgroupoid of $\pi_1(V_W, \{q_{C_1}, q_{C_2}\})$ (see Remark 2.3), the representation ρ^W constructed so far is however not the end of the story – that is, we need to know how to assign equivalences to the *near* large radius paths. Luckily for us, there is a natural source of extra "window-like" equivalences between two neighbouring phases coming from *fractional windows* (see Definition 4.24), introduced in [25]. These provide candidates for how to extend our representation $\rho^W : \mathcal{G}^W_{LR} \to \mathbf{Cat}_1$ from above to the whole of $\pi_1(V_W, \{q_{C_1}, q_{C_2}\})$. For a general FIPS, we don't know how to consistently pick these equivalences for all the near large radius paths, though see §2.4.3 for some progress in this direction. However, if we let W be any wall in the secondary fan and denote the two chambers on either side of W by C_1 and C_2, we can show:

Theorem A (Theorem 6.15)**.** *Suppose $Rk(L) = 2$. Then we can choose appropriate fractional windows to get a representation $\rho^W : \pi_1(V_W, \{q_{C_1}, q_{C_2}\}) \to \boldsymbol{Cat}_1$ such that $\rho(q_{C_i}) \cong D^b(X_{C_i})$.*

What makes this theorem feasible is that, for a 2d FIPS, we can understand $\pi_1(V_W, \{q_{C_1}, q_{C_2}\})$ explicitly and hence understand what relations we need to prove between our functors. This explicit description of the fundamental groupoid comes from the map on V_W with punctured cylinder fibres discussed above, whose fibre shown in Figure 2 (R). The basic observation is that, in the 2d case, this map is actually a *fibration* with base a small, possibly punctured, disk. This fibration then gives us an explicit description of $\pi_1(V_W, \{q_{C_1}, q_{C_2}\})$ in terms of the fundamental groupoid of the fibre and the monodromy around a distinguished point in the base. As we can present the fundamental groupoid of the fibre as a free groupoid, the only relations are the monodromy relations and, in the 2d case, we can describe the monodromy explicitly (see Lemma 6.5). Checking that these relations hold on ρ^W then boils down to properties (see Remark 6.12) of the semi-orthogonal decompositions used to define our fractional windows.

Remark 2.6. It's possible to glue together these near large radius groupoids across different walls and the representations ρ^W compatibly. The end result is a representation ρ of $\pi_1(U, \{q_C\})$ where $U \coloneqq \bigcup_{\text{Walls W}} V_W$. However, the individual representations ρ^W are not canonical (see Remark 2.5) and it's not obvious whether we can extend such an arbitrarily constructed ρ to a representation of $\pi_1(\text{FIPS}, \{q_C\})$ as in Conjecture A.

From here, there are two distinct directions in which to proceed and we deal with these in turn in the next two sections.

(1) How to extend the representation ρ to the whole FIPS in the 2d case
(2) How to deal with higher-dimensional FIPS

2.3. **Fundamental group representations of a 2d FIPS.** In general, we don't know how to choose the representations ρ^W from Theorem A for each wall W of the secondary fan such that, if we glue them together as in Remark 2.6, they extend to a representation of the whole FIPS. Nonetheless, for the particular example of the Octahedron VGIT, which we detail in §5.3 and §7.2, we are able to do this:

Theorem B (Theorem 7.16)**.** *In the Octahedron VGIT, we can choose representations ρ^W (as in Theorem A) for each wall W such that together they define a representation of $\pi_1(\mathit{FIPS}, \{q_C\})$. Hence Conjecture A holds in this example.*

By a quasi-projective form of the usual Lefschetz hyperplane theorem (see §9.2.1), we expect $\pi_1(U)$ to generate $\pi_1(\text{FIPS})$ in general. As such, to prove Theorem B, we should only need to prove some additional relations between our functors. Again there is a natural source of such relations in the context of VGIT called *(fractional) magic windows*, which were introduced in [18]. The relevant theory is reviewed in §4.2, in particular Definitions 4.31 and 4.35.

The proof of Theorem B then consists of two parts. First, we understand what relations we need to prove in $\pi_1(U)$. This is purely topological and relies on the method of Zariski–van-Kampen (detailed in §7.1). The idea here is to pick a nice pencil of curves on the FIPS and see how the discriminant "braids" as we go around critical values. Secondly, following on from Remark 2.6, we prove that we can choose the representation ρ^W on each wall W such that, when we glue them together, there are fractional magic windows which implement all these relations. This example is interesting in that we really need to use *fractional* magic windows as there are no ordinary magic windows.

Remark 2.7. We also use exactly the same strategy as part of the proof of Theorem C which we discuss below (see §7.3 for the details).

2.4. **Fundamental group representations of a higher-dimensional FIPS.** When the FIPS is higher-dimensional, its topology becomes even more complicated. However, as mentioned in §1, there is one class of examples where the representation in Conjecture A can be constructed – when the underlying T_L-representation is *quasi-symmetric*. In this case, we prove:

Proposition (Theorem 8.8, Proposition 8.14)**.** *For a quasi-symmetric representation, the GKZ discriminant locus is, after taking logs, the complexification of a real hyperplane arrangement and it agrees with the one constructed by Halpern-Leistner–Sam in* [24] *up to an overall shift.*

As [24], Proposition 6.6 constructs a representation of the complement of this (log)-hyperplane arrangement using window equivalences, we have immediately that:

Corollary 2.8. *For a quasi-symmetric toric VGIT, ρ gives a representation of $\pi_1(FIPS)$, thereby proving Conjecture A.*

The strategy for proving this result is the same as for Theorem B. In the quasi-symmetric case both parts – topological and magic window – are well-behaved. In terms of topology, there is a presentation of the fundamental groupoid of the complement of the complexification of a real hyperplane arrangement called the *Deligne groupoid* (see, for example, [15, 29, 30]). This makes it straightforward to understand what relations we need to prove between our window equivalences. Moreover, Halpern-Leistner–Sam [24] show that, to every such relation, there is a corresponding magic window which implements it.

Outside of the quasi-symmetric setting, both aspects of the problem are harder. On the magic window side, there are examples where magic windows are not sufficient to implement all the relations (indeed they may not exist at all). In fact, the Octahedron VGIT is such an example – see Example 4.34. Even fractional magic windows are not enough (even for a 2-dimensional FIPS), as Example 4.37 shows. The topology of FIPS is also typically more complicated than that of the complement of a hyperplane arrangement. Nonetheless, we can prove:

Theorem C (Theorem 9.35)**.** *Conjecture A holds for the non-quasi-symmetric "Triangle VGIT" whose FIPS, introduced in §9, is 3-dimensional and where the phases are (orbifold) resolutions of a certain 3-dimensional non-isolated $\mathbb{Z}_2 \times \mathbb{Z}_2$ quotient singularity*

There are two approaches to simplifying the topology of the FIPS one could take to prove such a theorem:

- Use the Lefschetz hyperplane theorem
- Take a cover of the FIPS

We come to these in turn in the next two sections.

2.4.1. *Lefschetz strategy.* To get an inductive approach to proving Conjecture A, we could try to use the Lefschetz hyperplane theorem which should, in principle, allow us to reduce the problem to several problems with lower dimensional FIPS. The ultimate aim behind this would be to reduce to the 2d case. We carry this out successfully in §9 for the Triangle VGIT and prove Theorem C from this perspective.

The basic idea behind this approach is that, if we pick a toric divisor in the secondary stack, then all the phases near that divisor can be described in terms of several simpler VGIT problems glued together (this can be phrased in terms of polyhedral subdivisions – see §3.3). In addition, the complement of the discriminant on that divisor can be described (see Theorem 3.33) analogously as a gluing together of the FIPS of the simpler VGITs. So we could hope that if we proved Conjecture A for these VGIT problems near some (or all) of the toric divisors then this might be enough to prove it for the original VGIT.

Topologically the idea to implement this comes from (a quasi-projective version of) the Lefschetz hyperplane theorem. This says that, when the FIPS is at least 3-dimensional, the region where a tubular neighbourhood of any ample toric divisor in the secondary stack meets the FIPS necessarily contains the homotopy 1-type. As the secondary stack is proper, such an ample toric divisor always exists.

However, in general, this region is not itself a tubular neighbourhood of the divisor in the FIPS. One issue is that many of the toric divisors often lie completely in the discriminant and so such regions are at best punctured tubular neighbourhoods. More seriously, the discriminant might intersect the divisor "non-transversely".

But if the discriminant meets such a toric divisor "transversely", then the topology of this region should be able to be understood in terms of the topology of the toric divisor. Hence we would have reduced the problem to several simpler problems with lower-dimensional FIPS and we could continue iterating this approach.

The two main difficulties with this strategy are proving transversality (see §9.2.1) and solving the 2-dimensional problem (which we have discussed in §2.3).

2.4.2. *Covering strategy.* Covers of the FIPS were used successfully by Donovan and Segal in [18] to prove Conjecture A in a class of non-quasi-symmetric examples. The idea is that, for these examples, there is a finite cover of the FIPS which is itself the FIPS of a quasi-symmetric VGIT and hence for which we can prove Conjecture A. Moreover they observe that the original VGIT corresponds to a certain "slice" of this quasi-symmetric VGIT.

We use this approach in §9.3 to construct an analogous cover of the FIPS of the Triangle VGIT. In this case, the "unsliced" VGIT arises as the representations of the underlying quiver (shown in Figure 27) of an NCCR on the original (singular) affine GIT quotient, in much the same way as in the examples in [18]. Having already constructed an action in §9.2, we content ourselves by just sketching how to use this cover to reconstruct the action on the Triangle VGIT in Theorem C.

Remark 2.9. The construction of the unsliced VGIT using NCCRs allows us to relate our story to actions of hyperplane complements arising in the work of Wemyss and Donovan [19, 36]. See Remark 9.48.

There are two issues with doing this covering strategy more generally:

- Slicing an "unsliced" VGIT in this way does *not* in general produce a finite cover between the FIPS of the unsliced VGIT and the FIPS of the sliced VGIT.
- Even if we have a finite cover arising in this way, this only helps us if we can prove Conjecture A for the "unsliced" VGIT. However, for a given VGIT, we don't know when we should expect it to arise as a slice of a quasi-symmetric one.

2.4.3. *Representation on near large radius paths.* Finally, in §10, we forget about the complicated topology of the FIPS and instead discuss an idea about how to generalise the construction of the representation ρ^W for near large radius paths in 2-dimensions (see Theorem A) to higher dimensions. Recall that, in the 2d case, we used fractional windows to construct ρ^W on near large radius paths. These exist more generally and give a natural guess for how to define ρ^W in higher dimensions. However, they depend on a semi-orthogonal decomposition (SOD) of $D^b(Z'_\lambda)$ where $\lambda \in L$ is a normal to the wall W and Z'_λ is the λ-fixed locus inside X_β where $\beta \in L^\vee$ is any element in the interior of W.

So which SOD should we pick to define ρ^W on our near large radius paths? On the one hand, there is a natural way to get SODs of $D^b(Z'_\lambda)$ because Z'_λ is itself a phase of another (usually not Calabi–Yau) VGIT. In recent years, general VGIT technology has been developed [6, 22] which, for a given set of paths in $L^\vee_\mathbb{R}$ connecting our phase to certain "minimal" phases – that is, phases for which K_X is nef – allows us to produce SODs of $D^b(Z'_\lambda)$.

On the other hand, we recall in §3.1 that the components ∇_Γ of the GKZ discriminant are labelled by faces Γ of the polytope $\Delta \subset N_\mathbb{R}$, which is the convex hull of the rays. The rays on Γ itself form a VGIT and there is a "complementary" VGIT called the Higgs VGIT. A minimal phase of the Higgs VGIT is called a *Higgs phase* associated to Γ and we denote it by Z_Γ. There is an intriguing conjecture of Aspinwall et al. [4], which (adapted to the present context) says:

Conjecture B ([4], Conjecture 5)**.** *Loops in our near large radius curve (Figure 2 (R)) about a point in ∇_Γ should correspond to twists about a spherical functor with source category $D^b(Z_\Gamma)$*

Remark 2.10. The physical intuition behind this (see [4] for much more detail) is that the FIPS is closely related to the space of central charges of D-branes. As such, when we approach a point in ∇_Γ, certain D-branes become "massless". These massless D-branes should form a well-defined category independent of the point in ∇_Γ – this is the category $D^b(Z_\Gamma)$ in the conjecture.

Then, if we take a stable object in $D^b(X)$ and vary its central charge around a point of ∇_Γ, massless objects in $D^b(Z_\Gamma)$ can destabilise it. To form a new stable object from the old one, we can combine it with the massless objects which destabilise it. This should give rise to an auto-equivalence of $D^b(X)$ which is what the twist about a spherical functor in the conjecture is supposed to represent.

It turns out that the minimal phases in the SODs above are actually Higgs phases and so it seems like the correct SODs to use as far as Conjecture B is concerned are the ones coming from VGIT as above.

However, if this were true, then we would expect that such SODs always exist and that the number of factors in these SODs should be independent of the extra data of the paths needed to define them. We show that such a Jordan-Hölder property holds for these SODs:

Theorem D (Theorem 10.4)**.** *Any appropriate set of paths in $L^\vee_{\mathbb{R}}$ starting at Z'_λ gives rise to full embeddings $i_{\Gamma,j} : D^b(Z_\Gamma) \to D^b(Z'_\lambda)$ (for some collection of faces Γ and $j = 1, \dots, n_{\Gamma,W}$) and an SOD of $D^b(Z'_\lambda)$ into these pieces. Moreover, the Γ which occur and the number $n_{\Gamma,W}$ are independent of the particular choice of paths.*

Remark 2.11. The W-dependence in $n_{\Gamma,W}$ comes from the W-dependence of Z'_λ.

The first part of this theorem is standard (see [6]). Our contribution is the second part.

If we let $m_{\Gamma,W}$ be the intersection multiplicity of ∇_Γ with the curve $Z(W)$, then, since there are $m_{\Gamma,W}$ points of ∇_Γ in the curve in Figure 2 (R), Conjecture B naturally leads us to predict:

Conjecture C (Conjecture 10.15)**.** *The number $n_{\Gamma,W}$ of embeddings of $D^b(Z_\Gamma)$ in Theorem D agrees with the intersection multiplicity $m_{\Gamma,W}$*

If this holds, we may pick any SOD $D^b(Z'_\lambda) = \langle \mathcal{A}_1, \dots \mathcal{A}_j, \dots \rangle$ from Theorem D and a basis $\{\gamma_j\}$ for the fundamental group $\pi_1(D)$ (where D is the disk in Figure 2 (R)) such that, if $\mathcal{A}_j$ is associated with Γ then γ_j loops around a puncture in D at a point of ∇_Γ. Then there is a natural spherical functor from $\mathcal{A}_j$ to $D^b(X)$ (see Remark 4.17) and we can define $\rho^W(\gamma_j)$ to be its twist. This at least gives a conjectural action which is consistent with Conjecture B.

Remark 2.12. Even if this conjecture holds, it not clear that any SOD can be found such that ρ^W extends to an action of the whole near large radius groupoid. The main difficulty is that we have no general way of understanding what the monodromy is.

3. Discriminants and the FIPS

In this section, we introduce some necessary background (largely following [20], Ch. 9 and 10) on principal A-determinants, the FIPS, secondary fans/polytopes/stacks and Horn uniformisation.

3.1. **The discriminant and the FIPS.** Abusing notation, let $A = \{\omega_j\} \subset N$ be the (numbered) set of rays of our VGIT. In this section, we only consider Calabi–Yau torus representations – that is, where the torus $T_L := L \otimes \mathbb{C}^*$ acts on $\mathbb{C}^n$ through SL_n. This allows us to find a height 1 affine hyperplane H – that is, of the form

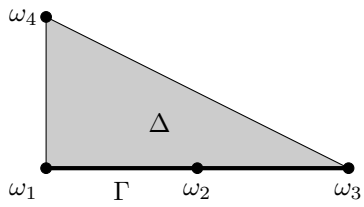

FIGURE 3. Δ is a redundant face of Δ but Γ is a minimal face

$\langle m, - \rangle = 1$ for some primitive $m \in M$ – on which all the rays ω_j lie. So we can equivalently think of A as a subset of the polytope $\Delta := \sigma \cap H$, where $\sigma \subset N_{\mathbb{R}}$ is the cone generated by all the rays. Since we always assume that the ray map A is surjective, $A \subset \Delta$ affinely generates $H \cap N$, which is a technical assumption needed for the results in [20] to hold.

Identifying elements $\omega \in N = M^\vee$ with characters x^ω of T_M, we may consider:

Definition 3.1. $\mathbb{C}^A := \{f(x) = \sum_{\omega \in A} a_\omega x^\omega\} \cong (\mathbb{C}^n)^\vee$ is the set of functions on T_M with exponents in A.

Definition 3.2. ([20], Ch. 9, Definition 1.2) Set

$$\nabla_0 := \{f(x) = \{a_\omega\}_{\omega \in A} \in \mathbb{C}^A \mid f \text{ has a critical point in } T_M\}$$

and $\nabla_A := \bar{\nabla}_0 \subset \mathbb{C}^A$. When ∇_A is a hypersurface, its defining equation is called the *A-discriminant* $\Delta_A(\{a_\omega\}_{\omega \in A})$. Otherwise we declare $\Delta_A = 1$.

If we pick a face Γ of Δ, then we can consider the set ∇_0 of functions in $\mathbb{C}^{A \cap \Gamma}$ with a critical point in T_{M_Γ} where $M_\Gamma := (\mathbb{R}\langle\Gamma\rangle \cap N)^\vee$. Exactly as in Definition 3.2, we define $\nabla_{A\cap\Gamma} = \bar{\nabla}_0 \subset \mathbb{C}^{A\cap\Gamma}$ and $\Delta_{A\cap\Gamma}$ to be the defining equation of $\nabla_{A\cap\Gamma}$ when this is a hypersurface (and 1 otherwise). In fact, for the purposes of defining the discriminant we mainly care about *minimal* faces.

Definition 3.3. For a face $\Gamma \subset \Delta$, we define the lattice L_Γ to be the lattice of relations between rays on Γ. We call the face Γ *minimal* if L_Γ is non-zero and, for every ray ω_i in Γ, there is some non-trivial relation $l \in L_\Gamma$ which involves ω_i. Non-minimal faces are called *redundant* (see [4], 3.2.2)

Remark 3.4. We can interpret this condition dually in terms of weights. Namely, Γ is minimal precisely when the VGIT associated to the rays on Γ (see §3.5) has no zero weights.

Since zero weights correspond to just adding a factor of $\mathbb{C}$ to the VGIT description, the VGIT associated to a redundant face is just the VGIT associated to a minimal face times $\mathbb{C}^k$ for some $k > 0$.

In fact, redundant faces which are not vertices (such as Δ in Figure 3) have $\Delta_{A\cap\Gamma} = 1$ since $\nabla_{A\cap\Gamma}$ has codimension greater than 1.

Example 3.5. We take A to be the four points in Δ in Figure 3, namely:

$$\omega_1 = (0,0,1), \quad \omega_2 = (1,0,1), \quad \omega_3 = (2,0,1), \quad \omega_4 = (0,1,1)$$

Then ∇_A is defined as the closure of those (a_1, a_2, a_3, a_4) such that $f(x, y, z) = z(a_1 + a_2x + a_3x^2 + a_4y)$ has a critical point in $(\mathbb{C}^*)^3$.

Explicitly, this says that there is such an (x, y, z) obeying:

$$z(a_2 + 2a_3x) = 0, \quad a_4z = 0, \quad a_1 + a_2x + a_3x^2 + a_4y = 0$$

As such, this is equivalent to $a_4 = 0$ and $a_1 + a_2x + a_3x^2$ having a multiple root. Thus $\nabla_A = \{a_4 = 0 = a_2^2 - 4a_1a_3\}$ and this has codimension 2 (so $\Delta_A = 1$). We note however that $\nabla_{A\cap\Gamma} = \{a_2^2 = 4a_1a_3\}$ (where Γ is the minimal face shown in Figure 3) has codimension 1 so $\Delta_{A\cap\Gamma} \neq 1$ is still interesting in this example.

Definition 3.6. The *principal A-determinant* $E_A(\{a_\omega\}_{\omega\in A}) := \prod_{\Gamma\subset\Delta} \Delta_{A\cap\Gamma}^{m_\Gamma} \in \mathcal{O}_{\mathbb{C}^A}(\mathbb{C}^A)$

Remark 3.7. Here the product is over all non-empty faces Γ of Δ (including Δ itself). By the preceding discussion about minimal faces, it's equivalent to take the product over all the vertices and minimal faces. The multiplicity $m_\Gamma \in \mathbb{Z}_{>0}$ is defined in [20], Ch. 10, 1.B but we will not need it in this thesis. Finally we interpret $\Delta_{A\cap\Gamma}$ as a function on $\mathbb{C}^A$ by pulling-back under the natural projection $p : \mathbb{C}^A \twoheadrightarrow \mathbb{C}^{A\cap\Gamma}$ induced by the inclusion $A \cap \Gamma \subset A$ and define $\nabla_\Gamma := p^*(\nabla_{A\cap\Gamma})$.

Remark 3.8. We can motivate E_A from the perspective of toric geometry as follows. Let $S_A \subset N$ be the semigroup generated by A and 0, and let $Y_A := \mathrm{Spec}(\mathbb{C}[S_A])$. Then $T_M \subset Y_A$ and we can consider $\mathbb{C}^A$ as functions on Y_A. At least when Y_A is smooth away from its torus fixed point, this allows us to define ∇_A alternatively in terms of the locus of $f \in \mathbb{C}^A$ where the twisted de Rham complex $(\Omega^\bullet_{Y_A}, \wedge df)$ fails to be exact (see [20], Ch. 10, Theorem 2.6 for details).

If instead we let D be the union of the toric divisors in Y_A and consider the locus where the *logarithmic* de Rham complex $(\Omega^\bullet_{Y_A}(\log D), \wedge df)$ ([20], Ch. 10, §2.A) fails to be exact, we arrive at Gelfand, Kapranov, and Zelevinsky's definition of the *principal A-determinant* E_A (c.f. [20], Ch. 10, Proposition 2.4). By [20], Ch. 10, Theorem 1.2, our definition of E_A is equal (up to a sign) to GKZ's definition.

We are now in a position to be able to define the FIPS based on [18], §4.1. Recall that T_M acts on $\mathbb{C}^A \cong (\mathbb{C}^n)^\vee$ via the dual short exact sequence from (1). Since ∇_A and $\{E_A = 0\}$ are invariant under T_M ([20], Ch. 9, 3.B), they descend to give divisors on the quotient stack $[\mathbb{C}^A/T_M]$. Abusing notation, we denote these divisors in the quotient stack by the same symbols.

Definition 3.9. The *FIPS* of the VGIT associated to A is $[\mathbb{C}^A \setminus \{E_A = 0\}/T_M]$. The *discriminant* (locus) is $\{E_A = 0\} \subset [\mathbb{C}^A/T_M]$.

Remark 3.10. With our definition of the discriminant locus and recalling the notation from Remark 3.7, we see that $\Delta_{A\cap\Gamma} \neq 1$ precisely when $\mathrm{codim}_{\mathbb{C}^{A\cap\Gamma}}(\nabla_{A\cap\Gamma}) = 1$. As such, ∇_Γ only appears in the discriminant when $\mathrm{codim}_{\mathbb{C}^A}(\nabla_\Gamma) = 1$ and so the

(reduced) discriminant locus is:

$$\bigcup_{\Gamma\subset\Delta|\mathrm{codim}_{\mathbb{C}^A}(\nabla_\Gamma)=1} \nabla_\Gamma$$

One might expect that $\bigcup_{\Gamma\subset\Delta}\nabla_\Gamma$ is a more natural definition but it is not clear to us whether this agrees with our definition. Namely, can there be points outside of the discriminant locus which nonetheless lie in ∇_Γ for some face Γ?

For later use, we name certain components of the discriminant as follows:

Definition 3.11. The *principal discriminant* of the VGIT associated to A is $\nabla_{pr} := \nabla_A$. When it is a hypersurface, we call it the *principal component* of the discriminant locus.

The components of the discriminant locus which are toric divisors are called the *toric* parts of the discriminant.

3.2. **The secondary fan and phases of the VGIT.** We recall that for any (not necessarily Calabi–Yau) toric VGIT, the space of (real) characters $L^\vee_{\mathbb{R}}$ of the torus T_L carries a natural fan structure (see [17], 3.4) – the so-called *secondary fan* – coming from the different possible GIT quotients of $\mathbb{C}^n$ by T_L. We introduce this here for a general linear toric VGIT.

Definition 3.12. Two characters β_1 and β_2 in $L^\vee$ are called *GIT equivalent* if the semistable loci $(\mathbb{C}^n)^{ss}_{\beta_1} = (\mathbb{C}^n)^{ss}_{\beta_2}$.

Definition/Theorem 3.13 ([14], §14.4)**.** The GIT equivalence classes of characters define a fan in $L^\vee_{\mathbb{R}}$ called the *secondary fan* whose rays include those generated by the non-zero weights β_i and whose support is the cone generated by all the weights. A *wall* of the secondary fan is a cone of codimension 1 and a *chamber* is a connected component of the complement of all the walls.

Remark 3.14. In the Calabi–Yau case, the weights sum to 0 and so the cone generated by the weights equals $L^\vee_{\mathbb{R}}$. Hence, for Calabi–Yau VGITs, the support of the secondary fan is $L^\vee_{\mathbb{R}}$.

Remark 3.15. In the setting of linear toric VGITs, there are several algorithms that can be used to calculate the secondary fan. One such algorithm is based on "generic characters" (see [14], Proposition 14.4.9). This particular algorithm makes clear that, if $\mathrm{Rk}(L^\vee) \leq 2$, every ray of the secondary fan has at least one weight on it. If the VGIT is also Calabi–Yau, the secondary fan is the unique fan with rays generated by the weights and with support $L^\vee_{\mathbb{R}}$ (see Remark 3.14).

Now that we understand the secondary fan, we introduce the dual notion of a secondary polytope.

Definition 3.16. A *secondary polytope* is any polyhedron in $L_{\mathbb{R}}$ whose normal fan is the secondary fan. If we start with a set of rays $A \subset N$, we denote any corresponding secondary polytope by $\Sigma(A)$.

Remark 3.17. For a non-Calabi–Yau VGIT, the secondary polytope need not be bounded (and so not really a polytope). However, by Remark 3.14, in the Calabi–Yau case $\Sigma(A)$ is actually a polytope.

In the Calabi–Yau case, we can link the principal A-determinant E_A (see Definition 3.6) with secondary polytopes by the following:

Theorem 3.18 ([20], Ch. 10, Theorem 1.4)**.** *The Newton polytope of E_A is a secondary polytope.*

Remark 3.19. In [20] (Ch. 7, Definition 1.6), the authors define *the* secondary polytope $\Sigma(A)$ in the Calabi–Yau case. It follows from Theorem 3.18 that their secondary polytope (which equals the Newton polytope of E_A) is a secondary polytope according to Definition 3.16. Our weaker combinatorial notion of secondary polytope will be sufficient for our purposes in this thesis.

It is clear from our definition of the secondary fan that it parametrises the possible GIT quotients in our VGIT and this allows us, in particular, to define *phases* of the VGIT.

Definition 3.20. For $\beta \in L^\vee$, the GIT quotient X_β is the Artin quotient stack $[(\mathbb{C}^n)^{ss}_\beta / T_L]$.

It follows immediately from the definition that any two GIT quotients whose polarisations lie in the same chamber C of the secondary fan are identical. As in §1, we define:

Definition 3.21. A *phase* X_C of the VGIT associated to the chamber C is X_β for any $\beta \in C \cap L^\vee$.

This is a smooth DM stack as there are no strictly semistable points for these quotients (see [14], Theorem 14.3.14).

If we prefer, we can think about the phases of the VGIT in terms of fans as follows. First, we recall:

Definition 3.22 ([16], Definition A.1)**.** A *stacky fan* $\mathbf{\Sigma}$ is the data $(\Lambda_1,\ \Lambda_2,\ \beta,\ \Sigma)$ where:

- Λ_2 is a finitely generated abelian group
- Λ_1 is a lattice and Σ is a fan in $(\Lambda_1)_\mathbb{R}$
- $\beta : \Lambda_1 \to \Lambda_2$ is a homomorphism with finite cokernel

By [20], Ch. 7, §2, the chamber C determines a quasi-projective simplicial – that is, all the cones are cones over simplices – fan $\Sigma_C \subset N_\mathbb{R}$ with support $\sigma = \mathrm{Cone}(\{\omega_i\})$, whose rays form a subset of the original rays $\{\omega_i\}$. Moreover, every such fan occurs for some chamber C. Then the phase X_C is the toric stack with stacky fan $(\mathbb{Z}^m, N, A|_{\mathbb{Z}^m}, \Sigma'_C)$ where $\mathbb{Z}^m \subset \mathbb{Z}^n$ indexes the rays in Σ_C and the cones in Σ'_C are $\sigma_J := \mathrm{Cone}(e_j | j \in J) \subset \mathbb{R}^m$ for those subsets $J \subset \{1, \cdots, m\}$ such that $A_\mathbb{R}(\sigma_J)$ is contained in a cone in Σ_C.

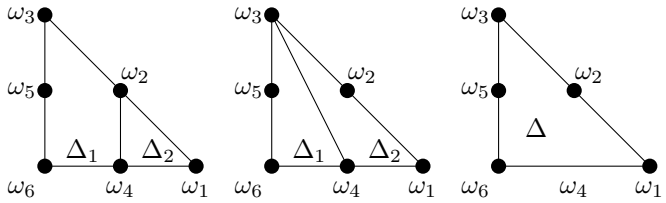

FIGURE 4. 3 polyhedral subdivisions of the triangle Δ

Remark 3.23. In the Calabi–Yau case, by slicing such fans by the height 1 hyperplane H (see the first paragraph of §3.1), we get a bijection between chambers in the secondary fan (or vertices in a secondary polytope) and (marked) "coherent" triangulations of Δ (see Definition 3.26). In this dictionary, coherence of the triangulation is equivalent to quasi-projectivity of the phase. For the precise meaning of triangulation, see Definition 3.24 below.

3.3. **Polyhedral subdivisions.** For a Calabi–Yau VGIT, we saw in Remark 3.23 that chambers of the secondary fan (or dually, vertices of a secondary polytope) corresponded to "coherent" triangulations of the polytope Δ living in the height 1 affine hyperplane $H \subset N_{\mathbb{R}}$. More generally, we'll see in Proposition 3.27 that we get a correspondence between faces of a secondary polytope and coherent *polyhedral subdivisions* of Δ.

Definition 3.24. ([20], Ch. 7, Definition 2.1) A *marked polytope* (Δ, A) is a pair where Δ is a convex polytope in the height 1 affine hyperplane H and A is a subset of $\Delta \cap N$ containing all the vertices of Δ.
A *polyhedral subdivision* of (Δ, A) is a finite number of marked polytopes (Δ_i, A_i) such that:

- $A_i \subset A$ and Δ_i is full-dimensional
- $\Delta_i \cap \Delta_j$ is a (possibly empty) face of both Δ_i and Δ_j and $A_i \cap (\Delta_i \cap \Delta_j) = A_j \cap (\Delta_i \cap \Delta_j)$
- $\bigcup_i \Delta_i = \Delta$

A *triangulation* of Δ is a polyhedral subdivision $\{(\Delta_i, A_i)\}$ of $(\Delta, \{\omega_i\})$ such that Δ_i are all simplices and A_i are the vertices of Δ_i.
The subdivision $S = \{(\Delta_i, A_i)\}$ *refines* $S' = \{(\Delta'_j, A'_j)\}$ if, for all j, the collection of (Δ_i, A_i) such that $\Delta_i \subset \Delta'_j$ forms a subdivision of (Δ'_j, A'_j).

Example 3.25. In Figure 4, we have drawn 3 polyhedral subdivisions of the triangle $\Delta = \mathrm{Conv}(\underline{0}, (2,0), (0,2))$ where A is the set of 6 points $\Delta \cap \mathbb{Z}^2$. The first and second have two pieces Δ_1 and Δ_2 and $A_i := \Delta_i \cap A$. The third has one piece $\Delta_1 = \Delta$, but A_1 is the set of five rays shown.

For other polyhedral subdivisions, see Figure 5. For all the 14 possible triangulations, see Figure 24.

We now want to define what it means for a subdivision S to be "coherent". For this, we recall that $\eta \in (\mathbb{R}^n)^\vee$ defines a convex, piecewise-affine function $\tilde{\eta}$ on Δ by

$\tilde{\eta}(q) = \min\{t \mid (q,t) \in \Delta_\eta\}$ where:

$$\Delta_\eta = \mathrm{Conv}\{(a,t) \in H \oplus \mathbb{R} \mid a \in A, t \geq \eta(a)\}$$

Definition 3.26 ([16], Definition A.10)**.** $\eta \in (\mathbb{R}^n)^\vee$ is a *defining function* for the polyhedral subdivision $S = \{(\Delta_i, A_i)\}$ if the convex, piecewise-affine function $\tilde{\eta}$ has the following properties:

- $\tilde{\eta}|_{\Delta_i}$ extends to an affine function ζ_i on H
- $\eta(a) = \zeta_i(a)$ precisely when $a \in A_i$

Moreover, if $\eta \in (\mathbb{Z}^n)^\vee$ and, for each i, ζ_i is integral with respect to the lattice $H \cap N$, we say η is an *integral* defining function. The subdivision S is called *coherent* if it has a defining function.

As mentioned above, the reason we care about such subdivisions is the following:

Proposition 3.27. *(*[20]*, Ch. 7, Theorem 2.4) Coherent polyhedral subdivisions S of $(\Delta, \{\omega_i\})$ are in bijection with faces F of a secondary polytope via $S \mapsto F(S)$, where $F(S)$ is the convex hull of all vertices corresponding to triangulations which refine S. Moreover, $F(S) \subset F(S') \iff S$ refines S'.*

Remark 3.28. We'll see in §9 that the three polyhedral subdivisions in Example 3.25 correspond to three 2-dimensional faces of a secondary polytope under this correspondence.

Remark 3.29. In §2, we mentioned how the phases of a VGIT near a toric divisor in the secondary stack were phases of simpler VGITs glued together. The above bijection now makes this precise. Namely, such a divisor corresponds to a facet in $\Sigma(A)$, which in turn corresponds to a certain polyhedral subdivision of our original VGIT. The phases near the toric divisor therefore correspond to triangulations which refine this particular subdivision. Each part (Δ_i, A_i) of this subdivision is the data for a new Calabi–Yau VGIT with fewer rays and hence is simpler. Moreover, the phases of the original VGIT near this toric divisor correspond to certain phases in each of these simpler VGITs glued together.

Remark 3.30. Following on from Remark 3.29, it is helpful to note that the phases associated to a face F of $\Sigma(A)$, which is dual to a k-dimensional cone σ, are precisely the phases of another toric VGIT. Unlike the original VGIT, this *face VGIT* associated to F is non-linear. Namely, we just replace the starting linear space $\mathbb{C}^n$ with the (non-linear) open subset $X_\sigma := (\mathbb{C}^n)^{ss}_\beta$ for any $\beta \in L^\vee$ in the relative interior of σ.

Moreover, if $L_\sigma \subset L$ denotes those 1-PS which pair trivially with σ, then, by construction of X_σ, only 1-PS in L_σ have fixed points in X_σ. As such, the secondary fan for the face VGIT is just the pull-back of the secondary fan for the T_{L_σ}-action on X_σ by the quotient map $L^\vee_{\mathbb{R}} \twoheadrightarrow L^\vee_{\mathbb{R}}/\langle\sigma\rangle$.

When $F(S)$ is an edge of $\Sigma(A)$ we can make Proposition 3.27 more explicit using the notion of circuits.

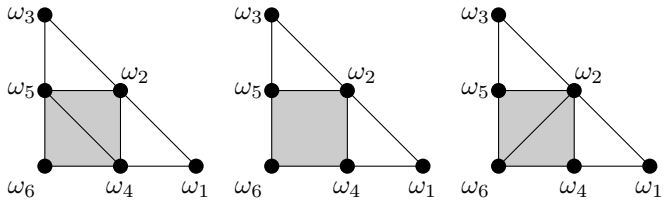

FIGURE 5. Two triangulations (L) and (R) of Δ related by an edge of $\Sigma(A)$ whose subdivision is shown in the centre

Definition 3.31. ([20], Ch. 7, Definition 1.B) A collection of rays $\{\omega_i\} \subset N$ forms a *circuit* if there is precisely one linear relation between the rays and this relation involves all the rays. A face $\Gamma \subset \Delta$ is called a *circuit* if the collection of all rays lying on Γ forms a circuit.

Then it can be shown (see [20], Ch. 7, Theorem 2.10) that the coherent polyhedral subdivisions S such that $F(S)$ is an edge of $\Sigma(A)$ correspond to certain circuits Z in A. Then two vertices of $\Sigma(A)$ are connected by $F(S)$ if the corresponding triangulations are the same outside $\mathrm{Conv}(Z)$ and inside $\mathrm{Conv}(Z)$ agree with one of the two possible triangulations of the circuit Z. Therefore the subdivision S corresponding to the circuit Z has $\mathrm{Conv}(Z)$ as one of its pieces.

Example 3.32. In Figure 5, we have drawn two triangulations of the triangle Δ from Example 3.25. The four rays $\omega_2, \omega_4, \omega_5, \omega_6$ form a circuit Z and outside $\mathrm{Conv}(Z)$ (shaded grey in the Figure) the two triangulations are identical. As such, the triangulations differ by the two possible triangulations of $\mathrm{Conv}(Z)$ and so are connected by an edge in the secondary polytope. The corresponding subdivision is shown in the middle of Figure 5. Geometrically, the birational map between the two corresponding phases is a standard flop.

We'll now turn to how the discriminant behaves when we restrict it to a face of a secondary polytope $\Sigma(A)$. So let $S = \{(\Delta_i, A_i)\}$ be a coherent subdivision and $F(S)$ be the corresponding face of $\Sigma(A)$. Since the Newton polytope of E_A is a secondary polytope (see Theorem 3.18), $E_A = \sum_{\phi \in \Sigma(A)} c_\phi \prod_{\omega \in A} a_\omega^{\phi(\omega)}$ and $F(S)$ corresponds to a collection of monomials of E_A. Therefore we can define the coefficient restriction $E_A|_{F(S)} := \sum_{\phi \in F(S)} c_\phi \prod_{\omega \in A} a_\omega^{\phi(\omega)}$. Then we have:

Theorem 3.33 ([20], Ch. 10, Theorem 1.12')**.** *$E_A|_{F(S)} = c \prod_i E_{A_i}^{m_i}$ where $\langle A_i \rangle$ is the abelian subgroup of N generated by the elements of A_i, $m_i = [N : \langle A_i \rangle]$ and c is some constant.*

Remark 3.34. This result tells us that the face $F(S)$ is built up from the secondary polytopes $\Sigma(A_i)$ of the simpler VGIT problems defined by A_i (see Remark 3.29). Specifically, it is a Minkowski sum of the $\Sigma(A_i)$.

3.4. **The secondary stack.** For a Calabi–Yau VGIT, defined by $A \subset N$ living in a height 1 affine hyperplane $H \subset N_{\mathbb{R}}$, we shall now describe how to enhance the secondary fan from §3.2 to a stacky fan, called the *stacky secondary fan*.

This stacky fan is defined by $\Lambda_2 = L^\vee$ and $\Lambda_1 = (\mathbb{Z}^{n'})^\vee$, where $e_i^\vee$ (for $i = 1, \cdots, n'$) indexes the rays ρ_i of the secondary fan and we assume that, if there are no rays with multiple weights on them, $e_i^\vee$ (for $i = 1, \cdots, n$) indexes the ray generated by β_i (see Definition 3.13). Then we may define $\tilde{\beta} : \Lambda_1 \to \Lambda_2$ by $\tilde{\beta}(e_i^\vee) = u_{\rho_i}$ where $u_{\rho_i} \in L^\vee$ is the primitive generator of ρ_i. Now a subset J of $\{1, \cdots, n'\}$ defines a cone $\sigma_J := \mathrm{Cone}(e_j^\vee | j \in J) \subset (\Lambda_1)_\mathbb{R}$. We define our fan Σ by declaring that σ_J is in Σ precisely when $\tilde{\beta}_\mathbb{R}(\sigma_J)$ is contained in a cone of the secondary fan.

Unfortunately, $\tilde{\beta}$ is not quite the right β for the stacky secondary fan. Instead, to define $\beta(e_i^\vee)$, we must consider the polyhedral subdivision S of Δ corresponding (using Proposition 3.27) to the facet of $\Sigma(A)$ dual to u_{ρ_i}. We let $c_S \in (\mathbb{Z}^n)^\vee$ be any primitive element in the $\mathbb{Z}$-linear span of the integral defining functions for S (see Definition 3.26) such that $Q(c_S) \in \rho_i$.

Example 3.35. For the 3 polyhedral subdivisions of the triangle in Figure 4 (reading left to right), we see that $e_1^\vee$, $2e_1^\vee + e_2^\vee$ and $e_4^\vee$ are integral defining functions for these subdivisions. Since they are primitive in $(\mathbb{Z}^6)^\vee$, we can choose c_S to be equal to them.

We define

$$\beta(e_i^\vee) := Q(c_S) \in L^\vee$$

With this definition, $\beta(e_i^\vee)$ is simply a positive integer multiple of $\tilde{\beta}(e_i^\vee)$.

Remark 3.36. One can check that, if the ray ρ_i of the secondary fan has a single weight – β_i say – lying on it, then $\beta(e_i^\vee) = \beta_i := Q(e_i^\vee)$. This is because we can take $c_S = e_i^\vee$ for such a subdivision.

By Remark 3.15, for a Calabi–Yau VGIT with $\mathrm{Rk}(L^\vee) \leq 2$, the secondary fan is the unique fan with rays generated by the weights and with support $L_\mathbb{R}^\vee$. As such, if this VGIT does not have multiple weights on the same ray, then it follows that $\beta = Q$. This will be the setup in the case of a 2d FIPS in §6.

Definition 3.37 ([16], Lemma A.31)**.** The *stacky secondary fan* consists of the data $((\mathbb{Z}^{n'})^\vee, L^\vee, \beta, \Sigma)$ as defined above.

Recall that, to any stacky fan $\mathbf{\Sigma}$, there is an associated toric stack (see [16], Definition A.2).

Definition 3.38. The *secondary stack* $\mathfrak{F}$ is the toric stack associated to the stacky secondary fan.

Remark 3.39. This definition of $\mathfrak{F}$ is equivalent to Definition A.28 in [16]. To see this, use [16], Lemma A.31 and note that, as we assume $A \subset N$ generates N, $K_A = 0$ and so $\Xi_A = L^\vee$.

Remark 3.40. It follows from Remark 3.14 that $\mathfrak{F}$ is proper (see [14], Theorem 3.1.19).

Remark 3.41. Instead of our definition of the FIPS (see Definition 3.9), it is perhaps more natural to define the FIPS as a complement inside $\mathfrak{F}$. To make this precise, observe that Theorem 3.18 tells us that E_A extends to a global section of a line bundle on $\mathfrak{F}$. Then we could have defined the FIPS as the complement of the zero locus of this section inside $\mathfrak{F}$.

One can show that the FIPS is an open substack of $\mathfrak{F}$ and is always a DM stack (see [18], §4.1). On the other hand, $\mathfrak{F}$ can have large isotropy groups. It follows from Remark 3.40 that $\mathfrak{F}$ is a toric compactification of the FIPS. This is one important reason why the secondary stack $\mathfrak{F}$ is such a central object in the study of the FIPS. It will sometimes be useful to think of the discriminant as living inside $\mathfrak{F}$ as opposed to $[\mathbb{C}^A/T_M]$ (see Definition 3.9).

Definition 3.42. The *discriminant* (locus) inside $\mathfrak{F}$ is the complement of the FIPS inside $\mathfrak{F}$.

If we abuse notation and let ∇_Γ also denote the closure of ∇_Γ in $\mathfrak{F}$, then the discriminant in $\mathfrak{F}$ is just the union of the components ∇_Γ for all faces Γ plus some extra toric divisors, indexed by rays of the secondary fan with no weights on them.

In fact, we can describe the toric part of the discriminant in $\mathfrak{F}$ completely. First, we note that the components ∇_{ω_i} of the discriminant in $\mathfrak{F}$ corresponding to rays ω_i which are vertices of Δ are toric as $\nabla_{\omega_i} = \{a_i = 0\}$ is in the discriminant. On the other hand, it is entirely possible to have toric divisors in the FIPS – that is, divisors which are not (wholly) in the discriminant locus. In fact, since ∇_Γ for Γ a non-vertex face of Δ is never a coordinate hyperplane in $\mathbb{C}^A$, it follows from the definition of the FIPS that divisors in the FIPS are indexed precisely by the i from 1 to n such that the ray $\omega_i \in N$ is not a vertex of Δ. The ray in the secondary fan corresponding to the toric divisor in the FIPS indexed by i is therefore the one generated by β_i.

It follows that the toric components of the discriminant in $\mathfrak{F}$ correspond to rays of the secondary fan with either no weights on or only weights corresponding to vertices of Δ. An elementary argument using the short exact sequences (1) shows that, whenever a ray in the secondary fan has multiple weights on it, all these weights must correspond to vertices of Δ. As such, the toric components of the discriminant in $\mathfrak{F}$ correspond to rays in the secondary fan with either no weights on them, 1 weight (corresponding to a vertex of Δ) or at least two weights.

We'll see in §5.1 that, if a chamber C contains in its closure a ray indexing a toric divisor in the FIPS, the phase X_C has smaller than expected Picard rank – that is, $< \mathrm{Rk}(L^\vee)$. We now consider the extreme case of this when we have an affine orbifold phase (whose Picard group is therefore finite). We'll see that *all* of the toric divisors near such a phase are in the FIPS.

The affine orbifold case: Suppose we have a linear toric VGIT with a phase (with corresponding chamber C in the secondary fan) which is an orbifold, $[\mathbb{C}^m/G]$ say

where $G \subset SL_m(\mathbb{C})$ is a finite abelian group. We'll see an explicit example of this situation with the Triangle VGIT in §9.

Then, as the fan for $[\mathbb{C}^m/G]$ consists of m linearly independent rays, Δ has to be an $(m-1)$-simplex (which we can assume has vertices $n_i e_i$ for $i = 1, \ldots, m$ for some $n_i \in \mathbb{Z}_{>0}$). It follows that G, which is the kernel of the ray map tensored with $\mathbb{C}^*$, is isomorphic to $\prod_{i=1}^m \mu_{n_i} \subset (\mathbb{C}^*)^m$. If there are n rays in Δ which are not vertices, then $\mathrm{Rk}(L^\vee) = n$. By definition, the FIPS is an open subset inside $[\mathbb{C}^{n+m}/T_M]$ (where the coordinate a_i on $\mathbb{C}^{n+m}$ corresponds to the ray ω_i in Δ).

As the toric components of the discriminant inside $[\mathbb{C}^{n+m}/T_M]$ are precisely $\{a_i = 0\}$ for i corresponding to the m vertices of Δ, in the FIPS $a_i \neq 0$ for such i and we can therefore use the T_M-action to set the m vertex coordinates to 1. For the vertex $n_i e_i$, this is ambiguous up to μ_{n_i} and hence we can describe the FIPS as the complement of the non-toric parts of the discriminant inside $[\mathbb{C}^n/G]$ where $G \subset (\mathbb{C}^*)^m$ acts by reparametrisation.

Since the non-toric parts of the discriminant avoid the torus fixed points in $\mathfrak{F}$, it follows that the torus fixed point $\underline{0} \in [\mathbb{C}^n/G]$ is in the FIPS and one checks that this corresponds to the chamber C associated with the orbifold phase. As the non-toric parts of the discriminant are not toric divisors, we see that, in the orbifold case, *all* the toric divisors near the orbifold phase are in the FIPS. This affine toric DM stack $[\mathbb{C}^n/G]$ which here partially compactifies the FIPS is a special case of the moduli stack $\mathcal{V}_A$ of full sections from [16], §A.4.

3.5. **The VGIT associated to a face.** Let Γ be a face of Δ and suppose n_Γ rays of the VGIT lie on Γ. Let $L_\Gamma \subset L$ be the lattice of relations between these rays. Then the rays in Γ define another Calabi–Yau VGIT – the VGIT on Γ – given by the exact sequence:

$$0 \to L_\Gamma \to \mathbb{Z}^{n_\Gamma} \to N_\Gamma \to 0$$

where $N_\Gamma \subset N$ is the sublattice generated by the rays in Γ.

In this section, we describe how the VGIT on Γ fits with the original VGIT. This leads naturally to the *Higgs* VGIT on Γ. We also discuss in Lemma 3.47 a handy bijection between minimal faces and certain subspaces in $L^\vee_{\mathbb{R}}$, which will be used in the proof of Proposition 8.14.

We begin by noting that the exact sequence defining the VGIT on Γ includes into the original exact sequence (where A is surjective by assumption) to give the following commutative diagram with exact rows and columns where q has finite cokernel (here the bottom row can just be defined as the cokernel of the inclusions

above them). Note that N'_Γ can have torsion.

(2)

$$\begin{array}{ccccccccc}
 & & 0 & & 0 & & 0 & & \\
 & & \downarrow & & \downarrow & & \downarrow & & \\
0 & \longrightarrow & L_\Gamma & \longrightarrow & \mathbb{Z}^{n_\Gamma} & \longrightarrow & N_\Gamma & \longrightarrow & 0 \\
 & & \downarrow & & \downarrow & & \downarrow{\scriptstyle i} & & \\
0 & \longrightarrow & L & \longrightarrow & \mathbb{Z}^{n} & \xrightarrow{A} & N & \longrightarrow & 0 \\
 & & \downarrow & & \downarrow & & \downarrow{\scriptstyle r} & & \\
0 & \longrightarrow & L'_\Gamma & \longrightarrow & \mathbb{Z}^{n-n_\Gamma} & \xrightarrow{q} & N'_\Gamma & & \\
 & & \downarrow & & \downarrow & & \downarrow & & \\
 & & 0 & & 0 & & 0 & &
\end{array}$$

If we want to think in terms of weights, we need to dualise this diagram. Setting $M_\Gamma \coloneqq N_\Gamma^\vee = \mathrm{Hom}(N_\Gamma, \mathbb{Z}), M'_\Gamma \coloneqq (N'_\Gamma)^\vee$ and noting that L, L_Γ and L'_Γ are all lattices, we get the following commutative diagram with exact rows and columns where Q_2 and $i^\vee$ have finite cokernel:

(3)

$$\begin{array}{ccccccccc}
 & & 0 & & 0 & & 0 & & \\
 & & \downarrow & & \downarrow & & \downarrow & & \\
0 & \longrightarrow & M'_\Gamma & \xrightarrow{j} & (\mathbb{Z}^{n-n_\Gamma})^\vee & \xrightarrow{Q_2} & (L'_\Gamma)^\vee & & \\
 & & \downarrow & & \downarrow & & \downarrow & & \\
0 & \longrightarrow & M & \longrightarrow & (\mathbb{Z}^{n})^\vee & \xrightarrow{Q} & L^\vee & \longrightarrow & 0 \\
 & & \downarrow{\scriptstyle i^\vee} & & \downarrow & & \downarrow{\scriptstyle p} & & \\
0 & \longrightarrow & M_\Gamma & \longrightarrow & (\mathbb{Z}^{n_\Gamma})^\vee & \xrightarrow{Q_1} & L_\Gamma^\vee & \longrightarrow & 0 \\
 & & & & \downarrow & & \downarrow & & \\
 & & & & 0 & & 0 & &
\end{array}$$

Borrowing our terminology from the physics' literature (see [4]), we define:

Definition 3.43. The *Higgs VGIT* on a face Γ is the VGIT with weights Q_2

Remark 3.44. As remarked in §2, the Higgs VGIT on Γ is "complementary" to the VGIT on Γ in the sense that it uses only the complementary set of weights. These correspond to rays ω_i not lying on Γ.

It follows from (3) that $\mathrm{Im}(Q_2)$ is the (co-finite) sub-lattice of $(L'_\Gamma)^\vee$ generated by the complementary weights. As such, $(L'_\Gamma)^\vee_{\mathbb{R}}$ is the linear subspace spanned by the complementary weights.

Remark 3.45. It is important to note that, unlike the VGIT on Γ, the Higgs VGIT on Γ is *not* necessarily Calabi–Yau. In particular, some phases may not be minimal – that is, their canonical divisor may not be nef. We shall explore this much more in §10.

Remark 3.46. The definition of the Higgs VGIT on Γ did not use the fact that Γ lives in the height 1 slice H or is a face of Δ. So more generally, if we have any linear toric VGIT and Γ is a linear subspace in $N_{\mathbb{R}}$ spanned by the rays on it, then we can define the Higgs VGIT as above.

When Γ is a minimal face, the corresponding subspace $(L'_\Gamma)^\vee_{\mathbb{R}} \subset L^\vee_{\mathbb{R}}$ of complementary weights has some special properties which we'll now see characterise it completely.

Lemma 3.47. *The map $\Gamma \mapsto (L'_\Gamma)^\vee_{\mathbb{R}}$ gives a bijection between:*

$$\left\{ \begin{array}{l} \textit{Minimal} \\ \textit{faces of } \Delta \end{array} \right\} \leftrightarrow \left\{ \begin{array}{l} \textit{Proper subspaces of } L^\vee_{\mathbb{R}} \textit{ spanned by the weights lying on} \\ \textit{them and with a positive relation between all these weights} \end{array} \right\}$$

Remark 3.48. Here by a *proper* subspace we mean a subspace that is not all of $L^\vee_{\mathbb{R}}$. A *positive* relation is a relation $\sum a_j \beta_j = 0$ where all $a_j \in \mathbb{Z}_{>0}$.

Proof. We first check that $(L'_\Gamma)^\vee_{\mathbb{R}}$ has these properties. Certainly $(L'_\Gamma)^\vee_{\mathbb{R}} = \ker p_{\mathbb{R}}$ (see (3)) is proper as $L_\Gamma \neq 0$ by minimality of Γ. Note that Remark 3.4 tells us that if Γ is minimal, then Q_1 has no zero weights. By (3), this is the same as saying that the only weights which lie on $(L'_\Gamma)^\vee_{\mathbb{R}}$ are complementary weights. Moreover, by the top row of (3), $(L'_\Gamma)^\vee_{\mathbb{R}}$ is spanned by the complementary weights and hence by all the weights lying on it. Since Γ is a face, there is $m \in M'_\Gamma$ such that $m(r(\omega_i)) > 0$ for all ω_i not lying on Γ. As such, $Q_2 \circ j(m)$ gives a positive relation between all the complementary weights and hence all the weights on $(L'_\Gamma)^\vee_{\mathbb{R}}$.

For injectivity, since Γ is minimal, the weights lying on $(L'_\Gamma)^\vee_{\mathbb{R}}$ are precisely the complementary weights. As such, if we know $(L'_\Gamma)^\vee_{\mathbb{R}}$ then we can recover the set of complementary weights and hence the set of rays on Γ. Taking the affine span of the corresponding ω_i in Δ recovers Γ so this map is injective.

For surjectivity, take a proper subspace H of $L^\vee_{\mathbb{R}}$ with the properties above. Then set $(L'_\Gamma)^\vee := H \cap L^\vee$ and let $Q_2 : (\mathbb{Z}^{n'})^\vee \to (L'_\Gamma)^\vee$ be the set of all weights lying on H. Then Q_2 has only finite cokernel and we set $M'_\Gamma := \ker Q_2$. Embedding this into the short exact sequences of weights on $L^\vee$ and taking the cokernel gives a commutative diagram of abelian groups similar to (3) which is exact everywhere apart from possibly the bottom left and top right corners and here the kernels and cokernels are finite. By definition of Q_2, the basis vectors in $(\mathbb{Z}^{n'})^\vee$ index all weights in $(L'_\Gamma)^\vee_{\mathbb{R}}$. As such, the map $Q_1 : (\mathbb{Z}^{n-n'})^\vee \to L^\vee_\Gamma$ has no zero weights.

Dualising this square over $\mathbb{R}$ gives a subspace $(N_\Gamma)_{\mathbb{R}} \subset N_{\mathbb{R}}$ which is generated by the rays indexed by basis vectors in $\mathbb{Z}^{n-n'}$. Intersecting $(N_\Gamma)_{\mathbb{R}}$ with Δ gives a slice $\Gamma \subset \Delta$. Since there is a positive relation between all the weights lying on $(L'_\Gamma)^\vee$, by the short exact sequence involving Q_2, this relation is of the form $Q_2 \circ j(m)$ for some $m \in M'_\Gamma$ such that $j(m) \in \mathbb{N}^{n'}$. Viewing m as a function on $N_{\mathbb{R}}$ which vanishes on Γ and is positive on all the rays indexed by $\mathbb{Z}^{n'}$ shows that Γ is in fact a face of Δ and $\mathbb{Z}^{n'} \to N'_\Gamma$ has no zero weights. Moreover, by Remark 3.4, as Q_1 has no zero weights, Γ is a minimal face.

Finally we need to check that H agrees with $(L'_\Gamma)^\vee_\mathbb{R}$ for this face Γ. Since we constructed the VGIT on Γ by taking *all* the rays on Γ, this follows from the fact that $\mathbb{Z}^{n'} \to N'_\Gamma$ has no zero weights – that is, the rays indexed by $\mathbb{Z}^{n-n'}$ are the only rays on Γ. □

Remark 3.49. We note that, amongst all proper subspaces $H \subset L^\vee_\mathbb{R}$ spanned by the weights lying on them (which here we call β_j for $j = 1, \cdots, k$) , those with a positive relation between all the weights can be characterised by $\mathrm{Cone}(\{\beta_j\}) = H$. To see this, note that if $\sum a_j\beta_j = 0$ is a positive relation (so a_j are all positive integers) then, for any i, $-a_i\beta_i = \sum_{j\neq i} a_j\beta_j$. So $-\beta_i \in \mathrm{Cone}(\{\beta_j\})$ for all i. Since the β_i span H, this gives that $\mathrm{Cone}(\{\beta_j\}) = H$. Conversely, if $\mathrm{Cone}(\{\beta_j\}) = H$, then, for any i, $-\beta_i = \sum a_j\beta_j$ where $a_j \geq 0$ are rational. Rearranging this tells us that, for any i, we have a relation $\sum a_j\beta_j = 0$ where $a_j \geq 0$ and $a_i = 1$. Summing these together for all i gives the desired positive relation between all the weights on H.

Using this characterisation, we observe that the subspaces from Lemma 3.47 necessarily have $-\sum_{j|\beta_j\in H} \beta_j \in \mathrm{Cone}(\{\beta_j\})$. By Theorem 3.13, this means that the canonical divisor of the Higgs VGIT lies in the support of its secondary fan and hence the Higgs phase is non-empty.

Remark 3.50. We observe that a polyhedral subdivision of (Δ, A) induces a polyhedral subdivision of $(\Gamma, A\cap\Gamma)$ for any face Γ of Δ. Moreover, from the description of the secondary fan in Remark 3.15 and the diagram (3), it follows that the natural quotient map $p : L^\vee \to L^\vee_\Gamma$ from (3) is actually a map of stacky secondary fans.

Remark 3.7 tells us that $\nabla_\Gamma \cap T_{L^\vee}$ is the pullback of $\nabla_{A\cap\Gamma} \cap T_{L^\vee_\Gamma}$ under $p \otimes \mathbb{C}^*$. Then it follows that $\nabla_\Gamma \subset \mathfrak{F}$ is actually the pullback of $\nabla_{A\cap\Gamma}$ from the secondary stack of the VGIT on Γ.

3.6. **Horn uniformisation.** First we recall ([20], Ch. 9, §3A) that the *logarithmic Gauss map* $\gamma_Z : Z \dashrightarrow \mathbb{P}^{m-1}$ of an irreducible hypersurface $Z \subset (\mathbb{C}^*)^m$ is the rational map taking a smooth point $z \in Z$ to $dl_z^{-1}(T_z Z)$ where l_z is multiplication by z in $(\mathbb{C}^*)^m$. Then we have:

Definition/Theorem 3.51. ([20], Ch. 9, 3.C) The *Horn uniformisation* is the rational map with image ∇_{pr} given by:

$$\mathbb{P}(L_\mathbb{C}) \dashrightarrow \nabla_{pr} \subset T_{L^\vee} = \mathrm{Hom}(L, \mathbb{C}^*)$$

$$\lambda \mapsto (l \mapsto \prod_{i=1}^{n} \langle\beta_i, \lambda\rangle^{\langle\beta_i, l\rangle})$$

In the case when ∇_{pr} is a hypersurface, this is a *birational* map with inverse given by $\gamma_{\nabla_{pr}}$.

If we pick a basis for L and corresponding coordinates $\lambda_1, \cdots, \lambda_k$ on $L_\mathbb{C}$, then (identifying $T_{L^\vee} \cong (\mathbb{C}^*)^k$) we may rewrite the Horn uniformisation as:

$$\mathbb{P}^{k-1} \dashrightarrow \nabla_{pr} \subset (\mathbb{C}^*)^k$$

$$[\lambda_1, \cdots, \lambda_k] \mapsto (\prod_{j=1}^{n} (\lambda_1 \beta_{j1} + \cdots + \lambda_k \beta_{jk})^{\beta_{ji}})_{i=1,\cdots,k} \tag{4}$$

where β_{ji} are the components of the weights $\beta_j \in L^\vee \cong \mathbb{Z}^k$ in the dual basis.

4. Windows

We now briefly recall the theory of grade restriction windows in the context of toric VGIT with $T_L \circlearrowright \mathbb{C}^n$. For more details, we refer the reader to Ballard–Favero–Katzarkov [6] and Halpern-Leistner [22]. Here we mainly follow the exposition and notation given in Halpern-Leistner–Shipman [25], §2.

Recalling Definition 3.20, we see that all GIT quotients X_β in the toric VGIT are open substacks inside the Artin stack $X_0 = [\mathbb{C}^n / T_L]$ and we denote the inclusions by i. Kempf and Ness showed how to equivariantly stratify the unstable locus – nowadays this is called the *Kempf-Ness stratification* – by locally-closed substacks $Y_{\lambda_i} \subset X_0$ called "blades". As such, $X_\beta = X_0 \backslash (\bigcup_{i=1}^k Y_{\lambda_i})$. These blades are indexed by $\lambda_i \in L$ for $i = 1, \cdots, k$ which are an ordered list of "destabilising 1-PS" determined by the choice of $\beta \in L^\vee$ (see the above references for details).

Definition 4.1. To any 1-PS λ, the *blade* $Y_\lambda := \{x \in X_0 | \lim_{t\to 0}(\lambda(t).x) \text{ exists in } X_0\}$.

Remark 4.2. If the group acting were not abelian, we would need to run the above procedure on a maximal torus and then take the G-orbits of the blades Y_λ.

Definition 4.3. For $\lambda \in L$, we let $Z^\lambda := [(\mathbb{C}^n)^\lambda / T_L] \subset X_0$ be the Artin quotient stack of the λ-fixed locus $(\mathbb{C}^n)^\lambda$ inside $\mathbb{C}^n$ by T_L and $Z'^\lambda := [(\mathbb{C}^n)^\lambda / (T_L/\mathrm{Im}(\lambda))]$ be the Artin quotient stack of the same locus by $T_L/\mathrm{Im}(\lambda)$, which still acts as λ acts trivially on $(\mathbb{C}^n)^\lambda$.

Definition 4.4. $D^b(Z^\lambda)_w$ is the full subcategory of $D^b(Z^\lambda)$ comprising of objects with λ-weight w. For $F^\bullet \in D^b(Z^\lambda)$, $(F^\bullet)_w$ denotes the λ-weight w summand of $F^\bullet$.

The blade and fixed locus fit into the following diagram, where i is the inclusion and $\pi(x) = \lim_{t\to 0}(\lambda(t).x)$.

$$\begin{array}{ccc} Y_\lambda & \xhookrightarrow{i} & X_0 \\ \downarrow{\scriptstyle \pi} & & \\ Z^\lambda & & \end{array}$$

As X_0 is smooth, π is then a locally trivial bundle of affine spaces over Z^λ.

Definition 4.5. Given a 1-PS $\lambda \in L$, we define $\kappa_\lambda := \det(N_{Y_\lambda/\mathbb{C}^n}) \in \mathrm{Pic}(Y_\lambda)$ and $\eta_\lambda := \mathrm{wt}_\lambda(\kappa_\lambda^\vee|_{Z^\lambda}) \in \mathbb{Z}$

With these definitions, one can show:

Lemma 4.6. *([22], Corollary 3.28) $i_{\lambda,w} := i_* \circ \pi^* : D^b(Z^\lambda)_w \to D^b(X_0)$ is fully faithful. Its left adjoint $i^L_{\lambda,w}(F^\bullet) = (F^\bullet|_{Z^\lambda})_w$ and its right adjoint $i^R_{\lambda,w}(F^\bullet) = (F^\bullet|_{Z^\lambda} \otimes \kappa_\lambda|_{Z^\lambda})_w$.*

Here, as always, $|_{Z^\lambda}$ is *derived* restriction to Z^λ and we note that $i_{\lambda,w}$ and $i_{\lambda^{-1},-w}$ are different functors, despite their source category being the same. When λ is obvious from the context, we abbreviate $i_{\lambda,w}$ to i_w.

Definition 4.7. The image of $i_{\lambda,w}$ is denoted by $A^\lambda_w \subset D^b(X_0)$. If $\mathcal{A} \subset D^b(Z^\lambda)_w$ is a full subcategory, $\mathcal{A}^\lambda_w \subset D^b(X_0)$ denotes its image under $i_{\lambda,w}$.

Definition 4.8. The *grade restriction window* $W_\lambda(w) \subset D^b(X_0)$ defined by a 1-PS $\lambda \in L$ and $w \in \mathbb{Z}$ is the full subcategory with objects $F^\bullet$ such that, for all i, $\mathrm{wt}_\lambda(\mathcal{H}^i(F^\bullet)|_{Z^\lambda}) \in [w, w + \eta_\lambda - 1]$. This numerical condition on $F^\bullet$ is called the *grade restriction rule* (for λ). We denote the inclusion $W_\lambda(w) \subset D^b(X_0)$ by j.

Then the foundational result of the theory of windows says:

Theorem 4.9. *([22], Theorem 2.10) Restriction $i^* \circ j : W_\lambda(w) \to D^b(X_0 \backslash Y_\lambda)$ is an equivalence of categories.*

If we want to make further deletions, we can set $X_0 := X_0 \backslash Y_\lambda$ and run the same argument again. Continuing inductively, if for each destabilising 1-PS λ_i appearing in the Kempf-Ness stratification for X_β we pick $w_i \in \mathbb{Z}$, we may define:

Definition 4.10. The full subcategory $W_{\underline{\lambda}}(\underline{w}) \subset D^b(X_0)$ (call this inclusion j) consists of objects $F^\bullet$ such that (for all $i = 1, \ldots, k$ and m) $\mathrm{wt}_{\lambda_i}(\mathcal{H}^m(F^\bullet)|_{Z^{\lambda_i} \backslash \bigcup_{l<i} Y_{\lambda_l}}) \in [w_i, w_i + \eta_{\lambda_i} - 1]$

Remark 4.11. This is a fiddly definition because we need to work with the locally closed subsets $Z^{\lambda_i} \backslash \bigcup_{l<i} Y_{\lambda_l}$. As such, a priori $W_{\underline{\lambda}}(\underline{w})$ depends on the ordering of our 1-PS λ_i. We'll see in §4.2 that magic windows (when they exist) give a much simpler description of $W_{\underline{\lambda}}(\underline{w})$ (for certain values of $\underline{w}$), which in particular shows that these categories don't depend on the ordering of the 1-PS.

Then applying Theorem 4.9 iteratively gives:

Theorem 4.12. *([22], Theorem 2.10) Restriction $i^* \circ j : W_{\underline{\lambda}}(\underline{w}) \to D^b(X_\beta)$ is an equivalence of categories.*

Remark 4.13. One can show that $i^* : D^b(X_0) \to D^b(X_\beta)$ is essentially surjective for any $\beta \in L^\vee$. Since we consider linear toric VGITs, $D^b(X_0)$ is generated by line bundles. It follows that $D^b(X_\beta)$ is generated by line bundles for all β, which makes these derived categories quite combinatorial objects.

Definition 4.14. $\mathcal{C}^\lambda_w$ is the full subcategory of $D^b(X_0)$ with objects $F^\bullet$ such that, for all i, $\mathrm{wt}_\lambda(\mathcal{H}^i(F^\bullet)|_{Z^\lambda}) \in [w, w + \eta_\lambda]$

It will be useful later to note that the inclusion $W_\lambda(w) \subset C^\lambda_w$ is admissible. In fact, we have:

Theorem 4.15. *([22], Theorem 2.10) There is a semi-orthogonal decomposition* $C_w^\lambda = \langle W_\lambda(w), A_w^\lambda \rangle = \langle A_w^\lambda, W_\lambda(w+1) \rangle$.

We now focus on crossing the wall W between two neighbouring chambers $C_\pm$, following [25], §3. Denote the two phases by X_+ and X_- and by $\lambda = \lambda_{C_-,C_+} \in L$ the primitive normal vector to W, which points towards C_-. Then we can arrange that there are the same number of destabilising 1-PS λ_i^+ for X_+ as there are λ_i^- for X_- (call this number k). Moreover we can assume that $\lambda_i^+ = \lambda_i^-$ for $i = 1, \cdots, k-1$ (call this common 1-PS λ_i) and that $\lambda_k^+ = (\lambda_k^-)^{-1} = \lambda$. If we let $X_0^\lambda = X_0 \backslash (\bigcup_{i=1}^{k-1} Y_{\lambda_i})$, then $X_\pm = X_0^\lambda \backslash Y_{\lambda^\pm}$. We denote the inclusions $X_\pm \subset X_0^\lambda$ by $i_\pm$.

The theory of windows outlined above works more generally with any smooth projective-over-affine variety in place of $\mathbb{C}^n$ and so we get windows $W_{\lambda^\pm}(w) \subset D^b(X_0^\lambda)$ for $D^b(X_\pm)$. If $\mathrm{wt}_\lambda \omega_X^\vee|_{Z^\lambda} = 0$, then one can check that $\eta_\lambda = \eta_{\lambda^{-1}}$ and, denoting this common value by η, we have that $W_\lambda(w) = W_{\lambda^{-1}}(-w-\eta+1)$. Thus it follows that:

Corollary 4.16. *([22], Proposition 4.5) Suppose* $wt_\lambda \omega_X^\vee|_{Z^\lambda} = 0$. *Then* $i_\pm^* : W_\lambda(w) \to D^b(X_\pm)$ *are both equivalences.*

Remark 4.17. If we let $Z_\lambda := Z^\lambda \cap X_0^\lambda$, we also get a fully faithful functor $i_w : D^b(Z_\lambda)_w \to D^b(X_0^\lambda)$ given by restricting the functor i_w from Lemma 4.6. Moreover, the functor $F_w := i_-^* \circ i_w : D^b(Z_\lambda)_w \to D^b(X_-)$ turns out to be spherical (see [25, 32]).

We observe that the assumption of Corollary 4.16 always holds when our VGIT is Calabi–Yau and hence we get equivalences between the derived categories of neighbouring phases.

Definition 4.18. For a Calabi–Yau VGIT, the equivalences (for any $w \in \mathbb{Z}$) $\phi_w := i_+^* \circ (i_-^*)^{-1} : D^b(X_-) \to W_{\lambda^{-1}}(-w-\eta+1) = W_\lambda(w) \to D^b(X_+)$ are called *window equivalences*.
The autoequivalences (for any $w \in \mathbb{Z}$) $\psi_w := \phi_w^{-1} \circ \phi_{w+1} : D^b(X_-) \to D^b(X_-)$ are called *window shifts*.

Since the secondary fan of a Calabi–Yau VGIT is connected (in fact, its support is $L_\mathbb{R}^\vee$), the theorem implies that all phases of a Calabi–Yau VGIT are derived equivalent via window equivalences.

Remark 4.19. The window shift ψ_w based at a phase X_- can be described more geometrically (see [25, 32]) as the twist about the spherical functor $F_w : D^b(Z_\lambda)_w \to D^b(X_-)$ from Remark 4.17.

When we're not in the Calabi–Yau setting, we don't expect to get equivalences between all the phases of our VGIT. Nonetheless, we can still use the theory of windows to describe how the derived categories of the phases on either side of a wall W differ (see [5, 6]). Suppose we pick $\lambda \in L$ to be primitive normal to W

such that $\mu_\lambda := \langle \lambda, -K\rangle \leq 0$, where $-K = \sum_i \beta_i$. We call the phase associated to the chamber C with $\langle \lambda, C\rangle \leq 0$ X_+, the other phase X_- and the quotient on the wall X_0 (this is intentionally ambiguous when $\mu_\lambda = 0$). Finally we let Z'_λ be the λ-fixed locus in X_0 (forgetting the trivial λ action).

Remark 4.20. Recall that a phase X is *minimal* if K_X is nef. So here X_- is the "more minimal" phase and X_+ is the "less minimal" phase.

The following theorem is just the extension of Corollary 4.16 to the case when $\mathrm{wt}_\lambda \omega_X^\vee|_{Z^\lambda} \neq 0$. By our choice of λ, $\eta_\lambda \geq \eta_{\lambda^{-1}}$ as $\mu_\lambda = \eta_{\lambda^{-1}} - \eta_\lambda \leq 0$. As such, $\phi_{-w-\eta_\lambda+1}$ using the window $W_{\lambda^{-1}}(w) \subset W_\lambda(-w-\eta_\lambda+1)$ for X_- still gives a full embedding.

Theorem 4.21 ([5], Theorem 3.1.4)**.** *For any $w \in \mathbb{Z}$, there are full embeddings $\phi_{-w-\eta_\lambda+1} : D^b(X_-) \to D^b(X_+)$ and $F_j : D^b(Z_{\lambda^{-1}})_j \to D^b(X_+)$ for $j = w, \dots, w-\mu_\lambda-1$ such that $\langle \mathrm{Im}\,\phi_{-w-\eta_\lambda+1}, \mathrm{Im}\,F_w, \dots, \mathrm{Im}\,F_{w-\mu_\lambda-1}\rangle$ is an SOD of $D^b(X_+)$ where $F_j = i_+^* \circ i_{\lambda^{-1},j}$ (c.f. Remark 4.17).*

Remark 4.22. This theorem follows from a mild generalisation of Theorem 4.15. Namely, if $W_\lambda(-w-\eta_\lambda+1) \subset D^b(X_0)$ is a window for $D^b(X_+)$ (of width η_λ), then there is an SOD $W_\lambda(-w-\eta_\lambda+1) = \langle W_{\lambda^{-1}}(w), A_w^{\lambda^{-1}}, \cdots, A_{w-\mu_\lambda-1}^{\lambda^{-1}}\rangle$, where $W_{\lambda^{-1}}(w)$ is a window for $D^b(X_-)$ (of width $\eta_{\lambda^{-1}}$) and $A_i^{\lambda^{-1}}$ is a copy of $D^b(Z_{\lambda^{-1}})_i$. Then Theorem 4.12 tells us that restricting from $W_\lambda(-w-\eta_\lambda+1)$ to $D^b(X_+)$ is an equivalence and restricting this SOD gives the functors and SOD described in the theorem.

From Theorem 4.15, we see that

$$R_{A_w^{\lambda^{-1}}}(W_{\lambda^{-1}}(w)) = W_{\lambda^{-1}}(w+1) = W_{\lambda^{-1}}(w) \otimes \mathcal{O}_{X_0}(\beta)$$

where β has λ^{-1}-weight 1. Restricting this to X_+ gives that $R_{\mathrm{Im}F_w}(\mathrm{Im}\phi_{-w-\eta_\lambda+1}) = \mathrm{Im}\phi_{-w-\eta_\lambda+1}(\beta)$. This property will be very useful in §6.2 where we will refer to it as the *window property* of $\mathrm{Im}\phi_{-w-\eta_\lambda+1}$.

Example 4.23. We consider the simplest case of this when X_0 is a rank 1 VGIT (so X_0 is of the form $[\mathbb{C}^n/\mathbb{C}^*]$) with no zero weights. Here λ is the primitive 1-PS pointing towards the minimal phase X_- and we denote by $\mathcal{O}(j)$ the line bundle with λ^{-1}-weight j. We observe that $\mu_\lambda = -|\sum_j \beta_j| = \eta_{\lambda^{-1}} - \eta_\lambda$. Then $Y_{\lambda^\pm} = \{x_i = 0 \mid \langle \beta_i, \lambda^\pm\rangle < 0\}$ and $X_\pm = X_0 \backslash Y_{\lambda^\pm}$ can be described geometrically as a vector bundle on a weighted projective space (which is given by $Y_{\lambda^\mp} \cap X_\pm = Y_{\lambda^\mp} \backslash \{0\}$).

Then Theorem 4.21 gives an SOD of $D^b(X_+)$ in terms of $D^b(X_-)$ and $-\mu_\lambda$ copies of $D^b(Z'_\lambda)$. As there are no zero weights, $Z'_\lambda = \underline{0}$ and so $D^b(Z_{\lambda^{-1}})_j = \langle \mathcal{O}_{Z_{\lambda^{-1}}}(j)\rangle$.

When $\mu_\lambda < 0$, it follows that $\mathrm{Im}F_j$ is generated by an exceptional object in $D^b(X_+)$, which is explicitly given by $\mathcal{O}_{Y_{\lambda^{-1}}\backslash\{0\}}(j)$. By Remark 4.13 we know

$$W_\lambda(-w-\eta_\lambda+1) = \langle \mathcal{O}_{X_0}(w), \cdots, \mathcal{O}_{X_0}(w+\eta_\lambda-1)\rangle$$

and similarly $W_{\lambda^{-1}}(w) = \langle \mathcal{O}_{X_0}(w), \cdots, \mathcal{O}_{X_0}(w+\eta_{\lambda^{-1}}-1)\rangle$.

Thus $\mathrm{Im}\phi_{-w-\eta_\lambda+1} = \langle \mathcal{O}_{X_+}(w), \cdots, \mathcal{O}_{X_+}(w+\eta_{\lambda^{-1}}-1)\rangle$ and our SOD is

$$D^b(X_+) = \langle \mathcal{O}_{X_+}(w), \cdots, \mathcal{O}_{X_+}(w+\eta_{\lambda^{-1}}-1), \mathcal{O}_{Y_{\lambda^{-1}}\backslash\{0\}}(w), \cdots, \mathcal{O}_{Y_{\lambda^{-1}}\backslash\{0\}}(w-\mu_\lambda-1)\rangle$$

4.1. **Fractional windows.** We now describe how to generalise the notion of windows to *fractional windows*, as introduced mathematically in [25]. This will give us an extra source of equivalences between neighbouring phases of our VGIT which we'll use in §6.2 to construct a (partial) fundamental group action when the FIPS is 2-dimensional.

Fix a 1-PS $\lambda \in L$, $w \in \mathbb{Z}$ and a semi-orthogonal decomposition $\langle \mathcal{A}, \mathcal{B} \rangle = D^b(Z^\lambda)_w$

Definition 4.24. The *fractional window* $F^w_\lambda(\langle \mathcal{A}, \mathcal{B} \rangle) \subset D^b(X_0)$ associated to this data is the full subcategory with objects $F^\bullet$ such that, for all i:

- $\mathrm{wt}_\lambda(\mathcal{H}^i(F^\bullet)|_{Z^\lambda}) \in [w, w+\eta]$
- $\mathrm{Hom}_{Z^\lambda}(\mathrm{wt}_w \mathcal{H}^i(F^\bullet)|_{Z^\lambda}, \mathcal{A}) = 0$
- $\mathrm{Hom}_{Z^\lambda}(\mathcal{B}, \mathrm{wt}_w(\mathcal{H}^i(F^\bullet)|_{Z^\lambda} \otimes \kappa_\lambda|_{Z^\lambda})) = 0$

This (partially numerical) condition on $F^\bullet$ is called the *fractional grade restriction rule* (for λ and $\langle \mathcal{A}, \mathcal{B} \rangle$).

Let's now consider crossing a wall between two neighbouring phases $X_\pm$. Our goal is to introduce *fractional window equivalences* in analogy to the usual window equivalences in Definition 4.18. As before, let $\lambda \in L$ be the primitive normal vector to the wall between the corresponding chambers pointing towards the X_- phase. We denote the quotient associated to the linearisation on the wall by X_0 and so $X_\pm = X_0 \backslash Y_{\lambda^\pm}$ (with the inclusion in X_0 denoted $i_\pm$).

If $\mathrm{wt}_\lambda \omega_X^\vee|_{Z^\lambda} = 0$, then $\eta_\lambda = \eta_{\lambda^{-1}}$ and so, since $F^w_\lambda(\langle \mathcal{A}, \mathcal{B} \rangle) \subset D^b(X_0)$ lives in λ-weights $[w, w+\eta]$, $F^{-w-\eta}_{\lambda^{-1}}(\langle \mathcal{C}, \mathcal{D} \rangle)$ has these same λ-weights, for any semi-orthogonal decomposition $\langle \mathcal{C}, \mathcal{D} \rangle = D^b(Z^{\lambda^{-1}})_{-w-\eta}$. When $\langle \mathcal{C}, \mathcal{D} \rangle$ is the "dual" SOD, we can do better:

Lemma 4.25. *Suppose $\omega_X^\vee|_{Z^\lambda} \cong \mathcal{O}_{Z^\lambda}$ and define $\mathcal{C}' := \mathcal{C} \otimes \kappa_\lambda^\vee|_{Z^\lambda}$. If at least one of $\mathcal{A}, \mathcal{B}$ is proper (that is, all morphisms are finite-dimensional vector spaces), then $\mathcal{B}^\vee := \mathcal{B}' \otimes \omega_{Z^\lambda}$, $\mathcal{A}^\vee = \mathcal{A}'$ gives an SOD of $D^b(Z^{\lambda^{-1}})_{-w-\eta} = D^b(Z^\lambda)_{w+\eta}$ such that $F^{-w-\eta}_{\lambda^{-1}}(\langle \mathcal{B}^\vee, \mathcal{A}^\vee \rangle) = F^w_\lambda(\langle \mathcal{A}, \mathcal{B} \rangle)$. Moreover, $i_\pm^* : F^w_\lambda(\langle \mathcal{A}, \mathcal{B} \rangle) \to D^b(X_\pm)$ are both equivalences.*

As before, in the Calabi–Yau setting, this allows us to construct equivalences.

Definition 4.26. For a Calabi–Yau VGIT, the equivalences (for any $w \in \mathbb{Z}$) $\chi_w := i_+^* \circ (i_-^*)^{-1} : D^b(X_-) \to F^{-w-\eta}_{\lambda^{-1}}(\langle \mathcal{B}^\vee, \mathcal{A}^\vee \rangle) = F^w_\lambda(\langle \mathcal{A}, \mathcal{B} \rangle) \to D^b(X_+)$ are called *fractional window equivalences.*

In the rest of this section, we recall some facts about how (fractional) windows in $D^b(X_0)$ behave under mutation. We shall use this in §6.2 (and only there) to help prove certain "monodromy relations" hold between our fractional window equivalences. Recalling the notation in Definition 4.7, we have the following extension of Theorem 4.15:

Theorem 4.27. *([25], Lemma 4.10) There is an SOD $C_w^\lambda = \langle \mathcal{A}_w^\lambda, F_\lambda^w(\langle \mathcal{A}, \mathcal{B}\rangle), \mathcal{B}_w^\lambda\rangle$ and hence $F_\lambda^w(\langle \mathcal{A}, \mathcal{B}\rangle) = R_{\mathcal{A}_w^\lambda}(W_\lambda(w)) = L_{\mathcal{B}_w^\lambda}(W_\lambda(w+1))$ (where L/R denote the left/right mutation functors respectively). Moreover, the following diagram commutes:*

$$\begin{array}{ccc} W_\lambda(w) & \xrightarrow{R_{\mathcal{A}_w^\lambda}} & F_\lambda^w(\langle \mathcal{A}, \mathcal{B}\rangle) \\ & {\scriptstyle i_+^*} \searrow \quad \swarrow {\scriptstyle i_+^*} & \\ & D^b(X_+) & \end{array}$$

More generally, if we have an SOD $D^b(Z^\lambda)_w = \langle E_1, \dots, E_n\rangle$ we can consider, for each $i = 1, \dots, n$, the subcategory $\mathcal{U}_i$ of $D^b(Z^\lambda)_w$ generated by the first i pieces of the above SOD and the subcategory $\mathcal{V}_i$ generated by the remaining pieces. These then give us fractional windows $F_\lambda^w(\langle \mathcal{U}_i, \mathcal{V}_i\rangle)$ for each i and it follows from Theorem 4.27 that:

Corollary 4.28. *The following diagram commutes:*

$$\begin{array}{ccc} F_\lambda^w(\langle \mathcal{U}_i, \mathcal{V}_i\rangle) & \xrightarrow{R_{E_{i+1}^\lambda}} & F_\lambda^w(\langle \mathcal{U}_{i+1}, \mathcal{V}_{i+1}\rangle) \\ & {\scriptstyle i_+^*} \searrow \quad \swarrow {\scriptstyle i_+^*} & \\ & D^b(X_+) & \end{array}$$

where, for notational simplicity, $E_{i+1}^\lambda := i_{\lambda,w}(E_{i+1})$.

If we consider again a wall-crossing between two neighbouring phases $X_\pm$ as before, we define $\mathcal{A}^+ := i_{\lambda,-w-\eta}(\mathcal{A})$ and $\mathcal{A}^- := i_{\lambda^{-1},w}(\mathcal{A})$. Then there is also a dual version of Corollary 4.28. Namely, if we have an SOD $D^b(Z^\lambda)_w = \langle E_1, \dots, E_n\rangle$, we can consider the (left) dual SOD $D^b(Z^\lambda)_w = \langle F_n, \dots, F_1\rangle$ where $F_i := L_{\langle E_1, \dots, E_{i-1}\rangle}(E_i)$. Note that $F_1 = E_1$ and $F_n = E_n \otimes \omega_{Z^\lambda}$. Tensoring with $\kappa_\lambda^\vee|_{Z^\lambda}$, we get an SOD $D^b(Z^{\lambda^{-1}})_{-w-\eta} = \langle F_n', \dots, F_1'\rangle$ and we call $\hat{\mathcal{U}}_i$ the subcategory of $D^b(Z^{\lambda^{-1}})_{-w-\eta}$ generated by the first i pieces of the SOD and $\hat{\mathcal{V}}_i$ the subcategory generated by the remaining pieces. Note that $\hat{\mathcal{U}}_i = \langle E_{n-i+1}', \cdots, E_n'\rangle \otimes \omega_{Z^\lambda} = \mathcal{V}_{n-i}' \otimes \omega_{Z^\lambda}$ and $\hat{\mathcal{V}}_i = \mathcal{U}_{n-i}'$. Then Lemma 4.25 gives that $F_\lambda^w(\langle \mathcal{U}_i, \mathcal{V}_i\rangle) = F_{\lambda^{-1}}^{-w-\eta}(\langle \mathcal{V}_{n-i}' \otimes \omega_{Z^\lambda}, \mathcal{U}_{n-i}'\rangle) = F_{\lambda^{-1}}^{-w-\eta}(\langle \hat{\mathcal{U}}_i, \hat{\mathcal{V}}_i\rangle)$ for all i and, from Corollary 4.28, we get:

Corollary 4.29. *The following diagram commutes:*

$$\begin{array}{ccc} F_\lambda^w(\langle \mathcal{U}_{i+1}, \mathcal{V}_{i+1}\rangle) & \xrightarrow{R_{F_{i+1}'^-}} & F_\lambda^w(\langle \mathcal{U}_i, \mathcal{V}_i\rangle) \\ & {\scriptstyle i_-^*} \searrow \quad \swarrow {\scriptstyle i_-^*} & \\ & D^b(X_-) & \end{array}$$

4.2. **Magic windows.** In this section, we define magic windows and see that they naturally lead to relations between window equivalences coming from different walls. This will be used extensively to construct our fundamental group representation for the non-quasi-symmetric examples in §7.2, §7.3 and §9. A good reference for this material is [18], §5.2 .

As we saw in Remark 4.11, the actual definition for the window $W^{\beta}_{\underline{\lambda}}(\underline{w})$ for a given phase X_β is given by imposing the grade restriction rule on the locally closed pieces $Z^{\lambda_i}\backslash\bigcup_{l<i} Y_{\lambda_l}$ for each destabilising 1-PS λ_i for that phase. Here we have added a β to the notation just to stress that this data depends upon the phase we are considering. More naïvely, we could just impose the grade restriction rules on the fixed loci Z^λ for all 1-PS λ defining walls in the secondary fan.

Definition 4.30. Let $MW(\underline{w}) \subset D^b([\mathbb{C}^n/T_L])$ be the full subcategory generated by all line bundles $\mathcal{O}(\beta)$ (for $\beta \in L^\vee$) which satisfy the grade restriction rule (starting at w_λ) for all walls W in the secondary fan. Explicitly, for each such W, if one of its primitive normal vectors is $\lambda \in L$, we require that $\langle \beta, \lambda\rangle \in [w_\lambda, w_\lambda + \eta_\lambda - 1]$.

Then it follows that $MW(\underline{w}) \subset W^{\beta}_{\underline{\lambda}}(\underline{w})$ for any β in a chamber of the secondary fan. Hence, by Corollary 4.16, restriction $i^* : MW(\underline{w}) \to D^b(X_\beta)$ is fully faithful for any phase. If this functor is essentially surjective, it follows that $MW(\underline{w}) = W^{\beta}_{\underline{\lambda}}(\underline{w})$ for all phases and so these windows admit a particularly nice description. We give this situation a name:

Definition 4.31. $MW(\underline{w})$ is a *magic window* if it generates (upon restriction) the derived category of one of the phases.

Remark 4.32. For an explicit example of magic windows, see the proof of Theorem 7.27 in §7.3.

Remark 4.33. We note that if $MW(\underline{w})$ is a magic window, then so is $MW(\underline{w}) \otimes \mathcal{O}(\beta) = MW(\underline{w}+\langle\beta,\lambda\rangle)$ for any $\beta \in L^\vee$. However, up to tensoring with line bundles, there are only finitely many magic windows.

The existence of magic windows requires a delicate balancing of the w_λ for all normal vectors λ, as there are usually more than $\mathrm{Rk}(L^\vee)$ destabilising 1-PS and so we are imposing more than $\mathrm{Rk}(L^\vee)$ inequalities on a $\mathrm{Rk}(L^\vee)$ space. As such, if the w_λ are not balanced we end up with no (or not enough) line bundles in $MW(\underline{w})$ to generate the phases.

In fact, even with such careful choices, magic windows are not guaranteed to exist.

Example 4.34. In the Octahedron VGIT (in §5.3) there are 3 (up to inverses) primitive 1-PS with non-trivial fixed loci – that is, $\lambda = (1,0), (0,1)$ and $(1,-1)$ – and all have $\eta_\lambda = 2$. Imposing the 3 grade restriction rules for these λ, we see that any category of the form $MW(\underline{w})$ has at most 3 line bundles in it. But we'll see in §5.3 that the phases are all isomorphic to Tot $\mathcal{O}_{\mathbb{P}^1\times\mathbb{P}^1}(-1,-1)^{\oplus 2}$ and so have rank 4 algebraic K_0-theory. As such, purely on K_0 grounds, there can be no magic windows.

In the Octahedron VGIT, we'll see (§7.2) that, although there are no magic windows, there are in fact fractional magic windows:

Definition 4.35. Suppose we have picked an SOD of $D^b(Z_\lambda)_{w_\lambda} = \langle \mathcal{A}^\lambda, \mathcal{B}^\lambda \rangle$ for each λ corresponding to a wall in the secondary fan. Let $FW(\underline{w}, \langle \mathcal{A}^*, \mathcal{B}^* \rangle) \subset D^b([\mathbb{C}^n/T_L])$ be the full subcategory generated by imposing fractional grade restriction rules (starting at w_λ) with respect to these SODs for each λ. We say that $FW(\underline{w}, \langle \mathcal{A}^*, \mathcal{B}^* \rangle)$ is a *fractional magic window* if this category generates (upon restriction) the derived category of one of the phases.

Remark 4.36. For both magic and fractional magic windows, generating one of the phases is equivalent (by Corollary 4.16) to generating all of the phases. Note also that, if we choose the trivial SOD of $D^b(Z_\lambda)_{w_\lambda}$ in the definition of a fractional magic window, this imposes the usual grade restriction rule. Hence magic windows are a special class of fractional magic windows.

If we push Example 4.34 a little further, we can construct examples where there aren't even any fractional magic windows.

Example 4.37. For $n > 2$, consider the VGIT with weights $Q : \mathbb{Z}^{3n} \to \mathbb{Z}^2 = L^\vee$:

$$\beta_1, \dots, \beta_n = (1,0), \beta_{n+1}, \dots, \beta_{2n} = (0,1), \beta_{2n+1}, \dots, \beta_{3n} = (-1,-1)$$

We note that the case $n = 2$ is exactly the Octahedron VGIT. As in the Octahedron, there are still only 3 interesting 1-PS but now $\eta = n$ for all these. If we impose the weight condition in all 3 fractional grade restriction rules, then the number of line bundles satisfying these grows slower than n^2 as function of n. But the phases of this VGIT are isomorphic to Tot $\mathcal{O}_{\mathbb{P}^{n-1}\times\mathbb{P}^{n-1}}(-1,-1)^{\oplus n}$ and so have algebraic K_0-theory of rank n^2. As such, for n sufficiently large, none of these examples can have fractional magic windows for purely numerical reasons.

Remark 4.38. There is no reason we couldn't widen the definition of fractional magic window by imposing fractional grade restriction rules with wider weight conditions but more orthogonality. However, we shall not need this here so will stick with Definition 4.35.

We have seen that for a magic window restriction gives an equivalence $MW(\underline{w}) \cong D^b(X_C)$ for any chamber C. Moreover, because of the weight condition, restriction from $MW(\underline{w})$ to any phase factors through $W_\lambda(w_\lambda)$ for any λ of interest. As such, we can interpret any window equivalence ϕ^λ_w (here the λ just keeps track of the wall) as lifting into $MW(\underline{w})$ (instead of $W_\lambda(w)$) and then restricting to the phase on the other side of the wall. Therefore we get a commutative diagram of functors, which is shown schematically in Figure 6, where all arrows denote restriction (and are equivalences) and $\lambda_1, \lambda_2 \in L$ define the $x-$ and $y-$axis respectively.

The reason we are interested in magic windows is that they imply certain relations between window equivalences coming from different walls. To see this, pick any starting chamber C. Then, if we pick a sequence of neighbouring chambers (separated by walls W_i with backward-pointing normals λ_i) ending back at C, the magic window $MW(\underline{w})$ gives the relation $\prod_i \phi^{\lambda_i}_{w_{\lambda_i}} = \mathrm{Id}_{D^b(X_C)}$. We call this a *magic*

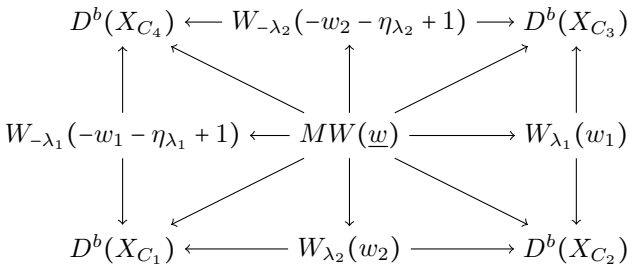

FIGURE 6. Commutative diagram of restrictions from a magic window

window relation. For example, in Figure 6, if $C = C_1$ and we follow a clockwise loop, then we get the relation $\phi^{\lambda_2}_{w_2} \circ \phi^{\lambda_1}_{w_1} \circ \phi^{-\lambda_2}_{-w_2-\eta_{\lambda_2}+1} \circ \phi^{-\lambda_1}_{-w_1-\eta_{\lambda_1}+1} = \mathrm{Id}_{D^b(X_{C_1})}$.

So a magic window gives a collection of relations, one for each loop of chambers. It's often convenient to think about this in terms of the secondary polytope $\Sigma(A)$ where such a loop corresponds exactly a loop in the 1-skeleton of $\Sigma(A)$. Since any such element can be factorised (up to changing basepoints) into loops around the 2-dimensional faces of $\Sigma(A)$ and changing basepoints does not introduce any more relations, we see that a magic window gives precisely one relation for each 2-dimensional face of $\Sigma(A)$.

Therefore, if we fix such a face and try to implement relations on it, a magic window for the whole VGIT (sometimes called a *global* magic window) is no more useful than a magic window for the VGIT near that face. This is particularly useful as the latter might exist even when the former don't. Nonetheless, as Example 4.34 shows, magic windows for the VGIT on a given 2-dimensional face still do not have to exist.

Remark 4.39. In a completely analogous way, fractional magic windows give rise to relations between fractional window equivalences coming from different walls.

5. At large radius

In this section, we describe certain regions of the FIPS of the Calabi–Yau VGIT defined by the rays $A \subset N$. For these regions we can (at least partially) understand the topology and this allows us in Proposition 5.20 to write down a representation on certain paths in such regions, in an analogous way to the 1d case discussed in §2.1.

The simplest regions are (analytic) open neighbourhoods V_C of the large radius limits p_C – that is, torus fixed points in $\mathfrak{F}$ – for each chamber C. We call these *large radius regions*. In §5.1, we describe how loops $\alpha \in \pi_1(V_C)$ correspond canonically to line bundles $\mathcal{O}(\beta)$ on X_C and hence to a canonical action of $\pi_1(V_C)$, given by tensoring with $\mathcal{O}(\beta)$.

We then move on to *curves at large radius* – that is, torus invariant curves in $\mathfrak{F}$. If W is the corresponding wall W in the secondary fan (which forms a wall of two chambers, C_1 and C_2 say), we denote this curve by $Z(W) \subset \mathfrak{F}$. In §5.2,

we describe an (analytic) open neighbourhood V_W of $Z(W)$ in the FIPS called the *near large radius region* associated to W (see Definition 5.6). V_W comes with a natural fibration structure which will enable us to simplify the description of $\pi_1(V_W, \{q_{C_1}, q_{C_2}\})$ – the so-called *near large radius groupoid*.

We then move on to describe a subgroupoid of the near large radius groupoid, called the *large radius groupoid* $\mathcal{G}_{LR}^W$ (see Definition 5.12) and a presentation which is analogous to the presentation in §2 of the fundamental groupoid of a 1d FIPS. By analogy with the 1d case, this allows us in Proposition 5.20 to use window equivalences (see Definition 4.18) to construct a representation ρ^W of the large radius groupoid for any wall W. In §5.3, to help the reader, we describe explicitly all these regions and their topology for the Octahedron VGIT.

5.1. **Large radius regions.** Recall that, when the FIPS was 1d (see §2.1), toric loops α near a large radius limit p_C (for C a chamber of the secondary fan) corresponded canonically to line bundles $\mathcal{O}(\beta)$ on the phase X_C.

To define such loops more generally, fix a chamber C and let $U'_C \subset \mathfrak{F}$ be the toric (Zariski) open neighbourhood of p_C in $\mathfrak{F}$. By applying [20], Ch. 6, Theorem 1.12 to the set of monomials of E_A and using Theorem 3.18 to observe that the convex hull of these monomials is the secondary polytope, we get:

Lemma 5.1. *For each chamber C, there is an (analytic) open neighbourhood W_C of p_C in $\mathfrak{F}$ which is invariant under the compact torus $T_{L^\vee}^{S^1}$ inside $T_{L^\vee}$ and avoids the non-toric parts of the discriminant. Moreover, this neighbourhood is a $T_{L^\vee}^{S^1}$-equivariant deformation retract of U'_C and this retract preserves the "real" subset $T_{L^\vee}^{\mathbb{R}} \subset T_{L^\vee}$. Finally, W_C is disjoint from $W_{C'}$ for all $C' \neq C$.*

Restricting W_C to the FIPS, we have:

Definition 5.2. $V_C := W_C \cap \mathrm{FIPS} = W_C \backslash \{\text{Toric part of the discriminant}\}$ is called a *large radius region* near p_C and we define $U_C := U'_C \backslash \{\text{Toric part of the discriminant}\}$

So V_C is an (analytic) open subset of the FIPS whose closure in $\mathfrak{F}$ contains p_C and such that $V_C \subset U_C$ is a deformation retract of the toric open subset U_C which preserves $T_{L^\vee}^{\mathbb{R}}$. Moreover, V_C is invariant under $T_{L^\vee}^{S^1}$ and is disjoint from $V_{C'}$ for $C' \neq C$.

In the case when all the toric divisors near p_C are in the discriminant, V_C is a punctured polydisk – that is, of the form $(D^*)^k \subset T_{L^\vee}$ where $k = \mathrm{Rk}(L^\vee) = \dim(\mathrm{FIPS})$ – and so $\pi_1(V_C) \cong \mathbb{Z}^k \cong L^\vee$. In other cases, some of the toric divisors containing p_C may not be in the discriminant and/or V_C may have an orbifold locus. Then $\pi_1(V_C) \cong \mathbb{Z}^{k'} \oplus G$ where G is a finite abelian group, $k' \leq k$ and we remember that, for us, π_1 always denotes the orbifold fundamental group(oid).

Definition 5.3. We call a (base)point $q_C \in V_C$ *real* if it lies in $T_{L^\vee}^{\mathbb{R}}$.

Pick any real basepoint q_C in V_C. Because our deformation retract $V_C \subset U_C$ preserves the real locus, $V_C \cap T_{L^\vee}^{\mathbb{R}} \subset U_C \cap T_{L^\vee}^{\mathbb{R}} = T_{L^\vee}^{\mathbb{R}} \cong \mathbb{R}_{>0}^k$ is a deformation retract

and hence $V_C \cap T^{\mathbb{R}}_{L^\vee}$ is contractible. As such, there is a canonical homotopy class of paths between any two real basepoints in V_C and so $\pi_1(V_C, q_C)$ is independent of the choice of q_C. Hence we can state:

Lemma 5.4. *There is a canonical isomorphism between $Pic(X_C)$ and $\pi_1(V_C, q_C)$*

Remark 5.5. The proof will show that $\pi_1(V_C, q_C)$ is generated by $\pi_1(T^{S^1}_{L^\vee}.q_C, q_C)$. As such, we refer to elements of $\pi_1(V_C, q_C)$ as *toric* loops. Since $\pi_1(T^{S^1}_{L^\vee}.q_C, q_C) \cong L^\vee$, we denote the toric loop at C corresponding to $\beta \in L^\vee$ by α^β_C.

Proof. Recall that the general theory of toric linear VGIT tells us that $\mathrm{Pic}(X_C) \cong L^\vee/\langle \beta_i \mid i \in I\rangle$ where $I \subset \{1, \dots, n\}$ indexes those $e_i \in \mathbb{Z}^n$ for which $\{a_i = 0\}$ is contained in the unstable locus for X_C. By the Hilbert-Mumford criterion, this condition on i equates to weights β_i for which there is a $\lambda \in L$ such that C meets the half-space $\mathcal{H}_\lambda = \{\langle -, \lambda\rangle > 0\} \subset L^\vee_{\mathbb{R}}$ and β_i is the only weight for which $\langle \beta_i, \lambda\rangle > 0$.

On the other hand, as $V_C \subset U_C$ is a deformation retract preserving the real locus, $\pi_1(V_C, q_C) \cong \pi_1(U_C, q'_C) \cong \pi_1(U_C, e)$ where $q'_C \in U_C$ is some real basepoint. The (orbifold) topology of toric varieties (see [14], Theorem 12.1.10) tells us that $\pi_1(U_C, e) \cong L^\vee/\langle \beta(e^\vee_j) \mid j \in J\rangle$ where J indexes the rays of the secondary fan in the maximal cone $\bar{C}$ whose associated toric divisors are not in the discriminant and β is the map with the same name from the stacky secondary fan (see §3.4). By the discussion immediately following Definition 3.11, $j \in J$ indexes rays in the secondary fan with a single weight β_j on them such that the ray $\omega_j \in N$ is not a vertex of Δ. By Remark 3.36, $\beta(e^\vee_j) = \beta_j$ for such j and so $\pi_1(V_C, q_C) \cong L^\vee/\langle \beta_j \mid j \in J\rangle$.

We claim that $\pi_1(V_C, q_C) \cong \mathrm{Pic}(X_C)$ canonically. Since the equivalences above are canonical, we need only show that $I = J$. To see this, take $\beta_i \in \bar{C}$ such that ω_i is not a vertex. Thus there is an integral relation $a_i\omega_i = \sum_{j\neq i} a_j\omega_j$ with $a_j \geq 0$ for all j and $a_i > 0$. This means that there is $\lambda \in L$ such that $\langle \beta_j, \lambda\rangle = -a_j \leq 0$ for all $j \neq i$ and $\langle \beta_i, \lambda\rangle = a_i > 0$. Moreover, as $\beta_i \in \bar{C}$ and $\langle \beta_i, \lambda\rangle = a_i > 0$, we see that C meets $\mathcal{H}_\lambda$.

Conversely, for any $\lambda \in L$, we get the relation $\sum_j \langle \beta_j, \lambda\rangle\omega_j = 0$ – that is, $\langle \beta_i, \lambda\rangle\omega_i = \sum_{j\neq i} -\langle \beta_j, \lambda\rangle\omega_j$. If $\beta_i \in I$, this means that ω_i can be written as a positive combination of some of the other rays (distinct from ω_i) since we assume the $\omega_i \in N$ generate distinct rays. Hence ω_i is not a vertex. Moreover, as C meets $\mathcal{H}_\lambda$ and all other weights β_j have $\langle \beta_j, \lambda\rangle \leq 0$, $\beta_i \in \bar{C}$. □

5.2. **Near large radius regions.** Now we move on to describing the near large radius region V_W near the toric curve $Z(W)$. It may be helpful to refer to the worked example in §5.3 whilst reading this section.

For each wall W in the secondary fan, label the two neighbouring chambers C_1 and C_2. Let $\lambda = \lambda_{C_1,C_2} \in L$ be the primitive normal to W pointing towards C_1. Pick an element $\beta_W \in L^\vee$ with λ-weight -1. The idea is that the orbit under the 1-PS corresponding to β_W of a point sufficiently close to $Z(W)$ will be where our push-off lies. The condition on β_W ensures that this orbit maps isomorphically (as opposed to being a finite cover) onto the rank 1 torus inside $Z(W)$.

We can describe this torically as follows. Quotienting by β_W projects $W \subset L^\vee_{\mathbb{R}}$ onto a full-dimensional cone $W \subset (L^\vee/\beta_W)_{\mathbb{R}}$. This induces a toric map $\pi' : U_W \to B'$ where U_W is the toric open subset of $\mathfrak{F}$ with fan $W \subset L^\vee_{\mathbb{R}}$ and B' is the affine toric variety associate to the cone $W \subset (L^\vee/\beta_W)_{\mathbb{R}}$. Note that B' has a unique torus fixed point $\underline{0}$ corresponding to the maximal cone W. The fibres of π' are exactly the orbits of β_W and the fibre over $\underline{0}$ is exactly $Z(W) \cap U_W$.

We now restrict π' to the FIPS so that the fibres become β_W-orbits punctured at points of the discriminant (marked with crosses in Figure 7 (L)). As b tends to $\underline{0}$, the β_W-orbit $\pi'^{-1}(b)$ breaks into several large radius curves $Z(W')$ (including $Z(W)$) and each of the points of the discriminant in $\pi'^{-1}(b)$ tends to one of the points $p_{W'}$ of the discriminant in $Z(W')$. Therefore for b sufficiently small, the points of the discriminant in $\pi'^{-1}(b)$ are naturally partitioned according to their limit point. For example, all the points in the grey region in Figure 7 (L) might limit to p_W.

As we are interested in only $Z(W)$, we want to focus on a subset of U_W which limits just to $Z(W)$. If we let $L^\vee_W := L^\vee/\langle W \cap L^\vee\rangle$, we note that the torus in $Z(W)$ can be described as $T_{L^\vee_W}$. Writing $\mathbb{C}^* \cong \mathbb{R}^\times_{>0} \times S^1$ in polar coordinates gives a canonical identification (as groups) $T_{L^\vee_W} \cong T^{\mathbb{R}}_{L^\vee_W} \times T^{S^1}_{L^\vee_W}$ where $T^{\mathbb{R}}_L := L \otimes \mathbb{R}^\times_{>0}$ and $T^{S^1}_L := L \otimes S^1$. To define our subset, pick a cylinder E (with boundary) in $T_{L^\vee_W} \subset Z(W)$ of the form $[a_1, a_2] \times S^1$ (where $a_1, a_2 \in \mathbb{R}_{>0}$ are sufficiently small and large respectively) under this identification. We define our subset $U'_W \subset U_W$ to be those points in U_W which limit to a point in E under any 1-PS $\beta \in L^\vee$ in the relative interior of W .

Then $\pi'|_{U'_W}$ has fibres which are cylinders (with boundary). However $\pi'|_{U'_W \cap \mathrm{FIPS}}$ is not a fibration over its image – this is because points of the discriminant in the fibres can either collide or go outside U'_W. If we let $B^o := \pi'(U'_W \cap \mathrm{FIPS}) \subset B'$ be the image, then B^o just consists of the complement in B' of the toric divisors in B' whose pre-image in U'_W is part of the discriminant. Then there is a critical locus $Z \subset B^o$ of codimension at least 1 over which $\pi'|_{U'_W \cap \mathrm{FIPS}}$ is not a fibration.

Then if we take $B \subset B^o$ to be a small (analytic) open neighbourhood of $\underline{0}$, we define V_W to be the open subset of the FIPS given by $U'_W \cap \pi'^{-1}(B) \cap \mathrm{FIPS}$. As such, V_W contains exactly the local structure of the FIPS near p_W. Note that B should be small enough such that any point in the discriminant in $U'_W \cap \pi'^{-1}(B)$ limits to p_W and no fibres of π' are contained in the discriminant.

Definition 5.6. We call V_W a *near large radius region* of the FIPS associated to the wall W.

We note that V_W comes with a map $\pi : V_W \to B$ (given by restricting π' to V_W) which is necessarily surjective. Moreover, V_W contains $E\backslash\{p_W\}$ precisely when $Z(W)$ is not part of the discriminant.

Remark 5.7. In §6, when the FIPS is 2d, we'll want to take B small enough such that π is also a fibration. This is not generally possible in higher dimensions.

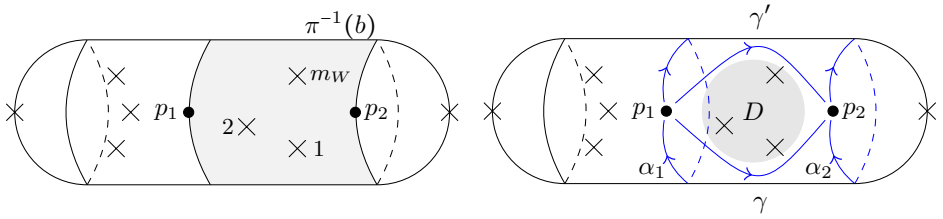

FIGURE 7. A fibre $\pi'^{-1}(b)$ (a β_W-orbit) with the region $\pi^{-1}(b)$ shaded (L) and some large radius paths in $\pi^{-1}(b)$ (R)

Definition 5.8. For a wall W in the secondary fan, we define m_W to be the intersection multiplicity of the non-toric components of the discriminant with $Z(W)$. Similarly, we define $m_{\Gamma,W}$ to be the intersection multiplicity of $Z(W)$ with the component ∇_Γ of the discriminant corresponding to the face $\Gamma \subset \Delta$ (see Remark 3.7).

The fibres $\pi^{-1}(b)$ for $b \in B\backslash Z$ are cylinders (with boundary) in $\pi'^{-1}(b)$ missing exactly m_W points (see Figure 7). If we pick a basepoint $b \in B\backslash Z$, the fibre $\pi^{-1}(b)$ plays the role of the push-off of $Z(W)$ for us.

Definition 5.9. If we pick 2 real basepoints p_1 and p_2 on the boundary of $\pi^{-1}(b)$ as shown in Figure 7 (L) (so that C_i corresponds to p_i), we refer to $\pi_1(V_W, \{p_1, p_2\})$ as the *near large radius groupoid*.

Now we move on to simplifying the description of the near large radius groupoid. This arises from a fibration structure on V_W. By definition of Z, $\pi|_{\pi^{-1}(B\backslash Z)}$ is a fibration. Moreover, this fibration has two natural sections defined as follows. Recall that we have the co-rank 1 torus $T_{L^\vee \cap W} \subset T_{L^\vee}$ and so taking the $T_{L^\vee \cap W}$-orbit of p_i defines a section s_i of π' in U_W over B'. Restricting these to V_W gives two sections s_1, s_2 of π over B since we do not delete any points of these orbits when we form V_W for B sufficiently small. This follows from the fact that the non-toric parts of the discriminant do not meet the large radius regions V_{C_1} or V_{C_2}.

Remark 5.10. By construction of the sections, toric loops in B (corresponding to elements of $\pi_1(T_{L^\vee/\beta_W}) \cong L^\vee/\beta_W$) lift to toric loops in $T_{L^\vee}$ (corresponding to elements in $\pi_1(T_{L^\vee}) \cong L^\vee$) via the splitting $L^\vee = \langle \beta_W \rangle \oplus L^\vee \cap \langle W \rangle$. We write $\beta = n\beta_W + \beta'$ under this equivalence, where $\beta' \in L^\vee$ has λ_{C_1,C_2}-weight 0.

Since $\pi|_{\pi^{-1}(B\backslash Z)}$ is a (locally trivial) fibration with sections, $\pi_1(\pi^{-1}(B\backslash Z), \{p_1, p_2\})$ can be understood in terms of monodromy on $\pi_1(\pi^{-1}(b), \{p_1, p_2\})$.

Remark 5.11. Later in §7.1, we will need a more general statement about the description of fundamental groupoids in terms of monodromy. As such, we defer precise definitions and results to there. For now, we just need that, in this setting, there is a way to define an action (which we call *monodromy*) of $\pi_1(B\backslash Z, b)$ on $\pi_1(\pi^{-1}(b), \{p_1, p_2\})$. Then Theorem 7.3 tells us that, since our sections s_i extend

over all of B, $\pi_1(V_W, \{p_1, p_2\})$ is generated by $\pi_1(\pi^{-1}(b), \{p_1, p_2\})$ and the sections $(s_i)_*(\pi_1(B, b))$ for $i = 1, 2$ subject only to relations coming from monodromy around loops in $B\backslash Z$.

However, even with this description to hand, in general $\pi_1(V_W, \{p_1, p_2\})$ is still hard to understand as the monodromy of the points of the discriminant in $\pi^{-1}(b)$ can be quite complicated. However, as mentioned in §2, for a 2d FIPS Z is actually empty. We'll explore this situation in §6.

In the general case, we now identify a subgroupoid – the *large radius groupoid* $\mathcal{G}_{LR}^W$ – of $\pi_1(V_W, \{p_1, p_2\})$ and a presentation for this subgroupoid which plays the analogue of the presentation for the FIPS in §2.1. For this, we observe that $E\backslash\{p_W\}$ is homotopy equivalent to $\pi^{-1}(b)\backslash D$ where D is a disk in $\pi^{-1}(b)$ punctured at all the points of the (non-toric) discriminant (see Figure 7 (R)). As such, the large radius paths α_i/γ in $Z(W)$ (see Figure 1) can be "pushed-off" using this identification to give large radius paths in the FIPS (in fact, in $\pi^{-1}(b)$) as shown in blue in Figure 7 (R).

As we vary $b \in B\backslash Z$, the points of the discriminant in $\pi^{-1}(b)$ undergo monodromy. But because B is sufficiently small and all these points limit to the single point p_W, we can assume that these points always lie in D over any $b \in B$. As such, our large radius paths in $\pi^{-1}(b)$ are invariant under all possible monodromies in $B\backslash Z$. Then the subgroupoid of $\pi_1(V_W, \{p_1, p_2\})$ generated by the large radius paths in $\pi^{-1}(b)$ and the sections is actually just the product $\pi_1(\pi^{-1}(b)\backslash D, \{p_1, p_2\}) \times \pi_1(B, b)$.

Definition 5.12. We call $\mathcal{G}_{LR}^W := \pi_1(\pi^{-1}(b)\backslash D, \{p_1, p_2\}) \times \pi_1(B, b)$ the *large radius groupoid* near the curve $Z(W)$. It is naturally a subgroupoid of the near large radius groupoid associated to W and hence comes with a natural map to $\pi_1(\mathrm{FIPS}, \{p_1, p_2\})$.

Remark 5.13. When the FIPS is 1-dimensional, this map $\mathcal{G}_{LR}^W \to \pi_1(\mathrm{FIPS}, \{p_1, p_2\})$ is always surjective and often an equivalence – we just have to add in the possible orbifold structure at the large radius limits in general. When the FIPS is higher-dimensional, this map is hardly ever surjective. This is because $\pi_1(V_W)$ for a single wall W rarely generates $\pi_1(\mathrm{FIPS})$ and, even if it does, in general not every path in $\pi_1(V_W)$ is a large radius path.

Remark 5.14. It's useful to have an explicit presentation of this groupoid in terms of toric loops and the paths γ. For this, we note that $\pi_1(\pi^{-1}(b)\backslash D, \{p_1, p_2\})$ is the free groupoid generated by the large radius paths α_1, α_2 and γ in Figure 7 (R).

By Remark 5.10, the toric loops in B (corresponding to $\beta' \in L^\vee \cap \langle W \rangle$) lift under s_i to toric loops in $T_{L^\vee}$ based at p_i which we'll denote by $\alpha_{C_i}^{\beta'}$ (c.f. Remark 5.5). Here we use the letter α because, as a toric loop, it plays an analogous role to α in $Z(W)$ (see Figure 1). Similarly we relabel α_i as $\alpha_{C_i}^{\beta_W}$ because this is exactly the toric loop based at p_i in the fibre $\pi^{-1}(b)$, which is a subset of a β_W-orbit. Finally we relabel γ as γ_{C_1,C_2}^0, the reason being that this extra integer superscript fixes the representation on γ in §5.4 (see Remark 5.21).

Then $\mathcal{G}_{LR}^W$ can be presented as the groupoid on p_1 and p_2 which is generated by $\alpha_{C_i}^{\beta}$ (for $i = 1, 2$ and all $\beta \in L^\vee$ where we use the splitting from Remark 5.10) and γ_{C_1,C_2}^0 subject to the relations:

(1) The map $L^\vee \to (\mathcal{G}_{LR}^W)_{p_i}, \beta \mapsto \alpha_{C_i}^{\beta}$ is a group homomorphism for $i = 1, 2$.
(2) If $\beta' \in L^\vee \cap W$ corresponds to a toric divisor in $\mathfrak{F}$ which meets the FIPS $\alpha_{C_i}^{\beta'} = e$ for $i = 1, 2$.
(3) γ_{C_1,C_2}^0 commutes with $\alpha_{C_i}^{\beta'}$ for $\beta' \in L^\vee \cap \langle W \rangle$.

By the correspondence in §5.1 between toric loops and the Picard group, the relations in (1) and (2) are a subset of the relations in $\mathrm{Pic}(X_{C_i})$ for $i = 1, 2$. Typically they are in fact a strict subset because in $\mathcal{G}_{LR}^W$ we do not impose the relations coming from the toric divisors in the regions V_{C_i} near p_i which lie in the FIPS but do not contain $Z(W)$.

Remark 5.15. Of course, there are many presentations of $\mathcal{G}_{LR}^W$. Another more symmetric one is given by adding a path in $\pi^{-1}(b)\backslash D$ from p_1 to p_2 which is the analogue of γ' in Figure 7 (R). We denote the corresponding path by γ_{C_1,C_2}^1. Then $\mathcal{G}_{LR}^W$ can be presented with this additional generator as subject to all the relations in Remark 5.14 plus the additional relation:

$$\gamma_{C_1,C_2}^1 = (\alpha_{C_2}^{\beta_W})^{-1} \circ \gamma_{C_1,C_2}^0 \circ \alpha_{C_1}^{\beta_W}$$

For an even more symmetric presentation, we could pick γ_{C_1,C_2}^0 and $\gamma_{C_2,C_1}^{-\eta_\lambda} := (\gamma_{C_1,C_2}^1)^{-1}$ as our non-toric generators, where $\lambda = \lambda_{C_1,C_2}$. Then in addition to all the relations in Remark 5.14 we have the additional relation:

$$\gamma_{C_2,C_1}^{-\eta_\lambda} \circ (\alpha_{C_2}^{\beta_W})^{-1} \circ \gamma_{C_1,C_2}^0 \circ \alpha_{C_1}^{\beta_W} = e$$

Remark 5.16. Having understood the large radius groupoid for a particular wall-crossing, it is natural to try to glue together these groupoids for nearby wall-crossings. Specifically suppose we have two walls W_1 and W_2 such that V_{W_1} and V_{W_2} meet in the large radius region V_C. Suppose we pick our basepoints p_1^i, p_2^i for wall-crossing W_i to be real and positive – that is, lie within $T_{L^\vee}^{\mathbb{R}}$ – and suppose p_1^1 and p_1^2 both correspond to the chamber C. Then there is a canonical homotopy class of paths connecting p_1^1 and p_1^2 in V_C, given by any real positive path in V_C which connects these two points. As such, there is a canonical way to identify these two basepoints in $\mathcal{G}_{LR}^{W_1}$ and $\mathcal{G}_{LR}^{W_2}$ respectively and hence glue them together as a groupoid with 3 basepoints. Similarly we could continue and glue together all such large radius groupoids into one big *large radius groupoid* $\mathcal{G}_{LR}$ with one basepoint for each chamber of the secondary fan. As each of the large radius groupoids comes with a map to $\pi_1(\mathrm{FIPS})$, $\mathcal{G}_{LR}$ comes with such a map too.

Remark 5.17. When the FIPS is more than 2-dimensional (the case we care about is the Triangle VGIT in §9), it will be useful to note that we can generalise this construction of push-offs of toric curves in $\mathfrak{F}$ to push-offs of higher-dimensional toric

subvarieties in $\mathfrak{F}$. In particular, let β be the generator of a ray in the secondary fan, corresponding to a toric divisor D in $\mathfrak{F}$, which we want to push-off into the FIPS. Then, instead of the 1-PS β_W, to define a fibration structure we now need to pick a co-rank 1 sublattice $L_\beta^\vee \subset L^\vee$. Equivalently, the fibration can be specified by the primitive normal $\lambda_\beta \in L$ to $L_\beta^\vee$. We require that $\langle \beta, \lambda_\beta \rangle = 1$ so that the fibres project isomorphically onto the torus $T_{L^\vee/\beta}$ inside D.

Then the fibration is the toric map $\pi' : U_\beta \to B'$ induced by quotienting by $L_\beta^\vee$ where the base B' is a 1-dimensional affine toric variety with a unique torus fixed point $\underline{0} \in B'$ and the fibres are orbits of the corresponding co-rank 1 subtorus $T_{L_\beta^\vee} \subset T_{L^\vee}$. As before, the push-off will lie in such a fibre sufficiently close to D.

Pick a closed subset $E \subset T_{L^\vee/\beta}$ in the open torus in D which is defined by inequalities (above we chose $a_1 \le |X| \le a_2$ where X was a toric coordinate on $T_{L_W^\vee}$) and such that E minus the discriminant is a deformation retract of D minus the discriminant. Then we consider the subset $U'_\beta \subset U_\beta$ of points which limit under the 1-PS β to E. So the fibres of $\pi'|_{U'_\beta}$ retain only what happens in π' near D.

Restricting to the FIPS and shrinking B' to a small (possibly punctured or orbifold) disk B, we end up with a near large radius region of the FIPS near D, which we denote $V_\beta \subset \text{FIPS}$. This comes with a surjective map $\pi : V_\beta \to B$. In fact, as we'll see in §6.1, the locus Z over which π fails to be a fibration is codimension 1, so we can assume that $Z = \varnothing$ and hence π is a fibration over B.

Pick basepoints p_i in the fibre $\pi^{-1}(b)$ over $b \in B$ in some (or all) of the large radius regions V_{C_i} near D. As before, these give rise to sections of π over B such that the canonical generating loop γ in B (corresponding to $\beta \in L^\vee/L_\beta^\vee$) lifts to the toric loop $\alpha_{C_i}^\beta \in \pi_1(T_{L^\vee}, p_i)$. Then, as in Remark 5.11, it follows that $\pi_1(V_\beta, \{p_i\})$ is generated by the fibre $\pi_1(\pi^{-1}(b), \{p_i\})$ and sections $(s_i)_*(\pi_1(B,b)) = \langle \alpha_{C_i}^\beta \rangle$ subject to the relations coming from monodromy around γ.

5.3. **The Octahedron VGIT.** As there was a lot of notation in the preceding discussion, to clarify things we now describe a simple example. This example is called the Octahedron VGIT and it has a 2-dimensional FIPS. Our aim is ultimately to show (see Theorem 7.16) that we can construct a representation of $\pi_1(\text{FIPS})$ on the phases but, for now, we content ourselves with understanding the preceding topology.

We start with the toric data. The Octahedron VGIT has weight matrix $Q : \mathbb{Z}^6 \to \mathbb{Z}^2$ given by:

$$Q = \begin{pmatrix} 1 & 1 & 0 & 0 & -1 & -1 \\ 0 & 0 & 1 & 1 & -1 & -1 \end{pmatrix}$$

Thus $L^\vee$ has rank 2 and one checks that there are 3 chambers whose unstable loci are indicated in Figure 8 (L). We label the walls and chambers as indicated in the figure.

We note that $e_1^\vee, e_3^\vee$ and $e_5^\vee$ are primitive integral defining functions (see Definition 3.26) for the 3 subdivisions corresponding to the 3 walls of the secondary fan. As

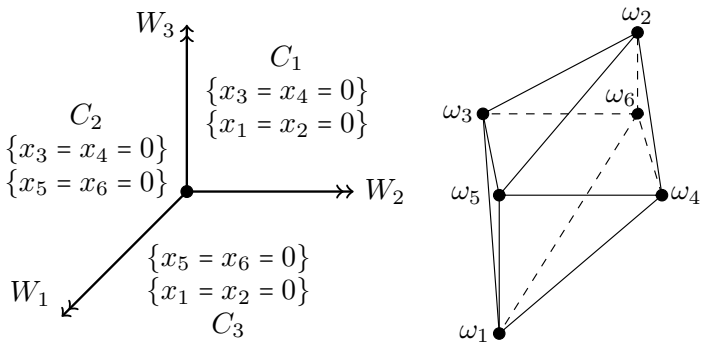

FIGURE 8. The secondary fan for the Octahedron VGIT with the unstable loci for the phases (L) and the octahedron Δ (R)

such, the stacky secondary fan (see §3.4) has 3 rays:

$$\beta(e_1^\vee) = (-1,-1), \beta(e_2^\vee) = (1,0), \beta(e_3^\vee) = (0,1)$$

It follows that the secondary stack $\mathfrak{F}$ is $\mathbb{P}^2$ with coordinates $[x,y,z]$.

One checks that the ray map $A : \mathbb{Z}^6 \to \mathbb{Z}^4$ can be described as:

$$A = \begin{pmatrix} 1 & 0 & 0 & 1 & 1 & 0 \\ 0 & 1 & 0 & 1 & 0 & 1 \\ -1 & 1 & 0 & 0 & 0 & 0 \\ 1 & 1 & 1 & 1 & 1 & 1 \end{pmatrix}$$

and so Δ, living in the height 1 slice $x_4 = 1$, is the octahedron shown in Figure 8 (R). As such, the phases are 4-dimensional toric Calabi–Yaus and, from thinking about the weights, are all globally isomorphic to Tot $\mathcal{O}_{\mathbb{P}^1\times\mathbb{P}^1}(-1,-1)^{\oplus 2}$.

Remark 5.18. From a different perspective, this VGIT arises as the representations (with dimension $(1,1,1)$) of the following quiver:

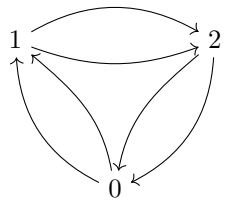

We now move on to the discriminant. As all the rays ω_i are vertices, the whole toric boundary is part of the discriminant. As all the edges and facets of the octahedron Δ are simplices, we only have one other component of the discriminant, namely the principal component ∇_{pr}. If we embed $T_{L^\vee} \subset \mathfrak{F} \cong \mathbb{P}^2$ using the first and third coordinates of $\mathbb{P}^2$, Horn uniformisation (see (4) in §3.6) describes ∇_{pr} as the

image of the map (which for dimension reasons is a morphism here):

$$\mathbb{P}^1 \to \mathbb{P}^2$$
$$[\lambda_1, \lambda_2] \mapsto [\lambda_1^2, (\lambda_1 + \lambda_2)^2, \lambda_2^2]$$

and hence ∇_{pr} is a smooth conic. Thus ∇_{pr} intersects each torus invariant curve $Z(W_i)$ in a single point with multiplicity 2 and so we conclude that $m_{W_i} = 2$.

Now we would like to understand the large radius groupoid associated to a wall. Let's choose the wall W_2 from Figure 8 (L). Then $Z(W_2) = \{x = 0\}$ and $U_{W_2} = \mathbb{P}^2 \backslash \{y = 0\} \cup \{z = 0\}$ (see Figure 9 (L)). Then $\lambda_{C_1,C_3} = (0, 1)$ and we can choose $\beta_{W_2} = (-1, -1)$. With these choices, the paths pushed off from $Z(W_2)$ will live in a β_{W_2}-orbit, also known as a line $\{x = bz\} \subset U_{W_2}$ for some $b \in \mathbb{C}$.

Explicitly following the construction, we consider the quotient map:

$$\mathbb{Z}^2 \to \mathbb{Z}^2 / \beta_{W_2} \cong \mathbb{Z}, (x_1, x_2) \mapsto x_1 - x_2$$

Then the affine toric variety B' corresponding to W_2/β_{W_2} is $\mathbb{C}$ with coordinate b, whose unique torus fixed point $\underline{0} = \{b = 0\}$. The map $\pi' : U_{W_2} \to \mathbb{C}$ can be described as $[x, y, z] \mapsto x/z$. Moreover, the fibre over $\underline{0}$ is exactly $Z(W_2) \cap U_{W_2}$.

Now we need to understand what happens when we restrict to the FIPS. From Horn uniformisation, we can compute that $\{x = bz\}$ meets ∇_{pr} at the 2 points $[b, (1 \pm \sqrt{b})^2, 1]$. We can see that, as $b \to 0$, these two points converge on the point $p_{W_2} = [0, 1, 1]$ in $Z(W_2)$. We pick the cylinder $E = \{[y, z] \mid a_1|y| \leq |z| \leq a_2|y|\}$ in $Z(W_2)$ for $a_1, a_2 \in \mathbb{R}_{>0}$ with $a_1 < 1$ and $a_2 > 1$. Then U'_{W_2} is those points in U_{W_2} which limit to E as $t \to 0$ under the 1-PS of $T_{L^\vee}$ corresponding to $(1, 0) \in L^\vee$, namely $t \mapsto [t, 1, 1]$. Thus $U'_{W_2} = \{[x, y, z] \mid a_1|y| \leq |z| \leq a_2|y|, y \neq 0, z \neq 0\}$ (see Figure 9 (L)).

However $\pi'|_{U'_{W_2} \cap \mathrm{FIPS}}$ is not a fibration over its image. We first note that its image $B^o = \pi'(U'_{W_2} \cap \mathrm{FIPS}) = B' \backslash \{b = 0\}$ as $Z(W_2)$ is part of the discriminant. Then we observe that, as $b \to 1$, one of the points of ∇_{pr} tends to $[1, 0, 1]$ which is not in U'_{W_2}. As such, π' is not a fibration at $b = 1$ and so $\{b = 1\} \subset Z$. However, so long as $a_1 \leq |1 \pm \sqrt{b}|^{-2} \leq a_2$ for both square-roots, we get a fibration on U'_{W_2}. As such, if we take $B \subset B^o$ to be a disk punctured at the origin satisfying this condition, then π will be a fibration over B as in Remark 5.7. Hence we end up with the near large radius region $V_{W_2} = U'_{W_2} \cap \pi'^{-1}(B) \cap \mathrm{FIPS}$ (see Figure 9 (L)).

If we take our basepoint $b = \{b = \epsilon\}$ with $\epsilon \in \mathbb{R}_{>0}$ small enough for b to be in B, then $\pi^{-1}(b)$ is a cylinder punctured in $m_{W_2} = 2$ points. Choosing $p_i = [\epsilon, 1/a_i, 1]$ in $\pi^{-1}(\epsilon)$, we get sections $s_i(b) = [b, 1/a_i, 1]$ over all of B. With these sections, the toric loop $\gamma : t \mapsto \epsilon e^{2\pi i t} \in B$ at b lifts to the toric loop (denoted $\alpha_{C_i}^{(1,0)}$) in $T_{L^\vee}$ corresponding to the 1-PS $(1, 0)$.

From here, we can now describe the large radius groupoid for W_2. Namely, as B is a punctured disk with no critical locus Z inside it, we can identify $\pi_1(B, b)$ with $\mathbb{Z}$ using γ and this is the only path in $B \backslash Z$ with interesting monodromy.

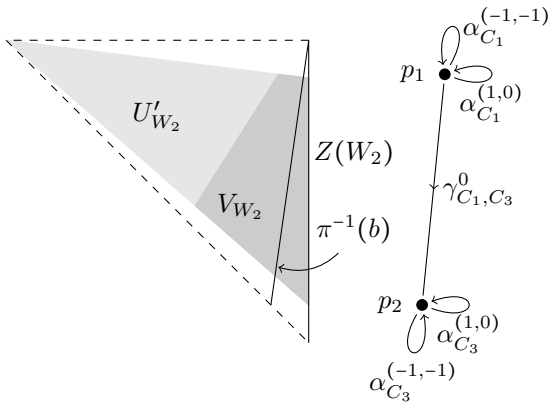

FIGURE 9. Images of regions U_{W_2} (everything except the dashed lines), U'_{W_2} (light grey), V_{W_2} (dark grey) and $\pi^{-1}(b)$ under the moment map for $\mathfrak{F} = \mathbb{P}^2$ (L) and generators for $\mathcal{G}_{LR}^{W_2}$ (R)

Remark 5.19. In fact, the monodromy around γ just permutes the two points of the discriminant, as shown in Figure 18 (L), but we will not need this here. We note that it indeed leaves all the paths in $\pi^{-1}(b)\backslash D$ alone.

Since we have a fibration of curves over a punctured disk, standard topology tells us that $\mathcal{G}_{LR}^{W_2}$ is generated by $\alpha_{C_i}^{(1,0)}$, $\alpha_{C_i}^{(-1,-1)}$ (for $i = 1, 3$) and $\gamma^0_{C_1,C_3}$ subject to $\alpha_{C_i}^{(1,0)}$ commuting with $\alpha_{C_i}^{(-1,-1)}$ and $\gamma^0_{C_1,C_3}$ (here (2) in Remark 5.14 is vacuous as we have deleted all the boundary). These generators are shown in Figure 9 (R).

5.4. **Representation on large radius paths.** Having pushed our paths in $Z(W)$ off into the FIPS, we now want to assign derived equivalences to these paths in analogy with the case of a 1d FIPS in §2. Recall that for a 1d FIPS, toric loops α gave us line bundles $\mathcal{O}(\beta)$ and hence the auto-equivalence $\otimes\mathcal{O}(\beta) : D^b(X_C) \to D^b(X_C)$. Moreover, paths of the form γ gave window equivalences between neighbouring phases.

Here, using the presentation of $\mathcal{G}_{LR}^W$ from Remark 5.14, exactly the same ideas give us:

Proposition 5.20. *For any wall W in the secondary fan, $\rho^W(\alpha_C^\beta) = \otimes\mathcal{O}(\beta)$ (using the correspondence in Lemma 5.4) and $\rho^W(\gamma^0_{C_1,C_2}) = \phi_0 : D^b(X_{C_1}) \to D^b(X_{C_2})$ (see Definition 4.18) describes a functor $\rho^W : \mathcal{G}_{LR}^W \to \boldsymbol{Cat}_1$ such that $\rho(q_{C_i}) \cong D^b(X_{C_i})$.*

Remark 5.21. We see here that there is an ambiguity in defining $\rho^W(\gamma^0_{C_1,C_2})$ – we could have chosen ϕ_w for any $w \in \mathbb{Z}$. Throughout, we fix this ambiguity by labelling all of the large radius paths with a superscript integer which specifies the corresponding window. As such, a large radius path labelled $\gamma^k_{C_1,C_2}$ will always correspond under ρ^W to ϕ_k.

Proof. All the relations in $\mathcal{G}_{LR}^W$ hold tautologically.

By Remark 5.14, we know relations (1) and (2) are just a subset of the relations in the Picard group. Lemma 5.4 tells us that the Picard group acts and so these relations hold.

For (3), we need to show that the window equivalence ϕ_0 commutes with tensoring by $\mathcal{O}(\beta')$ for $\beta' \in L^\vee \cap \langle W \rangle$ – that is, for $F \in D^b(X_{C_1})$, $\phi_0(F)(\beta') = \phi_0(F(\beta'))$. Recall that, by definition, $\phi_0(F)$ is the restriction to X_{C_2} of an element $\hat{F} \in W_\lambda(0)$ such that $\hat{F}|_{X_{C_1}} = F$. By Corollary 4.16, such an $\hat{F}$ is unique (up to isomorphism).

Then $\hat{F}(\beta') \in W_\lambda(0)$ too since β' has λ-weight 0 (see Remark 5.10). Moreover $\hat{F}(\beta')|_{X_{C_1}} = F(\beta')$. So $\hat{F}(\beta')$ is a lift to $W_\lambda(0)$ of $F(\beta')$ and so, by uniqueness, is the lift used in the definition of ϕ_0. So $\phi_0(F(\beta')) = \hat{F}(\beta')|_{X_{C_2}} = \phi_0(F)(\beta')$ as claimed.

□

Remark 5.22. If we use the first alternative presentation from Remark 5.15, then we can define $\rho^W(\gamma^1_{C_1,C_2}) = \phi_1 : D^b(X_{C_1}) \to D^b(X_{C_2})$. We then need to check one additional relation which says that, for $F \in D^b(X_{C_1})$, $\phi_1(F(-\beta_W)) = \phi_0(F)(-\beta_W)$ where β_W has λ-weight -1. This is pretty much the same as checking (3) above except that, because β_W has λ-weight -1, $\hat{F}(-\beta_W) \in W_\lambda(1)$ and so $\phi_1(F(-\beta_W)) = \hat{F}(-\beta_W)|_{X_{C_2}} = \phi_0(F)(-\beta_W)$.

If we use the second presentation in Remark 5.15, we can define $\rho^W(\gamma^{-\eta_\lambda}_{C_2,C_1}) = \phi_{-\eta_\lambda} : D^b(X_{C_2}) \to D^b(X_{C_1})$. We need then to check one additional relation. Using the relation we just checked, this can be simplified to $\phi_{-\eta_\lambda} = (\phi_1)^{-1}$. This holds since $W_{\lambda^{-1}}(-\eta_\lambda) = W_\lambda(1)$.

Example 5.23. We analyse what this representation looks like as we cross the wall W_2 in the Octahedron VGIT from §5.3. In this case, $\mathrm{Pic}(X_C) \cong L^\vee = \mathbb{Z}^2$ for all phases, where we label the line bundle $\mathcal{O}_{X_C}(a,b)$ accordingly. So $\alpha_{C_i}^{(a,b)}$ just acts by $\otimes \mathcal{O}_{X_C}(a,b)$. As a word of warning, we know that all phases are isomorphic to Tot $\mathcal{O}_{\mathbb{P}^1\times\mathbb{P}^1}(-1,-1)^{\oplus 2}$. However $\mathcal{O}_{X_C}(a,b)$ does not agree in general (though it does for X_{C_1}) with the pullback of $\mathcal{O}_{\mathbb{P}^1\times\mathbb{P}^1}(a,b)$ to the total space of this rank 2 vector bundle. This is because flops act non-trivially on divisors.

Now the large radius path $\gamma^0_{C_1,C_3}$ acts by the window equivalence ϕ_0, which involves lifting into the window $W_\lambda(0)$ where $\lambda := \lambda_{C_1,C_3} = (0,1)$. To understand this category, recall from Figure 8 (L), that in forming the phases for C_1 and C_3 we delete the stratum $\{x_1 = x_2 = 0\}$ from both and then there is one other unstable stratum that switches from $\{x_3 = x_4 = 0\}$ in C_1 to $\{x_5 = x_6 = 0\}$ in C_3. Therefore the phase on the wall $X_0^\lambda = [\mathbb{C}^6 \backslash \{x_1 = x_2 = 0\}/(\mathbb{C}^*)^2]$ and, recalling that $\eta = 2$ for all walls, $W_\lambda(0) \subset D^b(X_0^\lambda)$ is defined by having λ-weights in $[0,1]$. From the geometric description of X_{C_1} as Tot $\mathcal{O}_{\mathbb{P}^1\times\mathbb{P}^1}(-1,-1)^{\oplus 2}$, it follows that $D^b(X_{C_1})$ is generated by the 4 line bundles:

$$\mathcal{O}_{X_{C_1}}, \mathcal{O}(1,0)_{X_{C_1}}, \mathcal{O}_{X_{C_1}}(0,1), \mathcal{O}_{X_{C_1}}(1,1)$$

As these all have λ-weight in $[0,1]$, these lift to $W_\lambda(0)$ trivially. As such, ϕ_0 can be described as sending $\mathcal{O}_{X_{C_1}}(a,b) \mapsto \mathcal{O}_{X_{C_3}}(a,b)$ for these 4 values of (a,b). However, for other values of (a,b), ϕ_0 will do something non-trivial.

We now interpret this action geometrically using Remark 4.19 which says that the window shift $\psi_0 = \phi_0^{-1} \circ \phi_1$ on $D^b(X_{C_1})$ is the twist about an explicit spherical functor F. To do this, we observe that $Z'_\lambda = Z'^\lambda \cap X_0^\lambda = \{x_3 = x_4 = x_5 = x_6 = 0\} \cap X_0^\lambda \cong \mathbb{P}^1_{x_1,x_2}$ (where we recall that the prime means that we forget the trivial λ-action). Geometrically we interpret this by saying that, as we move from C_1 to W_2, $\mathbb{P}^1_{x_1,x_2} \times \mathbb{P}^1_{x_3,x_4}$ in X_{C_1} collapses along the first ruling to Z'_λ. Similarly as we go from W_2 to C_3, Z'_λ expands to become $\mathbb{P}^1_{x_1,x_2} \times \mathbb{P}^1_{x_5,x_6}$ in X_{C_3}.

Then $F = i^* \circ i_{\lambda,0} : D^b(\mathbb{P}^1_{x_1,x_2}) \to D^b(X_{C_1})$ is our spherical functor and $F(\mathcal{O}_{\mathbb{P}^1}(n)) = i_*\mathcal{O}_{\mathbb{P}^1 \times \mathbb{P}^1}(n,0)$ where $i : \mathbb{P}^1_{x_1,x_2} \times \mathbb{P}^1_{x_3,x_4} \subset X_{C_1}$ is the inclusion. As such, the image of F is concentrated on the collapsing locus in X_{C_1} and so the twist modifies objects in $D^b(X_{C_1})$ only along this locus.

Remark 5.24. We have seen in Remark 5.16 that we can canonically glue together the large radius groupoids for different walls along the large radius regions V_C near torus fixed points to get the large radius groupoid $\mathcal{G}_{LR}$. Moreover, since the action of $\pi_1(V_C)$ by tensoring with line bundles is canonical (see §5.1), ρ^W respects this gluing and so we get a representation ρ on $\mathcal{G}_{LR}$.

However this representation is not particularly useful in its own right. Firstly (see Remark 5.13) paths in $\mathcal{G}_{LR}$ need not generate $\pi_1(\text{FIPS})$. We'll show how to get around this issue for a 2d FIPS in §6. Also, in some cases of interest, $\mathcal{G}_{LR}$ does generate $\pi_1(\text{FIPS})$. For example, in the quasi-symmetric case treated in §8 the discriminant is a (log)-hyperplane arrangement and this holds.

However, even if $\mathcal{G}_{LR}$ does generate, the bigger issue is that the representation ρ^W is not canonical (see Remark 5.21). As such, when we start gluing these together, the representation becomes even less canonical. If we want to extend the representation of this groupoid to the whole of $\pi_1(\text{FIPS})$ (in the case when $\mathcal{G}_{LR}$ generates) we need to prove that the extra relations coming from the "interior" of the FIPS hold. But if we have made arbitrary choices of windows on different walls, then the composition of such functors is not going to admit a simple description. As such, there seems little use to this abstract gluing. Instead, when we come to construct such representations, we will need to choose a collection of paths and functors for these different walls which gives a simple description of the relations from the interior of the FIPS and the corresponding functors.

6. Near large radius in a 2d FIPS

In this section, we shall upgrade our action ρ^W on $\mathcal{G}_{LR}^W$ (see Proposition 5.20) to the full action of the near large radius groupoid in the case when we are crossing a wall W in a 2-dimensional FIPS. Recall from Remark 3.36 that, in this case, the stacky structure on $\mathfrak{F}$ is simple – that is, β from §3.4 is just given by the weights Q. To define our action, we shall need to define additional equivalences between

two neighbouring phases corresponding to the additional paths in $\pi_1(V_W, \{p_1, p_2\})$ which are not large radius paths – that is, not pushed off from the curve $Z(W) \subset \mathfrak{F}$ at large radius as described in §5.2. These equivalences will come from fractional windows (see Definition 4.24). Moreover, we need to check that the appropriate monodromy relations hold for these paths.

6.1. **Near large radius monodromy.** Recall from §5.2 that a choice of $\beta_W \in L^\vee$ allows us to define the near large radius region V_W. This space comes with a map $\pi : V_W \to B$ which is a fibration away from a locus $Z \subset B$ of codimension at least 1. The fibres $\pi^{-1}(b)$ are cylinders in a β_W-orbit in $T_{L^\vee}$ which have been punctured at the m_W points of the discriminant in $\pi^{-1}(b)$. We also saw that, if we picked 2 basepoints p_1, p_2 on $\pi^{-1}(b)$, we could define 2 sections s_i over B and $\pi_1(V_W, \{p_1, p_2\})$ is then generated by $\pi_1(\pi^{-1}(b), \{p_1, p_2\})$ and the sections $(s_i)_*(\pi_1(B, b))$ for $i = 1, 2$ subject only to relations coming from monodromy in $B \backslash Z$.

When the FIPS is 2-dimensional, B is a (possibly punctured or orbifold) disk which we can assume is small enough to miss any of the 0-dimensional locus Z. As such, we can assume $Z = \varnothing$ in this case and so we only have to impose monodromy relations coming from monodromy in B. As B is a (possibly punctured or orbifold) disk, $\pi_1(B, b)$ is generated by a single loop and so there is a single monodromy relation.

Remark 6.1. This is exactly what we saw in the Octahedron VGIT which we considered in §5.3.

In fact, the definition of B in §5.2 shows that $\pi_1(B, b)$ is naturally a quotient of $L^\vee/\beta_W$. As this lattice has a natural generator given by the primitive generator u_W of the ray of the secondary fan associated to W, so does $\pi_1(B, b)$. We give the monodromy with respect to this natural generating loop a name:

Definition 6.2. We define the *local monodromy* $\mathfrak{m} \in \mathrm{Aut}(\pi_1(\pi^{-1}(b), \{p_1, p_2\}))$ to be the monodromy action on $\pi^{-1}(b)$ associated to this generating loop in the base and sections s_1 and s_2.

We now want to know what $\mathfrak{m}$ looks like – this is Lemma 6.5. This will then allow us to construct our new action in §6.2. We begin by calculating the intersection multiplicity $m_{\Delta,W}$ of ∇_{pr} with $Z(W)$ (see Definition 5.8) explicitly from the combinatorial data. First, we observe that in dimension 2, the choice of β_W specifies a natural set of coordinates on U_W. Namely, there is a toric coordinate coming from B (which has a natural toric coordinate coming from the natural generator of $L^\vee/\beta_W$) and a toric coordinate coming from the natural generator β_W of $L^\vee/u_W$, where u_W is the primitive generator of W. When we draw pictures of monodromy such as Figure 10 we shall use the second toric coordinate above.

Lemma 6.3. *We may assume that our wall W is generated by $e_1 \in L^\vee = \mathbb{Z}^2$ and that $\beta_W = (0, 1)$. Then $m_{\Delta,W} = \max(\sum_{i|\beta_i \in \langle W \rangle} \beta_i^1, 0)$*

Proof. Take the toric open set U_W in $\mathfrak{F}$ associated to the ray generated by e_1. This has coordinates $(x_1, x_2) \in \mathbb{C} \times \mathbb{C}^*$ and $Z(W) = \{x_1 = 0\}$. Horn uniformisation for ∇_{pr} (see (4) in §3.6) is a *morphism* $\mathbb{P}^1 \to \mathfrak{F}$, which in these coordinates reads:

$$[\lambda_1, \lambda_2] \mapsto ((\prod_{\beta_i \in \langle W \rangle} {\beta_i^1}^{\beta_i^1}) \lambda_1^{\sum_{i|\beta_i \in \langle W \rangle} \beta_i^1} \prod_{\beta_i \notin \langle W \rangle} (\beta_i^1 \lambda_1 + \beta_i^2 \lambda_2)^{\beta_i^1}, \prod_{\beta_i \notin \langle W \rangle} (\beta_i^1 \lambda_1 + \beta_i^2 \lambda_2)^{\beta_i^2})$$

Since the x_2 coordinate must lie in $\mathbb{C}^*$ at the intersection of $Z(W)$ with ∇_{pr}, only weights lying on $\langle W \rangle$ contribute to the intersection. As such, there is at most one intersection point $[0, 1]$ and this contributes (with multiplicity $m_{\Delta,W} = \sum_{i|\beta_i \in \langle W \rangle} \beta_i^1$) precisely when $\sum_{i|\beta_i \in \langle W \rangle} \beta_i^1 > 0$. □

In dimension 2, the interaction of the components of the discriminant is also very restricted. Recall (see §3.1) that components of the discriminant (possibly empty) are indexed by minimal faces $\Gamma \subset \Delta$. Dually (see Lemma 3.47) they are indexed by proper subspaces in $L^\vee_{\mathbb{R}}$ with a positive relation, noting that, in dimension 2, these subspaces are automatically spanned by the weights on them. If W is such a subspace, we label the corresponding component ∇_W.

Lemma 6.4. *At most two components of the discriminant, namely ∇_{pr} (when $m_{\Delta,W} > 0$) and ∇_W (when $\langle W \rangle$ has a positive relation), meet $Z(W)$. In fact, there are 3 possibilities:*

	$Z(W)$ *meets* ∇_{pr}	$Z(W)$ *meets* ∇_W	m_W
Case 1	✓	✓	$m_{\Delta,W} + 1$
Case 2	✓	✗	$m_{\Delta,W}$
Case 3	✗	✓	1

Proof. The first part is a special case of Lemma 10.16, noting that the only subspaces of a 2d vector space of the form $(L'_\Gamma)^\vee_{\mathbb{R}}$ are 0 and lines ℓ for which there is a positive relation among the weights on ℓ. Moreover, such $\ell = \langle W \rangle$ are necessarily circuits as they are codimension 1. If we call the corresponding face Γ, Proposition 10.17 gives that $m_{\Gamma,W} = 1$ for either wall W on ℓ.

As the walls of the secondary fan are the tropicalisation of the non-toric discriminant, some component of the non-toric discriminant must hit the curve $Z(W)$ (This follows from [20], Ch. 6, Theorem 1.12b and Ch. 10, Theorem 1.4a). This leaves only the 3 possibilities in the table. □

As such, the fibre $\pi^{-1}(b)$ contains m_W points of the discriminant and at most one of these is from a non-principal component of the discriminant – such a point exists in Cases 1 and 3.

Lemma 6.5. *The local monodromy can be put into the following forms:*

Case 1: *Monodromy fixes the point of ∇_W in $\pi^{-1}(b)$ and cycles the points of ∇_{pr} around the point of ∇_W as in Figure 10 (L) .*

Case 2: *Monodromy cycles the points of ∇_{pr} in $\pi^{-1}(b)$ as in Figure 10 (R).*

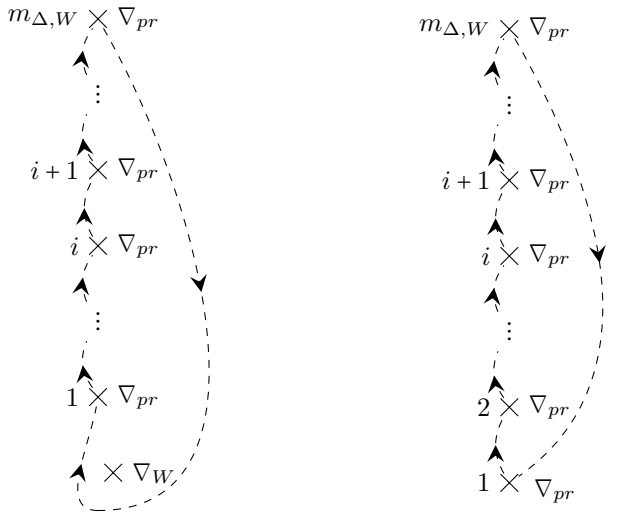

FIGURE 10. Standard forms for the local monodromy (dashed line) in Case 1 (L) and Case 2 (R)

Case 3: *Monodromy is trivial. This is the large radius description from §5.*

Proof. We have already observed in §5.2 that the monodromy is concentrated in the disk D in $\pi^{-1}(b)$. Write Horn uniformisation as in Lemma 6.3, using the affine coordinate $\Lambda = \lambda_1/\lambda_2$ on $\mathbb{P}^1$:

$$H : \Lambda \mapsto ((\prod_{\beta_i \in \langle W \rangle} {\beta_i^1}^{\beta_i^1})\Lambda^{m_{\Delta,W}} \prod_{\beta_i \notin \langle W \rangle} (\beta_i^1 \Lambda + \beta_i^2)^{\beta_i^1}, \prod_{\beta_i \notin \langle W \rangle} (\beta_i^1 \Lambda + \beta_i^2)^{\beta_i^2})$$

One checks that the intersection point $p_W = (0, p'_W)$ has a unique pre-image (namely $\Lambda = 0$) in $\mathbb{P}^1$ where $p'_W = \prod_{\beta_i \notin \langle W \rangle} {\beta_i^2}^{\beta_i^2}$.

Since we have written H with respect to the same coordinates on U_W which we used in the construction of V_W, we have that the projection π' is just projection onto the first coordinate. As such, as we go round a loop $\gamma(t) = e^{2\pi i t}$ in the base B, the Λ-coordinate of a point in ∇_{pr} roughly follows $t \mapsto \Lambda e^{2\pi i t/m_{\Delta,W}}$. As the natural coordinate coming from $\beta_W = (0,1)$ is x_2, we want to picture monodromy in terms of x_2. So expanding the x_2-coordinate of H near p_W in terms of Λ, we see that it equals $-p'_W m_{\Delta,W} \Lambda$ plus higher order terms in Λ (which, since $m_{\Delta,W} \neq 0$, play no role). Therefore (up to homotopy) the monodromy is as shown in Figure 10 (R) for Case 2. In Case 1, we just observe additionally that the x_2-coordinate of $\nabla_W = \{x_2 = p'_W\}$ is fixed and so the points in ∇_{pr} just cycle around the point in ∇_W. This gives the monodromy in Figure 10 (L) for Case 1. □

Remark 6.6. From the explicit form of H in the proof, it's easy to see that, although ∇_{pr} is singular in general, if ∇_{pr} meets $Z(W)$ (at p_W say), ∇_{pr} is smooth at p_W.

To see this, we compute that the derivative at $\Lambda = 0$ is $(0, -m_{\Delta,W} p'_W)$ for $m_{\Delta,W} > 1$ and $(\prod_{\beta_i \in \langle W \rangle} {\beta_i^1}^{\beta_i^1} \prod_{\beta_i \notin \langle W \rangle} {\beta_i^2}^{\beta_i^1}, -p'_W)$ for $m_{\Delta,W} = 1$, where we use that $-m_{\Delta,W} =$

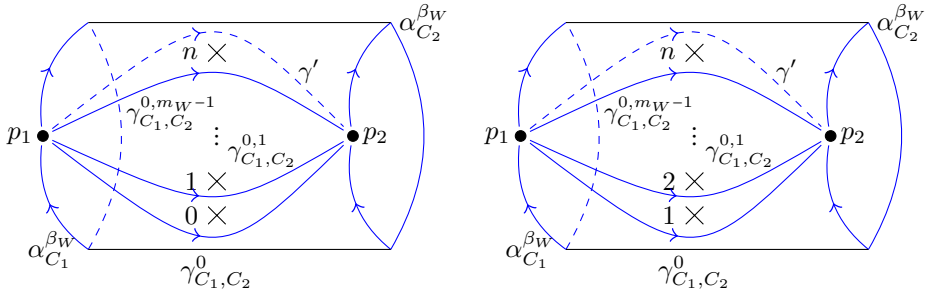

FIGURE 11. Free generators for $\pi_1(\pi^{-1}(b),\{p_1,p_2\})$ in Case 1 (L) and Case 2 (R) with an additional path γ' marked and $n = m_{\Delta,W}$

$\sum_{\beta_i\notin\langle W\rangle}\beta_i^1$ from the Calabi–Yau condition. As the proof shows H is injective near p_W, ∇_{pr} is smooth at p_W as claimed.

In fact, this gives another way to prove the lemma in Case 2 by noting that, at the smooth point p_W of ∇_{pr}, Taylor's theorem gives a standard form for the intersection of ∇_{pr} with $Z(W)$.

Finally, having described an explicit standard form for our monodromy, we label the point of ∇_W in Figure 10 by 0 (in case 1) and the points of ∇_{pr} by increasing integers from 1 up to $m_{\Delta,W}$ going from bottom to top. Then we pick the paths $\gamma_{C_1,C_2}^{0,i}$ and $\alpha_{C_i}^{\beta_W}$ shown in blue in Figure 11, which are free generators for $\pi_1(\pi^{-1}(b),\{p_1,p_2\})$. Note that $\gamma_{C_1,C_2}^{0,0}$ is exactly our large radius path γ_{C_1,C_2}^{0} from §5, so the *near* large radius paths correspond to $i\geq 1$. Again the notation $\gamma_{C_1,C_2}^{0,i}$ is supposed to also (partially) specify the representation on this path (see Remark 6.10).

Remark 6.7. As there are many ways to identify a given fibre $\pi^{-1}(b)$ with our standard form, this description is not canonical. Nonetheless, any such description will be enough for us to construct our action in §6.2.

It follows from our discussion at the beginning of this section and the description of the monodromy that these choices give a presentation of $\pi_1(V_W,\{p_1,p_2\})$ with generators $\gamma_{C_1,C_2}^{0,i}$ for $i=0,\dots,m_W-1$ and $\alpha_{C_j}^{\beta}$ for $j=1,2$ and $\beta\in L^\vee$ with relations:

(1) The map $L^\vee\to\pi_1(V_W,p_j),\beta\mapsto\alpha_{C_j}^{\beta}$ is a group homomorphism for $j=1,2$.
(2) If $\beta'\in L^\vee\cap W$ corresponds to a toric divisor in $\mathfrak{F}$ which meets the FIPS $\alpha_{C_j}^{\beta'}=e$ for $j=1,2$.
(3) (Monodromy relations) $\alpha_{C_2}^{u_W}\circ\gamma_{C_1,C_2}^{0,i}\circ\alpha_{C_1}^{-u_W}=\mathfrak{m}(\gamma_{C_1,C_2}^{0,i})$ for $i=0,\dots,m_W-1$.

As we have chosen $\gamma_{C_1,C_2}^{0,0}=\gamma_{C_1,C_2}^{0}$ and $\alpha_{C_i}^{\beta_W}$ here such that they agree with our large radius presentation from Remark 5.14, our notation is consistent under the inclusion $\mathcal{G}_{LR}^W\hookrightarrow\pi_1(V_W,\{p_1,p_2\})$.

Example 6.8. Here we revisit crossing the wall W_2 in Octahedron VGIT from §5.3. From Figure 8, we can see that $m_{\Delta,W_2}=2$ (calculated using Lemma 6.3), which agrees with our previous calculation. Moreover there is no positive relation

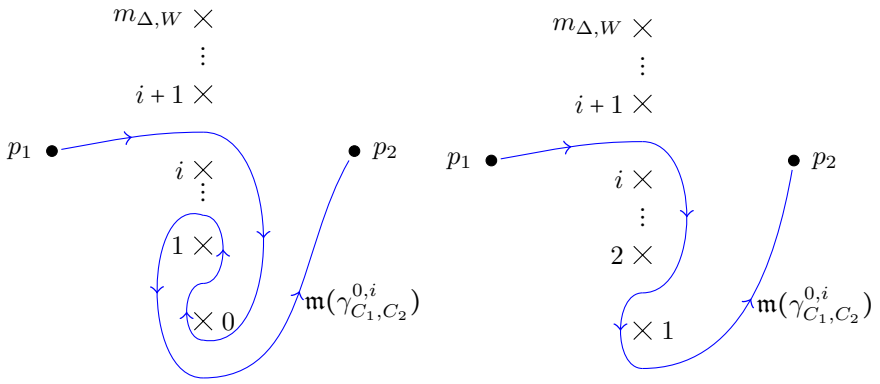

FIGURE 12. Effect of monodromy on the path $\gamma^{0,i}_{C_1,C_2}$ in $\pi^{-1}(b)$ (see Figure 11) in Case 1 (L) and Case 2 (R)

on $\langle W_2 \rangle$, as $-W_2$ is not is a ray in the secondary fan. So Lemma 6.4 tells us that we are in case 2 – in fact, we've seen that ∇_{pr} is the only component of the discriminant. Finally Lemma 6.5 tells us that the 2 points in $\pi^{-1}(b)$ should swap as in Figure 10 (R). Recalling that these points in $\pi^{-1}(b)$ are $[b, (1 \pm \sqrt{b})^2, 1]$, we can follow the monodromy explicitly around $b = \epsilon e^{2\pi i t}$ and see that it is given by Figure 18 (L). This agrees with Figure 10 (R).

6.2. **Representation on near large radius paths.** We shall now explain how we can extend the action of ρ^W on $\mathcal{G}^W_{LR}$ to $\pi_1(V_W, \{p_1, p_2\})$ by assigning certain fractional window equivalences (see Definition 4.24) to our extra generators $\gamma^{0,i}_{C_1,C_2}$ (for $i = 1, \dots, m_W - 1$). For this, we need to choose some specific SODs of $D^b(Z_\lambda)_0 = D^b(Z'_\lambda)$ where, as usual, $\lambda = \lambda_{C_1,C_2} \in L$ is the primitive normal to W pointing towards the chamber C_1. Recall that Z'_λ is a phase of the rank 1 linear toric VGIT given by the weights β_i lying on $\langle W \rangle$ – that is, the VGIT with $X_0 = Z'^\lambda$, the λ-fixed locus. We refer to this VGIT as the VGIT on Z'^λ or on W. Then Z'_λ is the phase of this VGIT which corresponds to the chamber W. We'll let $\hat{Z}_\lambda$ be the (possibly empty) other phase of this VGIT.

Remark 6.9. We note that the rank 1 VGIT on Z'^λ is generally not Calabi–Yau.

Remark 6.10. Here, as for the large radius representation (see Remark 5.21), we have an ambiguity in that we could use $D^b(Z_\lambda)_{w'}$ for any $w' \in \mathbb{Z}$ instead to define the representation on $\gamma^{0,i}_{C_1,C_2}$. In fact, on these paths ρ^W is even more ambiguous because, having fixed w', it requires a choice of SOD. We'll see below that the choice of such an SOD is specified by an additional integer $w \in \mathbb{Z}$ – this roughly corresponds to the ambiguity of writing our monodromy in standard form, as in Remark 6.7. We'll see in Remark 6.14 that the notation $\gamma^{0,i}_{C_1,C_2}$ is supposed to fix some of this ambiguity in ρ^W.

Recalling that Z'_λ is a *minimal* phase if $K_{Z'_\lambda}$ is nef, the 3 topological cases in Lemma 6.4 have geometric analogues as follows:

(1) Using the toric description of $K_{Z'_\lambda}$ (see [14], Theorem 8.2.3) $m_{\Delta,W} > 0$ means that $\hat{Z}_\lambda$ is minimal. Moreover since ∇_W intersects $Z(W)$, $\langle W \rangle$ has a positive relation and hence $\hat{Z}_\lambda \neq \varnothing$.
(2) As $m_{\Delta,W} > 0$, $\hat{Z}_\lambda$ is still the minimal phase, but as $\langle W \rangle$ does not have a positive relation $\hat{Z}_\lambda = \varnothing$.
(3) As $m_{\Delta,W} = 0$, Z'_λ is minimal.

Recalling Example 4.23 with $X_0 = Z'^\lambda$, the theory of wall-crossings in a (not necessarily Calabi–Yau) rank 1 toric linear VGIT gives an SOD of a maximal phase in terms of a minimal phase and some number of exceptional objects. If we let λ' be the primitive 1-PS in the VGIT on Z'^λ which points away from W, then these SODs are given explicitly in Example 4.23. With these choices, X_+/X_- in that example corresponds to $Z'_\lambda/\hat{Z}_\lambda$. We also note that $-\mu_{\lambda'} := \langle K_{Z'^\lambda}, \lambda' \rangle$ agrees with $m_{\Delta,W}$ when the former is positive. Thus the 3 geometric possibilities above have the 3 categorical analogues as follows:

(1) $D^b(Z'_\lambda) = \langle E_0, \mathcal{O}_{Y_{\lambda'^{-1}}}(w), \cdots, \mathcal{O}_{Y_{\lambda'^{-1}}}(w + m_{\Delta,W} - 1) \rangle$ where E_0 is a copy of $D^b(\hat{Z}_\lambda)$ embedded by $\phi_{-w-\eta_{\lambda'}+1}$.
(2) $D^b(Z'_\lambda) = \langle \mathcal{O}_{Z'_\lambda}(w), \cdots, \mathcal{O}_{Z'_\lambda}(w + m_{\Delta,W} - 1) \rangle$. In fact, Z'_λ is just a weighted projective space in this case and this is the standard Beilinson exceptional collection of line bundles (up to overall tensoring with a line bundle).
(3) We get the trivial SOD of $D^b(Z'_\lambda)$

We denote the exceptional objects $\mathcal{O}_{Y_{\lambda'^{-1}}}(w+i-1)$ by E_i for $i > 0$ and our SODs by $D^b(Z'_\lambda) = \langle E_0, E_1, \cdots, E_{m_{\Delta,W}} \rangle$ (where some of the E_i can be empty depending on the case). Here the labelling matches up with that of the points of the discriminant in $\pi^{-1}(b)$ that we saw in Figures 11 and 12. So E_0 is the single category associated with the single puncture of $\pi^{-1}(b)$ at a non-principal component ∇_W (in Cases 1 and 3) and E_i for $i > 0$ are the $m_{\Delta,W}$ exceptional objects associated with the $m_{\Delta,W}$ punctures in $\pi^{-1}(b)$ at ∇_{pr}.

Remark 6.11. These SODs are the simplest case of the more general story which we describe in §10.

Remark 6.12. There are two properties of these SODs that we will crucially use in the proof of Theorem 6.15.

- (Lefschetz property) $E_{i+1} = E_i(1)$ for $i > 0$.
- (Window property) $R_{E_1}(E_0) = E_0(u_W)$. This is just Remark 4.22, where we use that $\mathcal{O}(u_W)$ has λ'^{-1} weight 1.

Now, as in Corollary 4.28, our SOD $D^b(Z'_\lambda) = \langle E_0, E_1, \cdots, E_{m_{\Delta,W}} \rangle$ gives rise to fractional windows $F^0_\lambda(\langle \mathcal{U}_i, \mathcal{V}_i \rangle)$ where $\mathcal{U}_i$ is the category generated by the first i pieces of this SOD and $\mathcal{V}_i$ is generated by the remaining pieces. We then define $\rho^W(\gamma^{0,i}_{C_1,C_2})$ to be the fractional window equivalence χ_0 using this window.

Remark 6.13. Note that, for all the SODs above, one of $\mathcal{U}_i, \mathcal{V}_i$ is always proper and so, by Lemma 4.25, we do indeed get fractional window equivalences.

Remark 6.14. The notation here is supposed to fix some of the ambiguity in the definition of ρ^W, as in Remark 6.10. Namely, if we have fixed an SOD for the wall W, the superscripts in $\gamma^{0,i}_{C_1,C_2}$ tell us to use the fractional window with λ_{C_1,C_2}-weight 0 and $\mathcal{A}$ given by the i-th category $\mathcal{U}_i$.

We now prove:

Theorem 6.15. *In each of the 3 cases, any choice of SOD of $D^b(Z'_\lambda)$ of the form above gives a representation $\rho^W : \pi_1(V_W, \{p_1, p_2\}) \to \boldsymbol{Cat}_1$ which extends the large radius representation from Proposition 5.20.*

Remark 6.16. For the rest of this section, we simplify notation by letting X_0 denote the phase of the VGIT on the wall W, i_-^* be the restriction from $D^b(X_0)$ to $D^b(X_{C_1})$ and i_+^* be the restriction from $D^b(X_0)$ to $D^b(X_{C_2})$. $E' := E \otimes \kappa_\lambda^\vee|_{Z_\lambda}$ for $E \in D^b(Z'_\lambda)$. Recall the functor $i_{\lambda,w} : D^b(Z_\lambda)_w \to D^b(X_0)$ from Lemma 4.6. For an object or subcategory E in $D^b(Z'_\lambda)$, we let $E^\pm \in D^b(X_0)$ be the image of E under $i_{\lambda^\pm,0}$.

Example 6.17. For the wall W_2 in the Octahedron VGIT, we have seen in Example 6.8 that only the principal component contributes to the discriminant and so we are in case 2. Moreover, ∇_{pr} is a conic in $\mathfrak{F} = \mathbb{P}^2$ so $m_W = m_{\Delta,W} = 2$ and we have just one additional path $\gamma^{0,1}_{C_1,C_3}$. In Example 5.23, we have calculated $Z'_\lambda = \mathbb{P}^1_{x_1,x_2}$ where $\lambda = \lambda_{C_1,C_3} = (0,1)$. Thus Z'_λ is not minimal. Indeed, the VGIT on W_2 has two weights $\beta_1 = \beta_2 = 1 \in L^\vee := \mathbb{Z}$ and so the minimal phase of this VGIT, which we called $\hat{Z}_\lambda$ earlier, is empty. The SOD for case 2 is then $D^b(\mathbb{P}^1) = \langle \mathcal{O}(w), \mathcal{O}(w+1) \rangle$ for any $w \in \mathbb{Z}$.

We'll now describe explicitly the fractional window equivalence associated with the SOD $D^b(\mathbb{P}^1) = \langle \mathcal{O}, \mathcal{O}(1) \rangle$ – that is, the case $w = 0$ of the SOD above. First, we need to understand the fractional window $F^0_\lambda(\langle \mathcal{O}, \mathcal{O}(1) \rangle)$. By definition, a line bundle $\mathcal{O}(\beta)$ in $D^b(X_0)$ belongs to it if it has λ-weights in $[0,2]$ and has:

$$\mathrm{Hom}_{Z'_\lambda}(\mathcal{O}(\beta)|_{Z'_\lambda}, \mathcal{O}) = 0 \text{ and } \mathrm{Hom}_{Z'_\lambda}(\mathcal{O}(1), (\mathcal{O}(\beta) \otimes \kappa_\lambda)|_{Z'_\lambda}) = 0$$

where $\kappa_\lambda := \det(N_{Y_\lambda/X_0})$. Since we know $Y_\lambda = \{x_5 = x_6 = 0\}$, we see that $\kappa_\lambda \cong \mathcal{O}(-2,-2)$. Writing $\beta = (a,b) \in \mathbb{Z}^2$ (as in Example 5.23) so that $\mathcal{O}(a,b)|_{Z_\lambda} \cong \mathcal{O}(a)$ on $\mathbb{P}^1$, we see that $\mathcal{O}(a,b)$ satisfies these conditions precisely when $b \in [0,2]$ and if $b = 0$, $a = 1$ and if $b = 2$, $a = 2$. By Remark 4.13, these line bundles generate $F^0_\lambda(\langle \mathcal{O}, \mathcal{O}(1) \rangle)$. Thus $\rho^W(\gamma^{0,1}_{C_1,C_3})$ can be described as the functor sending $\mathcal{O}_{X_{C_1}}(a,b)$ for these values of (a,b) to $\mathcal{O}_{X_{C_3}}(a,b)$. As with the window equivalences in Example 5.23, $\rho^W(\gamma^{0,1}_{C_1,C_3})$ will act non-trivially on other line bundles.

We can again interpret this geometrically by considering what the auto-equivalence $\rho^W((\gamma^0_{C_1,C_3})^{-1} \circ \gamma^{0,1}_{C_1,C_3})$ looks like. It turns out (see Remark 6.24) that this is a spherical twist about $\mathcal{O}_{\mathbb{P}^1 \times \mathbb{P}^1}$, whereas we saw in Example 5.23 that the window shift was a twist about the whole category supported on the locus $\mathbb{P}^1 \times \mathbb{P}^1$ which collapses as we cross W_2. So the new auto-equivalences capture some extra geometric structure in the collapsing locus, in this case individual destabilising objects supported on this locus.

We now turn to the proof. Recall the presentation of $\pi_1(V_W, \{p_1, p_2\})$ after Remark 6.7. As we have already constructed ρ^W on large radius paths in Proposition 5.20, we need only check that the monodromy relations hold under ρ^W on the (strictly) near large radius paths $\gamma^{0,i}_{C_1,C_2}$ for $i = 1, \ldots, m_W - 1$. Note that Case 3 is therefore already solved. Explicitly, we need to show that:

$$\rho^W(\alpha_{C_2}^{u_W} \circ \gamma^{0,i}_{C_1,C_2} \circ \alpha_{C_1}^{-u_W}) = \rho^W(\mathfrak{m}(\gamma^{0,i}_{C_1,C_2})) \text{ for } i = 1, \cdots, m_W - 1$$

We do this by expressing both functors as sequences of lifts into certain fractional windows followed by restriction to a phase. We then simplify this description of these functors by using the mutations we introduced in §4.1. This allows us to rewrite the monodromy relation above as the equality of two sequences of mutation functors associated to certain subcategories of $D^b(X_0)$. We then check that these functors agree by (general calculus of mutations and) the Lefschetz and window properties of our SOD from Remark 6.12.

We first note that tensoring by a line bundle with λ-weight 0, lifting into a fractional window and then tensoring by the inverse line bundle can be described as lifting into a different fractional window:

Lemma 6.18. *$\rho^W(\alpha_{C_2}^{u_W} \circ \gamma^{0,i}_{C_1,C_2} \circ \alpha_{C_1}^{-u_W}) = i_+^* \circ (i_-^*)^{-1}$ where $(i_-^*)^{-1}$ is the lift from $D^b(X_{C_1})$ into $F^0_\lambda(\langle \mathcal{U}_i(u_W), \mathcal{V}_i(u_W)\rangle)$.*

Proof. By definition, the functor on the left-hand side is $\otimes\mathcal{O}(u_W) \circ \rho^W(\gamma^{0,i}_{C_1,C_2}) \circ \otimes\mathcal{O}(-u_W)$. First note that the fractional window in the statement makes sense as $\langle \mathcal{U}_i(u_W), \mathcal{V}_i(u_W)\rangle$ is an SOD of $D^b(Z'_\lambda)$ as u_W has λ-weight 0. It is not hard to see that

$$F^0_\lambda(\langle \mathcal{U}_i(u_W), \mathcal{V}_i(u_W)\rangle) = F^0_\lambda(\langle \mathcal{U}_i, \mathcal{V}_i\rangle) \otimes \mathcal{O}(u_W)$$

Given this, if $G \in F^0_\lambda(\langle \mathcal{U}_i, \mathcal{V}_i\rangle)$ is a lift of $F(-u_W) \in D^b(X_{C_1})$, then $G(u_W)$ is a lift of F to $F^0_\lambda(\langle \mathcal{U}_i(u_W), \mathcal{V}_i(u_W)\rangle)$. Hence $(i_-^*)^{-1}(F) \cong G(u_W)$ and so:

$$\rho^W(\alpha_{C_2}^{u_W} \circ \gamma^{0,i}_{C_1,C_2} \circ \alpha_{C_1}^{-u_W})(F) = G|_{X_{C_2}} \otimes \mathcal{O}(u_W) = G(u_W)|_{X_{C_2}} = i_+^* \circ (i_-^*)^{-1}(F)$$

□

Now we turn to understanding $\rho^W(\mathfrak{m}(\gamma^{0,i}_{C_1,C_2}))$. Recall the disk D (see §5.2) in $\pi^{-1}(b)$ containing all the punctures at points of the discriminant (we'll assume it contains the basepoints p_1, p_2 too) and which we assume is in the standard form from Figure 10. As $\mathfrak{m}(\gamma^{0,i}_{C_1,C_2}) \in \pi_1(D, p_1, p_2)$ and $\pi_1(D, p_1, p_2)$ is freely generated by $\gamma^{0,i}_{C_1,C_2}$ (for $i = 0, \cdots, m_W - 1$) and γ' (see Figure 11), $\rho^W(\mathfrak{m}(\gamma^{0,i}_{C_1,C_2}))$ can be described via a sequence of lifts into the fractional windows $F^0_\lambda(\langle \mathcal{U}_i, \mathcal{V}_i\rangle)$ followed by restriction to a phase. Moreover Figure 12 tells us explicitly what this sequence is. It therefore seems natural to split these functors into two by introducing:

- Additional basepoints e_i (for $i = 0, \cdots, m_W$) in D whose corresponding categories $\rho^W(e_i) := F^0_\lambda(\langle \mathcal{U}_i, \mathcal{V}_i\rangle) = F^{-\eta}_{\lambda^{-1}}(\langle \mathcal{V}'_{n-i} \otimes \omega_{Z'_\lambda}, \mathcal{U}'_{n-i}\rangle)$
- Additional paths $\delta_i^\pm$ such that $\rho^W(\delta_i^\pm) := i_\pm^*$.

These are shown in Figure 13 (T) where $n := m_W$.

We can naturally incorporate the discussion of mutations in §4.1 into this picture by introducing additional paths $\epsilon_i^{\pm}$ as shown in Figure 13 (T). Then $\pi_1(D, \{p_i, e_j\})$ can be presented with generators $\epsilon_i^{\pm}, \delta_i^{\pm}$ shown in Figure 13 (T) subject to the relations $\delta_i^{\pm}\epsilon_i^{\pm} = \delta_{i-1}^{\pm}$ for $i = 1, \dots, n$.

Remark 6.19. In this presentation, $\gamma_{C_1,C_2}^{0,i}$ corresponds to the path $\delta_i^+ \circ (\delta_i^-)^{-1}$.

Moreover, Corollary 4.28 tells us that $\rho^W((\delta_i^+)^{-1} \circ \delta_{i-1}^+) = R_{E_i^+}$ and so we define $\rho^W(\epsilon_i^+) \coloneqq R_{E_i^+}$. Similarly Corollary 4.29 tells us to define $\rho^W(\epsilon_i^-) \coloneqq L_{F_i'^-}$, where we recall that $\langle F_{m_{\Delta,W}}, \cdots, F_0\rangle$ is the left-dual SOD to $D^b(Z'_\lambda) = \langle E_0, \cdots, E_{m_{\Delta,W}}\rangle$. Then ρ^W in this presentation is depicted in Figure 13 (B).

What's more, we have shown that ρ^W extends to a functor on $\pi_1(D, \{p_i, e_j\})$. Noting that $\rho^W(e_0) = F_\lambda^0(\langle \mathcal{U}_0, \mathcal{V}_0\rangle) = W_\lambda(0)$ and $\rho^W(e_n) = F_\lambda^0(\langle \mathcal{U}_{m_{\Delta,W}}, \mathcal{V}_{m_{\Delta,W}}\rangle) = W_\lambda(1)$, we see that ρ^W agrees with our representation on large radius paths in $\pi_1(D, \{p_1, p_2\})$.

Remark 6.20. We might worry that to understand $\rho^W(\mathfrak{m}(\gamma_{C_1,C_2}^{0,i}))$ we have to understand the dual SOD too, which will involve more complicated objects. Actually, it turns out that we don't, because the ϵ_j^- appearing in the description of $\mathfrak{m}(\gamma_{C_1,C_2}^{0,i})$ in the presentation above only come in terms of the form $\epsilon_j^- \circ \cdots \circ \epsilon_1^-$. By Theorem 4.27, the associated functor $\rho^W(\epsilon_i^- \circ \cdots \circ \epsilon_1^-) = L_{\mathcal{V}'^-_{n-i}}$ and $\mathcal{V}'^-_{n-i} = \langle E_1'^-, \dots, E_i'^-\rangle$ can be described in terms of only the E_i rather than the dual F_i.

Remark 6.21. Before we launch into the proof, it will be helpful to recall the combinatorics of mutations. Recall that if E, F are two subcategories, $L_{\langle E,F\rangle} = L_E \circ L_F$ and $R_E = L_E^{-1}$. Therefore we have that $L_E \circ L_F = L_{\langle E,F\rangle} = L_{\langle F, R_F(E)\rangle} = L_F \circ L_{R_F(E)}$. In particular, if E and F are orthogonal, L_E and L_F commute.

We now turn to the proof of the theorem.

Proof. We know from Lemma 6.18 that $\rho^W(\alpha_{C_2}^{u_W} \circ \gamma_{C_1,C_2}^{0,i} \circ \alpha_{C_1}^{-u_W})$ can be expressed as a particular fractional window equivalence. Comparing Figures 12 and 13, we see how to write $\rho^W(\mathfrak{m}(\gamma_{C_1,C_2}^{0,i}))$ in terms of lifting into certain fractional windows and restricting to phases. Here we write this expression down in both cases and mess around with mutations to get the result. We start with Case 2, as it's simpler.

Case 2: Compare Figures 12 (R) and 13. We see that $\rho^W(\mathfrak{m}(\gamma_{C_1,C_2}^{0,i}))$ can be expressed as the composition of functors from $D^b(X_{C_1})$ to $D^b(X_{C_2})$ going clockwise around the following diagram, where we note that $F_1'^- = E_1'^-$ (as $F_1 = E_1$). Moreover, we have seen that $\rho^W(\alpha_{C_2}^{u_W} \circ \gamma_{C_1,C_2}^{0,i} \circ \alpha_{C_1}^{-u_W})$ can be expressed as the functor around the bottom.

$$\begin{array}{ccccc}
F_\lambda^0(\langle \mathcal{U}_{i+1}, \mathcal{V}_{i+1}\rangle) & \xrightarrow{L_{\langle E_2^+, \dots E_{i+1}^+\rangle}} & F_\lambda^0(\langle \mathcal{U}_1, \mathcal{V}_1\rangle) & \xrightarrow{R_{F_1'^- = R_{E_1'^-}}} & W_\lambda(0) \\
\downarrow{\scriptstyle i_-^*} & \swarrow{\scriptstyle L_{E_1'^-}} & & \searrow{\scriptstyle L_{\mathcal{U}_i^+(u_W)}} & \downarrow{\scriptstyle i_+^*} \\
D^b(X_{C_1}) & \xleftarrow[i_-^*]{} & F_\lambda^0(\langle \mathcal{U}_i(u_W), \mathcal{V}_i(u_W)\rangle) & \xrightarrow{i_+^*} & D^b(X_{C_2})
\end{array}$$

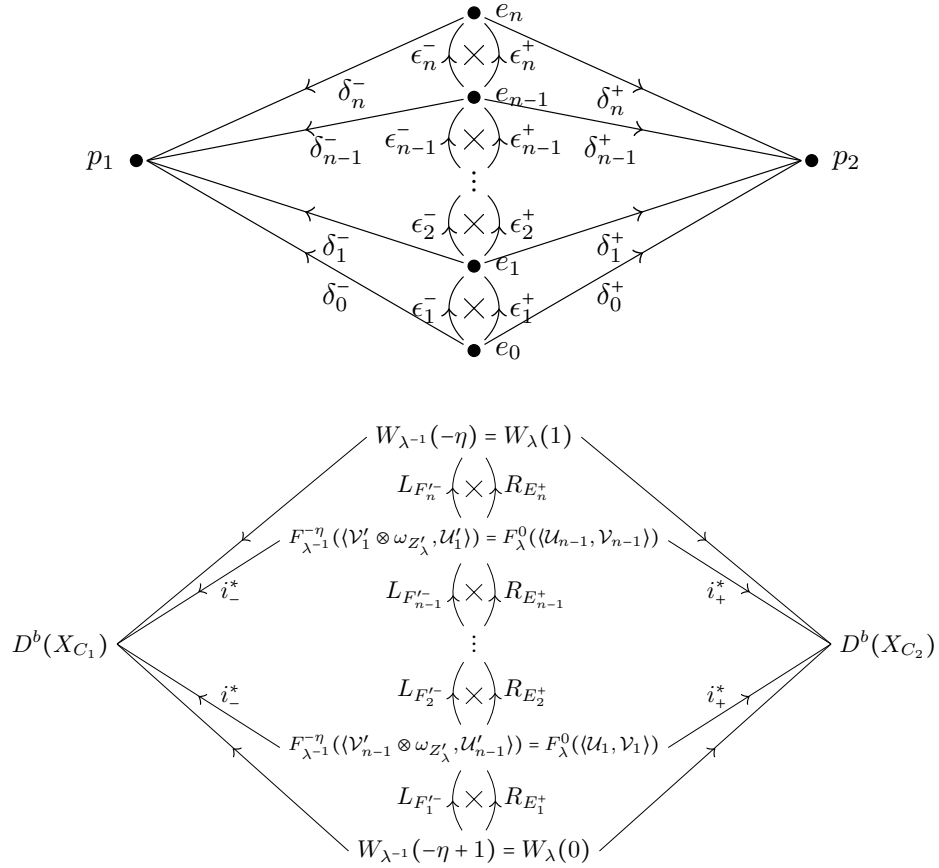

FIGURE 13. Generators for $\pi_1(D, \{p_i, e_j\})$ (T) and the corresponding functor ρ^W (B)

So we are reduced to showing this diagram commutes. Now we remove any reference to the phases (and so only have to deal with mutating subcategories of $D^b(X_0)$) by using Lemma 6.22 to express the compositions $(i_\pm^*)^{-1} \circ i_\pm^*$ in terms of mutations – these are indicated by the dotted lines in the diagram above. Thus we are reduced to showing:

$$L_{E'^-_1} \circ L_{\mathcal{U}_i^+(u_W)} = L_{\langle E_2^+, \dots E_{i+1}^+ \rangle} \circ L_{E'^-_1}$$

But $\mathcal{U}_i^+(u_W) = \langle E_2^+, \cdots, E_{i+1}^+ \rangle$ by the Lefschetz property and these subcategories are orthogonal by Lemma 6.23. Hence we are done by Remark 6.21.

Case 1: Compare Figures 12 (L) and 13. We see that $\rho^W(\mathfrak{m}(\gamma_{C_1,C_2}^{0,i}))$ can be expressed as the composition of functors from $D^b(X_{C_1})$ to $D^b(X_{C_2})$ going clockwise around the following diagram, noting that $F_0'^- = E_0'^-$ (as $F_0 = E_0$) and $R_{F_0'^-} \circ R_{F_1'^-} = R_{\langle E_0'^-, E_1'^- \rangle}$ by Remark 6.20. Moreover, we have seen that $\rho^W(\alpha_{C_2}^{u_W} \circ \gamma_{C_1,C_2}^{0,i} \circ \alpha_{C_1}^{-u_W})$ can be expressed as the anti-clockwise functor with same source and target.

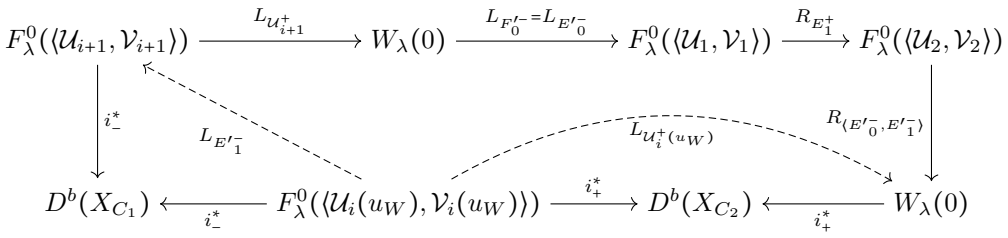

So we are reduced to showing this diagram commutes. Now we remove any reference to the phases (and so only have to deal with mutating subcategories of $D^b(X_0)$) by using Lemma 6.22 to express the compositions $(i^*_\pm)^{-1} \circ i^*_\pm$ in terms of mutations – these are indicated by the dotted lines in the diagram above. Thus we are reduced to showing:

$$L_{E'^-_0} \circ L_{\langle E^+_0, \dots E^+_{i+1}\rangle} \circ L_{E'^-_1} = L_{E^+_1} \circ L_{E'^-_0} \circ L_{E'^-_1} \circ L_{\mathcal{U}^+_i(u_W)}$$

By Remark 6.21, swapping the first pair of functors in the right-hand functor and then swapping the second pair of functors shows that the right-hand functor equals:

$$L_{E'^-_0} \circ L_{R_{E'^-_0}(E^+_1)} \circ L_{L_{E'^-_1}(\mathcal{U}^+_i(u_W))} \circ L_{E'^-_1}$$

By Lemma 6.23, E^+_1 and ${E'}^-_0$ are orthogonal (noting that E_1 has compact support) and hence $R_{E'^-_0}(E^+_1) = E^+_1$.

By the Lefschetz property of E_i for $i > 0$, $\mathcal{U}^+_i(u_W)) = \langle E^+_0(u_W), E^+_2, \dots, E^+_{i+1}\rangle$. Since by Lemma 6.23, E^+_i and ${E'}^-_1$ are orthogonal for $i > 1$, $L_{E'^-_1}(E^+_i) = E^+_i$. Similarly, noting that E_1 is compactly supported and, by the window property,

$$\mathrm{Hom}(E_0(u_W), E_1) = \mathrm{Hom}(R_{E_1}(E_0), E_1) = \mathrm{Hom}(E_0, L_{E_1}(E_1)) = 0$$

Lemma 6.23 gives $L_{E'^-_1}(E^+_0(u_W)) = E^+_0(u_W)$. Thus $L_{E'^-_1}(\mathcal{U}^+_i(u_W)) = \mathcal{U}^+_i(u_W)$ and the right-hand functor equals:

$$L_{E'^-_0} \circ L_{\langle E^+_1, E^+_0(u_W), E^+_2, \dots E^+_{i+1}\rangle)} \circ L_{E'^-_1}$$

Since, by the window property,

$$\langle E^+_1, E^+_0(u_W), E^+_2, \dots E^+_{i+1}\rangle = \langle E^+_1, R_{E^+_1}(E^+_0), \dots, E^+_{i+1}\rangle = \langle E^+_0, E^+_1, \dots, E^+_{i+1}\rangle$$

we see that this functor agrees with the left-hand functor.

□

We now prove the two missing lemmas from the proof of Theorem 6.15. The first tells us that we can rewrite certain compositions of functors in the commutative diagrams in that proof as left mutations.

Lemma 6.22. $(i^*_+)^{-1} \circ i^*_+ : F^0_\lambda(\langle \mathcal{U}_i(u_W), \mathcal{V}_i(u_W)\rangle) \to W_\lambda(0)$ *is the left mutation* $L_{\mathcal{U}^+_i(u_W)}$. *Similarly* $(i^*_-)^{-1} \circ i^*_- : F^0_\lambda(\langle \mathcal{U}_i(u_W), \mathcal{V}_i(u_W)\rangle) \to F^0_\lambda(\langle \mathcal{U}_{i+1}, \mathcal{V}_{i+1}\rangle)$ *is the left mutation* $L_{E'^-_1}$.

Proof. To check that the compositions are as claimed, we first check that the mutations indicated do indeed map the source to the target. For the compositions $(i_+^*)^{-1} \circ i_+^*$, this follows from Theorem 4.27 with $\mathcal{A} = \mathcal{U}_i(u_W)$ and $\mathcal{B} = \mathcal{V}_i(u_W)$. For the compositions $(i_-^*)^{-1} \circ i_-^*$, it similarly follows from Theorem 4.27 after we rewrite the relevant categories in terms of λ^{-1} using Lemma 4.25. Explicitly, we have:

$$F_\lambda^0(\langle \mathcal{U}_i(u_W), \mathcal{V}_i(u_W)\rangle) = F_{\lambda^{-1}}^{-\eta}(\langle \mathcal{V}'_{n-i}(u_W) \otimes \omega_{Z_\lambda}, \mathcal{U}'_{n-i}(u_W)\rangle)$$

$$F_\lambda^0(\langle \mathcal{U}_{i+1}, \mathcal{V}_{i+1}\rangle) = F_{\lambda^{-1}}^{-\eta}(\langle \mathcal{V}'_{n-i-1} \otimes \omega_{Z_\lambda}, \mathcal{U}'_{n-i-1}\rangle$$

By the Lefschetz property , we see that:

$$\mathcal{V}_i(u_W) = \langle E_{i+1}, \dots, E_{m_{\Delta,W}}, E_{m_{\Delta,W}}(u_W)\rangle = \langle \mathcal{V}_{i+1}, E_{m_{\Delta,W}}(u_W)\rangle$$

Thus, since $\omega_{Z_\lambda} \cong \mathcal{O}(-m_{\Delta,W} u_W)$ and $E_i(u_W) = E_{i+1}$ for $i > 0$, $\mathcal{V}_i(u_W) \otimes \omega_{Z_\lambda} = \langle \mathcal{V}_{i+1} \otimes \omega_{Z_\lambda}, E_1\rangle$. Hence $\mathcal{V}'_{n-i}(u_W) \otimes \omega_{Z_\lambda} = \langle \mathcal{V}'_{n-i-1} \otimes \omega_{Z_\lambda}, E'_1\rangle$.

By Corollary 4.28:

$L_{E_1'^-}$ maps $F_{\lambda^{-1}}^{-\eta}(\langle \mathcal{V}'_{n-i}(u_W) \otimes \omega_{Z_\lambda}, \mathcal{U}'_{n-i}(u_W)\rangle)$ to $F_{\lambda^{-1}}^{-\eta}(\langle \mathcal{V}'_{n-i-1} \otimes \omega_{Z_\lambda}, \langle E_1, \mathcal{U}_{n-i}(u_W)\rangle'\rangle)$

But we know that $\langle \mathcal{V}'_{n-i-1} \otimes \omega_{Z_\lambda}, \mathcal{U}'_{n-i-1}\rangle$ is an SOD of $D^b(Z_{\lambda^{-1}})_{-\eta}$ so $\langle E_1, \mathcal{U}_{n-i}(u_W)\rangle' = \mathcal{U}'_{n-i-1}$ and hence:

$$F_{\lambda^{-1}}^{-\eta}(\langle \mathcal{V}'_{n-i-1} \otimes \omega_{Z_\lambda}, \langle E_1, \mathcal{U}_{n-i}(u_W)\rangle'\rangle) = F_{\lambda^{-1}}^{-\eta}(\langle \mathcal{V}'_{n-i-1} \otimes \omega_{Z_\lambda}, \mathcal{U}'_{n-i-1}\rangle)$$

Finally, it remains to show that the mutation functors agree with $(i_\pm^*)^{-1} \circ i_\pm^*$. This follows immediately by noting that, for any $E \in D^b(Z'_\lambda)$, $E^\pm$ is supported on $Y_{\lambda^\pm}$ and hence $E^\pm|_{X_\pm} = 0$. So the claim follows by the formula for left mutation. □

Lemma 6.23. *If $E, F \in D^b(Z'_\lambda)$ are such that $Hom(F, E) = 0$ and at least one is compactly supported, then E'^- and F^+ are orthogonal.*

Proof. $\mathrm{Hom}_{D^b(X_0)}(E'^-, F^+) = \mathrm{Hom}_{D^b(Z'_\lambda)}(E'^-|_{Z'_\lambda}, F)$ using Lemma 4.6. As E^- is supported on $Y_{\lambda^{-1}}$ (of codimension c in X_0), we can use the Koszul resolution to show that $E^-|_{Z_\lambda} = E \otimes (\oplus_{i=0,\dots,c} \Lambda^i \mathcal{N}^\vee_{Y_{\lambda^{-1}}, X_0})|_{Z_\lambda}$. As E and $\kappa_\lambda^\vee$ have λ-weight 0 and η respectively:

$$E'^-|_{Z'_\lambda} = (E^- \otimes \kappa_\lambda^\vee)|_{Z_\lambda} = E \otimes \mathrm{wt}_{\lambda=-\eta}(\oplus_{i=0,\dots,c} \Lambda^i \mathcal{N}^\vee_{Y_{\lambda^{-1}}, X_0})|_{Z^\lambda} \otimes \kappa_\lambda^\vee|_{Z_\lambda}$$

As all λ-weights of $\mathcal{N}^\vee_{Y_{\lambda^{-1}}, X_0}|_{Z_\lambda}$ are strictly negative and $-\eta$ is the sum of all such weights, only $\det(\mathcal{N}^\vee_{Y_{\lambda^{-1}}, X_0})|_{Z_\lambda}$ has λ-weight $-\eta$, so $E'^-|_{Z'_\lambda} = E \otimes (\kappa_{\lambda^{-1}}^\vee \otimes \kappa_\lambda^\vee)|_{Z'_\lambda}$.

Taking determinants of the decomposition:

$$TX_0|_{Z_\lambda} = TZ'_\lambda \oplus \mathcal{N}_{Y_\lambda, X_0}|_{Z_\lambda} \oplus \mathcal{N}_{Y_{\lambda^{-1}}, X_0}|_{Z_\lambda}$$

along Z_λ, we see that $\omega_{X_0}|_{Z_\lambda} \cong \omega_{Z'_\lambda} \otimes (\kappa_\lambda^\vee \otimes \kappa_{\lambda^{-1}}^\vee)|_{Z_\lambda}$. As X_0 is Calabi–Yau, we see that $(\kappa_\lambda^\vee \otimes \kappa_{\lambda^{-1}}^\vee)|_{Z_\lambda} \cong \omega_{Z'_\lambda}^\vee$ and hence $E'^-|_{Z'_\lambda} = E \otimes \omega_{Z'_\lambda}^\vee$. Using this:

$$\begin{aligned}\mathrm{Hom}_{D^b(X_0)}(E'^-, F^+) &= \mathrm{Hom}_{D^b(Z'_\lambda)}(E'^-|_{Z'_\lambda}, F) = \mathrm{Hom}_{D^b(Z'_\lambda)}(E \otimes \omega_{Z'_\lambda}^\vee, F) \\ &= \mathrm{Hom}_{D^b(Z'_\lambda)}(E, F \otimes \omega_{Z'_\lambda}) = \mathrm{Hom}(F, E) = 0\end{aligned}$$

by Serre duality on Z'_λ (which is valid as at least one of E, F is compactly supported) and $\mathrm{Hom}(F, E) = 0$.

Similarly, using the right adjoint in Lemma 4.6:

$$\mathrm{Hom}_{D^b(X_0)}(F^+, E'^-) = \mathrm{Hom}_{D^b(Z'_\lambda)}(F, (E^-)|_{Z'_\lambda}) = \mathrm{Hom}(F, E) = 0$$

□

Remark 6.24. We can alternatively prove this result in terms of fundamental groups. It follows from [25] that the corresponding auto-equivalences $\rho^W((\gamma^{0,j-1}_{C_1,C_2})^{-1} \circ \gamma^{0,j}_{C_1,C_2})$ (known as *fractional* window shifts) can be described as the twist about the spherical functor $F_0 \circ i_{E_j} : \langle E_j \rangle \to D^b(X_{C_1})$ where $i_{E_j} : \langle E_j \rangle \to D^b(Z'_\lambda)$ is the inclusion of the j-th piece of the SOD and F_0 is the functor from Remark 4.19.

This proof is slightly less complicated than the one above as all the mutations are hidden in the description of the fractional window shifts. We have chosen the proof above because it maintains the groupoid perspective which we adopt in this thesis.

Remark 6.25. Having constructed this representation of $\pi_1(V_W)$ for each wall W, we can try to glue these all together along the large radius regions V_C near torus fixed points. We do this exactly as in Remark 5.16. By the (groupoid) van-Kampen theorem, this then give us a representation of the fundamental groupoid of a tubular neighbourhood of the toric boundary in any 2d FIPS. This is slightly more useful than the analogous large radius representation in Remark 5.24 as this groupoid should generate the fundamental groupoid of the FIPS. This follows from the Lefschetz hyperplane theorem (see Remark 9.12).

However, as in Remark 5.24, the fact that ρ^W is not canonical (see Remark 6.10) means that this abstract gluing is not very helpful when we try to extend the representation to $\pi_1(\mathrm{FIPS})$. In fact, ρ^W is even less canonical on near large radius paths as it depends on a choice of SOD, so the situation is only going to be worse.

7. Fundamental group representations of a 2d FIPS

From §6, we understand how to construct a representation on each region V_W near large radius. However (see Remark 6.25) gluing these regions and the representations on them together arbitrarily is not a good idea. In this section, we use a pencil on the secondary stack $\mathfrak{F}$ to help us pick these regions near different curves $Z(W)$ in the toric boundary in such a way that the relations between paths in these different regions become transparent.

In this section, we shall carry out this approach successfully for two examples, namely the Octahedron VGIT and the Pentagon VGIT and, as a result, will be able to construct the full representation of $\pi_1(\mathrm{FIPS})$. The strategy for doing so is the same in both cases:

(1) (Topology) Apply the Zariski–van-Kampen theorem (see Theorem 7.3) to our pencil to find a presentation for $\pi_1(\mathrm{FIPS})$ in terms of a specific choice

of near large radius regions (adapted to our pencil) plus some additional explicit relations $\mathcal{R}$.

(2) (Magic windows) Implement the relations in $\mathcal{R}$ using (fractional) magic windows (see §4.2).

Before we launch into these examples, it will be useful to present the Zariski–van-Kampen theorem in a suitably groupoid way.

7.1. **The Zariski–van-Kampen Theorem.** In this section, we describe a general technique to understand the fundamental group(oid) of a 2-dimensional FIPS using a pencil of curves, based on ideas of Zariski and van-Kampen. For a good introduction with lots of pictures, we refer to [13].

Suppose F is a (connected) complex surface with a surjective morphism $f : F \twoheadrightarrow C$ onto a curve C. We assume additionally that:

(1) Away from a finite set of critical values $Z \subset C$, $f' : F' \to B$ is a locally trivial fibration where $B := C \backslash Z$, $F' := f^{-1}(B) \subset F$ and $f' = f|_{F'}$. We denote by F_b the fibre over $b \in B$.
(2) The critical fibres $f^{-1}(z)$ for all $z \in Z$ are irreducible.
(3) We have picked points $\{b_i\}$ in B for $i = 1, \dots, n$.
(4) There are disjoint continuous sections $s_j : B \to F'$ of f' for $j = 1, \dots, m$. We define the basepoints in the fibre F_{b_i} to be $p_{ij} := s_j(b_i)$.

Remark 7.1. For Theorem 7.3, it is enough to have picked basepoints p_{ij} and then have sections $(s_j)_* : \pi_1(B, \{b_i\}) \hookrightarrow \pi_1(F', \{p_{ij}\})$ of f'_* at the level of π_1 for $j = 1, \dots, m$.

Recall that, if $B \subset F$ is an irreducible hypersurface, a *meridian* of B (see [13], Definition 4.13 for the precise definition) is roughly a loop in $F \backslash B$ given by travelling from your basepoint to nearby a smooth point of B, doing a small loop in $F \backslash B$ around this point and going back to your basepoint along the same path. Then we have:

Proposition 7.2 ([13], Proposition 1.2)**.** *For fixed j, k, if i denotes the inclusion $F \backslash B \subset F$ then $\ker(i_* : \pi_1(F \backslash B, p_{jk}) \twoheadrightarrow \pi_1(F, p_{jk}))$ is the normal subgroup generated by a meridian of B.*

This forms an important part of the proof of the following theorem, whose fundamental group version is standard (see, for example, [13], §2).

Theorem 7.3 (Groupoid version of the Zariski–van-Kampen theorem [35, 37])**.** *$\pi_1(F, \{p_{ij}\})$ is generated by:*

$\pi_1(F_{b_i}, \{p_{ij}\} \cap F_{b_i})$ (one copy for each i) and $(s_j)_*(\pi_1(B, \{b_i\}))$ (one copy for each j)

subject to the relations:

- *$\gamma'_z = e$ where γ'_z is a meridian in F around the critical fibre $f^{-1}(z)$ for $z \in Z$*

- *the monodromy relations* $(s_l)_*(\alpha) \circ \gamma \circ (s_k)_*(\alpha^{-1}) = m_\alpha(\gamma)$ *where* $\alpha \in \pi_1(B, b_i, b_j), \gamma \in \pi_1(F_{b_i}, p_{ik}, p_{il})$ *for any* i, j, k, l *and* $m_\alpha(\gamma) \in \pi_1(F_{b_j}, p_{jk}, p_{jl})$ *denotes the monodromy of* γ *along* α.

(Sketch). As in [13], §5, we can define monodromy along any path in the base for a locally trivial fibration by the homotopy lifting extension property. Then the same argument which shows the fundamental group of the total space of such a fibration (with a section) is the semi-direct product of the fundamental group of the fibre with the fundamental group of the base (where the latter acts on the former by monodromy), shows, by (1) and (4), that $\pi_1(F', \{p_{ij}\})$ is generated by $\pi_1(F_{b_i}, \{p_{ij}\} \cap F_{b_i})$ (one copy for each i) and $(s_j)_*(\pi_1(B, \{b_i\}))$ (one copy for each j) subject to $(s_l)_*(\alpha) \circ \gamma \circ (s_k)_*(\alpha^{-1}) = m_\alpha(\gamma)$.

Note that the map induced by inclusion $i_* : \pi_1(F', \{p_{ij}\}) \to \pi_1(F, \{p_{ij}\})$ is full as we are deleting fibres which are of real codimension 2. Its kernel consists only of loops and $\ker(i_*)_{p_{ij}} = \ker(i_* : \pi_1(F', p_{ij}) \to \pi_1(F, p_{ij}))$. By Proposition 7.2 and (2), we know that this is generated by a meridian γ'_z around the critical fibre $f^{-1}(z)$ for $z \in Z$. □

Remark 7.4. For our applications, we are always going to take f coming from a choice of pencil $\hat{f} : \mathfrak{F} \dashrightarrow \mathbb{P}^1$ on the secondary stack $\mathfrak{F}$. Then so long as the basepoints of $\hat{f}$ are contained in the discriminant, we can take $F = \mathrm{FIPS}$ and f to be the morphism $f := \hat{f}|_{\mathrm{FIPS}} \twoheadrightarrow C \subset \mathbb{P}^1$ with image C.

Remark 7.5. One particularly nice case of Theorem 7.3 is when the section s_j extends over $z \in Z$. If we denote this extension by s_j too, then $s_j \circ \gamma_z$ is a meridian around the critical fibre $f^{-1}(z)$ where $\gamma_z \in \pi_1(B, \{b_i\}_i)$ is (up to change of basepoint) a sufficiently small loop in B around z. As such, we can take $\gamma'_z = s_j \circ \gamma_z$ in Theorem 7.3. If we just have sections on π_1 (see Remark 7.1), then the analogue of the condition that s_j extends over $z \in Z$ is that $(s_j)_*(\gamma_z) = e$ in $\pi_1(F, \{p_{ij}\})$.

Example 7.6. Let's take F to be the complement in $\mathbb{C}^2_{X,Y}$ of the hyperplanes $\mathcal{A} := \{X = 1\} \cup \{Y = 1\}$ and the morphism f given by projection $f : (X, Y) \mapsto X$. So $C = \mathbb{C} \setminus \{X = 1\}$ and we have:

(1) f is a fibration over C (with fibre $F_b \cong \mathbb{C}_Y \setminus \{Y = 1\}$) and so $B = C$ and $Z = \varnothing$.
(2) Nothing to check
(3) Take $b_1, b_2 \in B$ with X-coordinate $\in \mathbb{R}_{>0}$ small and large respectively. These are shown at the bottom of Figure 14.
(4) Choose two disjoint sections $s_j(X) = (X, \epsilon_j)$ for $\epsilon_j \in \mathbb{R}_{>0}$ small and large respectively. So we have 4 basepoints $p_{11}, p_{21}, p_{22}, p_{12}$.

Here the sections extend over $Z = \varnothing$ trivially and so, using Remark 7.5, Theorem 7.3 says that $\pi_1(F, \{p_{ij}\})$ is generated by $\pi_1(F_{b_j}, \{p_{j1}, p_{j2}\})$ for $j = 1, 2$ and $s_j(\gamma_k)$ for $j, k = 1, 2$ where $\gamma_k \subset B$ are shown in blue in Figure 14 and freely generate

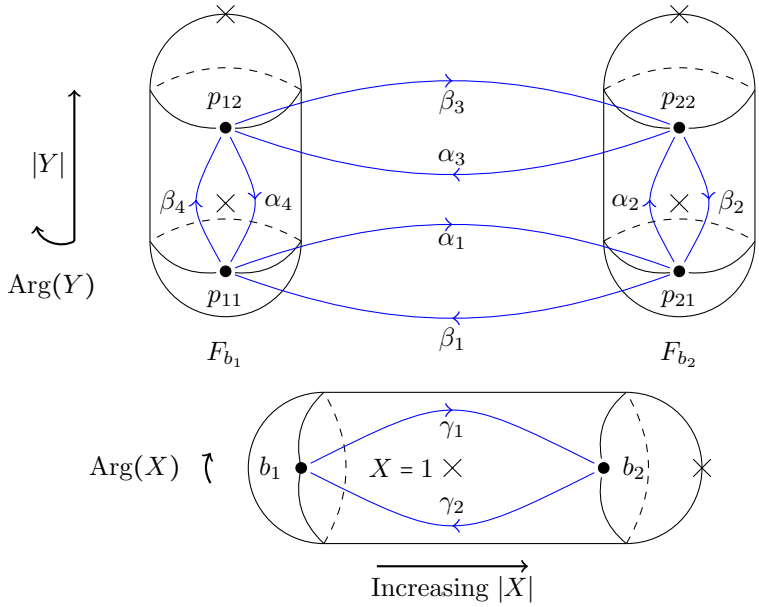

FIGURE 14. Generators for fundamental groupoids of fibres and base in Example 7.6

$\pi_1(B, \{b_1, b_2\})$. Moreover, since $Z = \varnothing$, we only have monodromy relations. As f is a trivial fibration and we have picked trivial sections, monodromy along any path is trivial.

Pick free generators for $\pi_1(F_{b_j}, \{p_{j1}, p_{j2}\})$ as shown in blue in Figure 14, where we are drawing the fibres by projecting onto $\mathbb{C}_Y$. Call $s_1(\gamma_1) =: \alpha_1, s_2(\gamma_1) = \beta_3, s_1(\gamma_2) = \beta_1$ and $s_2(\gamma_2) = \alpha_3$.

Finally we check that monodromy gives the following relations:

Monodromy along γ_1:

$$\alpha_1 \circ \alpha_4 \circ \beta_3^{-1} = \beta_2, \beta_3 \circ \beta_4 \circ \alpha_1^{-1} = \alpha_2$$

Monodromy along γ_2:

$$\beta_1 \circ \beta_2 \circ \alpha_3^{-1} = \alpha_4, \alpha_3 \circ \alpha_2 \circ \beta_1^{-1} = \beta_4$$

Remark 7.7. This description agrees with the Deligne groupoid of the real hyperplane arrangement given by $\mathcal{A}$ (see [29, 30]).

7.2. **The Octahedron VGIT.** Here we revisit the Octahedron VGIT from §5.3, which is visibly not quasi-symmetric (see Definition 8.1). Our aim is to construct a representation of its fundamental groupoid (see Theorem 7.16) following the strategy outlined at the start of this chapter. As such, the next section covers the topology and the subsequent section constructs the required magic windows.

7.2.1. *Topology using Zariski–van-Kampen.* In this section, we apply the Zariski–van-Kampen theorem to describe the topology of the FIPS for the Octahedron VGIT. The ultimate aim is to find a presentation for $\pi_1(\text{FIPS})$ in terms of specific near large radius regions plus some extra explicit relations.

Recall that $\mathfrak{F} \cong \mathbb{P}^2$ with coordinates $[x, y, z]$ and, in line with Remark 7.4, take the pencil $x = bz$ where $b \in \mathbb{C}$ is a coordinate on the base. This has a unique basepoint at $p_1 := [0, 1, 0]$ and, since the whole toric boundary is in the discriminant, we get a morphism:

$$f : \text{FIPS} \twoheadrightarrow C, [x, y, z] \mapsto x/z$$

where the image $C = \mathbb{C}^*_b$. Note that this agrees with the map π' from §5.3.

Remark 7.8. In coordinates $X = x/z, Y = y/z$ on the FIPS $\subset (\mathbb{C}^*)^2_{X,Y}$, $f(X, Y) = X$ and, using Horn uniformisation (see (4) in §3.6), there are two points of ∇_{pr} in the fibre $X = b$ with Y-coordinates $(1 \pm \sqrt{b})^2$.

Notation: $p_2 := [1, 0, 0], p_3 := [0, 0, 1]$. Let $Z(W_i)$ be the torus-invariant curve connecting p_{i+1}, p_{i+2} where the indices are read modulo 3 and W_i be the wall between the corresponding chambers, as labelled in Figure 8.

We now check that all the conditions in the Zariski–van-Kampen Theorem (Theorem 7.3) are satisfied:

(1) Since the elements of the pencil in $\mathfrak{F}$ are $\cong \mathbb{P}^1$ and the discriminant is a smooth conic plus the toric boundary, the generic fibre F_b of f is $\cong \mathbb{C}^* \setminus \{2 \text{ points}\}$. One checks that this is a locally trivial fibration over $C \setminus \{b = 1\}$. However, as b approaches 1, one of the points of the conic approaches $\{Y = 0\}$ in the fibre and so the critical locus $Z = \{b = 1\} \subset C$. The base B is shown at the bottom of Figure 16.
(2) $f^{-1}(1) \cong \mathbb{C}^* \setminus \{1 \text{ point}\}$ is irreducible.
(3) Pick two basepoints in B given by $b = b_1 \in \mathbb{R}_{>0}$ sufficiently large and $b = b_2 \in \mathbb{R}_{>0}$ sufficiently small. Then $\pi_1(B, \{b_1, b_2\})$ is the free groupoid on the paths ζ_1, ζ_2 and ζ_3 shown in blue at the bottom of Figure 16.
(4) Pick two sections s_j of f' for $j = 1, 2$, which we shall choose to lie in $\{Y = \epsilon_j\}$ for $\epsilon_1 \in \mathbb{R}_{>0}$ sufficiently large and $\epsilon_2 \in \mathbb{R}_{>0}$ sufficiently small. By Remark 7.1, we need only define lifts of ζ_i for $i = 1, 2, 3$. Defining $s_j(b) := (b, \epsilon_j) \in \mathbb{C}^2_{X,Y}$, we check that $s_j(\zeta_i)$ are such lifts.

Remark 7.9. Since the X-coordinates of the two points in $\nabla_{pr} \cap \{Y = \epsilon_1\}$ have large modulus, we have that $s_1(\gamma_z) = e$ where (as in Remark 7.5) γ_z is a small loop in B around $z = 1$. On the other hand, the X-coordinates of the two points in $\nabla_{pr} \cap \{Y = \epsilon_2\}$ are close to $X = 1$ and so $s_2(\gamma_z)$ (in addition to looping $X = 1$) loops around them too. Hence $s_2(\gamma_z)$ is *not* a meridian around the fibre F_1.

Then, using Remarks 7.5 and 7.9, the Zariski–van-Kampen Theorem (Theorem 7.3) gives us:

Corollary 7.10. *$\pi_1(FIPS, \{p_{ij}\})$ is generated by:*

$$\pi_1(F_{b_1}, \{p_{11}, p_{12}\}), \pi_1(F_{b_2}, \{p_{21}, p_{22}\}) \text{ and } s_j(\zeta_i) \text{ for } i = 1,2,3, j = 1,2$$

subject to the relation $s_1(\zeta_3) = s_1(\zeta_2\zeta_3\zeta_1^{-1})$ and the monodromy relations along ζ_i ($i = 1,2,3$).

We now want to understand this presentation in terms of imposing additional relations on $\pi_1(U)$ where $U \subset$ FIPS is a specific collection of near large radius regions in the FIPS glued together. Recall that the reason we want to do this is that we know from §6 how to define a representation on $\pi_1(U)$ for free.

So how should we pick U so that it can be compared easily with the presentation in Corollary 7.10? For this, we note that the choices made for the Zariski–van-Kampen Theorem give some natural choices of near large radius regions. Our choice of pencil on the FIPS means that F_{b_i} are $(1,1)$-orbits and so F_{b_1} is the push-off of $Z(W_3)$ defined by $\beta_{W_3} = (1,1)$. Similarly F_{b_2} is the push-off of $Z(W_2)$ defined by $\beta_{W_2} = (1,1)$. The section s_2 lies in an orbit of the 1-PS $(1,0)$ and so $\mathrm{Im}(s_2)$ lives in the push-off of $Z(W_1)$ defined by $\beta_{W_1} = (1,0)$. Similarly $\mathrm{Im}(s_1)$ lives in the push-off of $Z(W_3)$ defined by $\beta_{W_3} = (1,0)$.

Remark 7.11. Note that β_{W_1} is not fixed by the pencil itself but by the section s_2 and so different sections (which mean that s_2 lies in $\{X^nY = \epsilon\}$ for different n) give different natural choices for β_{W_1}.

The corresponding near large radius regions in the FIPS defined by these choices can be written explicitly as:

$$U_1 := \{|Y| \le \epsilon_2\}, U_2 := \{|X| \le b_2\}, U_3 := \{|X| \ge b_1\}, U_4 := \{|Y| \ge \epsilon_1\}$$

so that (for $i = 1,2,3$) U_i is the near large radius region near $Z(W_i)$ (defined by $\beta_{W_1} = (1,0), \beta_{W_2} = \beta_{W_3} = (1,1)$). The images Δ_i of the four subsets U_i under the moment map $\mu : \mathbb{P}^2 \twoheadrightarrow \Delta := \mu(\mathbb{P}^2)$ are shown in Figure 15 (R). Gluing them together, we define $U := \bigcup_{i=1,2,3,4} U_i$.

Remark 7.12. Because of how we chose β_{W_2} and β_{W_3}, we have that $U_3 = f^{-1}(D_1)$ and $U_2 = f^{-1}(D_2)$ where D_i is the punctured disk in C bounded by ζ_i for $i = 1,2$.

As we did at the end of §6.1, we now pick presentations of $\pi_1(F_{b_i}, \{p_{i1}, p_{i2}\})$ as free groupoids on the generators shown in blue in Figure 16, where the coordinate on the fibres is Y. We use the notation for near large radius paths from §6.1 so that, once an SOD on the wall W_i has been specified, we know what ρ^{W_i} on these paths is (see Remark 6.14). We have chosen these particular generators on the different fibres to make the monodromy relations as simple as possible. We also pick free generators for paths in $Y = \epsilon_2$ given by the two toric loops $\alpha_{C_i}^{(1,0)}$ (for $i = 2,3$) and the paths $\gamma_{C_2,C_3}^{0,0} := s_2(\zeta_3), \gamma_{C_3,C_2}^{0,1}$ shown in blue in Figure 17. We also define the path $\gamma_{C_1,C_3}^{0,1} := \alpha_{C_3}^{(1,1)} \circ \gamma_{C_1,C_3} \circ \alpha^{-1} \in \pi_1(F_{b_2}, \{p_{21}, p_{22}\})$ where γ_{C_1,C_3} is shown in Figure 16.

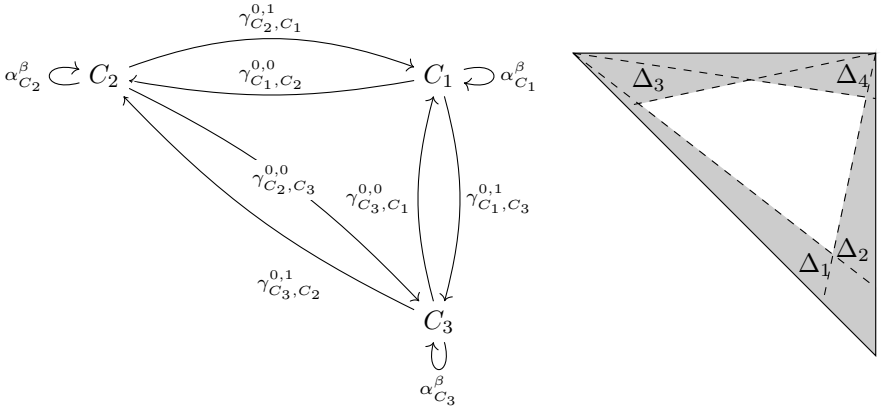

FIGURE 15. Generators of $\pi_1(U, \{p_{11}, p_{12}, p_{22}\})$ for the Octahedron VGIT (L) and image of near large radius regions covering U under the moment map (R)

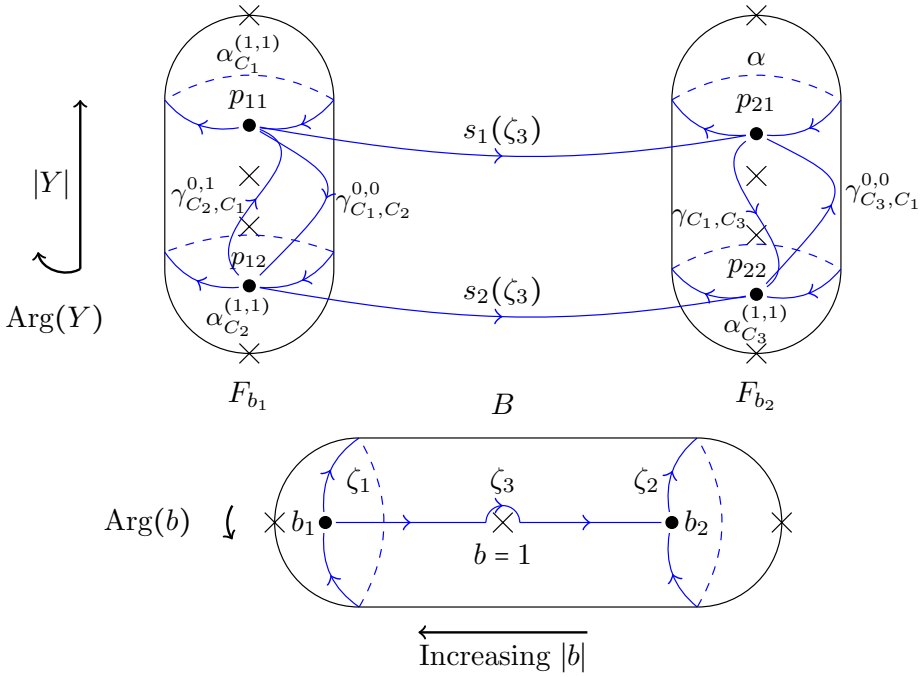

FIGURE 16. Generators for $\pi_1(F_{b_i}, \{p_{i1}, p_{i2}\})$ and $\pi_1(B, \{b_1, b_2\})$. The 2 points in ∇_{pr} in the fibre F_b are $Y = (1 \pm \sqrt{b})^2$

Remark 7.13. We note that the sections $s_j(\zeta_i)$ for $i = 1, 2$ actually define toric loops corresponding to $(1, 0)$. To be more in line with the notation of the previous sections, we therefore relabel $\alpha^{(1,0)}_{C_i} := s_i(\zeta_1)$ for $i = 1, 2$ and $\alpha^{(1,0)}_{C_3} := s_2(\zeta_2)$.

Now we repackage the presentation in Corollary 7.10 in terms of $\pi_1(U)$ and see what's left over. The near large radius region U_2 can be described in terms of F_{b_2}, $s_j(\zeta_2)$ and monodromy along ζ_2 (see Remark 7.12). Similarly U_3 can be described in terms of F_{b_1}, $\alpha^{(1,0)}_{C_j}$ (for $j = 1, 2$) and monodromy along ζ_1. We'll now see that the

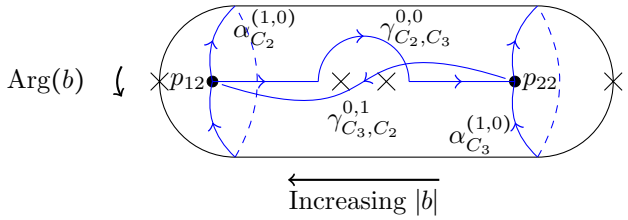

FIGURE 17. Free generators of $\pi_1(\{Y = \epsilon_2\}, \{p_{12}, p_{22}\})$

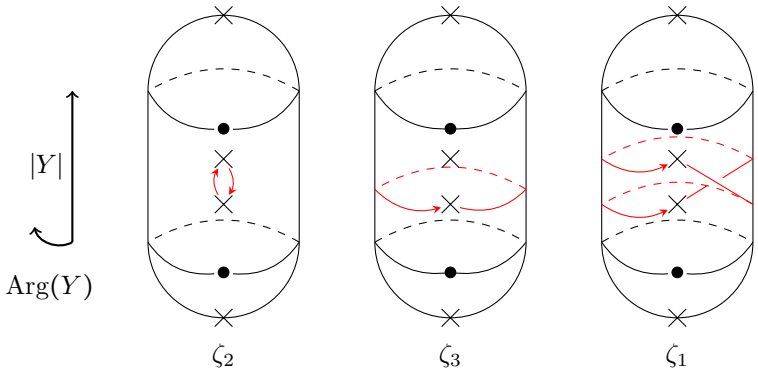

FIGURE 18. Monodromy of F_b around the 3 loops ζ_1, ζ_2 and ζ_3

additional relations on $\pi_1(U)$ only come from monodromy along ζ_3. More precisely, we get:

Proposition 7.14. *$\pi_1(FIPS, \{p_{11}, p_{12}, p_{22}\})$ is generated by $\pi_1(U, \{p_{11}, p_{12}, p_{22}\})$ subject to the relations:*

(1) $\gamma^{0,0}_{C_2,C_3} \circ \gamma^{0,0}_{C_1,C_2} = \gamma^{0,1}_{C_1,C_3}$
(2) $\gamma^{0,0}_{C_3,C_1} \circ \gamma^{0,0}_{C_2,C_3} = \gamma^{0,1}_{C_2,C_1}$
(3) $\gamma^{0,0}_{C_1,C_2} \circ \gamma^{0,0}_{C_3,C_1} = \gamma^{0,1}_{C_3,C_2}$

Remark 7.15. Recall that the presentation in Corollary 7.10 used the 4 basepoints p_{ij}. In the proposition above, we only use 3 of them (one near each p_i). Happily, there is a canonical equivalence $\pi_1(\text{FIPS}, \{p_{ij}\}) \cong \pi_1(\text{FIPS}, \{p_{11}, p_{12}, p_{22}\})$ using the canonical (homotopy class of) path between p_{11} and p_{21} near p_1 (see Remark 5.16) to identify p_{21} with p_{11}. In fact, as s_1 extends over $b = 1$, this path agrees with $s_1(\zeta_3)$. We abuse notation and denote by the same symbols the images in $\pi_1(\text{FIPS}, \{p_{11}, p_{12}, p_{22}\})$. For example, in $\pi_1(\text{FIPS}, \{p_{11}, p_{12}, p_{22}\})$ $\gamma^{0,0}_{C_3,C_1}$ refers to the path from p_{22} to p_{11} given by $s_1(\zeta_3)^{-1} \circ \gamma^{0,0}_{C_3,C_1}$. Under these identifications, $\pi_1(U, \{p_{11}, p_{12}, p_{22}\})$ is generated by the paths in Figure 15 (L).

Proof. For now, we work with all 4 basepoints p_{ij}. At the end, we will then remove p_{21}.

The monodromy around the loops ζ_i is shown in Figure 18, where we are projecting onto the Y-coordinate so the basepoints appear fixed and the path taken by the discriminant is indicated by the arrows.

Note that $\gamma^{0,1}_{C_3,C_2}$ is not among the generators in Corollary 7.10. We claim that we can write it in terms of them as $\gamma^{0,0}_{C_1,C_2} \circ s_1(\zeta_3^{-1}) \circ \gamma^{0,0}_{C_3,C_1}$. To see this, note that (as Figure 16 makes clear) under the projection $g : (X, Y) \mapsto Y$ $\gamma^{0,0}_{C_1,C_2}$ and $\gamma^{0,0}_{C_3,C_1}$ map to inverse paths in $B' = \mathbb{C}^*_Y \setminus \{Y = 1\}$. It is easy to see (because of the $\mathbb{Z}_3$-symmetry of the VGIT or explicitly) that g defines a fibration over these paths. We choose sections $s_j(b') = (b_j, b')$ living inside $X = b_j$ and so $s_2(g(\gamma^{0,0}_{C_3,C_1})) = \gamma^{0,0}_{C_3,C_1}$ and similarly $s_1(g(\gamma^{0,0}_{C_1,C_2})) = \gamma^{0,0}_{C_1,C_2}$. Therefore monodromy along such paths is defined and following $s_1(\zeta_3^{-1})$ along $g(\gamma^{0,0}_{C_1,C_2})$ gives a path in $Y = \epsilon_2$ from p_{22} to p_{12} which is homotopic to $\gamma^{0,0}_{C_1,C_2} \circ s_1(\zeta_3^{-1}) \circ \gamma^{0,0}_{C_3,C_1}$. One checks that it is, in fact, $\gamma^{0,1}_{C_3,C_2}$.

Now we package the presentation in Corollary 7.10 into pieces we understand and see what's left over. Note that, by Remark 7.12 and the Zariski–van-Kampen theorem applied to U_3, $\pi_1(F_{b_1}, \{p_{11}, p_{12}\})$, $\alpha^{(1,0)}_{C_1}$, $\alpha^{(1,0)}_{C_2}$ plus the monodromy relations along ζ_1 just give a copy of $\pi_1(U_3, \{p_{11}, p_{12}\})$. Similarly, $\pi_1(F_{b_2}, \{p_{21}, p_{22}\})$, $\alpha^{(1,0)}_{C_3}$, α plus the monodromy relations along ζ_2 give a copy of $\pi_1(U_2, \{p_{21}, p_{22}\})$.

By definition, $s_1(\zeta_3)$ lives in $U_4 \setminus \mathrm{Int}(U_2) \cup \mathrm{Int}(U_3)$. As we see from Figure 15, we can think of the region $U_2 \cup U_3 \cup U_4$ as the near large radius regions along $Z(W_2)$ and $Z(W_3)$ glued together along a large radius region near p_1. From this perspective, $s_1(\zeta_3)$ is just the canonical path between p_{11} and p_{21} in this large radius region. As such (see Remark 5.16), $\pi_1(U_2 \cup U_3 \cup U_4, \{p_{ij}\})$ is the groupoid generated by $\pi_1(U_2, \{p_{21}, p_{22}\})$, $\pi_1(U_3, \{p_{11}, p_{12}\})$ and $s_1(\zeta_3)$ subject to the relation $s_1(\zeta_3) = s_1(\zeta_2\zeta_3\zeta_1^{-1})$.

Therefore, packaging up our presentation of $\pi_1(\mathrm{FIPS})$ in this way, we see that $\pi_1(\mathrm{FIPS})$ is generated by $\pi_1(U_2 \cup U_3 \cup U_4)$ and $s_2(\zeta_3) = \gamma^{0,0}_{C_2,C_3}$ subject only to the monodromy relations along ζ_3.

Monodromy relations for ζ_3: In terms of b, near $b = 1$ ζ_3 is $t \mapsto 1 + \epsilon e^{-\pi i t}$ for $t \in [0, 1]$). Then we get monodromy relations:

- $\gamma^{0,0}_{C_2,C_3} \circ \alpha^{(1,1)}_{C_2} \circ (\gamma^{0,0}_{C_2,C_3})^{-1} = \alpha^{(1,1)}_{C_3}$
- $s_1(\zeta_3) \circ \alpha^{(1,1)}_{C_1} \circ s_1(\zeta_3)^{-1} = \alpha$
- $\gamma^{0,0}_{C_2,C_3} \circ \gamma^{0,0}_{C_1,C_2} \circ s_1(\zeta_3)^{-1} = \gamma^{0,1}_{C_1,C_3}$
- $s_1(\zeta_3) \circ \gamma^{0,1}_{C_2,C_1} \circ (\gamma^{0,0}_{C_2,C_3})^{-1} = \gamma^{0,0}_{C_3,C_1}$

If we use $s_1(\zeta_3)$ to identify p_{11} with p_{21}, then, using $s_1(\zeta_2) = s_1(\zeta_3\zeta_1\zeta_3^{-1})$ and $\alpha = s_1(\zeta_3) \circ \alpha^{(1,1)}_{C_1} \circ s_1(\zeta_3)^{-1}$ to get rid of these generators, we see that $\pi_1(\mathrm{FIPS}, \{p_{11}, p_{12}, p_{22}\})$ is generated by $\pi_1(U_2 \cup U_3 \cup U_4, \{p_{11}, p_{12}, p_{22}\})$ and $\gamma^{0,0}_{C_2,C_3}$ subject to relations (1) and (2) and monodromy invariance for $\gamma^{0,0}_{C_2,C_3}$.

If instead we present $\pi_1(\mathrm{FIPS}, \{p_{11}, p_{12}, p_{22}\})$ in terms of all the previous generators plus $\gamma^{0,1}_{C_3,C_2}$ and all the old relations plus relation (3), then we see that this presentation is generated by $\pi_1(U_2 \cup U_3 \cup U_4, \{p_{11}, p_{12}, p_{22}\})$, $\gamma^{0,0}_{C_2,C_3}$ and $\gamma^{0,1}_{C_3,C_2}$ subject to relations (1),(2),(3) and monodromy invariance for $\gamma^{0,0}_{C_2,C_3}$. Packaging $\gamma^{0,0}_{C_2,C_3}$ and $\gamma^{0,1}_{C_3,C_2}$ together to give the remaining generators of $\pi_1(U_1)$ and noting that the monodromy relation for $\gamma^{0,1}_{C_3,C_2}$ must follow automatically since it holds in

$\pi_1(\text{FIPS})$, we see that $\pi_1(\text{FIPS}, \{p_{11}, p_{12}, p_{22}\})$ is generated by $\pi_1(U, \{p_{11}, p_{12}, p_{22}\})$ subject to relations (1),(2) and (3) as claimed. □

7.2.2. *Fundamental groupoid representation.* By Proposition 7.14, we know that $\pi_1(\text{FIPS})$ is generated by $\pi_1(U)$ where U is covered by near large radius regions. Therefore, if we choose the SOD $D^b(Z'_\lambda) = \langle \mathcal{O}(-u_{W_i}), \mathcal{O} \rangle$, Theorem 6.15 gives us the near large radius representation ρ^{W_i} on $\pi_1(U_i)$ (for $i = 1, 2, 3$). Moreover, if we include U_4 too, Remark 6.25 tells us how to glue these all together to get a representation of $\pi_1(U)$.

We now check that the 3 extra relations in Proposition 7.14 hold. We have already noted in Example 4.34 that there are no magic windows in this example. However, it turns out that there are fractional magic windows.

Theorem 7.16. *$\pi_1(FIPS, \{p_{11}, p_{12}, p_{22}\})$ acts on the phases of the Octahedron VGIT such that, near the curve $Z(W_i)$, it recovers the representation ρ^{W_i} above.*

Proof. We note that

$$\mathcal{O}, \mathcal{O}(-1, 0), \mathcal{O}(-2, -1), \mathcal{O}(-1, -1)$$

satisfy the grade restriction rules for $\lambda_{C_2,C_3} = (-1, 1)$ (with $w_\lambda = 0$) and $\lambda_{C_3,C_1} = (0, -1)$ (with $w_\lambda = 0$) and the fractional grade restriction rule for $\lambda_{C_2,C_1} = (-1, 0)$ (with $w_\lambda = 0$) with respect to the SOD $D^b(Z^{\lambda_{C_2,C_1}})_0 = \langle \mathcal{O}(0, -1), \mathcal{O} \rangle$. Moreover, by the two standard Euler exact sequences on $\mathbb{P}^1 \times \mathbb{P}^1$ pulled back to X_{C_1}, the restrictions of these 4 line bundles to X_{C_1} generate $D^b(X_{C_1})$. Therefore these form a fractional magic window which, as in Remark 4.39, implements the relation (2).

Similarly,

$$\mathcal{O}, \mathcal{O}(0, 1), \mathcal{O}(1, 2), \mathcal{O}(1, 1)$$

form a fractional magic window which satisfies the grade restriction rules for λ_{C_2,C_3} (with $w_\lambda = 0$) and λ_{C_1,C_2} (with $w_\lambda = 0$) and the fractional grade restriction rule for λ_{C_1,C_3} (with $w_\lambda = 0$) with respect to the SOD $D^b(Z^{\lambda_{C_1,C_3}})_0 = \langle \mathcal{O}(-1, 0), \mathcal{O} \rangle$. This implements the relation (1).

Finally,

$$\mathcal{O}, \mathcal{O}(1, 0), \mathcal{O}(0, -1), \mathcal{O}(1, -1)$$

form a fractional magic window which satisfies the grade restriction rules for λ_{C_1,C_2} (with $w_\lambda = 0$) and λ_{C_3,C_1} (with $w_\lambda = 0$) and the fractional grade restriction rule for λ_{C_3,C_2} (with $w_\lambda = 0$) with respect to the SOD $D^b(Z^{\lambda_{C_3,C_2}})_0 = \langle \mathcal{O}(1, 1), \mathcal{O} \rangle$. This implements the relation (3). □

7.3. **The Pentagon VGIT.** We now introduce the Pentagon VGIT which, like the Octahedron VGIT, is not quasi-symmetric (see Definition 8.1) and has a 2d FIPS. The reason we are interested in this VGIT is that it occurs as one of the boundary problems for the Triangle VGIT in §9 and, as such, forms a vital part of the construction of the representation in that case.

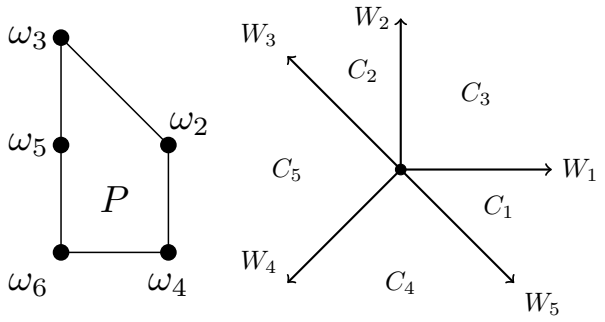

FIGURE 19. The polytope Δ formed by the rays (L) and the secondary fan for the Pentagon VGIT with chambers labelled (R)

The Pentagon VGIT is the linear Calabi–Yau toric VGIT $T_L \circlearrowright \mathbb{C}^5$ specified by the toric data $L = \mathbb{Z}^2 \to \mathbb{Z}^5 \xrightarrow{\hat{A}} \mathbb{Z}^3 = N$ where:

$$\hat{A} = \begin{pmatrix} 1 & 0 & 1 & 0 & 0 \\ 1 & 2 & 0 & 1 & 0 \\ 1 & 1 & 1 & 1 & 1 \end{pmatrix}$$

Therefore the rays live in the height 1 affine hyperplane $H = \{z = 1\}$ and Δ is a degenerate pentagon P (hence the name of the VGIT) as shown in Figure 19 (L).

Remark 7.17. The strange numbering of the rays in Figure 19 (L) comes from its relation to the Triangle VGIT (see §9.2.4 for more details)

By Remark 3.15, the secondary fan, shown in Figure 19 (R) with the chambers labelled, is the fan with support $L^\vee_{\mathbb{R}}$ and with rays generated by the columns of $\hat{Q} : (\mathbb{Z}^5)^\vee \to L^\vee$ where:

$$\hat{Q} = \begin{pmatrix} 1 & 0 & -1 & -1 & 1 \\ -1 & 1 & 1 & -1 & 0 \end{pmatrix}$$

Moreover, by Remark 3.36, the stacky secondary fan just has β (see §3.4) equal to $\hat{Q}$. Then standard toric geometry (see [14], §11.1) tells us that $\mathfrak{F}$ is the (weighted orbifold) blow-up of $\mathbb{P}^2$ (with coordinates $[a_3, a_6, a_5]$ where the numbering here corresponds to the numbering on the rays in Figure 19 (L)) at the basepoints of the pencil of conics given by $\alpha_1^2 a_3 a_6 = \alpha_2 a_5^2$, which (set-theoretically) are the two torus fixed points $[1, 0, 0]$ and $[0, 1, 0]$. As such, $\mathfrak{F}$ is a conic bundle over $\mathbb{P}(1, 2)$ (with coordinates $[\alpha_1, \alpha_2]$).

The discriminant for the Pentagon VGIT has two non-toric components, one (call it ∇_P) corresponding to the left hand edge of P and the other (the principal component ∇_{pr}) corresponding to P itself. Finally, there are four toric divisors corresponding to the four vertices of P. The secondary polytope with the toric components of the discriminant indicated by dashed lines is shown in Figure 26 (ignore the phases in this figure). One checks that ∇_P is the discriminant of a quadratic polynomial in one variable and so $\nabla_P = \{a_5^2 = 4a_3a_6\}$. As such, ∇_P is the conic fibre over $[\alpha_1, \alpha_2] = [2, 1]$ and intersects only $Z(W_3)$ and $Z(W_5)$, doing

so in each case transversely at a single point. One also checks that ∇_{pr} meets each of $Z(W_i)$ (for $i = 1, 2, 4$) transversely at one point. Therefore there are only large radius paths in the Pentagon and so we will only need to use the large radius representation ρ^W from Proposition 5.20.

Remark 7.18. The Pentagon VGIT occurs as a slice of the universal unfolding of the A_2 surface singularity in [18] (see also [8]). There Donovan and Segal observe that the universal unfolding is described by another VGIT whose FIPS is a double cover of the FIPS of the Pentagon. In fact, the fundamental group of the Pentagon FIPS is intimately related to the "mixed" braid group $B_{1,2} \subset B_3$ (see [18], §4.4). Similarly, the fundamental group of the FIPS of the universal unfolding is related to the "pure" braid group $PB_3 \subset B_3$ and this double cover corresponds to the fact that $B_{1,2}$ is an extension of $\mathbb{Z}_2$ by PB_3.

Now the VGIT describing the universal unfolding is quasi-symmetric and its FIPS, by Theorem 8.8, is a hyperplane complement. Since, by Corollary 2.8, the fundamental group of this FIPS acts, they are able to prove Conjecture A for this non-quasi-symmetric example. We shall discuss this approach more in §9.3 but the main drawback to generalising it is that it is difficult to determine when such nice covers exist (though see Remark 7.29 for an idea in this direction).

7.3.1. *Topology using Zariski–van-Kampen.* Our aim in the rest of this section (see Theorem 7.27) is to reconstruct Donovan and Segal's fundamental groupoid action (see [18]) directly – that is, forgetting about the nice double cover in Remark 7.18 – following the strategy outlined at the start of this chapter.

We start by using the Zariski–van-Kampen theorem to find a presentation for the fundamental groupoid. We begin with the pencil which presents $\mathfrak{F}$ as a conic bundle $\hat{f} : \mathfrak{F} \to \mathbb{P}(1,2)$ as described above. Pick coordinates X, Y on the toric open subset of $\mathfrak{F}$ near p_{C_3} such that $\{X = 0\} = Z(W_1)$ and $\{Y = 0\} = Z(W_2)$. Then one checks, by Horn uniformisation (see (4) in §3.6), that $\nabla_{pr} = \{X + Y = 1\}$ and $f(X, Y) = XY \in \mathbb{C}_\alpha$ (where $\alpha := \alpha_2/\alpha_1^2$). We have also seen that $\nabla_P = \{XY = 1/4\}$ is the fibre of f over $\alpha = 1/4$.

We now check that the conditions in the Zariski–van-Kampen Theorem (Theorem 7.3) hold for the morphism $f = \hat{f}|_{\mathrm{FIPS}} : \mathrm{FIPS} \twoheadrightarrow C \subset \mathbb{P}(1,2)$. Here $C := \mathrm{Im}(f) = \mathbb{P}(1,2)\backslash\{\alpha = 0, 1/4\}$ since the torus-invariant fibre over $\alpha_2 = 0$ (but *not* the torus-invariant fibre over $\alpha_1 = 0$) is part of the discriminant.

(1) The fibre $F_\alpha = \{XY = \alpha\}\backslash\{X + Y = 1\}$ is generically $\cong \mathbb{C}^* \backslash \{2 \text{ points}\}$ and one checks that there are two critical fibres, one over $\alpha = 1/4$ (which is not in FIPS anyway) and one over $\alpha_1 = 0$. As such, $Z = \{\alpha_1 = 0\}$ and so $B = C\backslash\{\alpha_1 = 0\}$.
(2) The fibre over $\alpha_1 = 0$ is $\cong \mathbb{C}^* \backslash \{1 \text{ point}\}$ and so is irreducible.
(3) We pick two basepoints $b_1, b_2 \in B$ with α-coordinate $\in \mathbb{R}_{>0}$ respectively less than/greater than $1/4$. We also pick free generators ζ_i of $\pi_1(B, \{b_1, b_2\})$ as shown in blue at the bottom of Figure 20 (in terms of α).

(4) By Remark 7.1, we need to pick disjoint lifts of ζ_i for $i = 1, 2, 3$. We shall choose two such lifts s_1 and s_2 lying in $\{Y = \epsilon\}$ and $\{X = \epsilon\}$ respectively for $\epsilon \in \mathbb{R}_{>0}$ sufficiently large. As usual, $p_{ij} := s_j(b_i)$ for $j = 1, 2$ denotes the two basepoints in F_{b_i}.

We note that neither of our sections extends over $\alpha_1 = 0$. This is because they lie in $\{X = \epsilon\}$ and $\{Y = \epsilon\}$ and these curves limit to the torus fixed point p_{C_4} and p_{C_5} respectively, which have been deleted. As such, Remark 7.5 does not apply. Nonetheless the meridians of $f^{-1}(\alpha_1 = 0)$ in the FIPS are easy to describe – in fact, we can just take $\gamma'_z = \alpha_{C_i}^{(-1,-1)}$ for $i = 4$ or 5. So the Zariski–van-Kampen theorem (Theorem 7.3) gives us:

Corollary 7.19. *$\pi_1(FIPS, \{p_{ij}\})$ is generated by:*

$$\pi_1(F_{b_1}, \{p_{11}, p_{12}\}), \pi_1(F_{b_2}, \{p_{21}, p_{22}\}) \text{ and } s_j(\zeta_i) \text{ for } i = 1, 2, 3, j = 1, 2$$

subject to $\alpha_{C_i}^{(-1,-1)} = e$ for $i = 4, 5$ and the monodromy relations for ζ_i ($i = 1, 2, 3$).

We now want to understand this presentation in terms of imposing additional relations on $\pi_1(U)$ where $U \subset$ FIPS is a specific collection of near large radius regions in the FIPS glued together. Recall that the reason we want to do this is that we know from §5.4 how to define a representation on $\pi_1(U)$ since there are only large radius paths in U.

So how should we pick U so that it can be compared easily with the presentation in Corollary 7.19? For this, we note that the choices made for the Zariski–van-Kampen Theorem give some natural choices of near large radius regions. Our choice of pencil means that the fibre F_{b_1} is a $(-1, 1)$-orbit and so F_{b_1} contains the push-off of $Z(W_1)$ and $Z(W_2)$ in the near large radius regions corresponding to $\beta_{W_1} = \beta_{W_2} = (-1, 1)$. Our choice of sections means that s_j lives in an orbit of the 1-PS corresponding to $(1, 0)$ and $(0, 1)$ respectively for $j = 1, 2$. Therefore $\mathrm{Im}(s_1)$ lives in the push-off of $Z(W_5)$ defined by $\beta_{W_5} = (1, 0)$. Similarly $\mathrm{Im}(s_2)$ lives in the push-off of $Z(W_3)$ defined by $\beta_{W_3} = (0, 1)$. We therefore relabel $s_j(\zeta_2) = \gamma^{-1}_{C_{j+3}, C_j}$ and $s_j(\zeta_1) = \gamma^{-1}_{C_j, C_{j+3}}$ in the notation from §5 to specify ρ^W on these paths.

Remark 7.20. Note however that we don't get a natural choice of near large radius region near $Z(W_4)$ from the Zariski–van-Kampen presentation. The natural guess would be the subset $\{|XY| \geq b_2\}$ with fibre F_{b_2}. This would correspond to choosing $\beta_{W_4} = (-1, 1)$. However, this is not a near large radius region near $Z(W_4)$ because $\langle \lambda_{C_4, C_5}, (-1, 1) \rangle \neq \pm 1$. Geometrically, this corresponds to the fact that the conic fibration f has a non-reduced fibre supported on $Z(W_4)$. Therefore instead we have to use a different fibration to push $\gamma^k_{C_4, C_5}$ off $Z(W_4)$.

These choices of β_{W_i} (for β_{W_4} we choose $(0, 1)$) lead us to pick the following regions in the FIPS:

$$U_1 := \{|XY| \leq b_1\}, U_2 := \{|Y| \geq \epsilon, |XY| \leq b_2\}$$

$$U_3 := \{|X| \geq \epsilon, |XY| \leq b_2\}, U_4 := \{|X| \geq \epsilon, |XY| \geq b_2\}$$

and $U_5 = V_{C_4}$ is a large radius region (see §5.1) containing p_{21}. The images Δ_i of the five subsets U_i under the moment map $\mu : \mathfrak{F} \twoheadrightarrow \Delta := \mathrm{Im}(\mu)$ are shown in Figure 22 (L). Gluing these regions together, we define $U := \bigcup_{i=1,2,3,4,5} U_i$.

Remark 7.21. Note that U_i for $i = 2, 3, 4$ are actual near large radius regions of the form V_W. On the other hand, U_1 is a neighbourhood of both curves $Z(W_1)$ and $Z(W_2)$ and so not of this form. Instead it's regions of the form V_{W_1}, V_{W_2} glued together near V_{C_3}. This is because the pencil f breaks into multiple boundary curves as $\alpha \to 0$. Then "large radius paths" in U_1 will correspond to a pair of large radius paths in V_{W_1} and V_{W_2} respectively. The reason we keep U_1 in one piece despite this extra complication is so that (by our choice of β_{W_1} and β_{W_2}) we have $U_1 = f^{-1}(D)$ where D is the punctured disk in C bounded by ζ_3 and f is our pencil. This will mean that the monodromy is easy to analyse in terms of U_1.

Remark 7.22. Here we take U_4 to be the near large radius region defined by $\beta_{W_4} = (0, 1)$, so that the push-off $\gamma^k_{C_4,C_5}$ is a path in the fibre $F = \{X = \epsilon\}$ (between a new basepoint p' say and p_{22}) and not the fibre F_{b_2}. As in Remark 5.16, the canonical path in U_5 between p' and p_{21} allows us to identify $\pi_1(U, \{p_{ij}, p'\}) \cong \pi_1(U, \{p_{ij}\})$ and one checks explicitly that the paths $\gamma^k_{C_4,C_5}$ get identified with the paths of the same name in F_{b_2} shown in Figure 20.

Since $Z(W_4)$ is not in the discriminant and hence is in U_4, $\alpha^{(-1,-1)}_{C_i} = e$ for $i = 4, 5$ and hence $\pi_1(U_4, \{p', p_{22}\}) \cong \pi_1(F, \{p', p_{22}\})$. Changing basepoints from p' to p_{21}, we therefore see that $\pi_1(U_4 \cup U_5, \{p_{21}, p_{22}\})$ is the subgroupoid of $\pi_1(\{|XY| \geq b_2\}, \{p_{21}, p_{22}\})$ generated by the paths $\gamma^k_{C_4,C_5}$ in F_{b_2} and the loops $\alpha^{(0,1)}_{C_i}$ for $i = 4, 5$.

We now pick presentations (as in Remark 5.15) of $\pi_1(F_{b_i}, \{p_{i1}, p_{i2}\})$ as free groupoids on the generators shown in blue in Figure 20, where we have drawn our fibres by projecting onto the X-coordinate. We have chosen these particular generators on the different fibres to make the monodromy relations as simple as possible.

Remark 7.23. We use the notation for large radius paths in U_i for $i = 2, 3, 4$ from §5 so that ρ^{W_i} is then automatically specified. Recall from Remark 7.21 however that U_1 is not a single near large radius region but a union of two such regions and so the generators $\gamma^{0/j}_{C_1,C_2}$ in F_{b_1} correspond to a large radius path $\gamma^0_{C_1,C_3}$ in V_{W_1} followed by a large radius path $\gamma^j_{C_3,C_2}$ in V_{W_2}. As such, this notation specifies the representation on these paths – namely, it's the sequence of window equivalences $\phi^{C_3,C_2}_j \circ \phi^{C_1,C_3}_0$. It should not be confused with $\gamma^{0,j}_{C_1,C_2}$ from §6 which specifies a (single) *fractional* window equivalence.

Another way of thinking about the representation on these paths is to introduce another basepoint near the torus fixed point p_{C_3}. Then the actual large radius paths $\gamma^0_{C_1,C_3}$ and $\gamma^j_{C_3,C_2}$ are paths in the fundamental groupoid with this extra basepoint and we know how to define the representation. Whilst this approach is

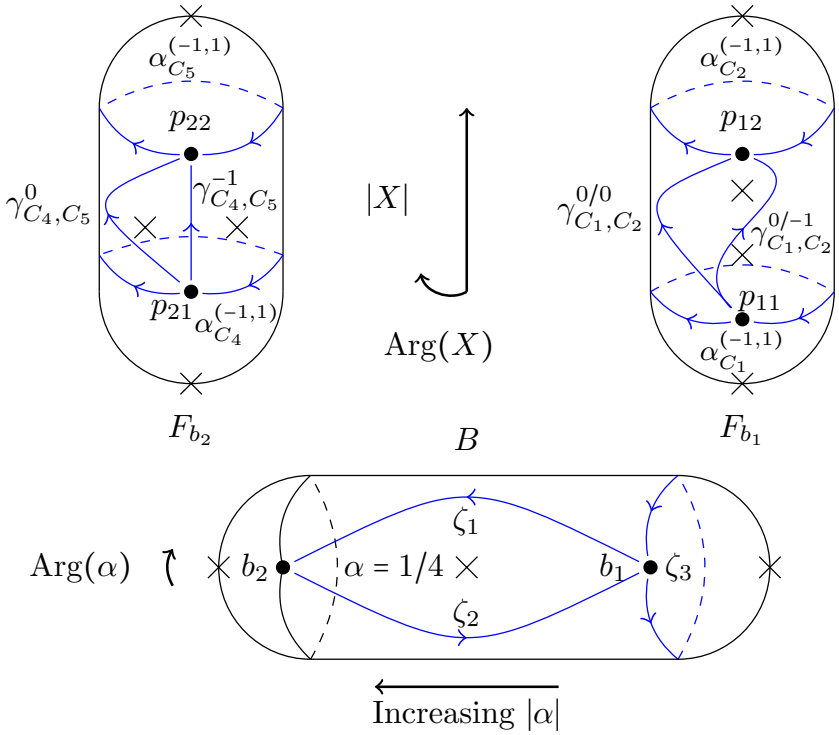

FIGURE 20. Generators for $\pi_1(F_{b_i}, \{p_{i1}, p_{i2}\})$ and $\pi_1(B, \{b_1, b_2\})$ for the Pentagon VGIT

natural from the large radius point of view in U_1, we do not pursue it here because it doesn't play so well with the presentation coming from the pencil. To use this presentation, we would need to extend this extra basepoint to a section of f. But the pencil doesn't split into multiple curves as $\alpha \to \infty$ and so this extra basepoint isn't natural from the large radius point of view near $Z(W_4)$.

Remark 7.24. Our choices of section mean that $s_1(\zeta_3)$ agrees with the toric loop $\alpha_{C_1}^{(-1,0)}$ and $s_2(\zeta_3)$ with $\alpha_{C_2}^{(0,-1)}$. To be in line with the notation from previous sections, we relabel $s_1(\zeta_3)$ by $\alpha_{C_1}^{(-1,0)}$ and $s_2(\zeta_3)$ by $\alpha_{C_2}^{(0,-1)}$.

Our choice of projection means that (for $i = 1, 2$) p_{i2} appear fixed under monodromy whilst p_{i1} (whose X-coordinate is α/ϵ) moves. In particular, around ζ_3, p_{11} does the non-trivial loop shown in Figure 21 (R). However, along ζ_1 and ζ_2, p_{i1} traces out a trivial loop so we draw it as fixed. Together with the fact that the two points of the fibre over α in the discriminant have X-coordinates $1/2 \pm \sqrt{1/4 - \alpha}$, this explains the monodromy shown in Figure 21.

Now we repackage the presentation in Corollary 7.19 in terms of $\pi_1(U)$ and see what's left over. Since the near large radius region U_1 can be described in terms of F_{b_1}, $\alpha_{C_1}^{(-1,0)}$,$\alpha_{C_2}^{(0,-1)}$ and monodromy along ζ_3 (see Remark 7.21), it turns out that the additional relations only come from monodromy along ζ_1 and ζ_2. More precisely, we get:

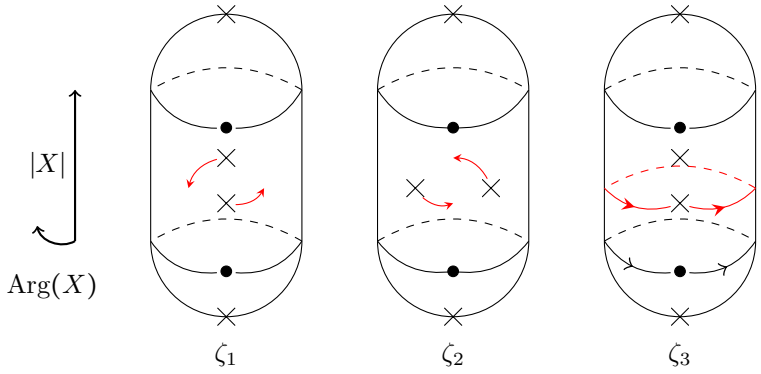

FIGURE 21. Monodromy around the 3 paths ζ_1, ζ_2 and ζ_3 for the Pentagon VGIT

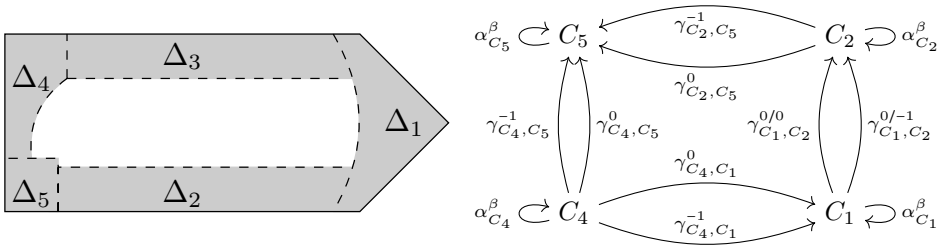

FIGURE 22. Image of near large radius regions under the moment map (L) and generators for $\pi_1(U)$ in the Pentagon VGIT (R)

Proposition 7.25. *$\pi_1(FIPS, \{p_{ij}\})$ is generated by $\pi_1(U, \{p_{ij}\})$ plus the 4 relations:*

(1) $\gamma^{-1}_{C_4,C_5} = \gamma^{-1}_{C_2,C_5} \circ \gamma^{0/-1}_{C_1,C_2} \circ \gamma^{0}_{C_4,C_1}$
(2) $\gamma^{0}_{C_4,C_5} = \gamma^{-1}_{C_2,C_5} \circ \gamma^{0/0}_{C_1,C_2} \circ \gamma^{0}_{C_4,C_1}$
(3) $\gamma^{0}_{C_4,C_5} = \gamma^{0}_{C_2,C_5} \circ \gamma^{0/0}_{C_1,C_2} \circ \gamma^{-1}_{C_4,C_1}$
(4) $\gamma^{-1}_{C_4,C_5} = \gamma^{0}_{C_2,C_5} \circ \gamma^{-1/0}_{C_1,C_2} \circ \gamma^{-1}_{C_4,C_1}$

where $\gamma^{-1/0}_{C_1,C_2}$ is the path in F_{b_1} given by $\gamma^{0/0}_{C_1,C_2}(\gamma^{0/-1}_{C_1,C_2})^{-1}\alpha^{(-1,1)}_{C_2}\gamma^{0/0}_{C_1,C_2}(\alpha^{(-1,1)}_{C_1})^{-1}$.

Remark 7.26. It will follow from the proof that $\pi_1(U, \{p_{ij}\})$ is generated by the paths in Figure 22 (R), where $\gamma^{0}_{C_4,C_1} := (\gamma^{-1}_{C_1,C_4})^{-1}$ and $\gamma^{0}_{C_2,C_5} := .(\gamma^{-1}_{C_5,C_2})^{-1}$.

Proof. Now we package this presentation into pieces we understand and see what's left over. Note that, by Remark 7.21 and the Zariski–van-Kampen theorem applied to U_1, $\pi_1(F_{b_1}, \{p_{11}, p_{12}\})$ and $s_j(\zeta_3)$ (for $j = 1$ and 2) together with the monodromy relations for ζ_3 give a presentation of $\pi_1(U_1, \{p_{11}, p_{12}\})$.

Also, monodromy of $\alpha^{(-1,1)}_{C_2}$ along ζ_1 and ζ_2^{-1} gives exactly monodromy invariance of $\gamma^{k}_{C_2,C_5}$ near the large radius curve $Z(W_3)$. Therefore the subgroupoid of $\pi_1(\text{FIPS}, \{p_{11}, p_{12}, p_{22}\})$ generated by $\pi_1(F_{b_1}, \{p_{11}, p_{12}\})$, $s_j(\zeta_3)$ (for $j = 1$ and 2), $\alpha^{(-1,1)}_{C_i}$ (for $i = 2, 5$) and $\gamma^{k}_{C_2,C_5}$ gives a presentation of $\pi_1(U_1 \cup U_3, \{p_{11}, p_{12}, p_{22}\})$.

In exactly the same way, using monodromy of $\alpha^{(-1,1)}_{C_1}$ along ζ_1 and ζ_2^{-1}, we get that the subgroupoid of $\pi_1(\text{FIPS}, \{p_{ij}\})$ generated by $\pi_1(F_{b_1}, \{p_{11}, p_{12}\})$, $s_j(\zeta_3)$

(for $j = 1$ and 2), $\alpha_{C_i}^{(-1,1)}$ (for $i = 1, 2, 4, 5$), γ_{C_2,C_5}^{k} and γ_{C_1,C_4}^{k} gives a presentation of $\pi_1(U_1 \cup U_2 \cup U_3, \{p_{ij}\})$.

By Remark 7.22, if we add in the two remaining free generators γ_{C_4,C_5}^{k} in $\pi_1(F_{b_2}, \{p_{21}, p_{22}\})$ and the relation $\alpha_{C_i}^{(-1,-1)} = e$ for $i = 4, 5$, we get a copy of $\pi_1(U, \{p_{ij}\})$.

Comparing with our presentation of $\pi_1(\mathrm{FIPS}, \{p_{ij}\})$, we see that the only relations left to implement are the monodromy of $\gamma_{C_1,C_2}^{0/k}$ along ζ_1 and ζ_2^{-1}. Using Figure 21, we see that:

- $m_{\zeta_1}(\gamma_{C_1,C_2}^{0/k}) = \gamma_{C_4,C_5}^{k}$ and so we get the relations $\gamma_{C_2,C_5}^{-1} \circ \gamma_{C_1,C_2}^{0/k} \circ (\gamma_{C_1,C_4}^{-1})^{-1} = \gamma_{C_4,C_5}^{k}$
- $m_{\zeta_2}(\gamma_{C_4,C_5}^{0}) = \gamma_{C_1,C_2}^{0/0}$ and so we get the relation $(\gamma_{C_2,C_5}^{0})^{-1} \circ \gamma_{C_4,C_5}^{0} \circ \gamma_{C_1,C_4}^{0} = \gamma_{C_1,C_2}^{0/0}$
- $m_{\zeta_2}(\gamma_{C_4,C_5}^{-1}) = \gamma_{C_1,C_2}^{-1/0}$ and so we get the relation $(\gamma_{C_2,C_5}^{0})^{-1} \circ \gamma_{C_4,C_5}^{-1} \circ \gamma_{C_1,C_4}^{0} = \gamma_{C_1,C_2}^{-1/0}$.

Therefore it follows that $\pi_1(\mathrm{FIPS}, \{p_{ij}\})$ is the quotient of $\pi_1(U, \{p_{ij}\})$ by the four relations stated. □

7.3.2. *Fundamental groupoid representation.* By Remark 7.23, our notation specifies how we are choosing the large radius representation ρ^W from Proposition 5.20 in each region V_W near a curve in the toric boundary. By Remark 5.24, these glue together (across U_5 also) to give a representation ρ of $\pi_1(U)$. In this section, we prove:

Theorem 7.27. *$\pi_1(FIPS, \{p_{ij}\})$ acts on the phases of the Pentagon VGIT so that it recovers the large radius representation ρ^W on each wall.*

Remark 7.28. This example shows that, while the structure of magic windows in the quasi-symmetric setting of §8 may be particularly nice, magic windows are sufficient to construct our fundamental group(oid) action in non-quasi-symmetric examples too.

Proof. By Proposition 7.25, we have an equivalence

$$\pi_1(\mathrm{FIPS}, \{p_{ij}\}) \cong \pi_1(U)/\langle (1), (2), (3), (4) \rangle$$

Since ρ is naturally a representation on $\pi_1(U)$, we only need to prove that there are 4 magic windows which implement these 4 additional relations.

One checks that the following 4 collections of 3 line bundles are magic windows whose parameters w_λ (see Definition 4.30) agree with those appearing in the relations (1) to (4) respectively:

$$\mathcal{O}, \mathcal{O}(-1, 0), \mathcal{O}(0, -1)$$
$$\mathcal{O}, \mathcal{O}(0, -1), \mathcal{O}(1, -1)$$
$$\mathcal{O}, \mathcal{O}(1, 0), \mathcal{O}(1, -1)$$
$$\mathcal{O}, \mathcal{O}(1, 0), \mathcal{O}(0, 1)$$

□

Remark 7.29. These 4 magic windows are the only ones which give relations between window equivalences with weights 0 or −1 – that is, between equivalences corresponding to large radius generators from the presentation in Theorem 7.27. In fact, in this example, every magic window is of this form up to tensoring with a line bundle.

The set of all magic windows is naturally indexed by the chambers of the affine hyperplane arrangement $\mathcal{A} = \{X \in \mathbb{Z}\} \cup \{Y \in \mathbb{Z}\} \cup \{X + Y \in \mathbb{Z}\}$. For a quasi-symmetric representation, there is a corresponding affine hyperplane arrangement (see Proposition 8.14) whose chambers also naturally index the magic windows. In this case $\mathcal{A}$ is the hyperplane arrangement associated to the quasi-symmetric VGIT with weights:

$$\mathbb{Z}^6 \twoheadrightarrow L^\vee = \mathbb{Z}^2, Q = \begin{pmatrix} 1 & -1 & 0 & 0 & 1 & -1 \\ 0 & 0 & 1 & -1 & -1 & 1 \end{pmatrix}$$

and this is exactly the "unsliced" VGIT whose slice is the Pentagon VGIT and which induces the covering map in [18]. More generally, one might hope that in other non-quasi-symmetric examples the combinatorics of the set of all magic windows might help to identify such an "unsliced" VGIT whose slice is the original VGIT.

8. The quasi-symmetric case

Definition 8.1. A representation $T_L \circlearrowright \mathbb{C}^n$ is *quasi-symmetric* if, for each line ℓ in $L^\vee_{\mathbb{R}}$, the sum of all the weights that lie on ℓ is zero.

Remark 8.2. In particular self-dual representations of T_L – that is, if $\beta \in L^\vee$ is a weight, then so is $-\beta$ – are quasi-symmetric. A simple example of a quasi-symmetric representation which is not self-dual is given by $L = \mathbb{Z} \to \mathbb{Z}^3, 1 \mapsto (1, -2, 1)$. This corresponds to the toric VGIT which describes the (orbifold) flop between $\mathrm{Tot}(\mathcal{O}_{\mathbb{P}^1}(-2))$ and $[\mathbb{C}^2 / \mathbb{Z}_2]$ where $\mathbb{Z}_2$ acts via $(-1, -1)$.

We note that quasi-symmetric representations are necessarily Calabi–Yau. Conversely, any Calabi–Yau representation with $\mathrm{Rk}(L) = 1$ is automatically quasi-symmetric.

Given that the general story of magic windows in the quasi-symmetric setting is worked out in [24], in this section we complete this circle of ideas by proving, in Theorem 8.8, that the (log-)discriminant locus is a hyperplane arrangement and, in Proposition 8.14, that it agrees with the combinatorial model used to construct the large radius representation in [24].

The proof of Theorem 8.8 is based on the following observation:

Lemma 8.3. *The representation $T_L \circlearrowright \mathbb{C}^n$ is quasi-symmetric if and only if ∇_{pr} is a point.*

Proof. Since the image of Horn uniformisation is ∇_{pr} ([20], Ch. 9, Theorem 3.3a), ∇_{pr} is a point if and only if its Horn uniformisation (see (4) in §3.6) is constant. Explicitly, this happens precisely when, for all i, $\prod_{j=1}^{n}(\lambda_1\beta_{j1}+\cdots+\lambda_k\beta_{jk})^{\beta_{ji}}$ is constant as a degree 0 element of $\mathbb{C}(\lambda_1,\cdots,\lambda_k)$. Since $\sum_{m=1}^{k}\lambda_m\beta_{jm}$ agrees with $\sum_{m=1}^{k}\lambda_m\beta_{Jm}$ (up to scaling) if and only if β_j and β_J lie on the same line in $L^\vee_{\mathbb{R}}$, decomposing $\prod_{j=1}^{n}(\lambda_1\beta_{j1}+\cdots+\lambda_k\beta_{jk})^{\beta_{ji}}$ into lines as $\prod_{\ell\subset L^\vee_{\mathbb{R}}}(\prod_{j|\beta_j\in\ell}(\sum_{m=1}^{k}\lambda_m\beta_{jm})^{\beta_{ji}})$ shows that this is constant if and only if each factor $\prod_{j|\beta_j\in\ell}(\sum_{m=1}^{k}\lambda_m\beta_{jm})^{\beta_{ji}}$ is constant for all i and all lines ℓ. Fix a primitive generator $\underline{\ell}=(l_1,\cdots,l_k)$ for ℓ and write each β_j on ℓ as $n_j\underline{\ell}$ for $n_j\in\mathbb{Z}$. Then

$$\prod_{j|\beta_j\in\ell}(\sum_{m=1}^{k}\lambda_m\beta_{jm})^{\beta_{ji}}=(\prod_{j|\beta_j\in\ell}n_j^{\beta_{ji}})(\sum_{m=1}^{k}\lambda_m l_m)^{\sum_{j|\beta_j\in\ell}\beta_{ji}}$$

is constant if and only if $\sum_{j|\beta_j\in\ell}\beta_{ji}=0$. Hence the result. □

Remark 8.4. The proof shows that, in the quasi-symmetric case, ∇_{pr} has i-th coordinate $\prod_{j=1}^{n}n_j^{\beta_{ji}}$.

8.1. **Hyperplanes associated to circuits.** If Γ is a circuit (see Definition 3.31), $T_{L^\vee_\Gamma}$ is a rank 1 torus, where we recall that $L^\vee_\Gamma$ contains the weights for the VGIT on Γ (see §3.5). Moreover, as a face which is a circuit is necessarily minimal (see Definition 3.3), $\nabla_{A\cap\Gamma}\subset T_{L^\vee_\Gamma}$ is a point. If we pick a generator $l_\Gamma\in L_\Gamma$, then this gives a coordinate x on $T_{L^\vee_\Gamma}$ and also allows us to identify $L^\vee_\Gamma\cong\mathbb{Z}$ via $\langle -,l_\Gamma\rangle$. Then Horn uniformisation tells us that $\nabla_{A\cap\Gamma}=\{x=c_\Gamma\}\subset T_{L^\vee_\Gamma}$ where $c_\Gamma=\prod_{j=1}^{n}m_j^{m_j}$ and $m_j=\langle\beta_j,l_\Gamma\rangle\in\mathbb{Z}$.

Remark 8.5. Note that $m_j^{m_j}$ is positive precisely when $m_j\geq 0$ or m_j is even. So c_Γ is positive precisely when it contains an even number of negative odd terms – that is, $\sum_{m_j<0}m_j\in 2\mathbb{Z}$. In the notation of §4, this is the same as η_{l_Γ} being even.

When we pull $\nabla_{A\cap\Gamma}$ back to $T_{L^\vee}$ under the map induced by $p:L^\vee\twoheadrightarrow L^\vee_\Gamma$ (see §3.5), it becomes the divisor $\nabla_\Gamma:=\{x^{l_\Gamma}=c_\Gamma\}$.

Remark 8.6. Since the universal cover $L^\vee_{\mathbb{C}}\to T_{L^\vee}$ is given in coordinates by taking the logarithm, we prefix the pullback under this cover of any object defined on $T_{L^\vee}$ by *log*. For example, the *log*-discriminant locus is the union of $\{\mathrm{Log}(\Delta_{A\cap\Gamma})=0\}$ over all faces $\Gamma\subset\Delta$, where $\mathrm{Log}:=\frac{\log}{2\pi i}$. As Log is multivalued, $\{\mathrm{Log}(\Delta_{A\cap\Gamma})=0\}$ consists of translates under $L^\vee$ of $\{\mathrm{Log}_{br}(\Delta_{A\cap\Gamma})=0\}$, where Log_{br} is the single-valued version of Log with arguments lying in $[0,2\pi)$. Note that $\Delta_{A\cap\Gamma}$ extends to a section of a line bundle on $\mathfrak{F}$ (see §3.4) and so, when we take logs, we are implicitly restricting this function to $T_{L^\vee}$. In particular, if Γ is a vertex of Δ, $\Delta_{A\cap\Gamma}$ is a toric coordinate on $T_{L^\vee}$ and the corresponding component of the log-discriminant locus is empty.

With this terminology, ∇_Γ is a log-hyperplane – if we pick a basis of L (and write $l_\Gamma=(l_1,\ldots,l_k)$ in this basis) and corresponding coordinates x_i on $T_{L^\vee}$, then $x^{l_\Gamma}=\prod_i x_i^{l_i}$ and $H_\Gamma:=\mathrm{Log}(\nabla_\Gamma)=\{(\mathrm{Log}(\underline{x})\in\mathbb{C}^k\mid\sum_i l_i\mathrm{Log}(x_i)\in\mathrm{Log}(c_\Gamma)+\mathbb{Z}\}$ is

a free $\mathbb{Z}$-orbit of complex affine hyperplanes. The upshot to this discussion is that faces Γ which are circuits give rise to log-hyperplanes in the discriminant locus.

Remark 8.7. If the original VGIT is quasi-symmetric and we write $\beta_j = n_j \underline{\ell}$ where (as in the proof of Lemma 8.3) $\underline{\ell}$ denotes a choice of primitive generator of the line $\ell = \langle \beta_j \rangle \subset L^\vee_{\mathbb{R}}$ we can compute:

(5)
$$c_\Gamma = \prod_{\ell \subset L^\vee_{\mathbb{R}}} \prod_{j|\beta_j \in \ell} (n_j \langle l_\Gamma, \underline{\ell} \rangle)^{\langle l_\Gamma, \beta_j \rangle} = \prod_{\ell \subset L^\vee_{\mathbb{R}}} \Big(\prod_{j|\beta_j \in \ell} n_j^{\langle l_\Gamma, \beta_j \rangle} \Big) \langle l_\Gamma, \underline{\ell} \rangle^{\sum_{j|\beta_j \in \ell} \langle l_\Gamma, \beta_j \rangle} = \prod_{j=1}^{n} n_j^{\langle l_\Gamma, \beta_j \rangle}$$

where, for the third equality, we used that quasi-symmetry implies $\sum_{j|\beta_j \in \ell} \beta_j = 0$.

If the original representation is actually self-dual (see Remark 8.2), we may pick half of the weights, which we index β_i, such that all the weights are of the form $\pm\beta_i$. Then the terms in c_Γ corresponding to $\pm\beta_i$ cancel up to a sign and we get that $c_\Gamma = \pm 1$ where the sign can be worked out using Remark 8.5. This means that $\mathfrak{I}(\mathrm{Log}(c_\Gamma)) = 0$ and hence H_Γ is the complexification of a real hyperplane. This is not true for general quasi-symmetric representations.

8.2. **The discriminant in the quasi-symmetric case.** In this section, we prove that, in the quasi-symmetric case, all components of the discriminant locus come from circuits.

Theorem 8.8. *The log-discriminant locus of a quasi-symmetric T_L-representation is an (affine) hyperplane arrangement. In this case, the hyperplanes are the H_Γ arising from the faces $\Gamma \subset \Delta$ which are circuits as in §8.1.*

Remark 8.9. By Remark 8.6, the log-discriminant locus doesn't contain toric components corresponding to vertices of Δ and so this theorem doesn't tell us anything about such components. In general in the quasi-symmetric case it is possible that the FIPS contains some toric divisors. In fact, the orbifold flop in Remark 8.2 gives such an example as the FIPS has a $\mathbb{Z}_2$-orbifold point corresponding to the phase $[\mathbb{C}^2/\mathbb{Z}_2]$. However, using the description from §5.1 of when a toric divisor is part of the discriminant, we can see that the FIPS of a quasi-symmetric VGIT only contains a toric divisor if there is a line and a complementary hyperplane in $L^\vee_{\mathbb{R}}$ such that any weight lies on one of these two subspaces. As such, typically the whole toric boundary of $\mathfrak{F}$ is in the discriminant and so the FIPS is actually equal to log-hyperplane complement in $T_{L^\vee}$ from the theorem.

Remark 8.10. By Remarks 8.4 and 8.7, $c_\Gamma = \prod_j n_j^{\langle l_\Gamma, \beta_j \rangle}$ agrees with the x^{l_Γ}-coordinate of ∇_{pr} in the quasi-symmetric case. Hence, $\nabla_{pr} \subset \nabla_\Gamma$ for all circuits Γ. By Theorem 8.8, this says that, in the quasi-symmetric case, ∇_{pr} is contained in all non-toric components of the discriminant locus (c.f. Remark 3.10).

Lemma 8.11. *If the representation $T_L \circlearrowright \mathbb{C}^n$ is quasi-symmetric and $\Gamma \subset \Delta$ is a face, then the induced representation $T_{L_\Gamma} \circlearrowright \mathbb{C}^{n_\Gamma}$ is quasi-symmetric also.*

Proof. Recall from (3) in §3.5 that the induced representation has weights $p(\beta_i)$ for all i such that $\omega_i \in \Gamma$, where $p : L^\vee \twoheadrightarrow L_\Gamma^\vee$ is the quotient map. Then it follows from (3) that all the other weights lie in $\ker p := (L'_\Gamma)^\vee$. As every lift $\hat{\ell} \subset L^\vee_{\mathbb{R}}$ of a line $\ell \subset (L_\Gamma^\vee)_{\mathbb{R}}$ is not contained in $(L'_\Gamma)^\vee_{\mathbb{R}}$, then the quasi-symmetry condition for all lifts $\hat{\ell}$ implies the quasi-symmetry condition for ℓ.

□

Proof of Theorem 8.8. By §8.1, we only need to show that if Γ is not a circuit, then $\Delta_{A\cap\Gamma}$ doesn't contribute to E_A. Since (non-vertex) redundant faces don't contribute to E_A, the space L_Γ of relations in such a Γ must have $\mathrm{Rk}(L_\Gamma) > 1$. By Lemma 8.11, as the T_L-representation is quasi-symmetric so is the T_{L_Γ}-representation. Then Lemma 8.3 tells us that $\nabla_{A\cap\Gamma}$ is a point and so $\nabla_\Gamma := p^*(\nabla_{A\cap\Gamma})$ has codimension at least 2. As such, $\Delta_{A\cap\Gamma}$ doesn't contribute to E_A. □

More generally, we note:

Lemma 8.12. *If the log-discriminant locus is a hyperplane arrangement, the hyperplanes are the H_Γ coming from faces Γ which are circuits, as in §8.1.*

Proof. Suppose that all the components ∇_Γ of the discriminant are log-hyperplanes. Since $\nabla_\Gamma = p^*(\nabla_{A\cap\Gamma})$, this implies that $\nabla_{A\cap\Gamma}$ is a log-hyperplane.

As such, we need only prove that if ∇_{pr} is a log-hyperplane, then $\mathrm{Rk}(L^\vee) = 1$, since it then follows that the T_L-representation has no zero weights and so is a circuit. To see the claim, note that the logarithmic Gauss map (see §3.6) of a log-hyperplane is the constant function. Then Theorem 3.51 implies that ∇_{pr} can only be a log-hyperplane if $\mathrm{Rk}(L^\vee) = 1$. □

Remark 8.13. This result implies that the secondary fan of a VGIT whose log-discriminant is a hyperplane arrangement is itself a hyperplane arrangement. In fact, we expect that such a VGIT is quasi-symmetric. It certainly follows from Lemma 8.12 that, if $\mathrm{Rk}(L) > 1$, ∇_{pr} is not part of the discriminant locus and so must be codimension at least 2. At least in 2-dimensions, this proves the claim as then ∇_{pr} is a point and we are done by Lemma 8.3.

8.3. **Explicit description of the hyperplane arrangement.** We conclude by showing that our log-discriminant hyperplane arrangement in $L^\vee_{\mathbb{C}}$ agrees with the one constructed by Halpern-Leistner–Sam in [24], Ch. 3. From Theorem 8.8, we know that our discriminant hyperplane arrangement, denoted $\mathcal{H}_{\mathrm{disc}}$, comes from faces $\Gamma \subset \Delta$ which are circuits. From §8.1, a circuit has a unique (up to sign) choice of generating relation $l_\Gamma \in L_\Gamma$ and our hyperplanes are $H_{\Gamma,n} := \{y \in L^\vee_{\mathbb{C}} \mid \langle l_\Gamma, y\rangle = \mathrm{Log}_{br}(c_\Gamma) + n\}$ where $n \in \mathbb{Z}$ and c_Γ is defined by (5) from §8.1. Note that the real hyperplane H_{l_Γ} defined by l_Γ is the hyperplane $(L'_\Gamma)^\vee_{\mathbb{R}}$ spanned by complementary weights from §3.5 and so $H_{\Gamma,n}$ is a translate of $(L'_\Gamma)^\vee_{\mathbb{C}}$ in $L^\vee_{\mathbb{C}}$.

In order to define their hyperplane arrangement, Halpern-Leistner–Sam introduce two polytopes in $L^\vee_{\mathbb{R}}$ associated to a T_L-representation:

$$\bar{\Sigma} := \Big\{ \sum_j a_j \beta_j \mid a_j \in [-1, 0] \Big\} =: \sum_j [-\beta_j, 0]$$

$$\bar{\nabla} := \Big\{ \beta \in L^\vee_{\mathbb{R}} \mid -\frac{\eta_l}{2} \leq \langle l, \beta \rangle \leq \frac{\eta_l}{2} \text{ for all } l \in L \Big\}$$

where $\eta_l := \max\{\langle l, \mu \rangle \mid \mu \in \bar{\Sigma}\}$. Moreover they show (see [24], Lemma 2.8) that for quasi-symmetric torus representations $\bar{\nabla} = \frac{1}{2}\bar{\Sigma}$. They then define a real hyperplane arrangement in $L^\vee_{\mathbb{R}}$ as the $L^\vee$-orbit (acting by translations) of the supporting affine hyperplanes H_F of the facets F of $\bar{\nabla}$. Their hyperplane arrangement, which we denote $\mathcal{H}_{\text{HLS}}$, is then the complexification of this real hyperplane arrangement. Note that, as the weights span $L^\vee$, $\bar{\Sigma}$ and $\bar{\nabla}$ are full-dimensional and so there is a unique supporting hyperplane H_F for each facet F. Therefore if we write $H_F = \{y \in L^\vee_{\mathbb{R}} \mid \langle l_F, y \rangle = c_F\}$, then the hyperplanes in $\mathcal{H}_{\text{HLS}}$ have the form $H_{F,n} := \{y \in L^\vee_{\mathbb{C}} \mid \langle l_F, y \rangle = c_F + n\}$.

These two hyperplane arrangements, $\mathcal{H}_{\text{disc}}$ and $\mathcal{H}_{\text{HLS}}$, cannot be precisely the same since $\text{Log}_{br}(c_\Gamma)$ can have non-zero imaginary part (though not in the self-dual case – see Remark 8.7) and hence $H_{\Gamma,n}$ cannot in general be the complexification of a real hyperplane in $L^\vee_{\mathbb{R}}$. However we do have:

Proposition 8.14. *For a quasi-symmetric T_L-representation, $\mathcal{H}_{disc} = \mathcal{H}_{HLS}$ after translating the latter by $-\frac{i}{2\pi}\sum_j \log(|\beta_j|)\beta_j \in iL^\vee_{\mathbb{R}}$ where $|\beta|$ is the lattice length of β.*

Proof. We start by determining the facets of $\bar{\nabla}$ using its description both in terms of inequalities and as a convex hull. By adding up all the weights on a ray inside a given line, we can assume that, for the purpose of determining the facets, on any line with weights our representation only has weights $\pm\beta_j$.

We first describe when $\beta \in \partial\bar{\nabla}$. As above, since our representation is quasi-symmetric, we have $\bar{\nabla} = \frac{1}{2}\bar{\Sigma}$. Hence we observe that $\beta \in \partial\bar{\nabla}$ precisely when $\beta = \sum_j a_j\beta_j$ with $a_j \in [-1/2, 1/2]$ and there is an $l \in L$ such that one of inequalities in the definition of $\bar{\nabla}$ is saturated i.e. $\langle l, \beta \rangle = \pm\frac{\eta_l}{2}$. Since $\bar{\nabla} = \frac{1}{2}\bar{\Sigma}$, $\frac{\eta_l}{2} = \max\{\langle l, \mu \rangle \mid \mu \in \bar{\nabla}\}$ and, as $\bar{\nabla} = -\bar{\nabla}$, $-\frac{\eta_l}{2} = \min\{\langle l, \mu \rangle \mid \mu \in \bar{\nabla}\}$. Write $\langle l, \beta \rangle = \sum_j a_j \langle l, \beta_j \rangle$ and, swapping β_j for $-\beta_j$ if necessary, suppose that $\langle l, \beta_j \rangle \geq 0$ for all j. Then we get an equality $\langle l, \beta \rangle = \pm\frac{\eta_l}{2}$ by making the coefficient a_j of β_j such that $\langle l, \beta_j \rangle > 0$ as large/small as possible. So $\beta \in \partial\bar{\nabla}$ precisely when it's of the form $\sum_{j|\langle l,\beta_j\rangle>0} \pm\beta_j/2 + \sum_{j|\langle l,\beta_j\rangle=0} a_j\beta_j$.

So we get a pair of facets $F_\pm$ of $\bar{\nabla}$, going through $\sum_{j|\langle l,\beta_j\rangle>0} \pm\beta_j/2$ respectively, precisely when the set of weights in the real hyperplane $H_l = \{\langle l, - \rangle = 0\} \subset L^\vee_{\mathbb{R}}$ span the whole hyperplane. Hence the supporting hyperplanes of the facets $F_\pm$ are $H_{F_\pm} = \{\langle l, - \rangle = \langle l, \sum_{j|\langle l,\beta_j\rangle>0} \pm\beta_j/2 \rangle\}$ whenever l satisfies this property. So for such an l, we can take $l_{F_\pm} := l$ and $c_{F_\pm} := \langle l, \sum_{j|\langle l,\beta_j\rangle>0} \pm\beta_j/2 \rangle$. Note that, as $\sum_{j|\langle l,\beta_j\rangle>0} \pm\beta_j/2$ differ by an element of $L^\vee$, $H_{F_+,m} = H_{F_-,m+n}$ for some $n \in \mathbb{Z}$, so we need only consider the hyperplanes corresponding to one of these faces. By convention, we choose to work with F_+.

We now show that there is a face Γ (which is necessarily a circuit) such that the real hyperplanes H_{l_F} and H_{l_Γ} in $L^\vee_{\mathbb{R}}$ are equal. Since the representation is quasi-symmetric, we have that $\sum_{j|\beta_j\in H_{l_F}}\beta_j = 0$ and hence we have a positive relation between all the weights on H_{l_F}. Since H_{l_F} is spanned by the weights lying on it, Lemma 3.47 guarantees that there is a (minimal) face Γ such that $H_{l_F} = (L'_\Gamma)^\vee_{\mathbb{R}}$. Calling l_Γ the defining equation of $(L'_\Gamma)^\vee_{\mathbb{R}}$, $H_{l_F} = H_{l_\Gamma}$ as claimed.

For this Γ, we now claim that the real hyperplanes $\mathfrak{R}(H_{F,0}) = \{y \in L^\vee_{\mathbb{R}} \mid \langle l_F, y\rangle = c_F\}$ and $\mathfrak{R}(H_{\Gamma,n}) = \{y \in L^\vee_{\mathbb{R}} \mid \langle l_\Gamma, y\rangle = \mathfrak{R}(\mathrm{Log}_{br}(c_\Gamma)) + n\}$ are the same for some $n \in \mathbb{Z}$. Hence $\mathfrak{R}(H_{F,m}) = \mathfrak{R}(H_{\Gamma,m+n})$ and so $\mathcal{H}_{\mathrm{HLS}}$ and $\mathcal{H}_{\mathrm{disc}}$ determine the same real hyperplane arrangements. To see the claim, recall that $c_F = \langle l, \sum_{j|\langle l,\beta_j\rangle>0}\beta_j/2\rangle$ and hence is a half-integer. On the other hand, $c_\Gamma \in \mathbb{Q}^\times$ so $\mathfrak{R}(\mathrm{Log}_{br}(c_\Gamma))$ is either 0 or 1/2 when c_Γ is respectively positive or negative. Since $H_{l_F} = H_{l_\Gamma}$, it suffices to prove that $c_\Gamma > 0$ precisely when $c_F \in \mathbb{Z}$. By Remark 8.5, $c_\Gamma > 0$ precisely when $\langle l_\Gamma, \sum_{j|\langle l_\Gamma,\beta_j\rangle<0}\beta_j/2\rangle \in \mathbb{Z}$. By quasi-symmetry $\sum_{j|\langle l_\Gamma,\beta_j\rangle<0}\beta_j/2 = -\sum_{j|\langle l_\Gamma,\beta_j\rangle>0}\beta_j/2$ and so this happens precisely when $c_F = \langle l_\Gamma, \sum_{j|\langle l_\Gamma,\beta_j\rangle>0}\beta_j/2\rangle \in \mathbb{Z}$.

The imaginary parts of our two hyperplane arrangements, $\mathfrak{I}(H_{F,m}) = \{y \in L^\vee_{\mathbb{R}} \mid \langle l_F, y\rangle = 0\}$ and $\mathfrak{I}(H_{\Gamma,m+n}) = \{y \in L^\vee_{\mathbb{R}} \mid \langle l_\Gamma, y\rangle = -\frac{1}{2\pi}\log(|c_\Gamma|)\}$, are different in general. However, by (5) in §8.1

$$\log(|c_\Gamma|) = \log(\prod_j |n_j|^{\langle l_\Gamma,\beta_j\rangle}) = \sum_j \langle l_\Gamma,\beta_j\rangle \log(|\beta_j|) = \langle l_\Gamma, \sum_j \log(|\beta_j|)\beta_j\rangle$$

So, if we set $z := -\frac{1}{2\pi}\sum_j \log(|\beta_j|)\beta_j$, $\mathfrak{I}(H_{F,m}) + z = \mathfrak{I}(H_{\Gamma,m+n})$ and so $H_{F,m} + iz = H_{\Gamma,m+n}$ and we are done. □

9. The Triangle VGIT

9.1. **Introduction.** In this section, we discuss the Triangle VGIT which has a 3d FIPS and is not quasi-symmetric. We shall construct the fundamental groupoid representation from two different perspectives, one based on the Lefschetz strategy (as discussed in §2.4.1) and the other based on the covering strategy (see §2.4.2).

The Triangle VGIT is given by the following toric data:

$$0 \to L = \mathbb{Z}^3 \xrightarrow{Q^\vee} \mathbb{Z}^6 \xrightarrow{A} N = \mathbb{Z}^3 \to 0$$

where

$$Q^\vee = \begin{pmatrix} 1 & 0 & 0 \\ -1 & -1 & 1 \\ 0 & 1 & 0 \\ -1 & 1 & -1 \\ 1 & -1 & -1 \\ 0 & 0 & 1 \end{pmatrix}, A = \begin{pmatrix} 2 & 1 & 0 & 1 & 0 & 0 \\ 0 & 1 & 2 & 0 & 1 & 0 \\ 1 & 1 & 1 & 1 & 1 & 1 \end{pmatrix}$$

As all the rays given by A lie in the affine hyperplane $n_3 = 1$, this is a Calabi–Yau VGIT. We note that Δ is a triangle (hence the name of the VGIT) with all its sides having lattice length 2. This choice of matrix A corresponds to the ordering of the

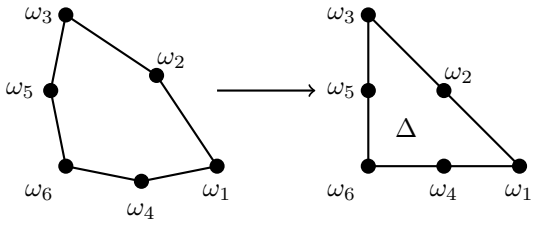

FIGURE 23. A hexagon degenerating to the triangle Δ with rays labelled

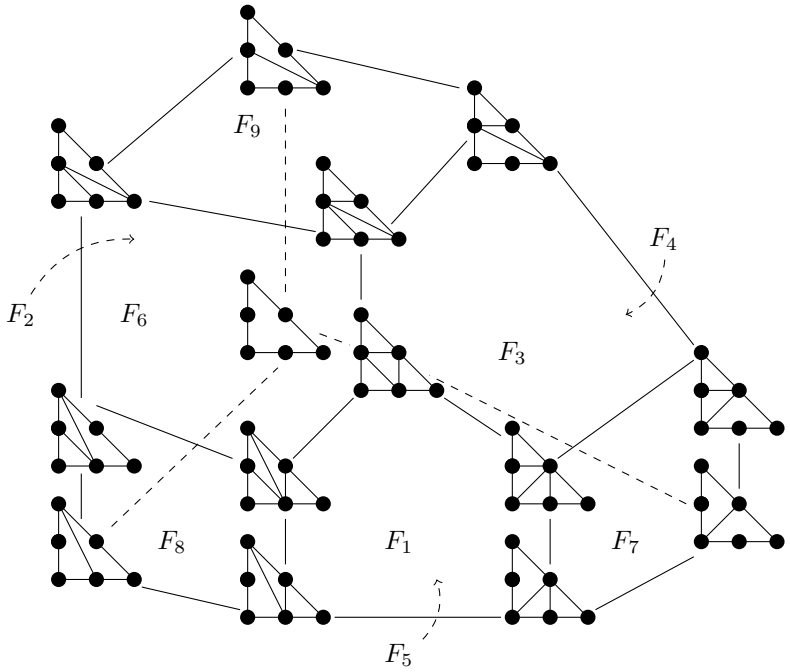

FIGURE 24. The secondary polytope of the Triangle VGIT

rays ω_i in N indicated in the right of Figure 23. We label by a_i the coordinate function on $\mathbb{C}^6$ corresponding to $e_i \in \mathbb{Z}^6$ and set $\beta_i := Q(e_i)$.

9.1.1. *The phases.* Phases of the Triangle VGIT correspond (see Remark 3.23) to all the possible triangulations of (the whole of) Δ with vertices at (some of) the integral points of Δ.

There are 14 phases in this problem. One way to see this is to view Δ as the degeneration of a hexagon in which some pairs of consecutive edges "straighten" to become edges of the triangle, as in Figure 23. This induces a bijection between triangulations of Δ as above and triangulations of the hexagon, which are counted by the fifth Catalan number $c_5 = 14$. The secondary polytope with all these 14 triangulations of Δ is illustrated in Figure 24.

In terms of the geometry, the phase at the back of Figure 24 with the trivial triangulation is the orbifold $[\mathbb{C}^3/G]$ where $G = \mathbb{Z}_2^{\oplus 2}$ embeds into $(\mathbb{C}^*)^3$ via the

matrices:

$$\sigma_1 = \begin{pmatrix} 1 & 0 & 0 \\ 0 & -1 & 0 \\ 0 & 0 & -1 \end{pmatrix}, \sigma_2 = \begin{pmatrix} -1 & 0 & 0 \\ 0 & 1 & 0 \\ 0 & 0 & -1 \end{pmatrix}, \sigma_3 = \begin{pmatrix} -1 & 0 & 0 \\ 0 & -1 & 0 \\ 0 & 0 & 1 \end{pmatrix} \tag{6}$$

We note that the three coordinate axes in $\mathbb{C}^3$ are the precisely the locus with non-trivial isotropy, and that, away from the origin, these have isotropy group $\mathbb{Z}_2$, corresponding to the 3 subgroups of G of order 2. At the origin, we get the full isotropy group G. The underlying toric variety has non-isolated singularities and can be described as the hypersurface singularity $\{xyz = u^2\} \subset \mathbb{C}^4_{xyzu}$.

The phase for the opposite chamber (in the centre of Figure 24 with the symmetric triangulation) has 3 compact curves which meet (at a unique point) as the axes in $\mathbb{C}^3$ do. These are the maximal compact toric cycles. In fact (see [11], Example 5.31 for more details), this phase can be described as $\mathrm{Hilb}^G(\mathbb{C}^3)$.

Remark 9.1. Since the triangulations into integral (not just simplicial) triangles all have 4 triangles, the geometric phases X of the VGIT have $e(X) = 4$ and so $K_0(X)_{\mathbb{Q}}$ has rank 4. As such, any magic window in $D^b([\mathbb{C}^6/T_L])$ should contain precisely 4 line bundles.

9.1.2. *The secondary stack.* We observe that the above bijection between triangulations of the hexagon and triangulations of the triangle can be extended to a bijection between any polyhedral subdivisions (see Definition 3.24) of the hexagon and triangle which respects the natural partial ordering of refinement. As such, we get a (combinatorial) isomorphism between these two secondary polytopes. Since (see [20], Ch. 7, Example 3.6) the secondary polytope of the hexagon is the 3-dimensional associahedron, we see that the secondary polytope $\Sigma(A)$ for the Triangle VGIT is the associahedron shown in Figure 24. By Proposition 3.27, the 9 facets of the associahedron $\Sigma(A)$ correspond to 9 polyhedral subdivisions of Δ with 2 free markings – some of these are shown in Figure 4.

The secondary fan can therefore be described as the normal fan to $\Sigma(A)$. Alternatively, we can use the more concrete procedure in Remark 3.15 to construct it directly from the original weights. Either way, we find that the rays of the secondary fan are generated by the columns of $Q' : \mathbb{Z}^9 \to \mathbb{Z}^3$ (these are the original weights β_i for $i = 1, \ldots, 6$ plus 3 new ones) where Q' is:

$$Q' = \begin{pmatrix} 1 & -1 & 0 & -1 & 1 & 0 & 1 & 1 & -1 \\ 0 & -1 & 1 & 1 & -1 & 0 & 1 & -1 & 1 \\ 0 & 1 & 0 & -1 & -1 & 1 & -1 & 1 & 1 \end{pmatrix}, A' = \begin{pmatrix} 2 & 1 & 0 & 1 & 0 & 0 & 0 & 0 & 0 \\ 0 & 1 & 2 & 0 & 1 & 0 & 0 & 0 & 0 \\ 1 & 1 & 1 & 1 & 1 & 1 & 0 & 0 & 0 \\ 0 & 1 & 0 & 0 & 0 & 0 & 1 & 0 & 0 \\ 0 & 0 & 0 & 1 & 0 & 0 & 0 & 1 & 0 \\ 0 & 0 & 0 & 0 & 1 & 0 & 0 & 0 & 1 \end{pmatrix}$$

Remark 9.2. We note that the secondary fan has an S_3-symmetry generated by permuting the standard basis vectors in $L^\vee = \mathbb{Z}^3$. This symmetry is induced by the

S_3-symmetry of Δ. There are 3 orbits of the facets of $\Sigma(A)$ under this symmetry and the 3 subdivisions in Figure 4 correspond to representatives.

To get the stacky secondary fan, we need to follow the procedure in §3.4. We claim that the map β describing this structure is Q'. To see this, recall Example 3.35. The three subdivisions considered there correspond to the following 3 rays of the secondary fan (in the above numbering):

$$\rho_1 = \mathbb{R}_{>0}\langle(1,0,0)\rangle \in \mathbb{R}^3, \rho_8 = \mathbb{R}_{>0}\langle(1,-1,1)\rangle, \rho_4 = \mathbb{R}_{>0}\langle(-1,1,-1)\rangle$$

It follows from the definition of β in §3.4 $\beta(e_1^\vee) = \beta_1 = Q'(e_1^\vee)$, $\beta(e_8^\vee) = 2\beta_1 + \beta_2 = Q'(e_8^\vee)$ and $\beta(e_4^\vee) = \beta_4 = Q'(e_4^\vee)$. As observed in Remark 9.2, the remaining elements $\beta(e_i^\vee) \in L^\vee$ are determined by the S_3-symmetry of Δ and so we see that $\beta = Q'$. We note that therefore the stacky secondary fan still has the S_3-symmetry from Remark 9.2.

It follows that the secondary stack can be described as the quotient of the open subset in $(\mathbb{C}^9)^\vee$ determined by the secondary fan (see §3.4) by $(\mathbb{C}^*)^6$ with weights $A' : \mathbb{Z}^9 \to \mathbb{Z}^6$. We set $\beta_i := Q'(e_i^\vee)$ for $i = 1, \dots, 9$ (noting that this agrees with our previous labels for the weights with $i = 1, \cdots, 6$) and label the facets of $\Sigma(A)$ corresponding to β_i by F_i, as shown in Figure 24.

9.1.3. *The FIPS.* To understand the FIPS, we need to understand the discriminant. It has 7 components in total corresponding to the 7 faces of Δ given by Δ itself (this corresponds to the principal component ∇_{pr}), the three edges of Δ (this gives three components ∇_i) and the three vertices of Δ.

In the coordinates a_i on $\mathbb{C}^6$, the vertex components correspond to the 3 toric divisors $a_1 = 0$, $a_3 = 0$ and $a_6 = 0$. This means that the FIPS lives inside $[\mathbb{C}^6 \setminus \bigcup_{i=1,3,6}\{a_i = 0\}/(\mathbb{C}^*)^3]$, which can be identified with $[\mathbb{C}^3/\mathbb{Z}_2^{\oplus 2}]$ where the "coordinates" on $\mathbb{C}^3$ are given by $u = a_2/\sqrt{a_1 a_3}, v = a_4/\sqrt{a_1 a_6}$ and $w = a_5/\sqrt{a_3 a_6}$ and $G = \mathbb{Z}_2^{\oplus 2}$ embeds into $(\mathbb{C}^*)^3$ exactly as in (6) in §9.1.1. As such, we have 3 lines of $\mathbb{Z}_2$-orbifold points in the FIPS degenerating into a G-orbifold point at the one remaining torus fixed point (corresponding to the origin).

Remark 9.3. This similarity between the orbifold phase of the Triangle VGIT (corresponding to a chamber C say) and the description of a small neighbourhood V_C in the FIPS of the torus fixed point p_C (see §5.1) is partially coincidental.

By the discussion of the orbifold case at the end of §3.4, we know that the FIPS of a VGIT with an orbifold phase $[\mathbb{C}^m/G]$ is an open subset (containing the origin and all neighbouring divisors) of $[\mathbb{C}^n/G]$ (where n is the number of rays which are not vertices of Δ) and the torus fixed point at the origin is p_C. Hence, in this setting, V_C is always a deformation retract of $[\mathbb{C}^n/G]$. So in the Triangle VGIT the only coincidence is that $m = n = 3$. In general, this does not have to hold. For example, in the case of $\mathrm{Tot}(K_{\mathbb{P}^{n-1}})$ flopping to $[\mathbb{C}^n/\mathbb{Z}_n]$, the FIPS is an open subset inside $[\mathbb{C}/\mathbb{Z}_n]$.

Now that we understand the ambient space, we turn to understanding the 4 remaining components of the discriminant. Following §3.1, we consider the family $\mathbb{C}^A$ of superpotentials given by $W = z(a_1x^2 + a_2xy + a_3y^2 + a_4x + a_5y + a_6)$. Then ∇_{pr} is given by the discriminant of W, namely those a_i for which W has a critical point in $(\mathbb{C}^*)^3$. This can therefore be described as:

$$\det\begin{pmatrix} a_1 & a_2/2 & a_4/2 \\ a_2/2 & a_3 & a_5/2 \\ a_4/2 & a_5/2 & a_6 \end{pmatrix} = 0$$

Similarly, ∇_i is the discriminant of the quadratic polynomial in one variable corresponding to restricting W to the edge opposite ω_1, ω_3 and ω_6 for $i = 1, 2, 3$ respectively. As such, $\nabla_1 = \{a_3a_6 = 4a_5^2\}$, $\nabla_2 = \{a_1a_6 = 4a_4^2\}$ and $\nabla_3 = \{a_1a_3 = 4a_2^2\}$. So the FIPS is the complement of $\nabla_{pr} \cup \bigcup_{i=1}^3 \nabla_i$ inside $[\mathbb{C}^3/G]$. In the coordinates u, v, w above, this can be written as $[\mathbb{C}^3 \setminus \{u^2 = 4, v^2 = 4, w^2 = 4, u^2 + v^2 + w^2 = uvw + 4\}/G]$.

Remark 9.4. One checks that ∇_{pr} has a unique singular point inside $[\mathbb{C}^3/G]$, which is a node at $(u, v, w) = (2, 2, 2)$.

Remark 9.5. We can also think about the discriminant locus inside the secondary stack $\mathfrak{F}$ (see Definition 3.42). In this case, the discriminant comprises the toric divisors $a_i = 0$ for $i = 1, 3, 6, 7, 8, 9$ as well as the 4 non-toric components above.

9.2. **The Lefschetz strategy.** Now that we understand the FIPS of the Triangle VGIT, we turn to proving that its fundamental groupoid acts. Recall from §2.4.1 that our basic strategy is to reduce the problem to constructing representations on the simpler VGITs which arise on the boundary of the secondary stack. We have already met some of these in Figure 4. Then the reduced problem will be to construct representations of $\pi_1(\mathrm{FIPS}(F_i))$, where F_i is the face of the secondary polytope corresponding to $\beta_i \in L^\vee$ (see Figure 24) and $\mathrm{FIPS}(F_i)$ is the complement of the discriminant in the corresponding toric divisor $D_i' \subset \mathfrak{F}$ (if this divisor is a (toric) component of the discriminant, we don't delete this component so $\mathrm{FIPS}(F_i)$ is always non-empty).

Remark 9.6. Calling this complement $\mathrm{FIPS}(F_i)$ is an abuse of notation because this space is not the FIPS of any Calabi–Yau VGIT in general. However, for the faces F_i in the Triangle VGIT, $\mathrm{FIPS}(F_i)$ will actually either be the FIPS of such a VGIT or a product of two such FIPS.

The crucial thing that allows us topologically to reduce to the boundary is that we can find an ample (reducible) toric divisor D on $\mathfrak{F}$ such that all its components meet the non-toric part of the discriminant "transversely" (see the discussion following Lemma 9.20). In particular, all the torus invariant curves $Z(W)$ in D intersect exactly one component of the discriminant and do so transversely. In general, to describe the topology of a neighbourhood of D in the FIPS we would have to include additional near large radius paths, living in the push-offs (see §5.2) of

the large radius curves $Z(W)$, as well as additional relations between these, living in the push-offs (see Remark 5.17) of the large radius divisors D_i' which make up D. Here transversality implies that these push-offs still look like $Z(W)$ and D_i' respectively – that is, there is no distinction between large radius and near large radius near these curves and divisors. As a result, it is enough to construct the representation on all of the divisors D_i' contained in D and check that these glue together over the curves $Z(W)$ where two such divisors meet.

Remark 9.7. Though the details in this section are specific to the Triangle VGIT, we expect that, whenever we can find a divisor D as above, very similar arguments would allow us to reduce constructing the representation of $\pi_1(\mathrm{FIPS})$ to constructing representations of $\pi_1(\mathrm{FIPS}(F_i))$ where F_i label the facets corresponding to components of D.

Remark 9.8. We note that there are curves $Z(W)$ in $\mathfrak{F}$ which intersect more than one component of the discriminant. In fact, for the particular ample divisor D we will choose, any curve $Z(W)$ not in D has this property – this is one reason for our choice of D in the first place. One can check that the curves not in D meet two components of the discriminant – namely, ∇_{pr} and one of the ∇_i – each with multiplicity one. So understanding the near large radius representation near these walls would involve SODs.

We'll now go over the strategy for proving this result. We'll then fill in the missing details in later sections.

(1) First we delete the locus $Y = \bigcup_{i=2,4,5} D_i'$ from the FIPS to get $\mathrm{FIPS}^o := \mathrm{FIPS}\backslash Y$. Noting that Y is the union of the toric divisors in the FIPS, we see that the stacky locus of the FIPS is contained in Y. This locus causes technical complications, both for the Lefschetz hyperplane theorem and for the existence of some push-offs that we will need. By Proposition 7.2, we know that $\pi_1(\mathrm{FIPS})$ is just the quotient of $\pi_1(\mathrm{FIPS}^o)$ by the meridians around D_i' (for $i = 2, 4, 5$), which are precisely the toric loops α^{β_i}. Therefore, to construct our representation ρ, it suffices to construct a representation of $\pi_1(\mathrm{FIPS}^o)$ which acts trivially on α^{β_i}. Since the representation ρ we construct on $\pi_1(\mathrm{FIPS}^o)$ will act in the canonical way (see §5.1) on toric loops (including α^{β_i}), this property will be automatic as the corresponding line bundles are trivial (since the divisors making up Y are in the FIPS).
(2) Using the Lefschetz hyperplane theorem (see Corollary 9.14) with the toric hyperplane $D := 4(D_1' + D_3' + D_6') + 6(D_7' + D_8' + D_9')$, we'll see that there is a family depending on $\epsilon \in \mathbb{R}_{>0}$ of neighbourhoods U_ϵ of D in FIPS^o which, for ϵ sufficiently small, contains the homotopy 1-type and so $\pi_1(\mathrm{FIPS}^o) \cong \pi_1(U_\epsilon)$.
(3) So we want to understand $\pi_1(U_\epsilon)$. For this, we'll introduce another family of neighbourhoods of D in FIPS^o depending on $\delta \in \mathbb{R}_{>0}$ called V_δ. By construction, we understand the topology of V_δ better than that of U_ϵ. We'll

show (see Lemma 9.18) that they are homotopy equivalent for δ sufficiently small and so we can work with V_δ instead.

Explicitly, V_δ is defined by gluing together near large radius regions near torus invariant divisors, curves and points in D. Specifically, recall the near large radius regions V_β, V_W and V_C from §5.2 near these respective toric subvarieties, where β is a ray of the secondary fan, W is a 2-dimensional cone and C is a chamber. The construction of these regions depend on certain choices, but, having made all these choices (see Lemma 9.17), we can define the region $V_\delta := \bigcup V_{C_k} \cup \bigcup V_{W_j} \cup \bigcup V_{\beta_i} \subset \mathrm{FIPS}^o$ which will be a neighbourhood of D in FIPS^o.

(4) By the van-Kampen theorem, $\pi_1(V_\delta)$ is obtained by gluing together the fundamental groupoids of the cover. Moreover, we know from Proposition 5.20 how to define our representation on near large radius regions V_C and V_W near torus invariant points and curves respectively. This is because there are no near large radius complications for the curves $Z(W)$ in D, as we remarked at the beginning of this section. We also know from Remark 5.24 that the representations on these regions near points and curves glue together canonically to give a representation ρ of the fundamental groupoid of the region $\bigcup V_{C_k} \cup \bigcup V_{W_j} \subset V_\delta \subset \mathrm{FIPS}^o$.

(5) Now we want to define the representations ρ^i on $\pi_1(V_{\beta_i})$. Recall that the regions V_{W_j} and V_{β_i} come with a fibration structure, which here we denote by π_{W_j} and π_{β_i} respectively. Then the base B of this fibration is a punctured 2-dimensional polydisk and a punctured disk respectively. Therefore, the fibres $\pi_{W_j}^{-1}(b)$ and $\pi_{\beta_i}^{-1}(b)$ are 1- and 2-dimensional respectively and play the role of the push-off of the large radius curve $Z(W_j)$ and large radius divisor $\mathrm{FIPS}^o(F_i)$, where $\mathrm{FIPS}^o(F_i)$ is the complement of the toric boundary in $\mathrm{FIPS}(F_i)$. Then Remark 5.17 tells us that $\pi_1(V_{\beta_i}) \cong \pi_1(\pi_{\beta_i}^{-1}(b)) \rtimes \langle \alpha^{\beta_i} \rangle$ where the action on $\pi_1(\pi_{\beta_i}^{-1}(b))$ is by monodromy around B. Since the discriminant locus is transverse to D, we get (see Lemma 9.20) a homotopy equivalence $\pi_{\beta_i}^{-1}(b) \simeq \mathrm{FIPS}^o(F_i)$. We've already remarked that the monodromy in V_W near the large radius curve $Z(W)$ is trivial. We'll see that all the generators of $\pi_1(\pi_{\beta_i}^{-1}(b))$ live in regions of the form V_W and so it follows that the monodromy action on $\pi_1(\pi_{\beta_i}^{-1}(b))$ is trivial. Therefore $\pi_1(V_{\beta_i}) \cong \pi_1(\mathrm{FIPS}^o(F_i)) \times \langle \alpha^{\beta_i} \rangle$.

(6) Up to the S_3-symmetry of the Triangle VGIT, there are only two possibilities for $\mathrm{FIPS}^o(F_i)$. For $i = 7, 8, 9$, $\mathrm{FIPS}^o(F_i)$ can be described as the hyperplane complement from Example 7.6 (with the coordinates axes deleted). Hence $\pi_1(\mathrm{FIPS}^o(F_i))$ has a simple presentation, generated by large radius paths subject to 4 additional explicit relations. For $i = 1, 3, 6$, $\mathrm{FIPS}(F_i)$ is exactly the FIPS of the Pentagon VGIT from §7.3 and so again we have already described an explicit presentation generated by large radius paths in Proposition 7.25.

Given these explicit presentations of $\pi_1(\mathrm{FIPS}^o(F_i))$, we can construct a representation of them on the Triangle VGIT. Moreover, this extends naturally (α^{β_i} acts by tensoring by the corresponding line bundle) to give representations ρ^i of $\pi_1(V_{\beta_i})$ for i in D.

(7) Finally, we check that ρ^i and ρ glue together on intersections.

Remark 9.9. In (1), we remarked that, since the FIPS is stacky, we want to delete the stacky locus and work on FIPS^o instead. Alternatively, we could just use a stacky quasi-projective Lefschetz theorem but, unfortunately, such a theorem at this level of generality doesn't seem to exist yet (though see [23] for a stacky projective Lefschetz theorem). As such, we adopt a roundabout approach to using the Lefschetz hyperplane theorem by passing through the coarse moduli space $|\mathfrak{F}|$, which is a singular toric variety, and using the quasi-projective Lefschetz theorem for singular schemes which we review in §9.2.1.

So what we have left to check is as follows:

(1) (§9.2.1) Check that D is ample and use the Lefschetz hyperplane theorem.
(2) (§9.2.2) Pick the data defining the regions V_{β_i} for each D_i' in D, V_{W_j} for each wall W_j in D and V_{C_k} for each chamber C_k in D. These regions all depend on $\delta \in \mathbb{R}_{>0}$ but we drop this from the notation. This data defines V_δ.
(3) (§9.2.2) Prove $\pi_1(U_\epsilon) \cong \pi_1(V_\delta)$ for δ sufficiently small.
(4) (§9.2.2) Prove that the 2-dimensional fibre $\pi_{\beta_i}^{-1}(b)$ of $\pi_{\beta_i} : V_{\beta_i} \to B$ is homotopy equivalent to $\mathrm{FIPS}^o(F_i)$.
(5) (§9.2.3 and §9.2.4) Construct representations $\rho^i : \pi_1(\mathrm{FIPS}^o(F_i)) \to \mathbf{Cat}_1$ for each i in D. By the S_3-symmetry, we actually need only do this for $i = 1, 8$.
(6) (§9.2.5) Check that ρ and ρ^i glue together

Remark 9.10. It will follow from our eventual description of $\pi_1(\mathrm{FIPS})$ that the fundamental *group* based at the phase which is isomorphic to $\mathrm{Hilb}^G(\mathbb{C}^3)$, which here we call X_3, is generated by toric loops plus certain loops consisting of large radius paths. Up to the S_3-symmetry, in fact the generating loops of the second type live solely in the push-off of $\mathrm{FIPS}(F_1)$. If we pick 5 basepoints p_i near the torus fixed points p_{C_i} in D_1' (see Figure 26), such loops are roughly given by:

(1) Going from p_3 to p_1 and back to p_3, looping the component ∇_{pr}.
(2) Going from p_3 to p_2 and back to p_3, looping the component ∇_{pr}.
(3) Going from p_3 to p_1, then to p_4 and back to p_1 (looping the component ∇_1) and finally back to p_3 along the original path.
(4) Going from p_3 to p_2, then to p_5 and back to p_2 (looping the component ∇_1) and finally back to p_3 along the original path.

The corresponding autoequivalences are as follows:

(1) We let X_1 be the phase corresponding to C_1 and $Z_{4,5}$ denote the curve in X_3 corresponding to the codimension 1 cone generated by the rays ω_4 and

ω_5. Then $Z_{4,5}$ is a $\mathbb{P}^1$ with $\mathcal{N}_{Z_{4,5}/X_3} \cong \mathcal{O}_{\mathbb{P}^1}(-1)^{\oplus 2}$. Then looping ∇_{pr} gives a spherical twist around a sheaf supported on $Z_{4,5}$.

(2) We let X_2 be the phase corresponding to C_2 and $Z_{2,5}$ denote the curve in X_3 corresponding to the codimension 1 cone generated by the rays ω_2 and ω_5. Then $Z_{2,5}$ has the same normal bundle as $Z_{4,5}$ and looping ∇_{pr} gives a spherical twist around a sheaf supported on $Z_{2,5}$.

(3) Use a window equivalence to identify X_3 with the phase X_1. In X_1, the toric divisor D_5 is fibred over a base $\mathbb{C}$ with fibre a $\mathbb{P}^1$ and $\mathcal{N}_{D_5/X_1} \cong \mathcal{O}_{D_5}(-2)$, so this is a family of (-2)-curves. Then the auto-equivalence corresponding to looping around ∇_1 is a family version of spherical twists around (-2)-curves in a surface. In particular, this auto-equivalence is supported on D_5.

(4) Use a window equivalence to identify X_3 with the phase X_2. Again, the toric divisor D_5 is fibred over a base $\mathbb{C}$ with fibre a $\mathbb{P}^1$ and $\mathcal{N}_{D_5/X_2} \cong \mathcal{O}_{D_5}(-2)$, so this is a family of (-2)-curves. Then the auto-equivalence corresponding to looping around ∇_1 is again a family version of spherical twists around (-2)-curves in a surface and hence supported on D_5.

9.2.1. *The Lefschetz hyperplane theorem.* The version of the quasi-projective Lefschetz hyperplane theorem that we will need is:

Theorem 9.11 ([26], Theorem 1.1.1)**.** *Let X be a projective subvariety in $\mathbb{P}^N$, $Z \subset X$ a subvariety and L a hyperplane in $\mathbb{P}^N$ such that $X \backslash (Z \cup L)$ is non-singular. Identifying $\mathbb{P}^N \backslash L$ with $\mathbb{C}^N_{z_1,\dots,z_N}$, we let $V_R(L) := \mathbb{P}^N \backslash \{\sum |z_i|^2 < R\}$ be a tubular neighbourhood of L in $\mathbb{P}^N$. Then $X \backslash Z$ has the homotopy type of a space obtained from $V_R(L) \cap (X \backslash Z)$ (for R sufficiently large) by adding cells of dimension at least $dim_{\mathbb{C}}(X)$ (where this homotopy equivalence is the identity on $V_R(L) \cap (X \backslash Z)$).*

One can prove this via Morse theory analogously to Andreotti and Frankel's proof of the usual projective Lefschetz theorem [2]. The subtlety is controlling the (pseudo-)gradient flow so that it preserves Z, which can be very singular. The key technique for doing this is using an algebraic Whitney stratification of X such that Z is a union of strata. We'll return to this in Lemma 9.20.

Remark 9.12. This theorem should be enough to see the claim in Remark 6.25 that, when the FIPS is 2-dimensional, $\pi_1(U)$ generates $\pi_1(\text{FIPS})$ where U is the union of the near large radius regions V_W for all walls W. Certainly, it follows from the theorem that some tubular neighbourhood of the toric boundary generates $\pi_1(\text{FIPS})$ by taking $X = |\mathfrak{F}|$, Z the discriminant and L an ample (reducible) toric divisor containing all irreducible toric divisors with multiplicity at least 1. Then, noting $X \backslash L \cong T_{L^\vee}$ is smooth, the homotopy 1-type of the FIPS ($= X \backslash Z$) is generated by $V_R(L) \cap \text{FIPS}$, which is a tubular neighbourhood of the toric boundary in the FIPS. This tubular neighbourhood should be homotopic to U by a similar argument to Lemma 9.18 below, but we haven't checked the details.

We apply Theorem 9.11 to the Triangle VGIT as follows. Recall that we denote the toric divisor in $\mathfrak{F}$ corresponding to β_i by D_i'.

Lemma 9.13. *The torus invariant divisor (invariant also under the S_3-symmetry) $D = a(D_1' + D_3' + D_6') + b(D_7' + D_8' + D_9')$ is ample precisely when $a > 0, b > 0$ and $2a > b > a$.*

Proof. By standard toric geometry ([14], Theorem 6.1.14), we need to prove that the piecewise-linear function on the secondary fan which sends $\beta_i \mapsto -a$ for $i = 1, 3, 6$, $\beta_j \mapsto -b$ for $j = 7, 8, 9$ and $\beta_k \mapsto 0$ for $k = 2, 4, 5$ is strictly convex. This is a straightforward computation. □

Now let $|\mathfrak{F}|$ be the singular toric variety corresponding to the secondary fan – that is, the coarse moduli space of $\mathfrak{F}$. Then it follows from [14], Theorem 6.1.14 that $D \coloneqq 4(D_1' + D_3' + D_6') + 6(D_7' + D_8' + D_9')$ is a very ample divisor on $|\mathfrak{F}|$ and we take $|\mathfrak{F}|$ embedded in $\mathbb{P}^N$ by the complete linear series on D. As such, we have a hyperplane $L \subset \mathbb{P}^N$ such that $L \cap |\mathfrak{F}| = D$. Let $Z \coloneqq \bigcup_{i=1,\cdots,9} D_i' \cup \nabla_{pr} \cup \bigcup_{j=1,2,3} \nabla_j \subset |\mathfrak{F}|$ be the union of all components of the discriminant as well as the 3 toric divisors in the FIPS, so that $|\mathfrak{F}| \backslash Z = \mathrm{FIPS}^o$.

Corollary 9.14. *Define $U_\epsilon \coloneqq \mathbb{P}^N \backslash \{\frac{1}{\sum |z_i|^2} > \epsilon\} \cap FIPS^o$. Then U_ϵ, for ϵ sufficiently small, has the same homotopy 1-type as $FIPS^o$. In particular, $\pi_1(FIPS^o) \cong \pi_1(U_\epsilon)$.*

Proof. Take $X = |\mathfrak{F}|$ and Z and L as above. Then $X \backslash (Z \cup L) \subset T_{L^\vee}$ is non-singular so we may apply Theorem 9.11. As $\dim(X) = 3$, we get that $X \backslash Z = \mathrm{FIPS}^o$ has the same homotopy 1-type as $V_{1/\epsilon}(L) \cap \mathrm{FIPS}^o = U_\epsilon$ for ϵ sufficiently small. □

9.2.2. *Near large radius regions near D.* In this section, we define the various near large radius regions whose union is a neighbourhood V_δ of D in FIPS^o and prove the fiddly results which describe their topology.

Most of the notation here aligns with §5.2. Additionally, recalling that β_i define the rays of the secondary fan, we let $W_{ij} = \langle \beta_i, \beta_j \rangle$ be the wall – that is, codimension 1 cone in the secondary fan – generated by β_i and β_j when this really is a cone of the secondary fan and $W_{ij} = \varnothing$ when it isn't. Similarly, we let $C_{ijk} = \langle \beta_i, \beta_j, \beta_k \rangle$ when this is a maximal cone of the secondary fan and $C_{ijk} = \varnothing$ when it isn't.

Recall from §5.2 that to define the near large radius region $V_W \subset \mathrm{FIPS}^o$ near the large radius curve $Z(W)$ we need to pick a fibration structure. This is determined by choosing $\beta_W \in L^\vee$ such that $\langle \beta_W, \lambda_W \rangle = \pm 1$ (here $\lambda_W \in L$ is either choice of primitive normal to W) and then the corresponding 1-dimensional fibres will be contained in β_W-orbits. Similarly, to define the fibration structure on the near large radius region V_β near a toric divisor, we need to pick $\lambda_\beta \in L$ such that $\langle \beta, \lambda_\beta \rangle = 1$ and the fibres will live in orbits of the rank 2 torus $T_{L_\beta^\vee}$, where $L_\beta^\vee = \{\langle -, \lambda_\beta \rangle = 0\} \subset L^\vee$. Recall from Figure 24 that there are 13 non-empty chambers C_{ijk} near D, 18 non-empty walls W_{ij} near D and 6 rays β_i near D. Up to the S_3-symmetry of the

secondary fan, we need only focus on 4 of these walls (say $W_{16}, W_{15}, W_{18}, W_{58}$) and 2 of these rays (say β_1, β_8). For these walls and rays, we pick the following data:

- $\lambda_{\beta_1} = (1,0,0), \lambda_{\beta_8} = (0,-1,0)$
- $\beta_{W_{16}} = (0,1,0), \beta_{W_{15}} = (0,0,1), \beta_{W_{18}} = (0,0,1), \beta_{W_{58}} = (1,0,0)$

Now that we have fixed the fibration structure, we need to pick the subsets V_{β_i} and $V_{W_{ij}}$ near D_i' and $Z(W_{ij})$ respectively. This amounts to two choices:

- A closed subset $E_{W_{ij}} \subset T_{L^\vee/W_{ij}}$ of the open torus inside $Z(W_{ij})$ which is a deformation retract and a similar region $E_{\beta_i} \subset T_{L^\vee/\beta_i}$ inside the open torus in D_i' such that $\mathrm{FIPS}^o(F_i) \cap E_{\beta_i} \subset \mathrm{FIPS}^o(F_i)$ is a deformation retract. We then consider only points in $\mathfrak{F}$ which limit under any of the 1-PS in the relative interior of the wall W_{ij} to $E_{W_{ij}}$ and similarly only points which limit under β_i to E_{β_i}.
- Having made this choice, we then need to shrink the base B' of the fibration to a region B in order to guarantee that it remains a fibration when we delete the discriminant.

Remark 9.15. This section would be a lot simpler if we could just pick regions V_{β_i} near each divisor D_i' in D which together form a neighbourhood of D. Unfortunately, as we have seen in 2-dimensions, we can't just take $E_{\beta_i} = T_{L^\vee/\beta_i}$ because the rank 2 $T_{L^\vee_{\beta_i}}$-orbit (in which the fibres of π_{β_i} live) typically limits to multiple divisors in $\mathfrak{F}$. As such, the whole of this orbit doesn't remain near D_i' and we have to define V_{β_i} using a region E_{β_i} which is strictly smaller than $T_{L^\vee_{\beta_i}}$. But then $V_{\beta_i} \cap V_{\beta_j}$ is strictly smaller than $V_{W_{ij}}$ and so the regions V_{β_i} on their own won't form a neighbourhood of D. Thus we are forced to add in regions of the form $V_{W_{ij}}$.

We also need these regions to depend on $\delta \in \mathbb{R}_{>0}$ in such a way that, as $\delta \to 0$, these regions shrink down to the corresponding divisor D_i' and curve $Z(W_{ij})$. We accomplish this by picking an explicit punctured (poly)disk B in the base of the fibration which depends on δ, as we now describe.

- Since there are no toric divisors in FIPS^o, we must delete the fibre over the torus fixed point $\underline{0} \in B'$ for V_β to be a subset of FIPS^o. Thus $\pi_\beta : V_\beta \to B$ is a fibration over a punctured disk B. Here B has a natural coordinate b coming from the natural coordinate on the toric variety $B' (\cong \mathbb{C})$ in which it sits. Then we can take $B = B_\delta = \{|b| \leq \delta\} \subset \mathbb{C}^*$ and so the subset V_β^δ also depends on δ. Explicitly, if we take coordinates X, Y, Z on the torus $T_{L^\vee}$ such that $\pi_{\beta_i}^*(b) = x^{\lambda_{\beta_i}} = X$ and $Y, Z \in L$ are invariant under the 1-PS β_i – that is, lie in the hyperplane defined by β_i – then $V_{\beta_i}^\delta = \{|X| \leq \delta, (Y,Z) \in E_{\beta_i}\}$.
- Recall (see §5.2) that $\pi_W : V_W \to B$ is only a fibration away from a divisor $Z \subset B$ where B is a punctured polydisk. However, in this case, as all the walls W near D have intersection multiplicity $m_W = 1$, π_W is a fibration over all of B. The affine toric variety B' for the walls W_{16}, W_{15}, W_{18} is just $\mathbb{C}^2_{b_1,b_2}$ and for W_{58} is the smooth orbifold $[\mathbb{C}^2_{b_1,b_2}/\mathbb{Z}_2]$ (B' is an orbifold here because $Z(W_{58})$ supports a $\mathbb{Z}_2$-orbifold locus – see §9.2.3). Then we

can take $B = B_\delta = \{|b_1| \leq \delta, |b_2| \leq \delta\} \subset (\mathbb{C}^*)^2$ for the first 3 walls and $B = B_\delta = \{|b_1| \leq \sqrt{\delta}, |b_2| \leq \sqrt{\delta}\}/\mathbb{Z}_2 \subset (\mathbb{C}^*)^2/\mathbb{Z}_2$ for W_{58}. Again the subset V_W^δ also depends on δ. Explicitly, if we take coordinates X, Y, Z on $T_{L^\vee}$ such that $\pi^*_{W_{ij}}(b_1) = X, \pi^*_{W_{ij}}(b_2) = Y$ and $Z = x^{\lambda_{W_{ij}}}$ then $V^\delta_{W_{ij}} = \{|X| \leq \delta, |Y| \leq \delta, Z \in E_{W_{ij}}\}$.

- For the punctured polydisk V_C, we pick a description of the toric open set $U_C \subset \mathfrak{F}$ as $[\mathbb{C}^3/G]$ with coordinates b_i on $\mathbb{C}^3$ for $i = 1, 2, 3$. Then we can choose $V_C^\delta = \{|b_1| \leq \delta, |b_2| \leq \delta, |b_3| \leq \delta\}/G \subset (\mathbb{C}^*)^3/G$.

So each near large radius region we are considering depends on a choice of δ which in principle we could vary independently. But we are looking to glue all of these regions together to construct a single family V_δ of neighbourhoods of D in FIPS^o which depends on δ and shrinks down to D as $\delta \to 0$. As such, for each β_i, we're going to pick an increasing continuous function $f_i : \mathbb{R}_{>0} \to \mathbb{R}_{>0}$ and take $V_{\beta_i}^{f_i(\delta)}$ as part of our neighbourhood. Similarly for W_{ij} and C_{ijk} we're going to pick f_{ij} and f_{ijk} and take the corresponding subsets $V_{W_{ij}}^{f_{ij}(\delta)}$ and $V_{C_{ijk}}^{f_{ijk}(\delta)}$ as part of our neighbourhood.

Remark 9.16. Note that, in order to maintain the property that the union of these regions is a neighbourhood on D for all δ sufficiently small (as in (1) in Lemma 9.17), the regions E_{β_i} and $E_{W_{ij}}$ also need to depend on δ – in fact, they should grow with δ, since the punctured polydisks $V_{C_{ijk}}$ shrink with δ.

The next lemma says that, for every δ, we can make all these additional choices in such a way that we can guarantee that their union is a neighbourhood of D in FIPS^o. Moreover, it says that, for every δ, we can choose the intersections between these regions to be particularly simple. This will make the gluing relations between the representations ρ^i on different faces transparent when we come to check them in §9.2.5.

Lemma 9.17. *We can define subsets $V_{\beta_i}^{f_i(\delta)} \subset FIPS^o$ near each D_i' in D, $V_{W_{ij}}^{f_{ij}(\delta)}$ near each $Z(W_{ij})$ in D and $V_{C_{ijk}}^{f_{ijk}(\delta)}$ near each torus fixed point in D which have the following properties:*

(1) *If we define:*

$$V_\delta := \bigcup V_{C_{ijk}}^{f_{ijk}(\delta)} \cup \bigcup V_{W_{ij}}^{f_{ij}(\delta)} \cup \bigcup V_{\beta_i}^{f_i(\delta)} \subset FIPS^o$$

then $V_{\delta'} \subset V_\delta$ for $\delta' \leq \delta$ and the closure $\bar{V}_\delta$ in $|\mathfrak{F}|$ is a neighbourhood of D.

(2) $\bigcap_{\delta \downarrow 0} \bar{V}_\delta = D$

(3) *The subsets respect the S_3-symmetry (see Remark 9.2)*

(4) *Two of these subsets meet precisely if one of the corresponding toric subvarieties of $|\mathfrak{F}|$ is contained in the other.*

(5) $V_{\beta_i}^{f_i(\delta)} \cap V_{W_{ij}}^{f_{ij}(\delta)} \subset V_{W_{ij}}^{f_{ij}(\delta)}$ *(where $V_{W_{ij}}^{f_{ij}(\delta)} = \varnothing$ if $W_{ij} = \varnothing$) is a deformation retract*

(6) $V_{\beta_i}^{f_i(\delta)} \cap V_{C_{ijk}}^{f_{ijk}(\delta)} \subset V_{C_{ijk}}^{f_{ijk}(\delta)}$ *(where $V_{C_{ijk}}^{f_{ijk}(\delta)} = \varnothing$ if $C_{ijk} = \varnothing$) is a deformation retract*

(7) $V_{W_{ij}}^{f_{ij}(\delta)} \cap V_{C_{ijk}}^{f_{ijk}(\delta)} \subset V_{C_{ijk}}^{f_{ijk}(\delta)}$ *is a deformation retract*

Proof. This is elementary but tedious so we don't give all the details. Start by taking coordinates on $T_{L^\vee} \cong (\mathbb{C}^*)^3_{X,Y,Z}$ which correspond to the standard basis in $L^\vee = \mathbb{Z}^3$. As $\lambda_{\beta_1} = (1,0,0)$, $x^{\lambda_{\beta_1}} = X$ is the coordinate on the base B and Y, Z are invariant under β_1 so $V_{\beta_1}^\delta = \{|X| \leq \delta, (Y,Z) \in E_{\beta_1}\}$. We can choose $E_{\beta_1} = \{|Y| \leq 1/\delta, |Z| \leq 1/\delta\}$: this is a valid choice of E_{β_1} because the co-rank 1 torus orbit $X = \delta$ in $V_{\beta_1}^\delta$ stays bounded as $Y \to 0$ and $Z \to 0$ – otherwise, we would have to delete a small neighbourhood of $Y = 0$ and $Z = 0$ from E_{β_1} too. With this choice, $V_{\beta_1}^\delta = \{|X| \leq \delta, |Y| \leq 1/\delta, |Z| \leq 1/\delta\}$. Then the S_3-symmetry implies that $V_{\beta_6}^\delta = \{|X| \leq 1/\delta, |Y| \leq 1/\delta, |Z| \leq \delta\}$. Hence $V_{\beta_1}^\delta \cap V_{\beta_6}^\delta = \{|X| \leq \delta, |Y| \leq 1/\delta, |Z| \leq \delta\}$ for δ sufficiently small. But $\beta_{W_{16}} = (0,1,0)$ and so X, Z are coordinates on the base B and, as $\lambda_{W_{16}} = (0,1,0)$, $x^{\lambda_{W_{16}}} = Y$ and so $V_{W_{16}}^\delta = \{|X| \leq \delta, |Z| \leq \delta, Y \in E_{W_{16}}\}$. Hence if we define $E_{W_{16}} \subset Z(W_{16})$ to be the cylinder $|Y| \leq 1/\delta$, we see that we can guarantee $V_{\beta_1}^\delta \cap V_{\beta_6}^\delta = V_{W_{16}}^\delta$ in this case. Continuing in this way, we can find the other near large radius regions and check the relevant properties. Note that in general, we are not able to guarantee that the intersections are actually equal, just a deformation retract of the smaller one. □

We assume from now on that we have fixed such a choice of regions for each δ and drop the explicit choices from the notation. For example, V_{β_i} will refer to $V_{\beta_i}^{f_i(\delta)}$ with a choice of E_{β_i} as in Lemma 9.17.

Lemma 9.18. *For ϵ sufficiently small, U_ϵ is homotopy equivalent to V_δ.*

Proof. It suffices to show that:

- For any δ sufficiently small, we can find ϵ such that $U_\epsilon \subset V_\delta$
- For any ϵ sufficiently small, we can find δ such that $V_\delta \subset U_\epsilon$
- For any $\epsilon' \leq \epsilon$ sufficiently small, the inclusion $U_{\epsilon'} \subset U_\epsilon$ is a homotopy equivalence.
- For any $\delta' \leq \delta$ sufficiently small, the inclusion $V_{\delta'} \subset V_\delta$ from Lemma 9.17 (1) is a homotopy epimorphism.

To see that these four properties are sufficient, use them to find a $V_\delta \subset U_\epsilon$ and a $U_{\epsilon'} \subset V_\delta$. Then the inclusion $U_{\epsilon'} \subset U_\epsilon$ is a homotopy equivalence which factors through V_δ and so $U_{\epsilon'} \subset V_\delta$ is a homotopy monomorphism. Now find a $V_{\delta'} \subset U_{\epsilon'}$. Similarly the inclusion $V_{\delta'} \subset V_\delta$ is a homotopy epimorphism which factors through $U_{\epsilon'}$ and so the inclusion $U_{\epsilon'} \subset V_\delta$ is a homotopy epimorphism. Being a homotopy monomorphism and epimorphism is enough to guarantee that the inclusion $U_{\epsilon'} \subset V_\delta$ is a homotopy equivalence.

We now check these properties:

- For contradiction, suppose we could find a sequence $x_i \in V_{\delta_i}$ with $\delta_i \downarrow 0$ such that $x_i \notin U_\epsilon$. Then the closure $\bar{V}_\delta$ in $|\mathfrak{F}|$ is compact and so some subsequence x_j converges to $x \in \bar{V}_\delta$. But then $x \in \bigcap \bar{V}_\delta = D$ by (2) in Lemma 9.17. But $x_j \notin U_\epsilon$ means that $f(x_j) > \epsilon$ where $f := \frac{1}{\sum |z_i|^2} : |\mathfrak{F}| \to [0, \infty]$ is the function

in the definition of U_ϵ. Thus $f(x) \neq 0$. This is a contradiction as f vanishes precisely on D.

- For contradiction, suppose we could find a sequence $x_i \in U_{\epsilon_i}$ with $\epsilon_i \downarrow 0$ such that $x_i \notin V_\delta$. Then the closure $\bar{U}_\epsilon$ of U_ϵ in $|\mathfrak{F}|$ is compact and so some subsequence x_j converges to $x \in \bar{U}_\epsilon$. But then $x \in \bigcap \bar{U}_\epsilon = D$ since $\bar{U}_\epsilon = \{f \leq \epsilon\}$ where f is the function above. But, by (1) in Lemma 9.17, $\bar{V}_\delta$ is a neighbourhood of D in $|\mathfrak{F}|$ and so $x_i \in V_\delta$ for i sufficiently large, which is a contradiction.
- The fact that U_ϵ is homotopy equivalent to $U_{\epsilon'}$ follows immediately from [26], §1.4.3. This is basically because we can modify the gradient flow of f to preserve the discriminant.
- To show that the inclusion $V_{\delta'} \subset V_\delta$ is a homotopy epimorphism, it suffices to construct a vector field on V_δ whose time-1 flow is contained in $V_{\delta'}$. To do this, we first construct a nowhere-zero vector field on each near large radius region V^δ (this notation refers to any of the regions $V^\delta_{\beta_i}, V^\delta_{W_{ij}}, V^\delta_{C_{ijk}}$ and should not be confused with their union V_δ) in our cover whose time-1 flow is contained in $V^{\delta'}$. By construction, on each region we can find a 1-PS of $T_{L^\vee}$ whose flow preserves the closure $\bar{V}^\delta$ in $|\mathfrak{F}|$ and shrinks the (poly)disk in the base B. In fact, any $\beta \in L^\vee$ in the interior of the corresponding cone of the secondary fan will do. Then the time-1 flow sends $\bar{V}^\delta$ to $\bar{V}^{\delta'}$ for $\delta' < \delta$.

  Unfortunately, this flow doesn't preserve the discriminant in general but, near the discriminant, we can modify it using an algebraic Whitney stratification as in the proof of Lemma 9.20 so that it does whilst continuing to preserve $\bar{V}^\delta$ and shrinking the (poly)disk in B (it follows that this vector field is nowhere-zero). As such, this modified time-1 flow still sends $\bar{V}^\delta$ to $\bar{V}^{\delta'}$ and hence sends V^δ to $V^{\delta'}$ as desired. We note in passing that, because we only need our flow to send V^δ to $V^{\delta'}$ and not to D, we do not need transversality of D to the discriminant here since the fibres of the fibration on V^δ away from D are already transverse to the discriminant (by our choice of B).

  Having constructed these vector fields on each region in our cover, we then use a partition of unity to glue them together to get a vector field on V_δ. Because we are forming positive linear combinations of vector fields which preserve the discriminant, the glued vector field also preserves the discriminant. Moreover, because each vector field shrinks the corresponding (poly)disk in the base and we are taking a positive linear combination of them, the glued vector field also has this property. As such, it is nowhere-zero and, in fact, its flow must send $\bar{V}_\delta$ to $\bar{V}_{\delta'}$. This implies that the flow sends V_δ to $V_{\delta'}$ as desired.

□

Remark 9.19. We note that in the proof we don't use any form of transversality to D so we could hope that this result holds more generally.

We now turn to understanding the push-offs into FIPS^o of the toric divisors D_i' that make up D.

Lemma 9.20. *The fibre $\pi_{\beta_i}^{-1}(\delta)$ of $\pi_{\beta_i} : V_{\beta_i} \to B$ is homotopy equivalent to $FIPS^o(F_i)$ for all i in D.*

What makes this result possible is that the discriminant is "transverse" to the divisors in D. As we have already remarked in §2, the discriminant is singular – in fact, it's reducible – and so here transverse doesn't make sense. We'll see in the proof that what matters is that each toric divisor D_i' in D is transverse to every stratum of an algebraic Whitney stratification (see [21], Part 1, §1.2) of the discriminant locus.

Remark 9.21. Whilst the proof below involves explicit descriptions of the various regions, the only property of the discriminant which it uses is that the components of the discriminant and their intersections are smooth near D. This allows us to construct a particularly nice algebraic Whitney stratification which is easily seen to be transverse to D.

Remark 9.22. In principle, we need to know the same result for the 1-dimensional fibres of $\pi_{W_{ij}}$ – that is, that they are homotopy equivalent to the complement of the discriminant in $Z(W_{ij})$. However, this is immediately clear from the explicit description of these regions in §5.2 since the intersection multiplicity $m_{W_{ij}} = 1$ and so the fibres of $\pi_{W_{ij}}$ are cylinders punctured at a single point. Nonetheless, if we wanted, we could use a similar proof to construct a flow which realises this homotopy equivalence.

Proof. By our choice of E_{β_i}, $E_{\beta_i} \cap \mathrm{FIPS}^o(F_i)$ is a deformation retract of $\mathrm{FIPS}^o(F_i)$. The basic idea of the proof is to observe that π_{β_i} extends over the closure $\bar{V}_{\beta_i}$ to the proper map $\pi'_{\beta_i} : \bar{V}_{\beta_i} \to B'$ (from the construction of V_{β_i} in §5.2) such that, if we delete the non-toric parts of the discriminant, the fibre of π'_{β_i} over $\underline{0} \in B'$ is $E_{\beta_i} \cap \mathrm{FIPS}^o(F_i)$ and the fibre over $\delta \in B'$ is $\pi_{\beta_i}^{-1}(\delta)$. As such, it will suffice to identify fibres of π'_{β_i} near $\underline{0}$ in such a way as to preserve the non-toric parts of the discriminant. This identification uses Thom's first isotopy lemma (see [21], Part 1, §1.5) which is valid because of the transversality mentioned above. In what follows, we shall construct a flow giving rise to this identification explicitly, as we will need the identification to have certain properties (see Remark 9.23) in §9.2.5.

Firstly, by (3) from Lemma 9.17, we have chosen V_{β_i} to respect the S_3-symmetry of the Triangle VGIT and so it will suffice to prove this for coset representatives of the faces F_i in D – here we choose $i = 1, 8$. The standard basis of $L^\vee = \mathbb{Z}^3$ identifies $T_{L^\vee} \cong (\mathbb{C}^*)^3_{X,Y,Z}$ in such a way that X, Y, Z are coordinates on the toric open subset $U_{C_{136}}$ of $|\mathfrak{F}|$. In particular, these give coordinates near D_1. Then one checks that

$X' = XY$, $Y' = Y^{-1}$ and $Z' = YZ$ give coordinates on the toric open subset $U_{C_{168}}$ which is near D_8.

For $i = 8$, we therefore use coordinates X', Y', Z'. Since $\lambda_{\beta_8} = (0, -1, 0)$, $x^{\lambda_{\beta_8}} = Y'$ and so $V_{\beta_8} \subset \mathrm{FIPS}^o$ is of the form $\{|Y'| \leq \delta, (X', Z') \in E_{\beta_8}\}$, $\pi_{\beta_8}^{-1}(\delta)$ is the hyperplane $\{Y' = \delta\} \subset V_{\beta_8}$ and $D_8' \cap U_{C_{168}} = \{Y' = 0\}$. In these coordinates, $\nabla_1 = \{Z' = 1/4\}$ and $\nabla_3 = \{X' = 1/4\}$. Moreover, we shall see in §9.2.3 that these are the only two components that meet D_8'. As such, for δ sufficiently small, V_{β_8} is just the complement of these two hyperplanes (and the toric boundary) in the closure $\bar{V}_{\beta_8}$ in $|\mathfrak{F}|$. Then it is straightforward that the gradient flow of $|Y'|^2$ on $\bar{V}_{\beta_8}$ preserves V_{β_8} (and fixes E_{β_8} in D_8') and the limiting flow identifies $\pi_{\beta_8}^{-1}(\delta)$ with $E_{\beta_8} \cap \mathrm{FIPS}^o(F_8)$.

For $i = 1$, we use coordinates X, Y, Z. Since $\beta_1 = (1, 0, 0)$, $x^{\lambda_{\beta_1}} = X$ and $V_{\beta_1} \subset \mathrm{FIPS}^o$ is of the form $\{|X| \leq \delta, (Y, Z) \in E_{\beta_1}\}$, $\pi_{\beta_1}^{-1}(\delta) = \{X = \delta\} \subset V_{\beta_1}$ and $D_1' \cap U_{C_{136}} = \{X = 0\}$. In these coordinates, $\nabla_{pr} = \{4XYZ + 1 = X + Y + Z\}, \nabla_1 = \{YZ = 1/4\}$. Moreover, we'll see in §9.2.4 that only these two components of the discriminant meet the toric divisor D_1'. As such, for δ sufficiently small V_{β_1} is just the complement of these two components (and the toric boundary) in the closure $\bar{V}_{\beta_1}$ in $|\mathfrak{F}|$.

Unfortunately, this case is harder than the $i = 8$ case as the gradient flow of $|X|^2$ does not preserve the discriminant. However, we can modify the gradient flow of $|X|^2$ such that it does. To this end, we pick an algebraic stratification of the closure $\bar{V}_{\beta_1}$ as follows. Let

$$V_0 := \nabla_{pr} \cap \nabla_1 = \{Y = Z = 1/2\}, V_1 := \nabla_{pr} \backslash V_0, V_2 := \nabla_1 \backslash V_0, V_3 := \bar{V}_{\beta_1} \backslash \nabla_1 \cup \nabla_{pr}$$

Then $\mathcal{V} = \{V_i\}$ is a stratification of $\bar{V}_{\beta_1}$ with non-singular strata such that the discriminant $Z = \bigcup_{i=0,1,2} V_i$ is a union of strata. Moreover, since the closure of each stratum in $\bar{V}_{\beta_1}$ is smooth, it follows that $\mathcal{V}$ satisfies Whitney's condition b) (see [21], Part 1, §1.2).

An easy check confirms that the toric divisor D_1' in $\mathfrak{F}$ is transverse to all the strata V_i. Then, as in [26], §1.3.4, we can modify the gradient vector field of $|X|^2$ near the discriminant in $\bar{V}_{\beta_1}$ so that the new vector field preserves the discriminant. To see this, starting with V_0 and working up to $\bar{V}_{\beta_1}$, Whitney's condition b) guarantees that we can find a vector field v on an open neighbourhood U of Z in $\bar{V}_{\beta_1}$ which preserves each stratum and which lifts (under π_{β_1}') the gradient vector field of $|X|^2$. As each torus invariant curve $Z(W)$ in D_1' is transverse to the discriminant, the part of the boundary $\partial \bar{V}_{\beta_1}$ near $Z(W)$ is also transverse to the discriminant. As such, we can assume that v is tangent to these parts of the boundary in U – that is, the subset $\{(X, Y, Z) \in U \mid (Y, Z) \in \partial E_{\beta_1}\}$.

Using a partition of unity to glue together v on U with the gradient vector field of $|X|^2$ outside U gives a vector field on $\bar{V}_{\beta_1}$ which preserves Z (and the "horizontal" part of the boundary mentioned above) and identifies fibres of π_{β_1}'. Therefore the limiting flow identifies $\pi_{\beta_1}'^{-1}(\delta)$ with E_{β_1} in such a way that the open subset $\pi_{\beta_1}^{-1}(\delta)$ of the former gets identified with $E_{\beta_1} \cap \mathrm{FIPS}^o(F_1)$. This is what we wanted, so we are done. □

Remark 9.23. Here we collect a few properties of the homotopy equivalence constructed in the proof of the previous lemma which will be needed in §9.2.5 to check the gluing relations between the representations ρ^i associated to different faces.

Away from the (non-toric parts of the) discriminant, the flow is just the gradient flow of $|X|^2$ where $X = x^{\lambda_{\beta_i}}$ is the coordinate on the torus $T_{L^\vee}$ defining the fibration π_{β_i} on V_{β_i}. As toric loops α^β in $\pi_{\beta_i}^{-1}(\delta)$ are not near the discriminant, this means that they get identified with toric loops $\alpha^{\bar\beta}$ in $\mathrm{FIPS}^o(F_i)$ where $\bar\beta = \beta \in L^\vee/\beta_i$.

As the flow preserves the horizontal part of the boundary, it identifies the region $V_{W_{ij}} \cap V_{\beta_i} \subset V_{\beta_i}$ with a region near $Z(W_{ij})$ inside $E_{\beta_i} \cap \mathrm{FIPS}^o(F_i)$. Moreover, it sends large radius paths living in a fibre $\pi_{W_{ij}}^{-1}(b)$ in this boundary (hence contained in a $\beta_{W_{ij}}$-orbit) to large radius paths which live in a $\bar\beta_{W_{ij}}$-orbit, where $\bar\beta_{W_{ij}} := \beta_{W_{ij}} \in L^\vee/\beta_i$.

9.2.3. *Representation for the face F_8.* In this section, we describe the secondary stack for the VGIT on F_8, which we call $\mathfrak{F}(F_8)$, and the complement of the discriminant in $\mathfrak{F}(F_8)$, which we call $\mathrm{FIPS}(F_8)$. We then construct a representation ρ^8 of $\pi_1(\mathrm{FIPS}^o(F_8))$ on the phases of the Triangle VGIT, where $\mathrm{FIPS}^o(F_8)$ is the complement of any remaining parts of the toric boundary in $\mathrm{FIPS}(F_8)$.

The polyhedral subdivision associated to F_8 (shown in the middle of Figure 25 (L)) is the product of 2 *independent* VGITs – that is, to get the phases we can triangulate each polygon independently of the other. As such, $\mathfrak{F}(F_8)$ is the product of the secondary stacks of the constituent VGITs and hence $\mathfrak{F}(F_8) \cong \mathbb{P}(2,1)\times\mathbb{P}(2,1)$ (with coordinates (b_1, b_2) for the first factor and (b_6, b_5) for the second).

Alternatively we can see this directly by quotienting $L^\vee$ by $\beta_8 = (1,-1,1)$ via

$$p_8 : L^\vee = \mathbb{Z}^3 \twoheadrightarrow L^\vee/\beta_8 \cong \mathbb{Z}^2, (x,y,z) \mapsto (x+y, y+z)$$

and checking that the projection of the stacky secondary fan nearby β_8 gives the stacky fan for $\mathbb{P}(2,1)\times\mathbb{P}(2,1)$. The generators – that is, β from §3.4 applied to the standard basis – of this fan are $\bar\beta_i := p_8(\beta_i)$ for β_i adjacent to β_8 – that is, for $i = 1,2,5,6$ – and are shown in Figure 25 (R).

The four phases of the Triangle VGIT near F_8 are shown in Figure 25 (L). Using Theorem 3.33, one checks that the discriminant (shown as the dashed lines in Figure 25 (L)) consists of the two toric divisors $\{b_1 = 0\}$ and $\{b_6 = 0\}$ as well as the two lines $\ell_1 := \{b_5^2 = 4b_6\}$ and $\ell_2 := \{b_2^2 = 4b_1\}$. As such, $\mathrm{FIPS}(F_8)$ is the complement of these four lines in $\mathfrak{F}(F_8)$ and is therefore the product of two copies of $\mathrm{FIPS}(F_8') := \mathbb{P}(2,1)\backslash\{[0,1],[1,2]\}$.

Remark 9.24. We note that $\mathrm{FIPS}(F_8')$ is the FIPS for the linear rank 1 toric VGIT defined by either of the 2 pieces of the subdivision associated to F_8. We'll refer to either of these two VGITs (defined by toric data of the form $L = \mathbb{Z} \xrightarrow{Q^\vee} \mathbb{Z}^4 \to N = \mathbb{Z}^3$ where $Q^\vee = (1,-2,1,0)$) as the VGIT on F_8'.

Remark 9.25. Note that in $\mathrm{FIPS}(F_8)$ there are two lines of $\mathbb{Z}_2$-orbifold points (namely $\{b_2 = 0\}$ and $\{b_5 = 0\}$) meeting in a $\mathbb{Z}_2^{\oplus 2}$-orbifold point at the bottom

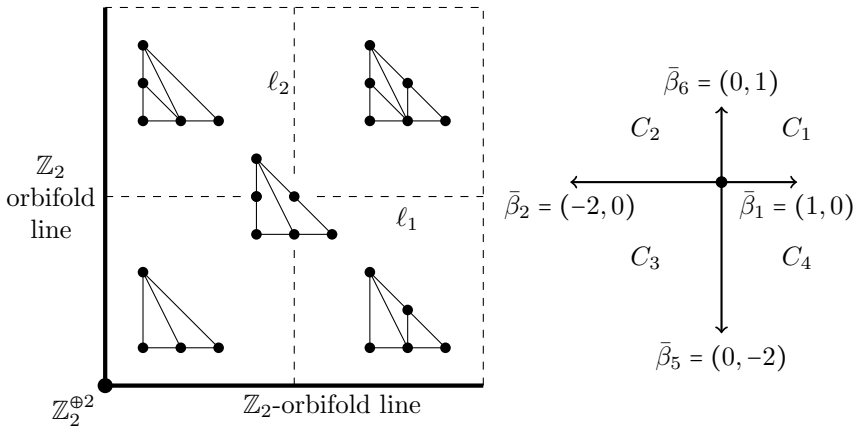

FIGURE 25. The secondary polytope (with the four phases shown) (L) and secondary fan (R) of the VGIT on the face F_8

left corner of Figure 25 (L). This $\mathbb{Z}_2^{\oplus 2}$-orbifold point in D_8' in turn meets one of the lines of $\mathbb{Z}_2$-orbifold points in the FIPS of the Triangle VGIT (see §9.1.3). As mentioned in §9.2, these orbifold points are why it is easier from a technical point of view to work with FIPS^o. Here we see that $\mathrm{FIPS}^o(F_8) \cong (\mathbb{C}^*)^2 \backslash (\ell_1 \cup \ell_2)$ indeed has no orbifold points to worry about.

We now move on to constructing the representation ρ^8. The topology in this case is straightforward. Recall that in Example 7.6 we considered the hyperplane arrangement $\{X = 1\} \cup \{Y = 1\}$ inside $\mathbb{C}^2_{X,Y}$. Then picking coordinates $X := 4b_1/b_2^2$, $Y := 4b_6/b_5^2$ gives an isomorphism between the open subset of D_8' away from the orbifold locus and $\mathbb{C}^2_{X,Y}$ in such a way that $\mathrm{FIPS}^o(F_8)$ gets identified with $(\mathbb{C}^*)^2 \backslash \{X = 1\} \cup \{Y = 1\}$. Note that, under this identification, the generating paths α_i, β_i from Example 7.6 correspond to large radius paths in the regions $\{|Y| < r\}$, $\{|X| > 1/r\}$, $\{|Y| > 1/r\}$, $\{|X| < r\}$ respectively for $i = 1, \cdots, 4$ and for any r sufficiently small. If we glue these four regions together to get:

$$U := \{|Y| < r\} \cup \{|X| > 1/r\} \cup \{|Y| > 1/r\} \cup \{|X| < r\} \subset \mathbb{C}^2 \backslash \{X = 1\} \cup \{Y = 1\}$$

then we can interpret Example 7.6 as saying that $\pi_1(\mathbb{C}^2 \backslash \{X = 1\} \cup \{Y = 1\})$ is generated by $\pi_1(U)$ subject to 4 explicit relations.

Remark 9.26. This region U is analogous to the large radius regions with the same name in §7.

If we now delete the coordinate hyperplanes $X = 0$ and $Y = 0$, we'll see that this gives the following presentation for $\pi_1(\mathrm{FIPS}^o(F_8))$:

Lemma 9.27. *If we let $U' := U \cap FIPS^o(F_8)$, $\pi_1(FIPS^o(F_8)) \cong \pi_1(U')/\mathcal{R}_{F_8}$ where $\mathcal{R}_{F_8}$ is the normal subgroupoid generated by the relations:*

(1) $\gamma^{-1}_{C_4,C_1} \circ \gamma^{-1}_{C_3,C_4} = \gamma^{-1}_{C_2,C_1} \circ \gamma^{-1}_{C_3,C_2}$
(2) $\gamma^{-1}_{C_3,C_4} \circ \gamma^{-1}_{C_2,C_3} = \gamma^{-1}_{C_1,C_4} \circ \gamma^{-1}_{C_2,C_1}$

(3) $\gamma_{C_1,C_2}^{-1} \circ \gamma_{C_4,C_1}^{-1} = \gamma_{C_3,C_2}^{-1} \circ \gamma_{C_4,C_3}^{-1}$
(4) $\gamma_{C_2,C_3}^{-1} \circ \gamma_{C_1,C_2}^{-1} = \gamma_{C_4,C_3}^{-1} \circ \gamma_{C_1,C_4}^{-1}$

Remark 9.28. Here we have relabelled the generating paths α_i, β_i from Example 7.6 as follows:

$$\alpha_i \mapsto \gamma_{C_i,C_{i+1}}^{-1}, \beta_i \mapsto \gamma_{C_{i+1},C_i}^{-1}$$

where we read the indices modulo 4 and the chambers C_i are as in Figure 25 (R). As in Remark 5.21, this is to fully specify the large radius representation on these paths – namely, it sends γ_{C_i,C_j}^{-1} to the window equivalence from $D^b(X_{C_i})$ to $D^b(X_{C_j})$ using the window with λ_{C_i,C_j}-weight -1.

Note that this presentation using both $\gamma_{C_i,C_{i+1}}^{-1}$ and $\gamma_{C_{i+1},C_i}^{-1}$ as generators on each wall is not minimal – instead, we could have just picked one of these. If we had picked a different presentation with one such large radius generator for each wall (chosen compatibly), we would only have to prove one additional relation. However, as we can easily implement these four relations above, the difference is cosmetic and so we stick with the presentation we know.

Proof. Under the relabelling above, Example 7.6 gives an equivalence $\bar{\phi} : \pi_1(U)/\mathcal{R}_{F_8} \cong \pi_1(\mathbb{C}^2 \setminus \{X = 1\} \cup \{Y = 1\})$. The 4 relations in $\mathcal{R}_{F_8}$ do not go near the coordinate axes in $\mathbb{C}^2$, so they still hold in $\mathrm{FIPS}^o(F_8)$. As such, since $U' \subset (\mathbb{C}^*)^2 \setminus \{X = 1\} \cup \{Y = 1\} \cong \mathrm{FIPS}^o(F_8)$, inclusion gives a functor $\phi : \pi_1(U')/\mathcal{R}_{F_8} \to \pi_1(\mathrm{FIPS}^o(F_8))$ which lifts the equivalence $\bar{\phi}$. By Proposition 7.2, we know that the kernels of the maps $\pi_1(\mathrm{FIPS}^o(F_8)) \to \pi_1(\mathrm{FIPS}(F_8))$ and $\pi_1(U')/\mathcal{R}_{F_8} \to \pi_1(U)/\mathcal{R}_{F_8}$ are generated by the same meridians. Hence ϕ is an equivalence. □

Because the intersections of the discriminant with the toric boundary are transverse, there are no additional near large radius paths and we know (see Proposition 5.20) how to define our representation (as in Remark 9.28) on each near large radius region. Then Remark 5.24 tells us that these glue together to automatically give a representation ρ^8 of $\pi_1(U')$ on the Triangle VGIT. In fact, we have:

Proposition 9.29. *There is a representation $\rho^8 : \pi_1(FIPS^o(F_8)) \to \boldsymbol{Cat}_1$ on the phases of the Triangle VGIT near F_8.*

Proof. By Lemma 9.27, we just need to check that the 4 relations in $\mathcal{R}_{F_8}$ hold for the Triangle VGIT. One checks that the following 4 collections of 4 line bundles form magic windows for the Triangle VGIT (where the relevant walls are defined by $\lambda_{C_1,C_4} = (0,1,1) \in L$ and $\lambda_{C_1,C_2} = (1,1,0) \in L$):

(1) $\mathcal{O}, \mathcal{O}(1,0,0), \mathcal{O}(0,0,1), \mathcal{O}(0,1,0)$
(2) $\mathcal{O}, \mathcal{O}(0,1,-1), \mathcal{O}(0,0,-1), \mathcal{O}(1,0,-1)$
(3) $\mathcal{O}, \mathcal{O}(-1,0,0), \mathcal{O}(-1,1,0), \mathcal{O}(-1,0,1)$
(4) $\mathcal{O}, \mathcal{O}(0,-1,1), \mathcal{O}(1,-1,0), \mathcal{O}(0,-1,0)$

One then checks that the weights w_λ in the i-th magic window agree with those occurring in the i-th relation in $\mathcal{R}_{F_8}$. □

Remark 9.30. There are easier ways to see the 4 relations $\mathcal{R}_{F_8}$ on F_8 hold than by magic windows – here's a more geometric reason. If we pick a single basepoint corresponding to the phase X_{C_1}, then loops around the two non-toric components of the discriminant ℓ_1 and ℓ_2 generate the fundamental group of the complement of U' in $\mathrm{FIPS}^o(F_8)$. Moreover, as this complement is homotopic to a 2-torus, there is just one relation between these loops saying that they commute.

To see that this holds on the level of functors, we recall (see Remark 9.10) that these generators, corresponding to window shifts on X_{C_1} with respect to λ_{C_1,C_4} and λ_{C_1,C_2} respectively, can be thought of as twists T_{F_i} of a spherical functor F_i for $i = 1, 2$ supported on the toric divisors D_5 and D_2 in X_{C_1} respectively. As $T_{F_1} \circ T_{F_2} \circ T_{F_1}^{-1} = T_{T_{F_1} \circ F_2}$, to prove commutativity it suffices to show that $T_{F_1} \circ F_2 = F_2$. But as the image of F_1 is supported on D_5, T_{F_1} only modifies any complex of sheaves along this locus. Since D_5 and D_2 are disjoint in X_{C_1}, the image of F_2 is supported away from D_5 and so it is left alone by T_{F_1}. Hence the functors commute.

9.2.4. *Representation for the face F_1.* In this section, we observe that the VGIT on F_1 is (nearly) identical to the Pentagon VGIT in §7.3. In particular, the complement of the discriminant in $\mathfrak{F}(F_1)$, which we call $\mathrm{FIPS}(F_1)$, is the FIPS of the Pentagon VGIT. We then construct a representation ρ^1 of $\pi_1(\mathrm{FIPS}^o(F_1))$ on the phases of the Triangle VGIT, which we have basically already done in Theorem 7.27.

The polyhedral subdivision corresponding to the face F_1 is shown in the centre of Figure 26. This makes it clear that the phases of the Triangle VGIT on F_1 correspond to triangulations of the quadrilateral P (shaded grey) and hence the secondary stack $\mathfrak{F}(F_1)$ of the VGIT on F_1 (see Remark 3.30) is the secondary stack of the VGIT on P. But the VGIT on P is exactly the Pentagon VGIT from §7.3 and hence the phases of the Pentagon VGIT are open subsets of the phases of the Triangle VGIT near F_1. Moreover, by Theorem 3.33, since the discriminant of the VGIT associated to the right hand triangle in the polyhedral subdivision in the centre of Figure 26 is trivial, the discriminant for the face VGIT equals the discriminant for the Pentagon VGIT. Hence $\mathrm{FIPS}(F_1)$ is the FIPS of the Pentagon VGIT.

We now want to construct the representation ρ^1 on the phases of the Triangle VGIT. Recall that in Proposition 7.25 we constructed an equivalence $\bar{\phi} : \pi_1(U)/\mathcal{R}_{F_1} \cong \pi_1(\mathrm{FIPS}(F_1))$ where U was a particular choice of large radius region inside $\mathrm{FIPS}(F_1)$ and $\mathcal{R}_{F_1}$ consisted of 4 explicit relations. Now we check what happens to this presentation once we delete the remaining toric divisor in $\mathrm{FIPS}(F_8)$.

Lemma 9.31. *If we let $U' := U \cap FIPS^o(F_1)$, $\pi_1(FIPS^o(F_1)) \cong \pi_1(U')/\mathcal{R}_{F_1}$.*

Proof. We note that inclusion induces a functor $\phi : \pi_1(U')/\mathcal{R}_{F_1} \to \pi_1(\mathrm{FIPS}^o(F_1))$ as the relations in R_{F_1} do not meet the toric boundary. We note that ϕ lifts the equivalence $\bar{\phi}$. By Proposition 7.2, $\pi_1(\mathrm{FIPS}(F_1))$ and $\pi_1(U)/\mathcal{R}_{F_1}$ are quotients of $\pi_1(\mathrm{FIPS}^o(F_1))$ and $\pi_1(U')/\mathcal{R}_{F_1}$ respectively by the toric loops $\alpha_{C_i}^{(-1,-1)}$ for $i = 4, 5$ in both cases. Therefore the functor ϕ must be an equivalence. □

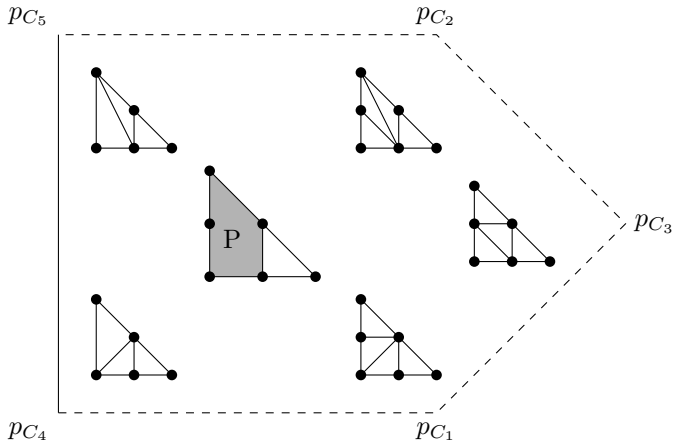

FIGURE 26. The secondary polytope of the VGIT on the face F_1, which is also the secondary polytope of the Pentagon VGIT

We can now construct the representation ρ^1:

Proposition 9.32. *The large radius representation ρ of $\pi_1(U')$ acting on the phases of the Triangle VGIT near F_1 gives the representation ρ^1 on $\pi_1(FIPS^o(F_1))$.*

Proof. By Lemma 9.31, we just have to prove that ρ satisfies the additional 4 relations in $\mathcal{R}_{F_1}$. One checks explicitly that the following 4 collections of 4 line bundles are indeed magic windows for the Triangle VGIT (where the relevant walls are defined by $\lambda = (0,1,0), (0,1,1), (0,1,-1), (0,0,1) \in L$):

(1) $\mathcal{O}, \mathcal{O}(1,0,0), \mathcal{O}(0,1,0), \mathcal{O}(0,0,1)$
(2) $\mathcal{O}, \mathcal{O}(-1,0,0), \mathcal{O}(0,-1,0), \mathcal{O}(0,0,-1)$
(3) $\mathcal{O}, \mathcal{O}(0,1,0), \mathcal{O}(0,1,-1), \mathcal{O}(-1,1,0)$
(4) $\mathcal{O}, \mathcal{O}(0,0,-1), \mathcal{O}(0,1,-1), \mathcal{O}(1,0,-1)$

Moreover, one can check that the weights w_λ in the i-th magic window agrees with those occurring in the i-th relation in $\mathcal{R}_{F_1}$. □

Remark 9.33. Recall that the phases of the Pentagon VGIT are open subsets within the phases of the Triangle VGIT on F_1. Then the 4 magic windows used in the proof above to implement the relations in $\mathcal{R}_{F_1}$ on the Triangle VGIT restrict to the Pentagon VGIT to give the magic windows we used to construct our representation for the Pentagon VGIT in Theorem 7.27.

Remark 9.34. Instead of picking magic windows on the Triangle VGIT to construct the representation ρ^1, we could just observe that the representation of $\pi_1(\mathrm{FIPS}^o(F_1))$ on the phases of the Pentagon VGIT (from Theorem 7.27) extends to the phases of the Triangle VGIT. This is because the phases in the Pentagon are just the complement of a fixed divisor in the phases in the Triangle and so we can set ρ^1 to be the identity on complexes supported on this divisor. The reason that this defines a valid extension is that ρ^1 is the identity in the toric open subset

of the Pentagon's phases near this divisor. This is because the generators of the fundamental group all correspond to twists about spherical functors whose image is concentrated on the flopping loci and hence the twists are the identity away from this locus.

9.2.5. *Fundamental groupoid representation.* In the previous subsections we have constructed representations ρ^1 of $\pi_1(\mathrm{FIPS}^o(F_1))$ and ρ^8 of $\pi_1(\mathrm{FIPS}^o(F_8))$ on the phases of the Triangle VGIT. Up to the S_3-symmetry, these are the only possibilities and so it follows that we have constructed ρ^i on $\pi_1(\mathrm{FIPS}^o(F_i))$ for all i in D. Our aim in this section is to follow the strategy outlined at the start of §9.2 to piece all these representations together compatibly to construct a representation of $\pi_1(\mathrm{FIPS}^o)$.

Theorem 9.35. *$\pi_1(FIPS)$ acts on the phases of the Triangle VGIT in such a way that the representation on the phases near a divisor D_i' in D agrees with ρ^i.*

Given the work of the previous sections, the proof largely boils down to checking that the representations ρ^i and ρ^j agree on the paths in $V_{W_{ij}}$.

Remark 9.36. Here we remark briefly on basepoints. The construction of the regions V_{β_i} and $V_{W_{ij}}$ already involves choosing certain basepoints (in the positive real torus) in all of the regions $V_{C_{ijk}}$ which they intersect. Thus we end up with multiple basepoints in each of these regions but, thanks to Remark 5.16, we can canonically get rid of all but one of them to leave one basepoint p_{ijk} in each region $V_{C_{ijk}}$ near D. Our fundamental groupoids in this theorem will always be based at the set $\{p_{ijk}\}$ and so we drop it from the notation.

Proof. First observe that, by Proposition 7.2, it suffices to construct the representation for $\pi_1(\mathrm{FIPS}^o)$. By Lemmas 9.14 and 9.18, $\pi_1(\mathrm{FIPS}^o) \cong \pi_1(V_\delta)$ for δ sufficiently small. As V_δ is covered by the near large radius regions described in §9.2.2, the (groupoid) van-Kampen theorem (see [10]) tells us that $\pi_1(V_\delta)$ is just the fundamental groupoids of these regions glued together along intersections. Moreover, we know how to define a representation on the regions $V_{C_{ijk}}$ and $V_{W_{ij}}$, since we are in the large radius situation described in §5.4.

Next we note that the representation ρ^i of $\pi_1(\mathrm{FIPS}^o(F_i))$ naturally extends to a representation of $\pi_1(V_{\beta_i})$. This is because the fibration structure on V_{β_i} (see Remark 5.17) presents $\pi_1(V_{\beta_i})$ as $\pi_1(\pi_{\beta_i}^{-1}(\delta)) \rtimes \langle \alpha^{\beta_i} \rangle$. By Lemma 9.20, $\pi_1(\pi_{\beta_i}^{-1}(\delta)) \cong \pi_1(\mathrm{FIPS}^o(F_i))$. As the discriminant meets all the large radius curves $Z(W_{ij})$ in D transversely, the monodromy on $\pi_{\beta_i}^{-1}(\delta) \cap V_{W_{ij}}$ is trivial. By the presentations of $\pi_1(\mathrm{FIPS}^o(F_i))$ in §9.2.3 and §9.2.4, these regions generate $\pi_1(\pi_{\beta_i}^{-1}(\delta))$ and so the monodromy acts trivially on this groupoid. As such, $\pi_1(V_{\beta_i}) \cong \pi_1(\mathrm{FIPS}^o(F_i)) \times \langle \alpha^{\beta_i} \rangle$. Defining $\rho^i(\alpha^{\beta_i})$ in the usual way as tensoring by the corresponding line bundle, we observe (as in the usual large radius representation – see Proposition 5.20) that this commutes with all the functors in the representation ρ^i on $\pi_1(\mathrm{FIPS}^o(F_i))$ and hence gives a representation of $\pi_1(V_{\beta_i})$.

Recall (see Remark 5.21) that the representation of $\pi_1(V_{W_{ij}})$ was not completely canonical because we had to choose an integer to define our windows. Here we fix this ambiguity by declaring that it agrees with the representation ρ^i in the region $V_{W_{ij}} \cap V_{\beta_i}$, where we note that the presentation of this large radius groupoid coming from §9.2.3 and §9.2.4 agrees with the presentation in Remark 5.15.

As such, we have defined the representation on all pieces of the cover of V_δ and so we only need to check the gluing relations. But, by the careful construction of our cover (see Lemma 9.17), these gluing relations are easy to understand. First of all, by Remark 5.24, we know that we can glue together the large radius representations from Proposition 5.20 of the regions $V_{C_{ijk}}$ and $V_{W_{ij}}$. So we are just left to check how the representation ρ^i glues. Since $V_{\beta_i} \cap V_{\beta_j} = \varnothing$, we just have to check that ρ^i glues along the regions $V_{W_{ij}}$ and $V_{C_{ijk}}$.

By Lemma 9.17, $V_{\beta_i} \cap V_{W_{ij}}$ is a deformation retract of $V_{W_{ij}}$. Hence the gluing relations on this intersection say that ρ^i acts canonically on toric loops and in a way which agrees with ρ^j on large radius paths. Certainly, by the way we extended ρ^i to $\pi_1(V_{\beta_i})$ above, this is true for the toric loop α^{β_i}. For the remaining generators of $\pi_1(V_{W_{ij}})$ in our presentation, we need to consider what these get identified with under the homotopy equivalence $\pi_{\beta_i}^{-1}(\delta) \simeq \mathrm{FIPS}^o(F_i)$ in Lemma 9.20. Recall from Remark 9.23 that toric loops α^β in $\pi_{\beta_i}^{-1}(\delta)$ get identified with toric loops $\alpha^{\bar\beta}$ in $\mathrm{FIPS}^o(F_i)$ where $\bar\beta := \beta \in L^\vee/\beta_i$. So ρ^i acts canonically on them.

For large radius paths in $V_{W_{ij}}$, recall from Remark 9.23 that the homotopy equivalence $\pi_{\beta_i}^{-1}(\delta) \simeq \mathrm{FIPS}^o(F_i)$ sends large radius paths living in a $\beta_{W_{ij}}$-orbit inside $V_{W_{ij}}$ to large radius paths in a $\bar\beta_{W_{ij}}$-orbit inside $E_{\beta_i} \cap \mathrm{FIPS}^o(F_i)$, where $\bar\beta_{W_{ij}} := \beta_{W_{ij}} \in L^\vee/\beta_i$. We can check that $\bar\beta_{W_{ij}}$ agrees with how we have defined the corresponding large radius region in the presentations of $\pi_1(\mathrm{FIPS}^o(F_i))$ from §9.2.3 and §9.2.4. As such, ρ^i gives a window equivalence on the large radius paths in $V_{W_{ij}}$. Fixing a particular large radius path in $Z(W_{ij})$ and pushing it off into either $\mathrm{FIPS}^o(F_i)$ or $\mathrm{FIPS}^o(F_j)$, we check that the corresponding window equivalence assigned by ρ^i and ρ^j agree by chasing around their descriptions from §9.2.3 and §9.2.4. Therefore we are done with this gluing relation.

Finally, Lemma 9.17 says that $V_{\beta_i} \cap V_{C_{ijk}}$ is a deformation retract of $V_{C_{ijk}}$ and so the gluing relations on this intersection say that ρ^i acts in the canonical way on toric loops. We have already checked this above and so are done.

□

9.3. **The covering strategy.** When the FIPS has a complicated topology, one approach to simplify the description of the fundamental group is to take an appropriate finite cover of the FIPS. In the A_n-singularity case [18], Donovan and Segal show that there is a tower of covers of the FIPS of the A_n surface singularity which are FIPS for certain higher-dimensional VGITs containing the A_n surface singularity. In this section, our main aim (see Proposition 9.46) is to describe how we can construct an analogous cover for the Triangle VGIT. We then sketch how

the techniques in [18] should be able to reconstruct a representation on the phases of the Triangle VGIT, as in Theorem 9.35.

We first need to find the analogous higher-dimensional VGIT for the Triangle VGIT. We shall refer to the Triangle VGIT as the original VGIT and and the new VGIT (whose phases are of higher dimension) as the "unsliced" VGIT. We want the unsliced VGIT to be quasi-symmetric so that we have a guaranteed large radius representation of $\pi_1(\text{FIPS})$, as in Corollary 2.8.

Remark 9.37. We should say immediately that it seems unlikely that in general we can find a quasi-symmetric unsliced VGIT whose FIPS covers the original FIPS. We return to this in Remark 9.41.

Having said that, the FIPS is analogous to the stringy Kähler moduli space which should roughly be (c.f. [7]) the quotient of the space of stability conditions by autoequivalences. From this perspective, there seems to be a hyperplane complement lurking in that, if we rewrite the space of stability conditions modulo auto-equivalence as the space of (numerical) stability functions modulo the residual symmetries of cohomology, then the space of stability functions is roughly the hyperplane complement in $K_0(X)_{\mathbb{C}}$ given by deleting central charges Z such that $Z(\delta) = 0$ for some stable object δ.

In the A_n singularity case [18], Donovan and Segal find the unsliced VGIT by describing some of the phases of their original VGIT as a moduli space of representations (with all dimensions 1) of a quiver Q with (toric) relations I. Note that these moduli spaces do indeed describe a *toric* VGIT. Crucially, the quiver Q is self-dual – that is, for every arrow between two vertices, there is one in the opposite direction – and so the associated toric VGIT is quasi-symmetric, as desired. In fact, the T_L-representation being quasi-symmetric is the same thing as the quiver being self-dual.

Remark 9.38. The moduli spaces of representations depend on a stability parameter $\theta \in L^\vee_{\mathbb{R}}$ and we denote the moduli space of θ-semistable representations (with all dimensions 1) of (Q, I) by $\mathcal{M}_\theta(Q, I)$.

Then Donovan and Segal define the unsliced VGIT to be the representations of the free quiver Q and imposing the relations in I is "slicing". As such, the phases of the unsliced VGIT correspond to $\mathcal{M}_\theta(Q)$ for different values of θ.

Starting from the geometry of the VGIT, they construct such a quiver description by using the McKay correspondence for the associated quotient singularity. Explicitly, the basic case is the VGIT associated to the A_n surface singularity $\mathbb{C}^2 / \mathbb{Z}_{n+1}$. Here the quiver description is automatic and explicit by the 2-dimensional McKay correspondence. Namely, the McKay quiver is the $\tilde{A}_n$ quiver with its usual commuting relations.

Remark 9.39. In the context of the McKay correspondence, representations of the McKay quiver (with relations) with all dimensions 1 are called *G-constellations*.

Note that the $\tilde{A}_n$ quiver is indeed self-dual, as claimed earlier and so we know, by Theorem 8.8, that the FIPS of the unsliced VGIT is the complement of some hyperplanes. In fact, the hyperplane arrangement turns out to be the A_n-configuration of hyperplanes in $\mathbb{R}^n$.

Remark 9.40. We can also view this process of constructing a quiver description from the geometry as taking a non-commutative crepant resolution (NCCR) of the associated toric singularity. This allows us to extend the strategy above to non-quotient singularities where there is no McKay correspondence.

In the A_n case, the quotient singularity has a canonical NCCR coming from the stacky resolution $[\mathbb{C}^2 / \mathbb{Z}_{n+1}]$. More generally, for any toric orbifold singularity $\mathbb{C}^n / G$ (for $G \subset SL_n(\mathbb{C})$ abelian), we can take the NCCR given by $\bigoplus_i \mathcal{O}(\chi_i)$ where χ_i are the irreducible representations of G. Computing the endomorphism algebra gives back the McKay quiver of this representation of G with relations given by commutators. However, there is no reason that this quiver is self-dual.

Remark 9.41. If we consider toric VGITs arising as moduli spaces of representations of a quiver (as above), it seems unlikely that we can in general always find an equivalent description in terms of a self-dual quiver. This supports Remark 9.37 and explains why we are more interested in the Lefschetz strategy in §9.2.

For example, whilst we have a quiver description for the Octahedron VGIT (see Remark 5.18), it is not self-dual and we don't know whether such a quiver exists.

Despite Remark 9.41, in individual cases we can try to find such a self-dual quiver description by taking NCCRs of the corresponding toric singularity.

We now explain how this works for the Triangle VGIT, where we recall (see §9.1.1) that the corresponding singularity is the orbifold singularity $\mathbb{C}^3 / G$ (where $G = \mathbb{Z}_2^{\oplus 2}$). Because this is an orbifold singularity, we can use the 3-dimensional McKay correspondence (or equivalently the tautological NCCR in Remark 9.40). Then the McKay quiver Q has four vertices and is shown in Figure 27. We note that it is self-dual and so take the unsliced VGIT to be given by its (free) representations. The relations I are the commutators, so are given schematically by $xy = yx$, $xz = zx$ and $yz = zy$, and the Triangle VGIT corresponds to moduli spaces of G-constellations.

Remark 9.42. In dimensions 4 and above, the moduli space of G-constellations is not necessarily a projective crepant resolution of $\mathbb{C}^n / G$. On the other hand, the geometric phases of any Calabi–Yau toric VGIT resolving this singularity would be. As such, in these cases, we would have to abandon the McKay correspondence and resort to trying different NCCRs, as in Remark 9.40. Happily in the 3-dimensional abelian case, we know (see [12]) that every projective crepant resolution of the quotient singularity $\mathbb{C}^3 / G$ is a moduli space of G-constellations. In particular, all the geometric phases in the Triangle VGIT are of this form since our resolutions are Calabi–Yau too and hence crepant.

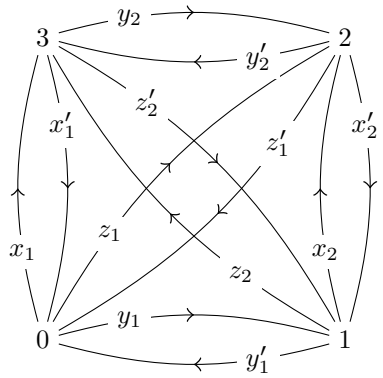

FIGURE 27. McKay quiver of $\mathbb{C}^3/G$

Now that we have constructed the unsliced VGIT, we want to construct a Galois cover $\mathrm{FIPS}_0 \to \mathrm{FIPS}_1$ where FIPS_0 is the FIPS of the unsliced VGIT and FIPS_1 is the FIPS of the Triangle VGIT. In the A_n-case, Donovan and Segal do this by finding a G-action on the secondary fan of the unsliced VGIT such that G acts freely on the chambers and such G-orbits correspond to phases of the unsliced VGIT which slice to give the same phase of the original VGIT – that is, under imposing the toric relations. So we shall look for a similar G-action on the secondary fan of the unsliced VGIT. We start with the toric data for the unsliced VGIT:

$$\mathbb{Z}^3 \xrightarrow{(Q')^\vee} \mathbb{Z}^{12} \xrightarrow{A'} \mathbb{Z}^9$$

where

$$(Q')^\vee = \begin{array}{c} x_1 \\ x_1' \\ y_1 \\ y_1' \\ z_1 \\ z_1' \\ x_2 \\ x_2' \\ y_2 \\ y_2' \\ z_2 \\ z_2' \end{array} \begin{pmatrix} 0 & 0 & 1 \\ 0 & 0 & -1 \\ 1 & 0 & 0 \\ -1 & 0 & 0 \\ 0 & 1 & 0 \\ 0 & -1 & 0 \\ -1 & 1 & 0 \\ 1 & -1 & 0 \\ 0 & 1 & -1 \\ 0 & -1 & 1 \\ -1 & 0 & 1 \\ 1 & 0 & -1 \end{pmatrix}, A' = \begin{array}{c} \end{array} \begin{array}{cccccccccccc} x_1 & x_1' & y_1 & y_1' & z_1 & z_1' & x_2 & x_2' & y_2 & y_2' & z_2 & z_2' \end{array} \begin{pmatrix} 1 & 1 & 0 & 0 & 0 & 0 & 0 & 0 & 0 & 0 & 0 & 0 \\ 0 & 0 & 1 & 1 & 0 & 0 & 0 & 0 & 0 & 0 & 0 & 0 \\ 0 & 0 & 0 & 0 & 1 & 1 & 0 & 0 & 0 & 0 & 0 & 0 \\ 0 & 0 & 0 & 0 & 0 & 0 & 1 & 1 & 0 & 0 & 0 & 0 \\ 0 & 0 & 0 & 0 & 0 & 0 & 0 & 0 & 1 & 1 & 0 & 0 \\ 0 & 0 & 0 & 0 & 0 & 0 & 0 & 0 & 0 & 0 & 1 & 1 \\ 1 & 0 & 0 & 1 & 0 & 0 & 0 & 0 & 0 & 0 & 0 & 1 \\ 0 & 1 & 0 & 0 & 1 & 0 & 0 & 0 & 0 & 1 & 0 & 0 \\ 0 & 0 & 0 & 0 & 0 & 0 & 0 & 1 & 1 & 0 & 1 & 0 \end{pmatrix}$$

Following Remark 3.15, we can therefore picture the secondary fan as in Figure 28 (L) (we use coordinates $X+Z, X+Y, Y+Z$ instead of the standard coordinates X, Y, Z here to make the symmetry clearer). The secondary polytope is therefore a "chamfered cube" (also known as a 4-truncated rhombic dodecahedron), which is shown in Figure 28 (R). This polyhedron has 32 vertices and 18 faces (12 hexagons

and 6 squares). As such, the unsliced VGIT has 32 phases. Note that we don't consider the stacky secondary fan here since we'll soon see that all the toric boundary is in the discriminant and so we can just work inside $T_{L^\vee}$.

In our case, slicing the phases of the unsliced VGIT gives the 4 geometric phases of the Triangle VGIT.

Remark 9.43. Note that we don't get all the phases of the Triangle VGIT by slicing. This is because all the phases of the unsliced VGIT are geometric – that is, have no orbifold locus – and, hence, so are all the sliced phases.

Now any G which acts freely on the chambers to give these 4 phases must have order 8. In fact, by computing which fans slice to a given fan of the Triangle VGIT, we can compute what the G-orbits of chambers in $L^\vee_{\mathbb{R}}$ should look like. So if we take $G = \mathbb{Z}_2^{\oplus 3}$ to be the group generated by "reflections" (not with the Euclidean metric) in the planes $Y + Z = 0, X + Z = 0$ and $X + Y = 0$ respectively, then this G preserves the secondary fan and has the correct G-orbits. For the secondary fan in Figure 28 (L), this amounts to actual reflections in the coordinate hyperplanes. This quotienting folds up the orthants in the secondary fan for the unsliced VGIT to give the secondary fan for the Triangle VGIT. Dually, with enough imagination, we can see how the chamfered cube folds up to give the associahedron. As such, this G seems like a sensible candidate.

Now we'll check that this G-action induces a G-action on FIPS_0. We start by understanding FIPS_0. From Theorem 8.8, the log-discriminant is a hyperplane arrangement whose log-hyperplanes correspond to hyperplanes in $L^\vee_{\mathbb{R}}$ spanned by the weights lying on them. Specifically, for each such hyperplane with normal l_Γ, the corresponding log-hyperplane takes the form $\nabla_\Gamma = \{x^{l_\Gamma} = c_\Gamma\}$ (see §8.1 for details). We can check that the hyperplanes in $L^\vee_{\mathbb{R}}$ of this form are precisely:

$$X = 0, Y = 0, Z = 0, X + Y = 0, X + Z = 0, Y + Z = 0, X + Y + Z = 0$$

To calculate ∇_Γ, we need to compute c_Γ for each of these. Since our T_L-representation is self-dual, by Remark 8.7, all the $c_\Gamma = \pm 1$. Calculating the correct signs and using Remark 8.9 to observe that all toric divisors are in the discriminant, we see that:

$$\mathrm{FIPS}_0 = (\mathbb{C}^*)^3 \backslash \{\alpha = -1, \beta = -1, \gamma = -1, \alpha\beta = 1, \beta\gamma = 1, \alpha\gamma = 1, \alpha\beta\gamma = -1\} \tag{7}$$

where

$$\alpha = \frac{x_2' y_1 z_2'}{x_2 y_1' z_2}, \beta = \frac{x_2 y_2 z_1}{x_2' y_2' z_1'}, \gamma = \frac{x_1 y_2' z_2}{x_1' y_2 z_2'}$$

Then the G-action on the secondary fan described above induces the following action on $(\mathbb{C}^*)^3$, which can be written explicitly in terms of generators $\sigma_1, \sigma_2, \sigma_3$ as:

$$\sigma_1 : (\alpha, \beta, \gamma) \mapsto (\alpha\beta\gamma, \frac{1}{\gamma}, \frac{1}{\beta}), \sigma_2 : (\alpha, \beta, \gamma) \mapsto (\frac{1}{\gamma}, \alpha\beta\gamma, \frac{1}{\alpha}), \sigma_3 : (\alpha, \beta, \gamma) \mapsto (\frac{1}{\beta}, \frac{1}{\alpha}, \alpha\beta\gamma)$$

[1]Figure By Watchduck (a.k.a. Tilman Piesk) - Own work, CC BY 4.0
https://commons.wikimedia.org/w/index.php?curid=66347020

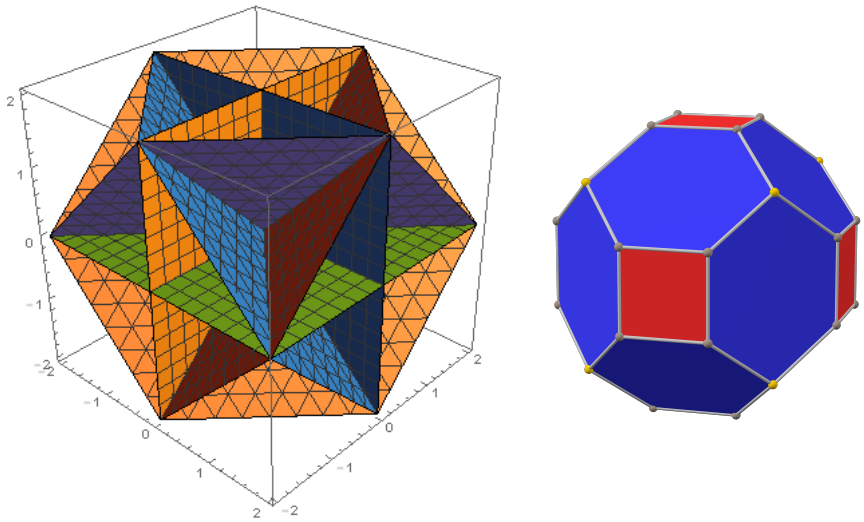

FIGURE 28. The secondary fan for the unsliced VGIT (L) and its secondary polytope, the "chamfered cube" (R) [1]

We can check that this G-action preserves the discriminant locus and so acts on FIPS_0.

Now that we have our candidate G-action, we want to show that $[\mathrm{FIPS}_0/G] \cong \mathrm{FIPS}_1$. One guess, following [31], as to how to define such a cover $\Phi : \mathrm{FIPS}_0 \to \mathrm{FIPS}_1$ is as follows. Suppose that the original VGIT is described by toric data $L \to \mathbb{Z}^n \xrightarrow{A} N$ and the unsliced VGIT is described by $L' \to \mathbb{Z}^{n'} \xrightarrow{A'} N'$. Since the phases of the original VGIT embed torically into the phases of the unsliced VGIT, we also have an embedding $i : N \hookrightarrow N'$ with the property that the rays of the original VGIT can be written as positive combinations of the rays in N'.

To construct our candidate for the covering map, we first construct a (possibly non-linear) map $\Phi : (\mathbb{C}^{n'})^\vee \to (\mathbb{C}^n)^\vee$. Let α_j be a way of writing $i(\omega_j)$ as a non-negative integral combination of the rays given by A'. As A' lives in a height one affine hyperplane in $N'_{\mathbb{R}}$, we note that there are only finitely many such α_j. We view α_j as the vector $(\alpha_j^k) \in \mathbb{N}^{n'}$ which sits in the commuting diagram:

$$\begin{array}{ccc} \mathbb{Z}^n & \xrightarrow[e_j \mapsto \omega_j]{A} & N \\ {\scriptstyle e_j \mapsto \alpha_j}\downarrow & & \downarrow{\scriptstyle i} \\ \mathbb{Z}^{n'} & \xrightarrow{A'} & N' \end{array}$$

Thus α defines a monomial function $(x')^{\alpha_j} := \prod_{k=1}^{n'} (x'_k)^{\alpha_j^k}$ on $(\mathbb{C}^{n'})^\vee$ and we can define $\Phi(x')(e_j) := \Phi_j(x') = \Sigma_{\alpha_j}(x')^{\alpha_j}$. By dualising the diagram above, we see that Φ intertwines the T_M and $T_{M'}$ actions along the map $i^\vee$ and so induces a map $[(\mathbb{C}^{n'})^\vee/T_{M'}] \to [(\mathbb{C}^n)^\vee/T_M]$. This is therefore a potential candidate to give a map between the two FIPS.

Remark 9.44. Note that we could put different coefficients in front of each monomial in Φ and it would still intertwine the actions. In fact, we'll use this flexibility for the Triangle VGIT – see Remark 9.45.

Unfortunately, in general, Φ doesn't respect the discriminant. However we'll now show (see Proposition 9.46) that it does for the Triangle VGIT and that, in fact, it is a G-cover. So first we construct the associated map $\Phi : (\mathbb{C}^{12})^\vee \to (\mathbb{C}^6)^\vee$ coming from imposing the commuting relations on the quiver Q. In total, there are 12 commuting relations (there are 4 vertices of Q and 3 pairs of commuting coordinates). But on the torus $(\mathbb{C}^*)^{12}$, 6 of these are redundant and, as such, the geometric phases of the Triangle VGIT can be described as the closure in the unsliced VGIT of the remaining 6 toric relations. These are encoded in a map $R : \mathbb{Z}^9 \to \mathbb{Z}^6$ whose kernel gives the embedding $i : N = \mathbb{Z}^3 \hookrightarrow N' = \mathbb{Z}^9$. When R is pre-composed with A', it gives the matrix

$$R \circ A' = \begin{pmatrix} 1 & 0 & -1 & 0 & 0 & 0 & -1 & 0 & 1 & 0 & 0 & 0 \\ 0 & 0 & 1 & 0 & -1 & 0 & 0 & 0 & 0 & -1 & 1 & 0 \\ 0 & 1 & 1 & 0 & 0 & 0 & 0 & -1 & -1 & 0 & 0 & 0 \\ 0 & 1 & 0 & 0 & 1 & 0 & -1 & 0 & 0 & 0 & 0 & -1 \\ 0 & -1 & 0 & 0 & 0 & 1 & 1 & 0 & 0 & 0 & -1 & 0 \\ 0 & 0 & 0 & 1 & 1 & 0 & 0 & 0 & -1 & 0 & -1 & 0 \end{pmatrix}$$

and we can compute that $i \circ A : \mathbb{Z}^6 \to \mathbb{Z}^9$ is given by:

$$\begin{pmatrix} 2 & 1 & 0 & 1 & 0 & 0 \\ 0 & 1 & 2 & 0 & 1 & 0 \\ 0 & 0 & 0 & 1 & 1 & 2 \\ 2 & 1 & 0 & 1 & 0 & 0 \\ 0 & 1 & 2 & 0 & 1 & 0 \\ 0 & 0 & 0 & 1 & 1 & 2 \\ 1 & 1 & 1 & 1 & 1 & 1 \\ 1 & 1 & 1 & 1 & 1 & 1 \\ 1 & 1 & 1 & 1 & 1 & 1 \end{pmatrix}$$

From here, one can check that $i(\omega_j)$ are the only rays in N' which occur on the slice given by i. Comparing this matrix and A', one can also see that there is a unique way to write $i(\omega_1), i(\omega_3)$ and $i(\omega_6)$ in terms of the rays in A' and precisely two ways to write each of the remaining three rays. This means that

$$\Phi(x) = (\Phi_1(x), \Phi_2(x), \Phi_3(x), \Phi_4(x), \Phi_5(x), \Phi_6(x))$$

where

$$\Phi_1(x) = -x_1x_1'x_2x_2', \Phi_2(x) = x_1y_1x_2'y_2' + x_1'y_1'x_2y_2, \Phi_3(x) = -y_1y_1'y_2y_2'$$

$$\Phi_4(x) = x_1z_1x_2z_2 + x_1'z_1'x_2'z_2', \Phi_5(x) = y_1y_2z_1z_2' + y_1'y_2'z_1'z_2, \Phi_6(x) = -z_1z_1'z_2z_2'$$

Remark 9.45. Actually, this Φ isn't exactly as we described before because we have chosen different coefficients for the monomials. This is needed for the next proposition to hold and shows that, in general, the coefficients appearing in Φ need to be chosen carefully if it's to have any hope of being a cover.

Now that we have constructed Φ for the Triangle, we can check:

Proposition 9.46. *Φ induces a map $FIPS_0 \to FIPS_1$ which is a G-cover.*

Proof. To show that we get a map between the FIPS, we claim that the pre-image under Φ of the discriminant of the Triangle VGIT is the discriminant of the unsliced VGIT. Let's start with the coordinate hyperplanes corresponding to vertices of our polytopes. By inspecting A', we see that every ray is a vertex whereas in the triangle Δ_1 only the first, third and sixth ray ω_i are vertices (see Figure 23). As Φ_1, Φ_3, Φ_6 are monomials which together involve all coordinates, the pre-image of the 3 coordinate hyperplanes $\{a_1 = 0\}, \{a_3 = 0\}, \{a_6 = 0\}$ in $\mathbb{C}^6$ is the union of all coordinate hyperplanes in $\mathbb{C}^{12}$.

We now move on to the pre-image of ∇_{pr}, which we recall has defining equation:

$$\Delta_{pr} := \det \begin{pmatrix} a_1 & a_2/2 & a_4/2 \\ a_2/2 & a_3 & a_5/2 \\ a_4/2 & a_5/2 & a_6 \end{pmatrix}$$

We observe that:

$$\Phi^*(\Delta_{pr}) = 1/4(x_1y_1z_1 + x_1'y_1'z_1')(x_2'y_1z_2' + x_2y_1'z_2)(x_2y_2z_1 + x_2'y_2'z_1')(x_1y_2'z_2 + x_1'y_2z_2')$$

Recalling that $\mathrm{FIPS}_0 \subset (\mathbb{C}^*)^{12}/T_{M'} \cong (\mathbb{C}^*)^3_{\alpha,\beta,\gamma}$, we may write $\Phi^*(\Delta_{pr})$ in these coordinates as $(\alpha\beta\gamma + 1)(\alpha + 1)(\beta + 1)(\gamma + 1)$ up to units. Comparing with the description of FIPS_0 in (7) above, we see that $\Phi^{-1}(\nabla_{pr})$ is a union of 4 components of the discriminant.

Finally, the 3 components of the discriminant ∇_i with equations $a_2^2 - 4a_1a_3$, $a_4^2 - 4a_1a_6$ and $a_5^2 - 4a_3a_6$ pullback under Φ to give $(x_1y_1x_2'y_2' - x_1'y_1'x_2y_2)^2$, $(x_1z_1x_2z_2 - x_1'z_1'x_2'z_2')^2$ and $(y_1y_2z_1z_2' - y_1'y_2'z_1'z_2)^2$ respectively – that is, $(\alpha\gamma - 1)^2$,$(\beta\gamma - 1)^2$ and $(\alpha\beta - 1)^2$. By the description of FIPS_0 in (7) again, we see that each of these pre-images is a component of the discriminant. As we have covered all components in the discriminant $\{E_{A_0} = 0\}$ of the unsliced VGIT, we conclude that Φ sends $\mathbb{C}^{12} \setminus \{E_{A_0} = 0\}$ to $\mathbb{C}^6 \setminus \{E_{A_1} = 0\}$ and hence descends to give a map $\Phi : \mathrm{FIPS}_0 \to \mathrm{FIPS}_1$.

To prove the covering statement, we shall show that the pullback $\hat{\Phi} : X \to \mathbb{C}^3_{uvw} \setminus \{E_{A_1} = 0\}$ of Φ under the $\mathbb{Z}_2^{\oplus 2}$-quotient map $\mathbb{C}^3_{uvw} \setminus \{E_{A_1} = 0\} \to \mathrm{FIPS}_1$ (see §9.1.3) is a G-cover, noting that X is a scheme as Φ is representable. We shall do this by showing that the non-empty fibres of $\hat{\Phi}$ are G-orbits. This implies that $\hat{\Phi}$ is an 8:1 cover of its image. Hence its image must be 3-dimensional and, since $\hat{\Phi}$ is proper, $\hat{\Phi}$ is surjective.

To prove that $\hat{\Phi}$ has fibres a G-orbit over its image, we need only show that Φ has fibres a G-orbit over its image. The fibre of Φ over $x \in \mathrm{FIPS}_1 \subset [\mathbb{C}^3/\mathbb{Z}_2^{\oplus 2}]$ is canonically isomorphic to $\mathrm{Aut}(x) \times \bar{\Phi}^{-1}(\pi(x))$ where $\bar{\Phi} = \pi \circ \Phi$ and

$$\pi : [\mathbb{C}^3/\mathbb{Z}_2^{\oplus 2}] \to \mathbb{C}^3/\mathbb{Z}_2^{\oplus 2} = \{xyz = u^2\} \subset \mathbb{C}^4_{xyzu}$$

is the projection to the coarse moduli space. Recall that x has non-trivial stabiliser only along the 3 coordinate axes – it has stabiliser $\cong \mathbb{Z}_2$ for all such points apart from the origin and, at the origin, the stabiliser is $\mathbb{Z}_2^{\oplus 2}$.

We may write $\bar{\Phi}$ in coordinates α, β, γ as:

$$\bar{\Phi}(\alpha,\beta,\gamma) = \left(\frac{(\alpha\gamma+1)^2}{\alpha\gamma}, \frac{(\beta\gamma+1)^2}{\beta\gamma}, \frac{(\alpha\beta+1)^2}{\alpha\beta}, -\frac{(\alpha\gamma+1)(\beta\gamma+1)(\alpha\beta+1)}{\alpha\beta\gamma}\right)$$

As such, we can check that $\bar{\Phi}$ is G-invariant by using the explicit G-action above so we need only check that the fibres consist of a single G-orbit.

Suppose $\bar{\Phi}(\alpha,\beta,\gamma) = \bar{\Phi}(\alpha',\beta',\gamma')$. Note that $\frac{(\alpha\gamma+1)^2}{\alpha\gamma} = \frac{(\alpha'\gamma'+1)^2}{\alpha'\gamma'}$ precisely when $\alpha\gamma = \alpha'\gamma'$ or $\frac{1}{\alpha'\gamma'}$ and similarly for the y and z terms. For fixed $\alpha\gamma$, $\beta\gamma$ and $\alpha\beta$ there are precisely 2 choices of α, β, γ (related by $-\mathrm{Id}$ on FIPS_0) with these values for the products. Moreover, these choices of α, β and γ have the same u-component of $\bar{\Phi}$ precisely when this component is 0.

As such, if $\bar{\Phi}(\alpha',\beta',\gamma')$ has non-zero u-component, then the fibre containing (α',β',γ') has 8 points, related by transformations sending $\alpha'\gamma' \mapsto \frac{1}{\alpha'\gamma'}$ etc. Comparing with σ_i, we see that this is a G-orbit.

If $\bar{\Phi}(\alpha',\beta',\gamma')$ has zero u-component, then it also has one of its other components equal to 0. One checks explicitly that, away from the x, y and z-axis, the 8 points in the fibre form a G-orbit. Similarly on these axes (but not at the origin) one checks that the 4 points in the fibre form a G-orbit and the 2 points over the origin also form a G-orbit.

□

So, exactly as in [18], we have constructed a Galois cover of the FIPS of the Triangle VGIT which is itself the FIPS of a quasi-symmetric VGIT. Having constructed a representation on the phases of the Triangle VGIT in §9.2, we now just sketch how our Galois cover should lead again to such a representation. We first observe that in the quasi-symmetric case we automatically have a large radius representation ρ on the phases of the unsliced VGIT from Corollary 2.8. To construct the representation on the phases of the Triangle VGIT, we want to "restrict" this representation to the slices.

Suppose we consider the two phases $X_\pm$ of the unsliced VGIT on either side of a wall, whose slices $Y_\pm$ are phases of the Triangle VGIT. The common open subset (which includes the open torus $T_{N'}$) gives a birational equivalence between the two

and we get a diagram as follows:

$$\begin{array}{ccc} X_- & \dashrightarrow & X_+ \\ \uparrow & & \uparrow \\ Y_- & \dashrightarrow & Y_+ \end{array}$$

Then ρ assigns a window equivalence $\phi_0 : D^b(X_-) \to D^b(X_+)$ to the corresponding large radius path. In the A_n-case (see [18], Proposition 5.17), this restricts to give an equivalence $\phi_0|_Y : D^b(Y_-) \to D^b(Y_+)$ between the sliced phases. If this restriction property holds for the Triangle VGIT, then as $\pi_1(\mathrm{FIPS}_0)$ is generated by such large radius paths and any relations between the functors ϕ_0 on the unsliced VGIT must continue to hold between the functors $\phi_0|_Y$ on the Triangle VGIT, we get a representation $\rho|_Y$ of $\pi_1(\mathrm{FIPS}_0)$ on the phases of the Triangle VGIT.

Remark 9.47. This restriction property for the Triangle VGIT does not follow directly from the same argument used for the A_n-examples in [18]. The difference is that the toric relations there were actual (invariant) functions whereas our relations are not – that is, neither of the monomials in any of our relations correspond to loops in the quiver. Geometrically, this corresponds to the fact that in the A_n-case we only slice away non-compact directions whereas for the Triangle we also slice away some compact directions. Note that the restriction property can be reinterpreted as a purely geometric statement about how the birational roof between two neighbouring phases of the unsliced VGIT behaves under slicing.

We also fully expect that the restrictions of these equivalences recovers the representation from Theorem 9.35. For this, we would have to check that window equivalences between neighbouring phases of the unsliced VGIT in distinct G-orbits restricted to window equivalences between phases of the Triangle VGIT and that window equivalences between neighbouring phases of the unsliced VGIT in the same G-orbit restricted to family spherical twists arising from a trivial family of $\mathbb{P}^1$s over $\mathbb{C}$ with normal bundle $\mathcal{O}(-2)$, as in the description of our representation in Remark 9.10.

Given the representation $\rho|_Y$ of $\pi_1(\mathrm{FIPS}_0)$ on the phases of the Triangle VGIT, it is largely formal to construct the representation of $\pi_1(\mathrm{FIPS}_1)$. Namely, as the G-orbits of chambers correspond to identical sliced phases, we have a canonical G-representation on the sliced phases by the identity.

Moreover, the large radius representation $\rho|_Y$ is G-equivariant. For this, we just need to check that the equivalences $(\phi_0^{C_1,C_2})|_Y$ and $(\phi_0^{g(C_1),g(C_2)})|_Y$ on the sliced phases agree for any $g \in G$. This holds because there is a G-action on $N' = \mathbb{Z}^9$ which preserves the set of rays of the unsliced VGIT and is compatible with our G-action on $L^\vee$ in the sense that two chambers in $L^\vee_{\mathbb{R}}$ differ by $g \in G$ precisely when the corresponding fans in $N'_{\mathbb{R}}$ differ by permuting the rays according to g. This compatibility means that everything about the wall crossing from C_1 to C_2 (such as the unstable loci on each side, the fixed locus etc.) agrees under the action of g

on the corresponding phases with the wall crossing from $g(C_1)$ to $g(C_2)$. As such, $\phi_0^{C_1,C_2}$ and $\phi_0^{g(C_1),g(C_2)}$ agree up to the action of g and the same thing continues to hold on the sliced phases (where the G-action is trivial). To see that we have such a G-action on N', observe that the G-action on the secondary fan preserves the set of weights of the unsliced VGIT. This follows immediately from Figure 28 (L) since the rays in the secondary fan which are not weights of the unsliced VGIT are the 6 rays lying on the coordinate axes in that figure (these correspond to the 6 square faces of the chamfered cube) and these are obviously permuted by reflection in the coordinate hyperplanes. Then this G-action on $L^\vee$ lifts to a G-action on $(\mathbb{Z}^n)^\vee$ which records the permutation of the weights. Dually, this induces the desired G-action on N' which preserves the set of rays.

Since $\rho|_Y$ is G-equivariant, we can combine it with the trivial G-action to get a representation of $\pi_1(\mathrm{FIPS}_0) \rtimes G$ where this is the semidirect product of a group with a groupoid (see [10], §11 for details). But it is known (ibid.) that $\pi_1(\mathrm{FIPS}_0) \rtimes G \cong \pi_1([\mathrm{FIPS}_0/G])$. Since $\mathrm{FIPS}_1 \cong [\mathrm{FIPS}_0/G]$, it follows that we have constructed a representation of $\pi_1(\mathrm{FIPS}_1)$, as desired.

Remark 9.48. This covering perspective on the Triangle VGIT has a lot of similarities with recent work of Donovan and Wemyss [19, 36]. In their setting, we would start with the 3-fold cD_4 singularity $Y := \mathbb{C}^3 / \mathbb{Z}_2^{\oplus 2} \cong \{xyz = u^2\} \subset \mathbb{C}^4_{xyzu}$ and a geometric crepant resolution $\pi : X \to Y$, which for us is given by a geometric phase of the Triangle VGIT. Here there is a natural such choice given by the maximally symmetric phase X_0, which can be described as $\mathrm{Hilb}^G(\mathbb{C}^3)$. This choice of a phase can be interpreted as an NCCR on Y by pushing down (by π) the bundle of sections of the universal subscheme on X_0. This can be alternatively described by choosing the affine orbifold phase $\pi' : [\mathbb{C}^3/G] \to Y$ and the associated NCCR $\bigoplus_{\chi \in \mathcal{X}^*(G)} \pi'_* \mathcal{O}(\chi)$ on Y (see Remark 9.40). Either way, we end up with the NCCR given by the McKay quiver in Figure 27.

To run the machinery in [19], we would then mutate this NCCR and use moduli tracking to compute the real hyperplane arrangement $\mathcal{H}$. This gives exactly the walls of the secondary fan for FIPS_0. In [36], §7.2 Example 7.6, Wemyss computes that there are 4 minimal models, obtained from X_0 by individually flopping the 3 exceptional curves. It follows that all other mutated algebras are just isomorphic to these and one can check that the chambers corresponding to the same algebra are precisely the G-orbits we have chosen above.

In [19], Donovan and Wemyss construct an action of the Deligne groupoid $\mathcal{G}_\mathcal{H}$ of the hyperplane arrangement $\mathcal{H}$ on the models of certain isolated 3-fold singularities by applying flop (or mutation) functors. However our 3-fold singularity is non-isolated which means that their techniques do not apply directly. However they do construct certain autoequivalences, called "J-twists", even when there are no actual flop functors – that is, between phases in the same G-orbit. In the Triangle VGIT, these "J-twists" should just be the family spherical twists we saw arising

in Remark 9.47. So in their language, our action combines J-twists with the usual flop functors to construct a representation of $\mathcal{G}_{\mathcal{H}}$.

10. Near large radius in higher-dimensions

We finish by discussing a conjectural way to describe the representation on paths near a large radius curve $Z(W)$ in any dimension, which is supposed to generalise the representation ρ^W from the 2d case in Theorem 6.15. So suppose we are crossing a wall W in the secondary fan from a chamber C_1 to C_2. Let $\lambda := \lambda_{C_1,C_2} \in L$ be the primitive normal (pointing towards C_1) and let $Z^\lambda = [(\mathbb{C}^n)^\lambda/T_L]$ and $Z'^\lambda = [(\mathbb{C}^n)^\lambda/(T_L/\lambda)]$ be the λ-fixed locus. Then Z'^λ is itself a linear toric VGIT and its weights are precisely those of the original VGIT lying in the hyperplane $\langle W\rangle$ (where we view these weights as living inside $\langle W\rangle \cap L^\vee$). We observe that W is contained (as a full-dimensional subcone) in a unique cone of the secondary fan for the VGIT on Z^λ and Z'^λ (which lies in $L^\vee_{\mathbb{R}}$ and $\langle W\rangle$ respectively). We call the corresponding quotients Z_λ and Z'_λ respectively.

Unlike in dimension 2, in general we can have many components of the discriminant intersecting $Z(W)$. Recall from §3.1 that such components correspond to faces Γ of Δ and to such a face we have associated (see Definition 3.43) a Higgs VGIT. As mentioned in §2, typically these VGITs are not Calabi–Yau.

Definition 10.1. A *Higgs phase* Z_Γ associated to a face Γ of Δ is any minimal phase of the Higgs VGIT – that is, a phase whose canonical bundle is nef.

Remark 10.2. Following Remark 3.46, this definition actually makes sense when we start with *any* linear toric VGIT, not necessarily a Calabi–Yau one.

Recall (see Proposition 5.20) that currently we have a representation ρ^W on large radius paths. Moreover, by Remark 4.19, loops at large radius based at the chamber C_1 correspond under ρ^W to twists about a spherical functor $F_w : D^b(Z_\lambda)_w \to D^b(X_{C_1})$. Here, as we did in 2-dimensions, we focus on the case $w = 0$ when $D^b(Z_\lambda)_w = D^b(Z'_\lambda)$. For general w, we note that, having chosen β_W of λ-weight -1 to define our near large radius paths (see §5.2), $\otimes\mathcal{O}(-w\beta_W)$ gives an equivalence between $D^b(Z'_\lambda)$ and $D^b(Z_\lambda)_w$.

Then, as described in Conjecture B, we would like to define our representation on loops near the large radius curve $Z(W)$ around ∇_Γ by twists about spherical functors (see [3] for precise definitions) with source category $D^b(Z_\Gamma)$. One source (and for us the only source) of such functors is from SODs of $D^b(Z'_\lambda)$ into "minimal" pieces of the form $D^b(Z_\Gamma)$.

Remark 10.3. In general, if we take a piece $\mathcal{A}$ of an SOD of the source category of a spherical functor F, it is not true that $F|_{\mathcal{A}}$ is spherical. However our spherical functor F_0 has the special property that its cotwist is (up to a shift) the Serre functor on $D^b(Z'_\lambda)$ and so (see [1], Proposition 1.1) $F_0|_{\mathcal{A}}$ is, in fact, spherical.

The SODs which we use are of a special form coming from the fact that Z'_λ is a phase in a linear toric VGIT. The main result of this section (Theorem 10.4) says that SODs into minimal factors of the form $D^b(Z_\Gamma)$ always exist and, moreover, the number of pieces of the form $D^b(Z_\Gamma)$ in any SOD coming from VGIT is an intrinsic quantity. This is therefore a Jordan-Hölder type theorem for these SODs. As we shall now see, it holds for a general linear toric VGIT. In §10.2, we will return to Conjecture B and the representation on near large radius paths in the Calabi–Yau case.

10.1. **SODs from wall-crossings.** Fix a wall W in the secondary fan of a toric (not necessarily Calabi–Yau) VGIT with primitive normal $\lambda_W \in L$ chosen so that $\mu_{\lambda_W} := \langle \lambda_W, -K \rangle \geq 0$, where $-K = \sum_i \beta_i$. We call the phase associated to the chamber C (adjacent to W) with $\langle \lambda_W, C \rangle \geq 0$ X_+, the other phase X_- and the quotient on the wall X_W (this is intentionally ambiguous when $\mu_{\lambda_W} = 0$). Finally we let Z'_{λ_W} be the λ_W-fixed locus in X_W (forgetting the trivial λ_W action). Then, for any $d \in \mathbb{Z}$, Theorem 4.21 gives full embeddings $\Phi_d : D^b(X_-) \to D^b(X_+)$ and $i_j : D^b(Z'_{\lambda_W}) \to D^b(X_+)$ for $j = 1, \dots, \mu_{\lambda_W}$ such that $\langle \operatorname{Im} \Phi_d, \operatorname{Im} i_1, \dots, \operatorname{Im} i_\mu \rangle$ is an SOD of $D^b(X_+)$.

Now pick a path $\gamma : [0,1] \to L^\vee_{\mathbb{R}}$ starting at a chamber whose corresponding phase X_0 is minimal (this may be empty) and ending at a phase X_1. This path should avoid any codimension 2 cones in the secondary fan and, whenever it crosses a wall, it does so in the direction from X_- to X_+. If we label the normals to the walls W_i along γ by λ_i for $i = 1, \dots, k$, then Theorem 4.21 gives us full embeddings $\Phi : D^b(X_0) \to D^b(X_1)$ and $i_{i,j} : D^b(Z'_{\lambda_i}) \to D^b(X_1)$ for $i = 1, \dots, k$ and $j = 1, \dots, \mu_{\lambda_i}$.

Continuing inductively, if Z'_{λ_i} is not minimal for some i, then we can decompose $D^b(Z'_{\lambda_i})$ further so long as, for such i, we choose similar paths γ_i (in the hyperplane $\langle W_i \rangle$) for the VGITs on Z'^{λ_i} going from a minimal phase to the phase Z'_{λ_i}. The choices of these paths is shown schematically in Figure 29. If we keep going, this eventually terminates as each linear subspace in which these paths live has strictly smaller dimension than the preceding one. Then the end result is an SOD of $D^b(X_1)$ whose pieces are $D^b(Z_\Gamma)$ for various faces Γ, which are necessarily minimal (see Definition 3.3) because we always take all the weights on the corresponding subspace (see Lemma 3.47). This gives the first part of the following:

Theorem 10.4. *Given a choice of paths as above, we get a number of full embeddings $i_{\Gamma,j} : D^b(Z_\Gamma) \to D^b(X_1)$ (for some collection of minimal faces Γ and $j = 1, \dots, n_\Gamma$) and an SOD of $D^b(X_1)$ into these pieces. Moreover, the Γ which occur and the number n_Γ are independent of the particular choice of these paths.*

Remark 10.5. It was shown in [28] that the Jordan-Hölder property doesn't hold in general for derived categories of smooth projective varieties, so this theorem is really using the fact that X_1 is a phase of a linear toric VGIT and that we are choosing a particular class of SODs of $D^b(X_1)$ which use this structure.

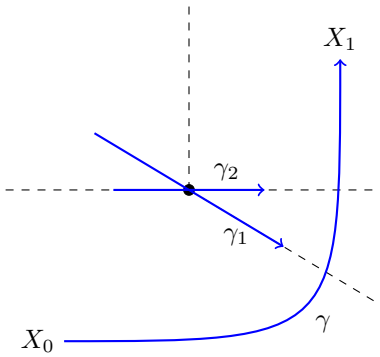

FIGURE 29. A choice of paths giving an SOD as in Theorem 10.4

We now turn to the proof of the second part of the theorem above. Suppose the VGIT for X_1 can be described as $T_L \circlearrowright \mathbb{C}^n$ and let its secondary fan in $L^\vee_{\mathbb{R}}$ be Σ. Pick any choice of paths $\gamma, \gamma_1, \ldots, \gamma_i, \ldots$ in $L^\vee_{\mathbb{R}}$ as in the theorem. We shall prove the theorem by induction on $\mathrm{Rk}(L^\vee)$, noting that when $\mathrm{Rk}(L^\vee) = 1$ there is only one choice of path and so we have nothing to prove. As such, we can assume that the faces Γ and numbers n_Γ for the SODs of $D^b(Z'_\lambda)$ (and $D^b(Z'_{\lambda_1,\lambda_2})$) which occur along γ do not, in fact, depend upon $\gamma_1, \ldots, \gamma_i, \ldots$ and we therefore forget about these extra choices.

To prove Theorem 10.4 it suffices to show that the Γ and n_Γ occurring at walls along γ do not change whenever we go "the other way" around a codimension 2 cone in Σ for which this makes sense – in particular, γ has to go from a minimal phase in the corresponding 2-dimensional face to a maximal one. This claim follows since any two choices of paths γ are related by such moves. This observation will ultimately allow us to reduce to the case when $\mathrm{Rk}(L^\vee) = 2$.

So fix such a codimension 2 cone σ in Σ (corresponding to a 2-dimensional face F of the secondary polytope) and consider the quotient map $q : L^\vee \to L^\vee_\sigma$ where $L^\vee_\sigma$ is the rank 2 quotient lattice $L^\vee/\langle\sigma\rangle \cap L^\vee$. By Remark 3.30, the secondary fan for the VGIT on F is pulled-back from the secondary fan (in $(L^\vee_\sigma)_{\mathbb{R}}$) of the VGIT given by T_{L_σ} acting on X_σ. Moreover, the canonical direction in Σ given by K_{X_1} induces a canonical direction in this secondary fan given by $q(K_{X_1})$. This is depicted in Figure 30. From now on, we shall assume that X_0 is the minimal phase *in this face* and X_1 the maximal one.

Remark 10.6. In general there is no single maximal or minimal phase as we have assumed here. However, as there are no wall contributions between different choices of maximal (or minimal) phases, we are free to choose them as we wish.

In the notation from Figure 30, consider the two SODs of $D^b(X_1)$ coming from the paths labelled γ_1 and γ_2, where we have labelled each wall with the corresponding contribution to the derived categories as we move along γ_i. The categorical contributions on wall W come with multiplicity $\mu_{\lambda_W} = \langle \lambda_W, -q(K_{X_1})\rangle$. Then, to prove the theorem, it is enough to prove that these two SODs of $D^b(X_1)$ have the

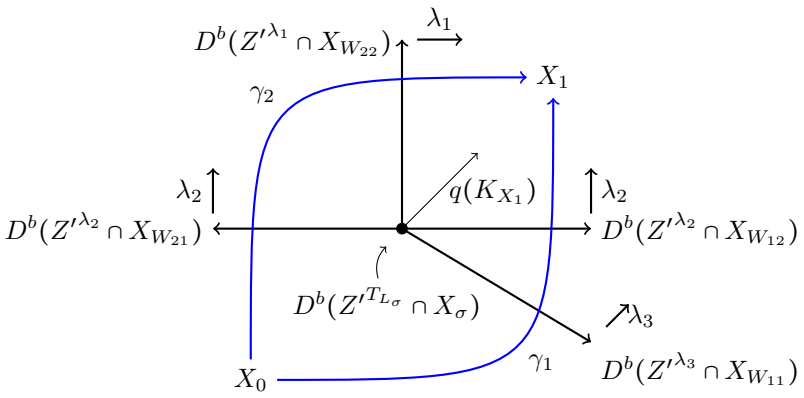

FIGURE 30. Two paths around the 2-dimensional face F superimposed on the secondary fan for the VGIT on F where W_{ij} is the j-th wall along γ_i

same minimal (in this face) factors with the same multiplicities. These minimal factors have 3 possible forms:

(1) $D^b(X_0)$
(2) $D^b(Z'^{\lambda} \cap X_W)$ when the line $\langle W \rangle$ contains two walls and $Z'^{\lambda} \cap X_W$ is a minimal phase of the VGIT on Z'^{λ}.
(3) $D^b(Z'^{T_{L_\sigma}} \cap X_\sigma)$

Lemma 10.7. *The multiplicities (in the two SODs of $D^b(X_1)$) of the minimal factors (1) and (2) agree.*

Proof. By Theorem 4.21, there is precisely one copy of $D^b(X_0)$ in each of these two SODs so this factor is easy.

For any two walls W_1, W_2 in the secondary fan for F which lie on a line (for example, the x-axis in Figure 30) with normal λ (pointing towards the maximal chamber), we add μ_λ copies of $D^b(Z'^{\lambda} \cap X_{W_1})$ if we follow γ_1 and μ_λ copies of $D^b(Z'^{\lambda} \cap X_{W_2})$ if we follow γ_2. One of these two categories is a minimal factor and, by Theorem 4.21, the other has an SOD with one copy of this minimal factor in. Therefore these factors have the same multiplicity in the two SODs of $D^b(X_1)$. □

Finally we consider the minimal factor (3). When two walls lie on a line, only the maximal phase (on that line) has factors of the form (3) in and so, for the purpose of counting the multiplicity of these factors, we can ignore the walls in such lines which correspond to minimal phases. Then we are only left with walls lying on distinct lines and, by Theorem 4.21, such a wall W with primitive generator $l_W \in (L_\sigma^\vee \cap \langle W \rangle)^\vee$ (such that $l_W(W) > 0$) contributes exactly $\mu_{\lambda_W} \mu_W^{\lambda_W}$ copies of $D^b(Z'^{T_{L_\sigma}} \cap X_\sigma)$ where the multiplicity $\mu_W^\lambda := \max(\langle -K_{Z^\lambda}, l_W \rangle, 0)$.

However in general, if we define:

$$\mu_{\gamma_i} := \sum_{\text{Walls } W \text{ along } \gamma_i} \mu_{\lambda_W} \mu_W^{\lambda_W}$$

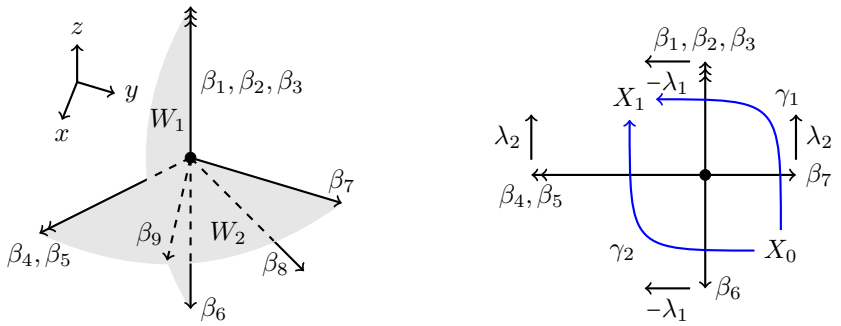

FIGURE 31. Weights β_i for $i = 1, \cdots, 8$ for Example 10.8 with the two extra walls W_i and one extra ray β_9 of the secondary fan shown (L) and the secondary fan in the face corresponding to β_9 (R)

μ_{γ_1} and μ_{γ_2} do not agree, as the following example shows.

Example 10.8. Take the following 8 weights in $L^\vee = \mathbb{Z}^3$.

$$\beta_1 = \beta_2 = \beta_3 = (0,0,1), \beta_4 = \beta_5 = (1,-2,0), \beta_6 = (0,0,-1), \beta_7 = (0,1,0), \beta_8 = (-2,1,-1)$$

These are shown in Figure 31 (L). The secondary fan for this VGIT has a single extra ray $\beta_9 = (1,0,0)$, which is the intersection of the two walls W_i in Figure 31 (L). Consider the 2-dimensional face corresponding to $\sigma = \beta_9$ shown in Figure 31 (R). Then the projection $q : L^\vee \to L^\vee_\sigma = \mathbb{Z}^2$ sends $(x,y,z) \mapsto (y,z)$ and one checks that $q(-K_{X_1}) = (-2,1)$ and so the minimal and maximal phases are as shown.

We shall now calculate μ_{γ_1} and μ_{γ_2} explicitly in this example. We have that $\mu_{-\lambda_1} = 2$ and $\mu_{\lambda_2} = 1$. Noting that the walls corresponding to β_6 and β_7 don't contribute to μ_{γ_2} and μ_{γ_1} respectively as they correspond to minimal phases for the VGIT on the wall, $\mu_{\gamma_1} = \mu_{-\lambda_1}\mu_W^{-\lambda_1} = 2 \times 2 = 4$ and $\mu_{\gamma_2} = \mu_{\lambda_2}\mu_W^{\lambda_2} = 1 \times 3 = 3$. Thus $\mu_{\gamma_1} \neq \mu_{\gamma_2}$.

In this example, the discrepancy between μ_{γ_1} and μ_{γ_2} came from the fact that the multiplicities μ_λ depend on all the weights but not all the weights (in this example β_8) affect the VGIT on the face F. However, in this example, Theorem 10.4 still holds because there is no contribution from the origin in Figure 31 (R) – that is, $Z'^{T_{L_\sigma}} \cap X_\sigma = \varnothing$.

More generally, we therefore have two cases to consider:

(1) $X_\sigma \cap Z'^{T_{L_\sigma}} = \varnothing$. In this case, μ_{γ_1} and μ_{γ_2} may differ but we don't care as far as Theorem 10.4 is concerned and so there is nothing left to check.
(2) $X_\sigma \cap Z'^{T_{L_\sigma}} \neq \varnothing$.

Remark 10.9. In case (1), the "wall" given by σ in any of the wall VGITs in F is not part of the secondary fan of these VGITs. We refer to this by saying that σ is a "fake wall". In Example 10.8, β_9 was a fake wall. More generally, whenever $\mathrm{Rk}(L^\vee) = 3$ and so σ is a ray β of the secondary fan, β defines a fake wall precisely when β has no weights on it.

Remark 10.10. For any 2-dimensional face F of the secondary polytope such that (1) holds, all the walls of the secondary fan for the VGIT on F must be lines. This follows because if there was a wall W in this secondary fan which was a ray, then, since $X_\sigma \cap Z'^{T_{L_\sigma}} = \varnothing$, the phases of the VGIT on $\langle W \rangle$ are the same and one of them is empty.

So we are left with case (2). The basic observation is:

Lemma 10.11. *If σ is not a fake wall – that is, $X_\sigma \cap Z'^{T_{L_\sigma}} \neq \varnothing$ – $q(\beta_i)$ lies on a wall of the secondary fan for the VGIT on F for all weights β_i which are not in $\langle \sigma \rangle$.*

Proof. By naturality of the semistable locus, $X_\sigma \cap Z'^{T_{L_\sigma}}$ corresponds to the phase of the linear toric VGIT on $Z'^{T_{L_\sigma}}$ whose chamber in $\langle \sigma \rangle$ is σ. Using the description of the support of the secondary fan of a linear toric VGIT (see [14], Theorem 14.4.7), $X_\sigma \cap Z'^{T_{L_\sigma}} \neq \varnothing$ implies that σ is contained in the cone generated by the weights which lie in $\langle \sigma \rangle$. Let's re-label these weights by $\beta_1, \ldots, \beta_n$.

Now take a weight β_i not lying in $\langle \sigma \rangle$ (so $i > n$) and consider $q(\beta_i)$. Let $\lambda \in L_\sigma$ be one of the primitive normal vectors to the line generated by $q(\beta_i)$. If $q(\beta_i)$ does not lie on a wall in the secondary fan for F, then it lies in a chamber of this fan. We let C be the maximal cone in Σ which corresponds to this chamber (so $\sigma \subset C$) and X_C denote the corresponding phase. Note that, by our choice of λ, $Z'^{\lambda} \cap X_C = \varnothing$.

Now λ defines a hyperplane in $L^\vee_{\mathbb{R}}$, which we call $\langle W \rangle$, on which the weights of the VGIT on Z'^{λ} lie. Then $Z'^{\lambda} \cap X_C = \varnothing$ implies that the open subset $\mathrm{Int}(C) \cap \langle W \rangle \subset \langle W \rangle$ is disjoint from the support of the secondary fan. But this is impossible because, if we let σ_i be the cone (of maximal dimension) generated by $\beta_1, \ldots, \beta_n$ and β_i in $\langle W \rangle$, then σ_i must meet $\mathrm{Int}(C) \cap \langle W \rangle$ since both are full-dimensional subsets of $\langle W \rangle$ containing σ in their closure and lying on the same side of $\langle \sigma \rangle$. As such, we have a contradiction and so $q(\beta_i)$ lies on a wall of the secondary fan for the VGIT on F. □

We are now in a position to complete the proof of Theorem 10.4.

Proof of Theorem 10.4. The first claim was dealt with before the statement of the theorem, so it only remains to show the second claim. Moreover, it suffices to prove that the two SODs coming from the two paths around a chosen 2-dimensional face F agree. We have also shown in Lemma 10.7 that the multiplicities of the minimal factors of the form $D^b(X_0)$ and coming from walls which are lines always agree. Therefore we are left with the minimal factor $X_\sigma \cap Z'^{T_{L_\sigma}}$ which we may assume is non-empty i.e. case (2). In this case, we need to show that $\mu_{\gamma_1} = \mu_{\gamma_2}$. For the purposes of showing this, as we have remarked, whenever we have two walls W_1 and W_2 lying on a line with normal λ, only one of $\mu^{\lambda}_{W_i}$ will be non-zero and so we can forget about the other side and assume that all walls lie on distinct lines. This means that, for any wall W, $\mu^{\lambda_W}_W = \sum_{i | q(\beta_i) \in W} |q(\beta_i)|$ and so, recalling that $u_W \in L^\vee$

is the primitive generator on the ray W:

$$u_W \mu_W^{\lambda_W} = \sum_{i|q(\beta_i)\in W} u_W |q(\beta_i)| = \sum_{i|q(\beta_i)\in W} q(\beta_i)$$

Pick an orientation on $L_\sigma^\vee$ such that γ_1 is positive with respect to this orientation. It follows that γ_2 is negative. We can find a unique primitive integral area form $\omega \in \Lambda^2 L_\sigma$ such that, if (u_1, u_2) are positively oriented (assume u_1 and u_2 are linearly independent) then $\omega(u_1, u_2) > 0$. This area form gives us an identification $L^\vee \to L, u \mapsto \omega(u, -)$ and, by definition of the $\lambda_W \in L$ occurring at walls W along γ_1, $\lambda_W = \omega(u_W, -)$. Similarly, for the λ_W coming from a wall W along γ_2, $\lambda_W = \omega(-u_W, -)$.

Then:

$$\begin{aligned}
\mu_{\gamma_1} - \mu_{\gamma_2} &= \langle q(-K_{X_1}), \sum_{\substack{\text{Walls } W \\ \text{along } \gamma_1}} \lambda_W \mu_W^{\lambda_W} - \sum_{\substack{\text{Walls } W \\ \text{along } \gamma_2}} \lambda_W \mu_W^{\lambda_W} \rangle \\
&= \omega(\sum_{\text{All walls } W} u_W \mu_W^{\lambda_W}, q(-K_{X_1})) \\
&= \omega(\sum_{\text{All walls } W} \sum_{i|q(\beta_i)\in W} q(\beta_i), q(-K_{X_1})) \\
&= \omega(q(-K_{X_1}), q(-K_{X_1})) = 0
\end{aligned}$$

where the penultimate equality comes from Lemma 10.11. □

Remark 10.12. Given Theorem 10.4, it is natural to ask if there is a more geometric interpretation of which minimal factors show up and their multiplicities n_Γ.

10.2. **Intersection multiplicities: a conjecture.** We return to the situation at the start of this section of crossing a single wall W between two phases of a Calabi–Yau VGIT. We want to apply the above technology to $X_1 = Z'_\lambda$ because we would like to define fractional windows and these come from SODs of $D^b(Z'_\lambda)$.

Definition 10.13. $n_{\Gamma,W}$ is the number n_Γ of pieces coming from Z_Γ in the SOD from Theorem 10.4 of the phase $X_1 = Z'_\lambda$ corresponding to W.

Remark 10.14. In this setting, the only faces Γ for which $n_{\Gamma,W}$ is non-zero are the ones for which the linear subspace $(L'_\Gamma)^\vee_\mathbb{R}$ spanned by the complementary weights (see §3.5) is contained in $\langle W \rangle$. This is because the Higgs VGITs occurring in the SOD of $D^b(X_1)$ from the previous section are defined by a subset of the weights of the VGIT on Z'^λ.

Unlike in the general case however, here we know how to define the discriminant (see Definition 3.2) and understand that its components correspond to minimal phases – that is, Higgs phases. Moreover, in light of the Conjecture of Aspinwall, Plesser and Wang (see Conjecture B in §2) and the fact that our SOD of $D^b(Z'_\lambda)$ gives rise to $n_{\Gamma,W}$ different spherical functors with source category $D^b(Z_\Gamma)$ (whose twists are fractional window shifts), it seems very natural to conjecture:

Conjecture 10.15. *The number $n_{\Gamma,W}$ agrees with the intersection multiplicity $m_{\Gamma,W}$ of ∇_Γ with the curve $Z(W)$.*

We don't know how to prove this in general as we usually don't have a method to understand $m_{\Gamma,W}$. However, as evidence for this conjecture, we can prove some special cases.

Lemma 10.16. *If Γ is such that $\langle W\rangle$ doesn't contain $(L'_\Gamma)^\vee$, then $m_{\Gamma,W} = 0$. By Remark 10.14, for such Γ, $n_{\Gamma,W} = 0$ also. As such, this agrees with Conjecture 10.15.*

Proof. As in Remark 3.50, ∇_Γ is the pullback of $\nabla_{A\cap\Gamma}$ under the map (of secondary stacks) induced by $p : L^\vee \to L_\Gamma^\vee$ where $\nabla_{A\cap\Gamma}$ is the principal component of the VGIT on Γ (whose weights lie in $L_\Gamma^\vee$ by definition). As such $m_{\Gamma,W} = \langle \nabla_{A\cap\Gamma}, p(Z(W))\rangle$.

Under p, the curve $Z(W)$ gets sent to either a toric fixed point or a toric curve and the latter happens precisely when $p(W)$ is a codimension 1 cone in $(L_\Gamma^\vee)_\mathbb{R}$ – that is, when $\langle W\rangle$ contains $(L'_\Gamma)^\vee =: \ker p$. As $\nabla_{A\cap\Gamma}$ always avoids the torus fixed points (see [20], Ch. 6, §1), for any wall such that $\langle W\rangle$ doesn't contain $(L'_\Gamma)^\vee$, $Z(W)$ is disjoint from ∇_Γ. □

If we push this a little further we get,

Proposition 10.17. *If Γ is a circuit, then $m_{\Gamma,W} = n_{\Gamma,W}$. This number is 1 precisely when $(L'_\Gamma)^\vee_\mathbb{R} = \langle W\rangle$ and 0 otherwise.*

Proof. By Remark 10.14 and the fact that $(L'_\Gamma)^\vee_\mathbb{R}$ is a hyperplane when Γ is a circuit, $n_{\Gamma,W} \neq 0$ precisely when $(L'_\Gamma)^\vee_\mathbb{R} = \langle W\rangle$ – that is, when the VGIT on W is the Higgs VGIT for Γ. Moreover, if $n_{\Gamma,W} \neq 0$, then $n_{\Gamma,W} = 1$ since Z_Γ is a phase in this VGIT and so this follows from Theorem 4.21.

On the other hand, from the proof of Lemma 10.16, we see that p maps $Z(W)$ to a toric curve precisely when $\langle W\rangle = (L'_\Gamma)^\vee_\mathbb{R}$ (as Γ is circuit, so $(L'_\Gamma)^\vee_\mathbb{R}$ is a hyperplane). Moreover, because $L_\Gamma^\vee$ is rank 1, such a toric curve must be the whole secondary stack and hence must meet $\nabla_{A\cap\Gamma}$. Thus we see that $m_{\Gamma,W} \neq 0$ precisely when $(L'_\Gamma)^\vee_\mathbb{R} = \langle W\rangle$ and that, if $m_{\Gamma,W} \neq 0$, $m_{\Gamma,W} = 1$ since $\nabla_{A\cap\Gamma}$ is always reduced and p maps $Z(W)$ isomorphically onto its image. □

Proposition 10.18. *If Γ is such that $Rk(L_\Gamma) = 2$, then $m_{\Gamma,W} = n_{\Gamma,W}$*

Proof. By Lemma 10.16, we need only consider Γ such that $(L'_\Gamma)^\vee_\mathbb{R} \subset \langle W\rangle$. Consider as usual the map of secondary stacks induced by $p : L^\vee \to L_\Gamma^\vee$. For such Γ, p sends W to a codimension 1 cone σ in the secondary fan for Γ, so $Z(W)$ gets mapped isomorphically to a boundary curve in the secondary stack for Γ. By Lemma 6.3, we have that:

$$m_{\Gamma,W} = \langle \nabla_{A\cap\Gamma}, p(Z(W))\rangle = \max\Big(\sum_{i|p(\beta_i)\in\langle\sigma\rangle} l(p(\beta_i)), 0\Big)$$

(where $l \in L_\Gamma$ obeys $l(u_\sigma) = 1$) and so $m_{\Gamma,W} = \max(\sum_{i|\beta_i\in\langle W\rangle} l'(\beta_i), 0)$, where $l' = p^*(l) \in L$.

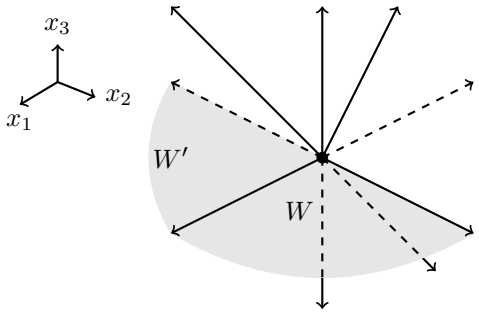

FIGURE 32. The weights in the setup of Example 10.21

On the other hand, $(L'_\Gamma)^\vee_\mathbb{R}$ is a hyperplane in $\langle W\rangle$ and so $n_{\Gamma,W} \neq 0$ precisely when $K_{Z'_\lambda}$ lies on the opposite side of $(L'_\Gamma)^\vee_\mathbb{R}$ to W – that is, when $\sum_{i|\beta_i\in\langle W\rangle} l'(\beta_i) > 0$. When $n_{\Gamma,W} \neq 0$, we only cross this wall $(L'_\Gamma)^\vee_\mathbb{R}$ once and, by Theorem 10.4, we can assume we pass through the Higgs chamber in $(L'_\Gamma)^\vee_\mathbb{R}$. Then Theorem 4.21 tells us that we get $n_{\Gamma,W} = \hat{l}(-K_{Z'_\lambda})$ copies of $D^b(Z_\Gamma)$, where $\hat{l} \in (\langle W\rangle \cap L^\vee)^\vee$ is the primitive normal to $(L'_\Gamma)^\vee_\mathbb{R}$ in $\langle W\rangle$ pointing towards W. But $\hat{l} = l'|_{\langle W\rangle}$ and so this quantity equals $\sum_{i|\beta_i\in\langle W\rangle} l'(\beta_i)$. □

Corollary 10.19. *For a 2-dimensional FIPS, Conjecture 10.15 holds.*

Proof. In a 2-dimensional FIPS (see Lemma 6.4) only ∇_{pr} and ∇_W can possibly meet $Z(W)$ and $\nabla_W = \nabla_\Gamma$ for a circuit Γ. Using Propositions 10.17 and 10.18, we have therefore covered all the possibilities. □

Remark 10.20. As these results show, it becomes harder to compute $m_{\Gamma,W}$ as Γ has more relations on it. In particular, of all the faces Γ, we should expect $m_{\Delta,W}$ to be the hardest to understand.

In the above results, we have crucially used Lemma 6.3 which relies on the fact that Horn uniformisation gives a morphism in dimension at most 2. In the case of a 3-dimensional FIPS, to which we now turn, only the multiplicities for $\Gamma = \Delta$ remain to be understood. However in this case, Horn uniformisation is generally only a *rational* map and this causes birational complications when computing $m_{\Gamma,W}$. Nonetheless in the simplest non-trivial 3-dimensional case, Horn uniformisation is still a morphism on the region we care about and so we can still show Conjecture 10.15 holds.

Example 10.21. Suppose that $L = \mathbb{Z}^3_{x_1,x_2,x_3}$ and that the weights are chosen such that the representation is Calabi–Yau and the only weights that lie on $\langle W\rangle = \{x_3 = 0\} = \mathbb{Z}^2$ lie on the 2 coordinate axes. Moreover we assume that $\beta_{x_j} = \sum_{i|\beta_i \text{ on } x_j\text{-axis}} \beta_i$ has positive x_j coordinate and that $\gcd(|\beta_i| \mid \beta_i \text{ on } x_j\text{-axis}) = 1$ (for $j = 1, 2$). Then $m_{\Delta,W} = n_{\Delta,W}$ and Conjecture 10.15 holds.

This situation is pictured in Figure 32. Note that there are at most 4 chambers for the VGIT on $\langle W\rangle$ and that, since β_{x_j} has positive x_j-coordinate for $j = 1, 2$, only

the chamber W in this VGIT given by the positive quadrant (which faces towards us in Figure 32) has $n_{\Delta,W} \neq 0$. Moreover, in this case, $n_{\Delta,W} = |\beta_{x_1}||\beta_{x_2}|$.

We now compute the intersection multiplicity of ∇_{pr} with $Z(W)$. For this, we use Horn uniformisation which is given by (see (4) in §3.6)

$$H : \mathbb{P}(L_{\mathbb{C}}) \dashrightarrow T_{L^\vee} = (\mathbb{C}^*)^3_{x_1,x_2,x_3}, [\lambda_1, \lambda_2, \lambda_3] \mapsto (\lambda_1^{|\beta_{x_1}|} \times \Lambda_1, \lambda_2^{|\beta_{x_2}|} \times \Lambda_2, \Lambda_3)$$

where $\Lambda_i(\lambda_1, \lambda_2, \lambda_3)$ are the factors in Horn uniformisation corresponding to weights not lying on $\langle W \rangle$ – that is, with non-zero λ_3-coordinate.

As in §5.2, a wall W and a choice of β_W gives a projection $\pi' : U_W \to B'$ such that $\pi'^{-1}(\underline{0}) = Z(W) \cap U_W$. Then $U_W = \mathbb{C}^2_{x_1,x_2} \times \mathbb{C}^*_{x_3}$ and, if we take $\beta_W = (0, 0, 1)$, π' is just the projection to the first 2 coordinates. Then $B' = \mathbb{C}^2_{x_1,x_2}$ and $\pi' \circ H : [\lambda_1, \lambda_2, \lambda_3] \mapsto (\lambda_1^{|\beta_{x_1}|} \times \Lambda_1, \lambda_2^{|\beta_{x_2}|} \times \Lambda_2)$.

Consider those elements in $\mathbb{P}(L_{\mathbb{C}})$ mapping to $Z(W)$ under H. As $\nabla_{pr} = \mathrm{Im}(H)$ avoids the torus fixed points, they must have $\Lambda_3 \neq 0$. Since all factors in Λ_3 (of the form $(\lambda_1\beta_{j1} + \lambda_2\beta_{j2} + \lambda_3\beta_{j3})^{\beta_{j3}}$ for β_j not lying in $\langle W \rangle$) have non-zero exponent, the only possibility is if $(\lambda_1\beta_{j1} + \lambda_2\beta_{j2} + \lambda_3\beta_{j3}) \neq 0$ for all such β_j. But since Λ_i has the same factors (with different exponents) for $i = 1, 2$ we conclude that $\Lambda_i \neq 0$. As such H actually defines a morphism on $H^{-1}(U_W)$ and $m_{\Delta,W} = \mathrm{Len}(H^*(Z(W) \cap U_W)) = \mathrm{Len}((\pi' \circ H)^*(\underline{0})) = \mathrm{Len}(\{\lambda_1^{|\beta_{x_1}|} = 0, \lambda_2^{|\beta_{x_2}|} = 0\}) = |\beta_{x_1}||\beta_{x_2}|$ as desired.

One can also check that $m_{\Delta,W'} = 0$ for the other chambers W'. As an example, take W' to be the wall shown in Figure 32. Then, if we compactify B' to $\mathbb{P}^1 \times \mathbb{P}^1$, $\pi' \circ H : [\lambda_1, \lambda_2, \lambda_3] \mapsto ([\lambda_1^{|\beta_{x_1}|} \times \Lambda_1 : 1], [\lambda_2^{|\beta_{x_2}|} \times \Lambda_2 : 1])$ and $Z(W') \cap U_{W'} = \pi'^*([0, 1], [1, 0])$. As above, the fact that $\Lambda_3 \neq 0$ means $\Lambda_i \neq 0$ for $i = 1, 2$ and so H is still a morphism on $H^{-1}(U_{W'})$. Moreover, $m_{\Delta,W'} = \mathrm{Len}(H^*(Z(W') \cap U_{W'})) = \mathrm{Len}((\pi' \circ H)^*(\underline{0})) = \mathrm{Len}(\varnothing) = 0$ as claimed.

Remark 10.22. We can prove the same statement in a few more complicated cases when $\mathrm{Rk}(L) = 3$. In all these examples, it seems natural to try to compactify the image of the projection using the secondary fan of the VGIT on Z'^{λ} and then resolve the indeterminacy in H using iterated blow-ups over the origin. Given the iterative nature of $n_{\Delta,W}$ it would seem natural to try to relate these blow-ups to walls in $\langle W \rangle$ but we don't know how to do this as, until H is resolved, we can't use it to compute intersection multiplicities.

Lastly, we observe that Conjecture 10.15 also holds for all wall-crossings in the Triangle VGIT (see §9) which has a 3-dimensional FIPS and is not of the form in Example 10.21.

Example 10.23. For every wall W in D, $Z(W)$ meets a unique component of the discriminant and does so with multiplicity 1. For any wall in F_8 (W_{i8} in the notation from §9.2.2) , $Z(W)$ meets ∇_i for a unique i, so $m_{i,W} = 1$ for this i and 0 for all other faces. The corresponding window shifts (see Remark 9.10) are family spherical twists over a base $Z'_\lambda \cong \mathbb{C}$. Moreover we check that the corresponding

VGIT on Z'^{λ} is given by:

$$Q : \mathbb{Z}^3 \to L^\vee \cap \langle W \rangle \cong \mathbb{Z}^2, Q = \begin{pmatrix} 1 & -1 & -1 \\ 0 & 1 & -1 \end{pmatrix}$$

Hence this VGIT has 3 phases and $K_{Z'_\lambda} = (1, 0)$. As such, any phase corresponding to one of the two chambers containing $K_{Z'_\lambda}$ is a Higgs phase and indeed Z'_λ is one of these, hence $n_{\Gamma,W} = 1$ for the face Γ such that $(L'_\Gamma)^\vee = L^\vee \cap \langle W \rangle$ and $n_{\Gamma,W} = 0$ for all others.

For the walls W_{16}, W_{13} and W_{15} (in the notation from §9.2.2) in the face F_1, $Z(W)$ meets ∇_{pr} so $m_{i,W} = 0$ for all i and $m_{\Delta,W} = 1$. The corresponding window shifts (see Remark 9.10) are spherical twists about a compact curve - indeed one sees that Z'_λ is a point – and hence Z'_λ is the Higgs phase Z_Δ, as expected.

For the 3 walls W_{24},W_{45},W_{25} not in D, $Z(W)$ meets ∇_{pr} transversely and one of the components ∇_i. Hence $m_{\Delta,W} = 1 = m_{i,W}$ and $m_{j,W} = 0$ for the other two j. These walls are chambers within $L^\vee \cap \langle W \rangle \cong \mathbb{Z}^2$ as above and correspond to the single non-minimal phase $Z'_\lambda \cong [\mathbb{C}/\mathbb{Z}_2]$. The SOD coming from wall-crossing is $D^b([\mathbb{C}/\mathbb{Z}_2]) = \langle D^b(\mathbb{C}), D^b(\mathrm{pt}) \rangle$ and so we get $n_{\Delta,W} = 1$ and one copy of another Higgs phase. One can check that it is indeed the correct Higgs phase.

References

[1] N. Addington, *New derived symmetries of some hyperkähler varieties*, Alg. Geom. 3(2):223-260, 2016

[2] A. Andreotti, T. Frankel, *The Lefschetz theorem on hyperplane sections*, Annals of Mathematics, 69 (1959), 713-717

[3] R. Anno, T. Logvinenko, *Spherical DG-functors*, arXiv:1309.5035, 2013

[4] P. Aspinwall, M. Plesser, K. Wang, *Mirror symmetry and discriminants*, arXiv-hep-th:1702.04661, 2017

[5] M. Ballard, C. Diemer, D. Favero, L. Katzarkov, G. Kerr, *The Mori Program and Non-Fano Toric Homological Mirror Symmetry*, arXiv:1302.0803, 2013

[6] M. Ballard, D. Favero, L. Katzarkov, *Variation of geometric invariant theory quotients and derived categories*, arXiv:1203.6643, 2012

[7] A. Bayer, T. Bridgeland, *Derived automorphism groups of K3 surfaces of Picard rank 1*, arXiv:1310.8266, 2016

[8] R. Bezrukavnikov, S. Riche, *Affine braid group actions on derived categories of Springer resolutions*, arXiv:1101.3702, 2011

[9] T. Bridgeland, *Stability conditions on triangulated categories*, Annals of Mathematics, 166 (2007), 317-345, arXiv:0212.237

[10] R. Brown, *Topology and Groupoids*, ISBN: 1-4196-2722-8, 2006

[11] A. Craw, *The McKay correspondence and representations of the McKay quiver*, University of Warwick Ph.D thesis, xviii + 134 pp, 2001.

[12] A. Craw, A. Ishii, *Flops of G-Hilb and equivalences of derived categories by variation of GIT quotient*, Duke Math.J.124:259-307, 2004

[13] J. Cogolludo-Agustín, *Braid Monodromy of Algebraic Curves*, https://riemann.unizar.es/ jicogo/papers/pau-bm.pdf

[14] D. Cox, J. Little, H. Schenck, *Toric Varieties*, Graduate Studies in Mathematics, Vol. 124, 2011

[15] P. Deligne, *Les immeubles des groupes de tresses généralisés*, Invent. Math. 17, 273–302, 1972

[16] C. Diemer, L. Katzarkov, G. Kerr, *Symplectomorphism group relations and degenerations of Landau-Ginzburg models*, arXiv:1204.2233v3, 2012

[17] I. Dolgachev, Y. Hu, *Variation of Geometric Invariant Theory Quotients*, arXiv:9402.008, 1994

[18] W. Donovan, E. Segal, *Mixed braid group actions from deformations of surface singularities*, arXiv:1310.7877, 2013

[19] W. Donovan, M. Wemyss, *Twists and braids for general 3-fold flops*, arXiv:1504.05320, 2015

[20] I. Gelfand, M. Kapranov, A. Zelevinsky, *Discriminants, Resultants, and Multidimensional Determinants*, Birkhäuser Boston, 1994

[21] M. Goresky, R. MacPherson, *Stratified Morse Theory*, Springer-Verlag, 1988

[22] D. Halpern-Leistner, *The derived category of a GIT quotient*, arXiv:1203.0276v2, 2012

[23] D. Halpern-Leistner, *Lefschetz Hyperplane Theorem for Stacks*, arXiv:1008.0891, 2010

[24] D. Halpern-Leistner, S. Sam, *Combinatorial Constructions of Derived Equivalences*, arXiv:1601.02030, 2016

[25] D. Halpern-Leistner, I. Shipman, *Autoequivalences of derived categories via geometric invariant theory*, arXiv:1303.5531, 2013

[26] H. Hamm, D. T. Lê, *Lefschetz theorems on quasi-projective varieties*, Bulletin de la S.M.F., Tome 113, p. 123-142, 1985

[27] M. Herbst, K. Hori, D. Page, *Phases of N=2 Theories in 1+1 Dimensions with Boundary*, DESY-07-154, CERN-PH-TH/2008-048, 2008

[28] A. Kuznetsov, *A simple counterexample to the Jordan-Hölder property for derived categories*, arXiv:1304.0903, 2013

[29] L. Paris, *The covers of a complexified real arrangement of hyperplanes and their fundamental groups*, Topology Appl. 53, no. 1, 75–103, 1993

[30] M. Salvetti, *Topology of the complement of real hyperplanes in* $\mathbb{C}^N$, Invent. Math. 88, no. 3, 603–618, 1987

[31] E. Segal, Unpublished note

[32] E. Segal, *Equivalences between GIT quotients of Landau-Ginzburg B-models*, Commun.Math.Phys.304:411-432, 2011

[33] Š. Špenko, M. Van den Bergh, *Non-commutative resolutions of quotient singularities*, arXiv:1502.05240, 2015

[34] W. Thurston, *The geometry and topology of Three-manifolds*, Electronic Version 1.1, http://www.msri.org/publications/books/gt3m, 2002

[35] E. Van Kampen, *On the connection between the fundamental groups of some related spaces*, Amer. J. Math. 55, no. 1-4, 261–267. MR 1506962, 1933

[36] M. Wemyss, *Aspects of the Homological Minimal Model Program*, arXiv:1411.7189, 2014

[37] O. Zariski, *On the Problem of Existence of Algebraic Functions of Two Variables Possessing a Given Branch Curve*, Amer. J. Math. 51, no. 2, 305–328. MR 1506719, 1929